

DEPOSITIONAL MECHANISM OF GREYWACKES

DEPOSITIONAL MECHANISM OF GREYWACKES,
CLORIDORME FORMATION (MIDDLE ORDOVICIAN),
GASPÉ, QUEBEC

by

BARHAM PARKASH

A Thesis

Submitted to the Faculty of Graduate Studies

in Partial Fulfilment of the Requirements

for the Degree

Doctor of Philosophy

McMaster University

May, 1969

DOCTOR OF PHILOSOPHY (1969)

MCMASTER UNIVERSITY

(Geology)

Hamilton, Ontario.

TITLE: Depositional Mechanism of
Greywackes, Cloridorme Formation
(Middle Ordovician), Gaspé,
Quebec.

AUTHOR: Barham Parkash, B.Sc. (Panjab University)
M.Tech. (Saugar
University)

SUPERVISOR: Professor G. V. Middleton

NUMBER OF PAGES: xv, 238

SCOPE AND CONTENTS:

A detailed study of sedimentary structures, textures and fabric of eight turbidite greywacke beds from the Cloridorme Formation (Middle Ordovician), Gaspé, Quebec, has been made. In light of the present knowledge of such features, implications of the above are considered in an attempt to understand the mode of deposition of sediment from turbidity currents.

ABSTRACT

Sedimentary structures, textures and fabric were studied in detail in eight turbidite greywacke beds from the Cloridorme Formation (Middle Ordovician), Gaspé, Quebec. The beds are exposed on the wave-cut platform near Grande Vallée and were traced for about two miles along the strike (276°), which is parallel to the average current direction (274°) as indicated by sole mark directions.

The beds under study show the following systematic downcurrent changes along the strike from east to west:

(i) Sole mark types show the following changes:

(1) tool marks such as grooves, prod marks and isolated flute marks, to (2) longitudinal ridges, longitudinal ridges with overlapping flute, closely spaced flutes, to (3) poorly developed, shallow longitudinal ridges with occasional cusped crossing bars, to (4) smooth bottom with occasional grooves.

(ii) There is an increase in variance of sole mark directions without a large change in the mean direction in most beds, but the sole mark direction changes by nearly 90° as one of the beds is traced from east to west along the strike.

(iii) Most of the beds are massive and are divided into two parts by a bedding joint. However, in the proximal region, if a bed is unusually thin, the bedding joint is absent and the bed shows slightly wavy, plane-laminated structure at places.

(iv) Grain orientations are generally statistically non-significant in the upper massive part of the bed in the proximal region and significant in the rest of the bed. Significant grain orientations and graptolite orientations show large deviations from the sole in the distal region. Deviations increase towards the top of the bed.

(v) The beds show a change from good grading to poor grading or slight reverse grading from the proximal to distal region.

It is considered that the beds were deposited by low concentration, highly turbulent currents. Deposition of the beds took place in two distinct phases. First a 'quick' bed separated from the current was sheared extensively by the overflowing current and on consolidation formed the lower part of the bed. Later deposition in the proximal region from the upper part of the current and the part close to the tail was by settling of individual particles from the suspension. Separation and consolidation of another 'quick' bed in some cases formed the upper part

of the beds in the distal region.

The depositing currents produced a good vertical and lateral grain size grading in the proximal region, but poor vertical grading in the distal region due to the loss of coarse grains and possibly increased concentration of flocculated clay. Also, the turbidity currents tended to "meander" greatly on slowing down in the distal region.

ACKNOWLEDGEMENTS

The author wishes to express his sincere gratitude to Professor G. V. Middleton, his research supervisor, for his guidance and encouragement during the progress of research and for many valuable suggestions for improving the manuscript.

Sincere thanks are extended to Drs. Paul Enos of Shell Oil (U.S.A.) and Roger G. Walker of the Geology Department, McMaster University. Dr. Enos showed the author important exposures of the Cloridorme Formation during a field trip in May, 1966, and made available many of his unpublished field notes. Dr. Walker visited the author in the field and made many helpful suggestions.

The following are thanked for their assistance: Art Troup and Harish Verma for assistance in numerous ways, Don Falkiner and Leonard Falkiner for preparation of thin sections, Jack Whorwood for photographic work and Miss S. Schonfeld for typing the final draft.

Financial assistance by the N.R.C. during summers 1966-68 and by the Geology Department, McMaster University during the academic sessions 1964-1969 is gratefully acknowledged.

TABLE OF CONTENTS

CHAPTER		PAGE
I	INTRODUCTION	1
	Rationale	1
	Area of Present Study	3
	Regional Setting	4
	Previous Work	9
	Structure and Stratigraphy	10
	Age	11
	Metamorphism	11
	Lithologies	12
II	FIELD DESCRIPTION	15
	Field Methods	15
	Field Description	18
	Bed G-68	33
	Bed G-67	38
	Bed G-66	44
	Beds G-65A and G-65	45
	Bed G-58	47
	Bed G-50	50
	Bed G-49	53
	Conclusions	55
III	GRAIN ORIENTATION STUDY	62
	Experimental Details	62
	Number of Measurements per Thin Section	64
	Accuracy and Consistency of Measurements	67
	Relationship Between Grain Orientations and Graptolite Orientations within a Hand Specimen	71
	Homogeneity of Samples	75

TABLE OF CONTENTS (cont'd)

CHAPTER		PAGE
III	Degree of Preferred Orientation and Deviation of Grain Orientations from the Sole	78
	Secondary Modes	104
	Imbrication	106
	Conclusions	112
IV	GRAIN SIZE AND SHAPE STUDY	115
	Experimental Details	115
	Relationship Between Mean Size and Maxi- mum Size	129
	Sphericity	132
	Vertical Grading	134
	Grading Characteristics and Grain Orientation	141
	Lateral Grading	142
	Sorting	145
	Skewness and Kurtosis	148
	Matrix	150
	Conclusions	152
V	DISCUSSION AND INTERPRETATION	153
	Changes in Internal Structure	154
	Variation in Sole Markings	160
	Lateral Changes in Sole Mark Directions	163
	Theory of Grain Orientation	166
	Mass deposition	166
	Direct deposition from suspension	169
	Deposition from a traction carpet	171
	Explanation of Observed Features of Grain Orientation in Light of Theory	174
	Degree of preferred orientation	174

TABLE OF CONTENTS (cont'd)

CHAPTER	PAGE
V	
Deviation of graptolites and grain orientations from the sole	177
Grading	181
Two Parts of a Bed	185
Synthesis: Depositional Mechanism of Greywackes	192
SUMMARY AND CONCLUSIONS	195
BIBLIOGRAPHY	200
APPENDICES	
I	
Grain Orientation Statistics	210
II	
Grain Imbrication Statistics	224
III	
Moment Measure Statistics	228

ILLUSTRATIONS

		PAGE
1.1	Cambrian and Ordovician flysch of the folded Appalachians.	5
1.2	Geology of Gaspé Peninsula.	6
1.3	Location of measured sections	7
1.4	Correlation of beds in a part of unit G, β -7 member.	Pocket
1.5	A view of the wave-cut platform looking west at section II ₄ .	8
2.1	Variation of bed thickness and sole mark directions along the strike.	Pocket
2.2a-	Relation of graptolite orientations to sole	
2.2g	mark directions in different beds.	20-23
2.3a-	Rose diagrams for sole mark directions for	
2.3h	the eight beds.	24-31
2.4	Side view of beds G-68, G-67 and G-66, 3250 yard point.	34
2.5	Side view of beds G-68, G-67 and G-66, 3200 yard point.	34
2.6	Side view of beds G-68, G-67 and G-66, 2560 yard point.	34
2.7	Side view of beds G-68, G-67 and G-66, 500 yard point.	34
2.8	Smooth base with curving grooves, bed G-68, 3250 yard point.	36
2.9	Delicate longitudinal ridges and scaly marks at the base of bed G-68, 2662 yard point.	36
2.10	Longitudinal ridges at the base of bed G-68, 1905 yard point.	36
2.11	Longitudinal ridges and load structures at the base of bed G-68, near 1100 yard point.	36

ILLUSTRATIONS (cont'd)

	PAGE
2.12 Sole marks at the base of beds G-68, G-67 and G-66, near 1100 yard point.	37
2.13 Poorly developed longitudinal ridges at the base of bed G-68, 400 yard point.	37
2.14 Small scale 'dish' structure in bed G-67, 1140 yard point.	37
2.15 Small scale 'dish' structure in bed G-67, near 1140 yard point.	37
2.16 Sharp nosed flute and some tool marks at the base of bed G-67, 2550 yard point.	40
2.17 Small 'scaly' structures filled with coarse grains at the base of bed G-67, 2495 yard point.	40
2.18 Mould of wrinkled mud bottom, bed G-67, 1850 yard point.	40
2.19 Longitudinal ridges with overlapping scaly structures, bed G-67, near 1100 yard point.	40
2.20 Fan shaped flutes filled with coarse grains, bed G-67 near 1100 yard point.	41
2.21 Shallow longitudinal ridges with cusped crossing bars, bed G-67, 125 yard point.	41
2.22 Poorly developed longitudinal ridges at the base of bed G-67, 125 yard point.	41
2.23 Grooves at the base of bed G-67, 80 yard point.	41
2.24a Base of bed G-67 showing orientation of argillite fragments, intrabed lineation and graptolites at the bedding joint and sole mark, 425 yard point.	43
2.24b Relationship between orientation of argillite fragments, graptolites and sole mark, bed G-67, 425 yard point.	43
2.25 A large groove with striated trough and with coarse grains, bed G-66, 2659 yard point.	46

ILLUSTRATIONS (cont'd)

	PAGE
2.26 Side view of beds G-65A and G-65. Argillite fragments in bed G-65A imbricate upstream.	46
2.27 Grooves on the rough bottom of bed G-65A, 3190 yard point.	46
2.28 Intrabed lineation and graptolites at the bedding joint deviate from the direction of groove at the base of the bed by 30°, 430 yard point.	46
2.29 Bed G-58 with faintly developed plane laminations towards the top, 1840 yard point.	49
2.30 Large irregular grooves modified by load casting at the base of bed G-58, 1800 yard point.	49
2.31 "Scaly" structures at the base of bed G-58, 80 yard point.	49
2.32 Internal lobate structure just below the bedding joint, bed G-50, near 1100 yard point.	49
2.33 Internal lobate structure below the bedding joint, bed G-50, near 1100 yard point.	51
2.34 Internal lobate structure just below the bedding joint in bed G-50, 550 yard point.	51
2.35 "Scaly" structures and longitudinal ridges at the base of bed G-50, near 1800 yard point.	51
2.36 Closely spaced flute marks, bed G-50, 1150 yard point.	51
2.37 Longitudinal ridges with crossing cusped bars, bed G-50, 1115 yard point.	52
2.38 Shallow longitudinal ridges with cusped crossing bars, bed G-50, 30 yard point.	52
2.39 Bed G-50 with coarse grains scattered throughout the lower part of the argillite overlying the sandy portion of the bed, 100 yard point.	52

ILLUSTRATIONS (cont'd)

	PAGE
2.40 Bed G-50 with irregular patterns of yellowish color in the middle, 450 yard point.	52
2.41 Side view of beds G-50 and G-49, 2600 yard point.	54
2.42 Side view of beds G-50 and G-49, 2410 yard point.	54
2.43 Crossing grooves at the base of bed G-49, 3130 yard point.	54
2.44 A large groove and a tool at the base of bed G-49, 3130 yard point.	54
3.1 Variation in vector mean and vector magnitude per cent with increase in number of measurements.	65
3.2 Grain orientation frequency distributions in operator experiment.	68
3.3 Vector mean and vector magnitude per cent in five thin sections in operator experiment.	69
3.4 Grain orientation frequency distributions in the specimen with large number of graptolite.	72
3.5- Grain orientation frequency distributions in the eight beds.	80-87
3.12	
3.13 Relation between vector mean directions of grain orientation distributions and sole directions for different beds.	88-91
3.14 Frequency distributions of deviations of significant grain orientations from sole directions.	93
3.15 Composite grain orientation frequency distributions for different beds.	103
3.16 Plot of angle of imbrication vs. grain size.	108
3.17 Polar plot of grain imbrications.	110
4.1- Cumulative curves of size distribution as determined by measuring two axes 'a' and 'b' (fig. 4.1) and by measuring only the longest axis (fig. 4.2) for bed G-66 at section II ₆ .	117
4.2	

ILLUSTRATIONS (cont'd)

	PAGE
4.3 Operator consistency in determination of the mean grain size and sorting.	120
4.4- Cumulative grain size distribution curves 4.11 for the eight beds.	121-128
4.12 Variation of the maximum grain size with the height above the base in beds G-68 and G-66.	130
4.13a-Variation of the mean grain size with the 4.13h height above the base in the eight beds.	136-138
4.14 Variation of the mean grain size at the base of the beds along the strike.	144
4.15 Plots of the dispersion vs. the mean grain size for beds G-68, G-67 and G-66.	146
4.16 Relationship between percentage of matrix and the mean grain size for beds G-68 and G-66.	151
5.1 Complete Turbidite Sequence	156

LIST OF TABLES

	PAGE
2.1 Summary of field directional data.	19
3.1 Determination of 'flatness' point.	67
3.2 Summary statistics: operator experiment - vector mean.	70
3.3 Analysis of variance: operator experiment - vector mean.	71
3.4 Experiment on relationship between graptolite and grain orientations in a hand specimen.	73
3.5 Homogeneity of grain fabric in a hand specimen - A. Data	76
B. Analysis of variance	77
3.6 Summary statistics of grain orientation study.	94
4.1 Summary statistics: operator experiment - mean size.	119
4.2 Analysis of variance - operator experiment - mean size.	129
4.3 Maximum grain size and matrix percentage in thin sections from beds G-68 and G-66.	131
4.4 Replicate sphericity determinations in operator experiment.	133
4.5 Analysis of variance of sphericity determinations in operator experiment.	133
4.6 Linear regression equations and correlation coefficients for relationship between k_1 and k_2 .	147

CHAPTER I

INTRODUCTION

Rationale

Studer (1827) introduced the term "flysch" to indicate an Upper Cretaceous geosynclinal sequence in the Alps consisting of alternating muddy sandstones and shales. "Flysch" was described as "Une formation qui se montre en général sous la forme de schistes et de grès gris noirâtre, mais qui prend un caractère très compliqué par la présence de blocs et de couches calcaire subordonnés, de grandes masses de brèches calcaire, de couches de quartz et de silex pyromaque noir et vert de poireau, etc." (Studer, 1827; in Dzulynski and Walton, 1965, p.1). Later the term flysch was extended to describe similar formations elsewhere. The origin of the sandstones in the flysch sequences remained enigmatic till 1950, when Kuenen and Migliorini (1950) in their classic paper, demonstrated experimentally that similar sandstones could be deposited by turbidity currents.

Recent researches on flysch sequences all over the world have resulted in exhaustive description of sole structures, paleocurrents, internal structures and facies variation in these beds (see Potter and Pettijohn, 1963 and Dzulynski and

Walton, 1965). Some insight into the formation of sole structures have been obtained by the experiments of Dzulynski and co-workers (Dzulynski and Walton, 1963; Dzulynski, 1965, 1966; Dzulynski and Simpson, 1966a,b). Theoretical studies (Bagnold, 1962; Sanders, 1963, 1965; Walker, 1965; Scheidegger and Potter, 1965; Walton, 1967) and experimental studies (Kuenen and Migliorini, 1950; Kuenen, 1951, 1965, 1966, 1967; Middleton, 1966a,b; 1967a,b) have resulted in some understanding of the deposition of sediment from turbidity currents and their hydraulics.

In the past, little attempt has been made to check in the field the validity of various hypotheses resulting from theoretical and experimental considerations, partly because individual beds in flysch sequences cannot be traced for long distances due to the tectonically disturbed nature of flysch sequences. Enos (1965) reported that individual greywacke beds from the flysch sequence of the Cloridorme Formation (Middle Ordovician), Gaspé, Quebec can be traced for about two miles along the strike and that the strike is almost parallel to the predominant current direction as deduced from sole mark directions. Thus, these beds offer an ideal situation for the study of turbidite sedimentation. The objective of the present study is to make a detailed field study of the sole mark types and directions, internal structures and laboratory study of texture of several of these

greywacke beds in the Cloridorme Formation and derive their depositional mechanism from these studies.

Area of Present Study

The present study deals with the detailed sedimentological characteristics of eight greywacke beds in the Cloridorme Formation (Middle Ordovician), Gaspé, Quebec. The eight greywacke beds belong to unit G of the β -7 member, the uppermost exposed portion of the formation in the central structural block (Enos, 1965). The unit G is exposed on an overturned limb of an anticline along the wave-cut platform (fig. 1.5) of the St. Lawrence Estuary between Petite Vallée and Grande Vallée, Gaspé, Quebec (fig. 1.3). The beds from the unit G are overturned to the south with a dip of 75° and strike along $N276^{\circ}$. The beds from unit G can be traced along the strike for about 3200 yards between sections II_4 and II_9 (fig. 1.3) and part of unit G measured at sections II_4 , II_5 , II_8 , II_6 and II_9 (fig. 1.3) is shown in figure 1.4. Enos (1965) noted that the predominant current direction (274°) as deduced from the sole mark directions is nearly parallel to the strike (276°).

The Cloridorme Formation is exposed along the north coast of Gaspé between Cap-des-Rosiers and Marsouins over a distance of 80 miles (McGerrigle, 1954). The outcrop belt

continues further inland as far as Ste-Anne-des-Monts for another 32 miles (fig. 1.2). The rocks consist of 7700 meters of greywackes, calcisiltites dolostones interbedded with grey argillite. The Cloridorme Formation may well be classified as flysch in the descriptive sense of Studer (1827). Most of these rocks are considered to be deposited by turbidity currents on the basis of sedimentary structures and reworked fauna (Enos, 1965).

Regional Setting

The Gaspé Peninsula is the extreme northern end of the Appalachian mountain system on the continental mainland and the Cloridorme Formation and the Cap-des-Rosiers Formation form a part of the exposure of eugeosynclinal assemblage of the folded Appalachians extending from southeastern Tennessee to Newfoundland (fig. 1.1).

The Gaspé Peninsula can be divided geologically into four main east-west trending belts (McGerrigle, 1950). The Cloridorme and Cap-des-Rosiers Formations form the northern-most belt and are a part of the northern limb of the east-west trending Gaspé Synclinorium. Volcanic flows and miogeosynclinal Silurian and Devonian rocks occupying the centre of the synclinorium form the second belt. The southern limb of the syncline consists of Ordovician rocks and constitutes the third belt. The

Fig. 1.1: Cambrian and Ordovician flysch of the folded Appalachians. After Enos, 1965.

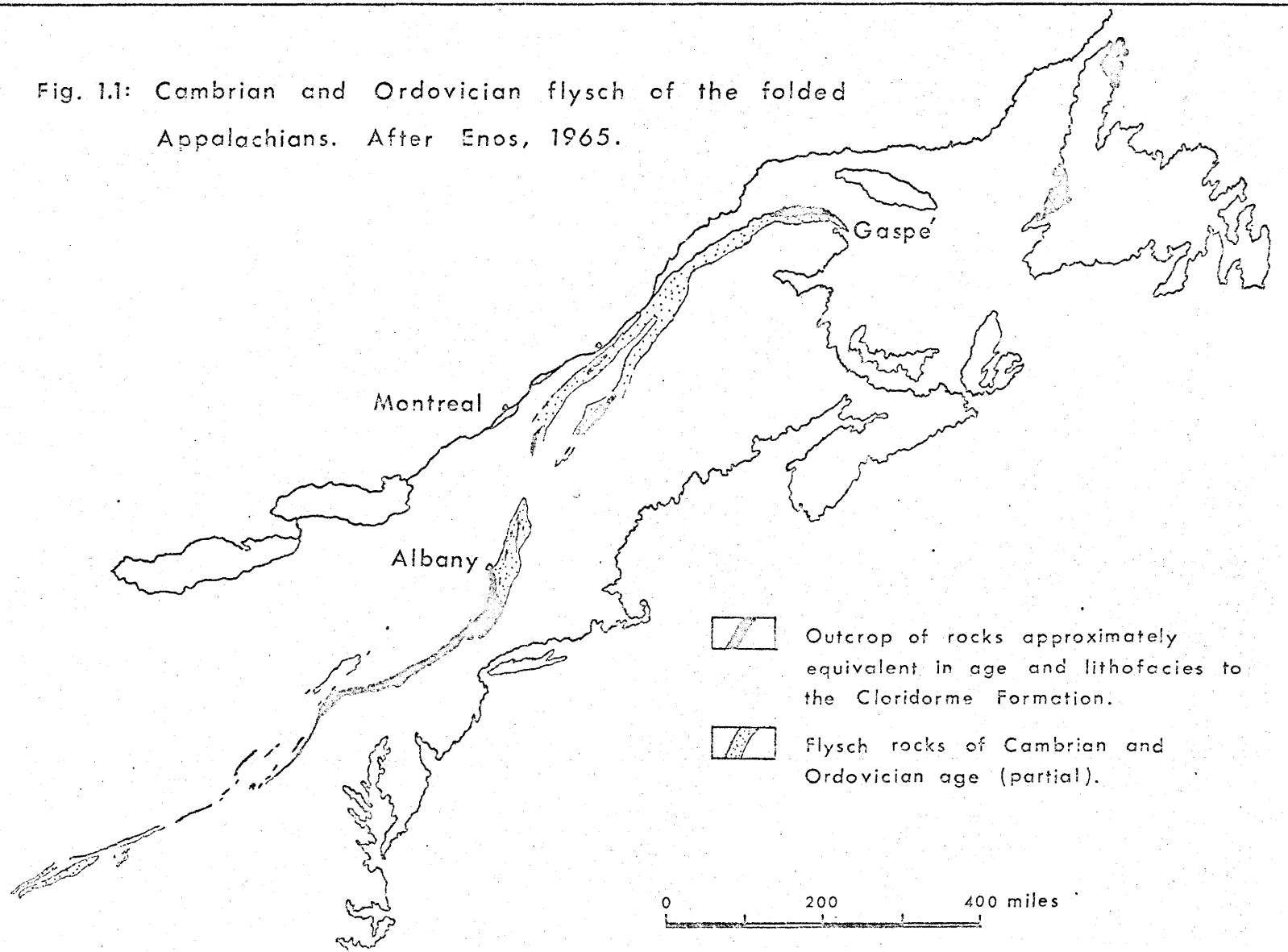





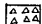









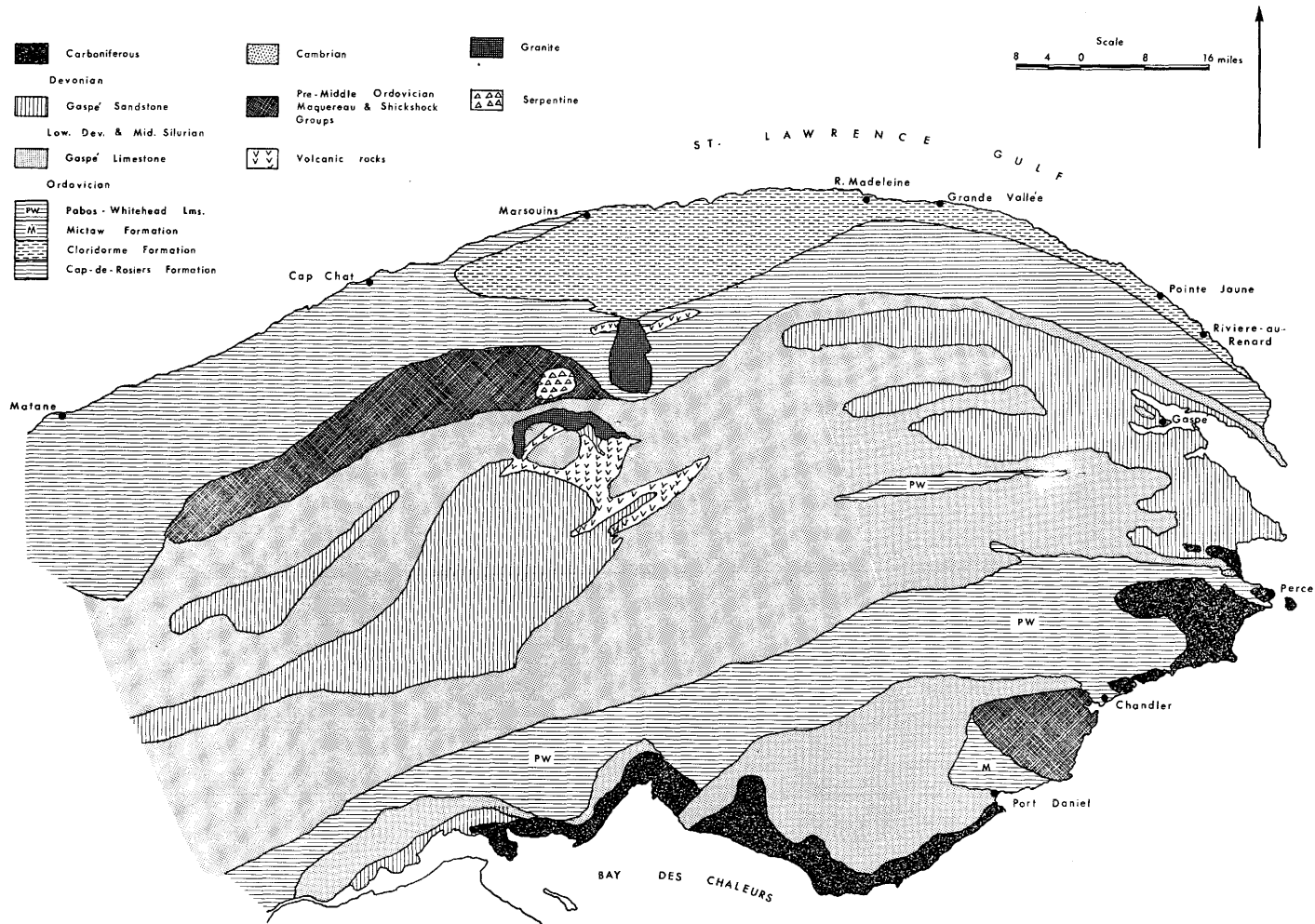


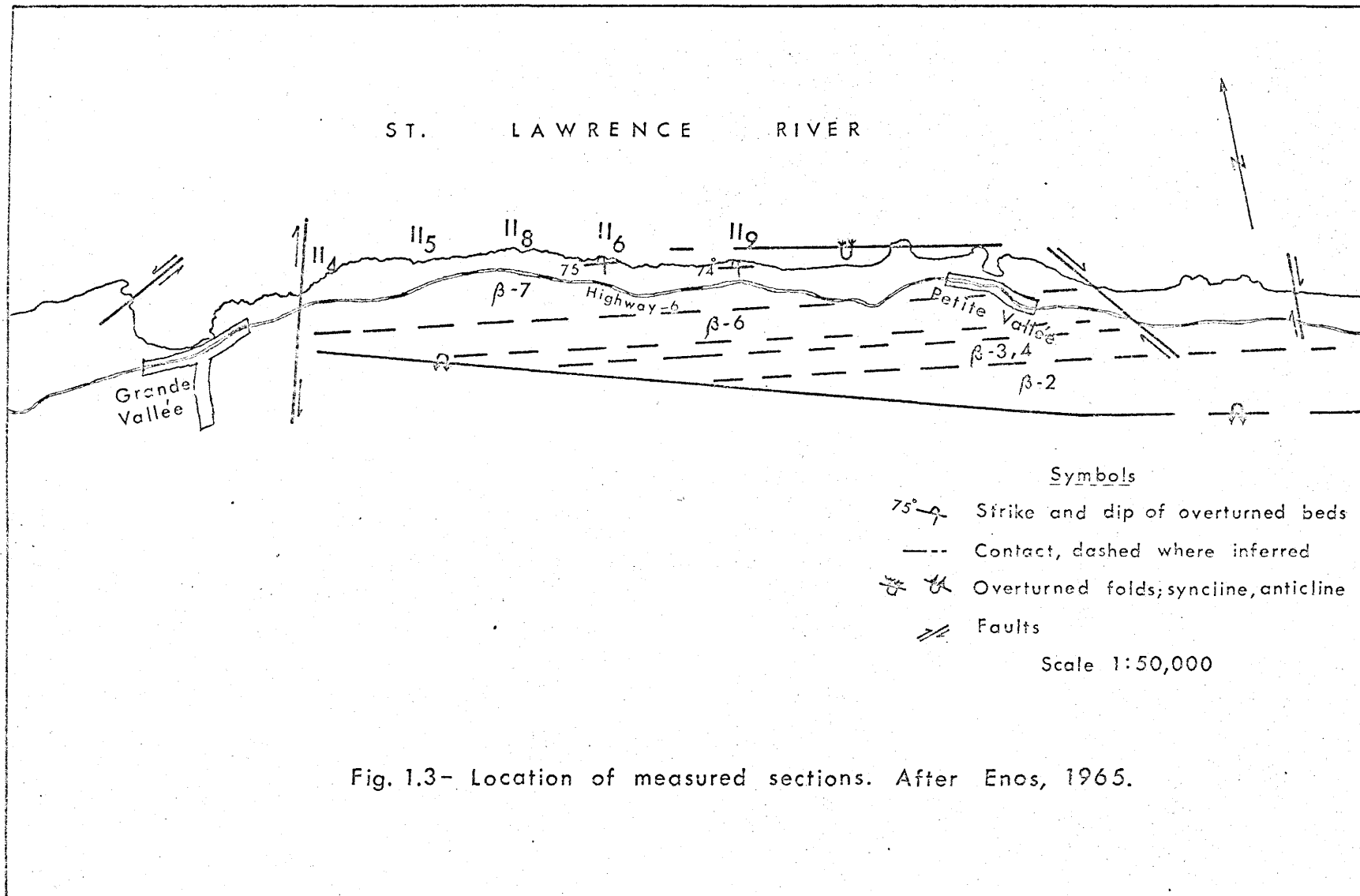
Fig. 1.2

Geology of Gaspé Peninsula
After McGerrigle, 1950

- | | | |
|---|---|--|
|  Carboniferous |  Cambrian |  Granite |
|  Devonian |  Pre-Middle Ordovician
Maquereau & Shickshock
Groups |  Serpentine |
|  Gaspé Sandstone |  Volcanic rocks | |
|  Low. Dev. & Mid. Silurian | | |
|  Gaspé Limestone | | |
|  Ordovician | | |
|  Pabos-Whitehead Lms. | | |
|  Miclaw Formation | | |
|  Cloridorme Formation | | |
|  Cap-de-Rosiers Formation | | |

Scale
8 4 0 8 16 miles





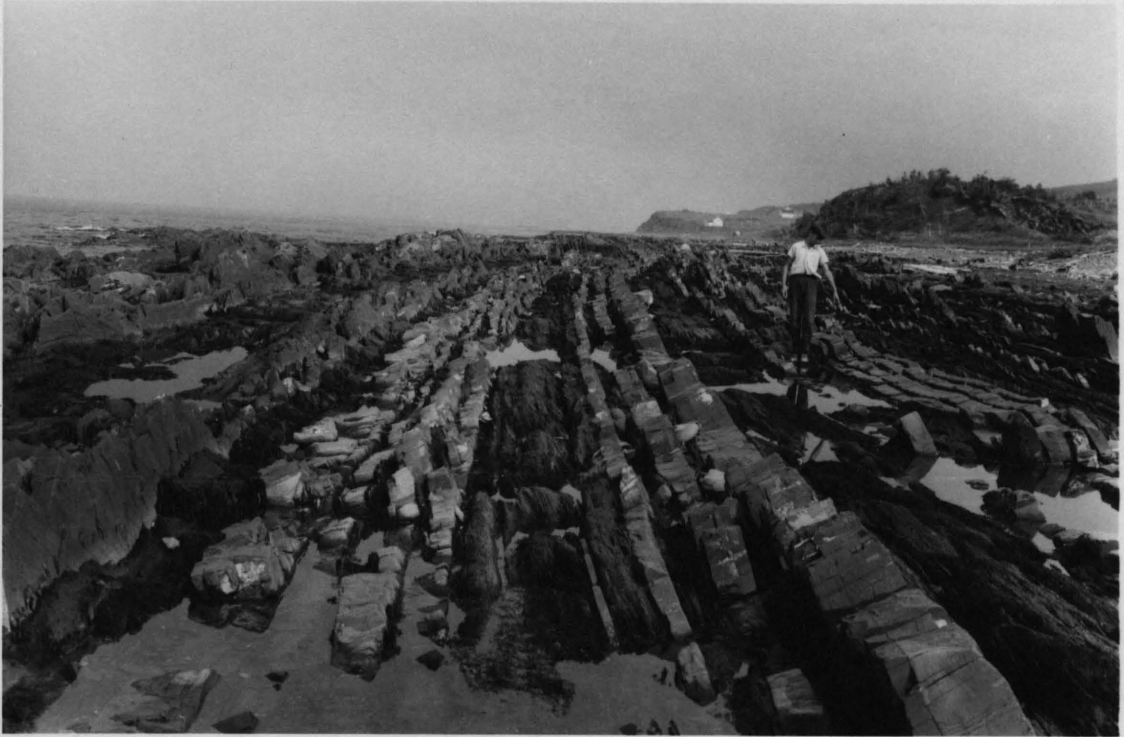


Fig. 1.5 - A view of the wave-cut platform looking east at section II4. The strike of the beds is east-west and the beds are overturned to the south. The observer stands between beds G-66 and G-65 (fig. 1.4). The top side and left side of the figure refer to east and north respectively.

southernmost belt consists of Pre-Cambrian, Ordovician and Silurian rocks and form the northern limb of another syncline which underlies Chaleur Bay and has been traced into New Brunswick.

The only exposed contact of the Cloridorme Formation is with the Cap-des-Rosiers Formation (Deepkill of McGerrigle, 1953; Lower Ordovician and Upper Cambrian in age). McGerrigle (1950, 1953) interpreted the contact between the formations as a normal one. Later studies by Enos (1965) show that the contact is probably faulted.

The Cloridorme Formation was deposited in the last phase of the filling up of 'Magog' eugeosyncline and later folded tightly along with older rocks in the Taconic orogeny.

Previous Work

McGerrigle (1959) briefly described the Middle Ordovician rocks exposed along the north coast of Gaspé. Enos (1965) named these rocks the Cloridorme Formation and made a detailed study of the stratigraphy, structure, paleocurrents and lateral variation in the greywacke sequence. The general description of the formation given here is based on Enos' work (1965).

Structure and Stratigraphy

Enos (1965) divided the whole area into three structural blocks: eastern, central and western. The stratigraphic sequence within each block was determined, but correlations between them were not possible probably due to missing stratigraphic intervals caused by structural dislocations separating the blocks. The eastern block is thrust over the central block along a fault that extends west from Pointe-Jaune. A transverse fault with unknown sense of displacement separates the central block from the western block at Grand-Ruisseau, 4 miles west of Grande Vallée.

The whole area is folded into asymmetric folds with fairly large amplitude. The folds are overturned to the north and fold axes are generally horizontal. However, a plunge of 2° to 8° is not unknown. Higher plunges of fold axes up to 45° east or west are recorded near the thrust faults.

Enos (1965) informally subdivided the Cloridorme Formation into 14 members grouped into 3 sequences, called α , β and γ . Each sequence is confined to one structural block so that the relationship between sequences is not known. The three sequences α , β and γ have 3, 7 and 4 members and are confined to the eastern, central and western

structural blocks respectively.

Age

The age of the Cloridorme Formation has long been recognized as Middle Ordovician and closely related to the Normanskill Formation of New York (Jones, 1934, McGerrigle, 1954, 1959). The New York Normanskill Formation was assigned by Berry (1962) to the Wilderness and early Trenton stages of Cooper's classification. Extensive graptolite collection made by Enos and identified by Berry show that the graptolites surprisingly belong to a very small number of species and the rocks are assigned to 'Orthograptus truncatus intermedius Zone' of late Wilderness and Trenton age (Enos, 1965). Only the uppermost Normanskill (upper part of Austin Glen member, Berry, 1962) is of this age, so that the Cloridorme Formation may correlate with the youngest Normanskill or overlying Canajoharie Formation.

Metamorphism

The rocks are considered to be metamorphosed to the lower green-schist facies on the basis of extensive development of chlorite and sericite on the cleavage surfaces and as alteration products of feldspars (Enos, 1965). Examination of greywackes in thin sections, however, shows no evidence

of rotation of or breaking of detrital minerals thus discounting the possibility of dimensional grain orientation being affected by metamorphism. Most greywacke beds are massive and do not show flow or fracture cleavage.

Lithologies

The Cloridorme Formation consists of coarse greywackes (15%), calcareous wackes (3%), calcisiltites (20%), dolostones, limestones, dolomitic argillite and volcanic ash (nearly 20%) interbedded with argillite (60%). The characteristics of different lithologies are fairly constant, but their abundances are quite variable in the formation. Greywackes, calcisiltites, and calcareous wackes exhibit typical turbidite structures such as flutes, longitudinal ridges, grooves, prod marks, bounce marks, current ripple lamination, convolute lamination and graded bedding.

Enos (1965) distinguished three types of greywackes in the Cloridorme Formation. Type one greywackes are coarse-grained and have an average thickness of 27 cm. They are massive and show good grading. Flutes and grooves are common sole marks. Type one greywackes grade into argillite in the downcurrent direction. Type two greywackes form the intermediate rock type between argillite and type one greywackes. Type two greywackes are finer-grained and contain

a higher percentage of matrix than type one greywackes. Petrographically, their average compositions (Enos, 1965, table 1) are:

Greywacke		Type 1	Type 2
Matrix	Argillaceous	17 %	48.4%
	Calcitic (cement in part)	16.7%	7.1%
Composition of detrital grains	Quartz	60 %	60 %
	Felspars	10 %	14 %
	Rock fragments	25 %	20.6%
	Mica	2 %	4.9%

Type three greywackes, though least common of all the three types of greywackes, may locally constitute a major clastic rock in a stratigraphic section. In most outcrops they have a layer a few centimeters thick from sandy to pebbly in grain size at the base of the bed and the average grain size of the rest of the bed is fine sand. The bed contains abundant calcisiltite fragments distributed throughout. They grade up into dolomitic argillite. Their average thickness is 85 cm.

Calcisiltites are medium bluish grey in colour and weather with a yellowish-brown coating. They are usually cross-laminated and rarely exhibit plane lamination. Flutes are common sole marks. Thickness varies from 1 cm to 100 cm. Calcareous wacke are similar in composition to calcisiltities, but are much coarser grained than calcisiltites. Thickness of calcareous wackes varies from 10 cm to 30 cm.

The greywacke beds under study are from unit G of the β -7 member of the formation. The abundance of various lithologies in unit G (figs. 1.4, 1.5) is fairly typical of the β -7 member. The β -7 member is characterized by a higher percentage of greywackes (38.3%) and a lower percentage of calcisilites (16.3%) than the average of the whole formation.

CHAPTER II

FIELD DESCRIPTION

This chapter deals with the detailed lateral changes observed in the field in the sole mark types and directions, internal structures and thickness of eight greywacke beds from unit G of β -7 member of the Cloridorme Formation. Unit G (along with unit H) was the subject of lateral changes in thickness by Enos (1965).

Field Methods

Because a very detailed study of the area under investigation was planned, an arbitrary bench mark with zero value was set up at the westernmost section II₄. Distances were measured in yards along the strike from this point and sub-stations were established at intervals of 100 yards by marking white paint marks on the prominent rock exposures. These sub-stations are marked in figure 2.1. Later these sub-stations were used in locating the observer's position along the outcrop. All locations along the outcrop are referred as distances in yards along the strike from the bench mark. The sections II₄, II₅, II₈, II₆ and II₉ (fig. 1.3) refer to 0, 570, 1180, 1975 and 3200 yards points

respectively. Note that the measured distance points increase to the east, i.e., they increase in the upstream direction.

As the strike of the beds varies only slightly ($276^{\circ} \pm 2^{\circ}$) in the area of study and the plunge of the fold is nearly zero, a simple dip-compensator described by Enos (1965) was used to record sole directions corrected for dip. The compensator consists of a plexi-glass plate ($8.2 \times 5.6 \times 0.5$ inches) mounted with a level and a protractor provided with a revolving arm. To measure a sole direction, the compensator is placed on the base of the bed and is moved till the level shows that the 0° - 180° line of the protractor is horizontal. Then the arm of the protractor is aligned with the sole direction and the angle of the sole direction with the strike is noted. This value is added to or subtracted from the strike value to obtain the corrected sole direction as described by Briggs and Cline (1967, p. 990).

Oriented samples were collected for all the eight beds at each of the five sections II₄, II₅, II₈, II₆ and II₉ for laboratory study of grain size and grain orientation. The strike and dip of the bed were marked accurately on the top or bottom surface of the specimen and an arrow along the side indicated the top side of the specimen. The specimens are numbered as II₆-50, II₉-68, etc., first giving the

field section followed by bed number.

Some of the beds are overlain by an argillite, 1-2 cm thick, which is topped by less than 1 cm thick cross-laminated calcisiltite. The argillite division may contain scattered sand grains, more commonly in the lower part. In measuring thickness of a bed, the top was taken at a point where the sand grains disappear because the upper calcisiltite division is not always present.

The greywacke beds under study are very rich in graptolites which commonly show a strong preferred orientation. In the field an attempt was made to split the bed parallel to the bedding plane at various levels and to note the graptolite orientation. The graptolite orientations for different beds are plotted in figure 2.2. The accuracy of graptolite orientation measurements is probably about $\pm 10^\circ$.

In order to study lateral changes in sole mark direction, sole mark direction measurements were taken, if possible, at intervals of 20 yards along the strike or even at shorter intervals, if the observed change in sole direction was marked. Sole directions selected to show maximum variation are plotted in figure 2.1. Cumulative frequency histograms with 10° class intervals are plotted in figure 2.3 for each of the beds for all the directional readings taken in each of the five tidal platforms separated

from each other by extension of the estuary inland in the form of 'anses' (coves) and the data is summarized in table 2.1.

Field Description

The beds studied are G-68, G-67, G-66, G-65A, G-65, G-58, G-50 and G-49 (fig. 1.4). They are less than 25 cm thick. For the most part, they are massive. All the beds show a fair degree of variation in thickness over the whole distance of study (fig. 2.1). They are type 1 greywackes (Enos, 1965), except that they may grade to type 2 greywacke (Enos, 1965) towards the top and that beds G-68, G-67, G-66 and G-65A grade to type 2 greywackes towards west.

In most localities, the beds can be divided into two parts. The two parts are separated by a bedding joint. Instead of a regular decrease in grain size from the bottom to the top of the bed, there is a sharp break in grain size at the joint. At the joint, a lineation (called intra-bed lineation here) commonly can be observed. An attempt was made to trace this line of discontinuity and it is shown by a dotted line in figure 2.1. This discontinuity may in some way be connected with the sedimentation history of the beds.

Intra-bed lineation has been described by Enos (1965)

Table 2.1

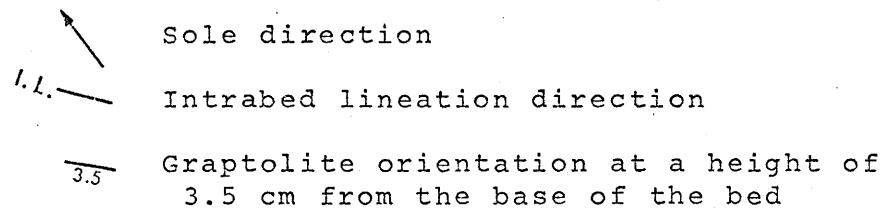
Summary of Field Directional Data

Bed	Block 1 0-230 yds.			Block 2 345-600 yds.			Block 3 800-1180 yds.			Block 4 1740-2225 yds.			Block 5 2440-3280 yds.			Cumulative 0-3280 yds.		
	n	Vector mean	Vector Magni- tude Per Cent	n	Vector mean	Vector Magni- tude Per Cent	n	Vector mean	Vector Magni- tude Per Cent	n	Vector mean	Vector Magni- tude Per Cent	n	Vector mean	Vector Magni- tude Per Cent	n	Vector mean	Vector Magni- tude Per Cent
G-68	20	286.8	95.80	28	285.5	94.07	17	289.2	99.79	15	285.9	99.48	17	284.8	99.27	98	286.0	97.19
	14	280.1	96.69	21	278.7	96.43	15	287.1	99.77	15	285.9	99.48	17	284.8	99.27	83	283.1	98.09
G-67	21	283.3	97.49	31	289.5	97.40	19	290.2	98.29							71	288.1	97.60
	14	279.6	99.20	17	281.5	99.23	15	286.6	99.88							47	282.7	99.32
G-66	19	281.7	95.93	29	286.2	99.15	23	285.9	93.92	15	284.8	99.11	11	282.9	99.53	98	284.7	97.30
	12	272.0	97.49	19	286.1	98.96	19	279.5	97.03	15	284.8	99.11	11	282.9	99.53	77	281.6	98.04
G-65A			Bed is absent				28	304.0	94.46	15	302.8	99.41	24	293.2	99.05	68	300.0	96.86
							20	300.7	95.78	14	302.8	99.36	22	294.1	99.12	57	298.4	97.79
G-65	23	222.0	97.25	26	209.6	93.95	24	267.4	92.32	31	298.9	97.88				105	252.2	76.65
	17	222.7	97.07	18	209.9	93.84	19	279.5	97.03	28	296.8	98.55				83	254.14	78.73
G-58																		
	30	249.3	96.60	16	255.3	90.97	12	273.7	99.45	15	235.5	98.93	16	237.5	94.22	91	248.6	95.47
G-50	25	276.1	97.77	16	271.6	99.11	15	278.1	99.16	15	289.3	99.10	12	298.8	98.35	86	281.2	95.71
	21	274.2	97.95	14	270.7	99.11	15	278.1	99.16	15	289.3	99.10	12	298.8	98.35	80	279.6	95.13
G-49	38	294.4	97.00	29	314.6	84.46				32	302.0	83.41	28	296.7	94.94	129	311.0	89.61
	31	299.1	98.54	21	322.3	84.79				30	301.1	82.92	25	296.9	94.54	109	303.3	89.57

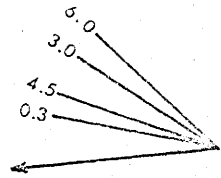
Note: (i) n is the number of measurements.

(ii) Orientation statistics in the upper column for each bed are for sole marks and intrabed lineation taken together and those in the lower column pertain to sole marks only.

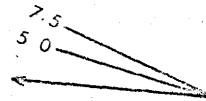
Fig. 2.2a-2.2g - Relation of graptolite orientations to sole mark directions in different beds.



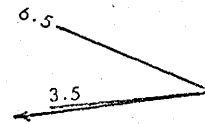
BED G-68



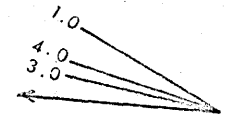
130 yds.



400 yds.



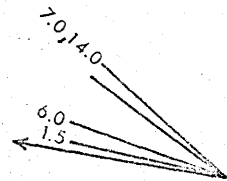
430 yds.



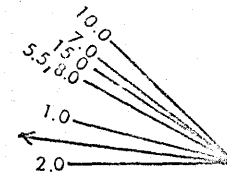
1140 yds.

Fig. 2.2a

BED G-67



120 yds.



425 yds.

Fig. 2.2b

BED G-66

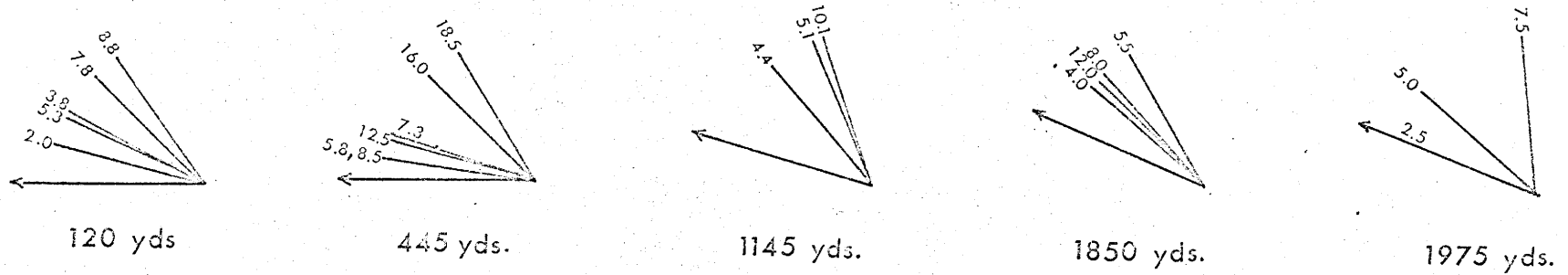


Fig. 2.2c

BED G-65A



Fig. 2.2d

BED G-65

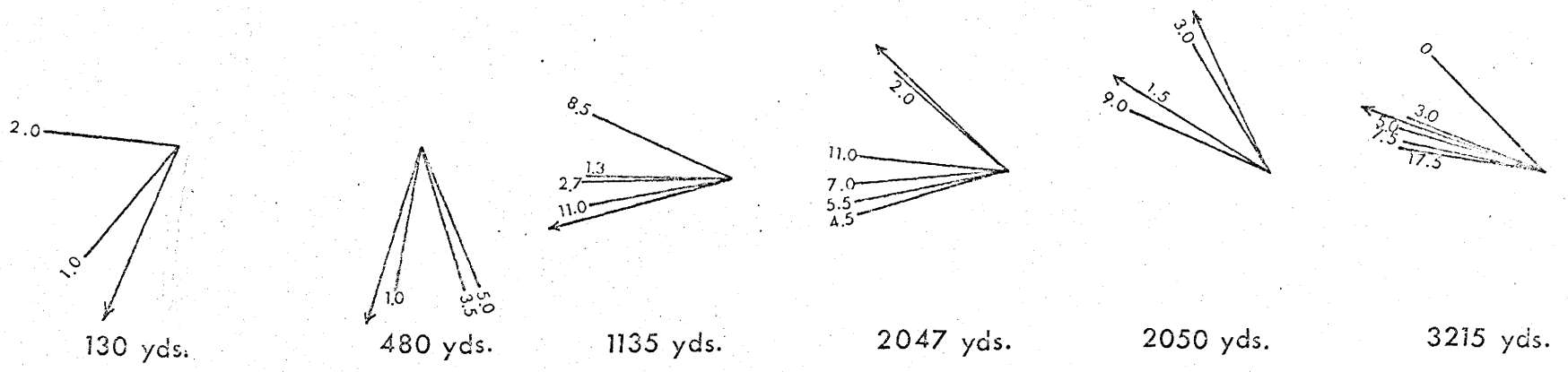


Fig. 2.2e

BED G-50

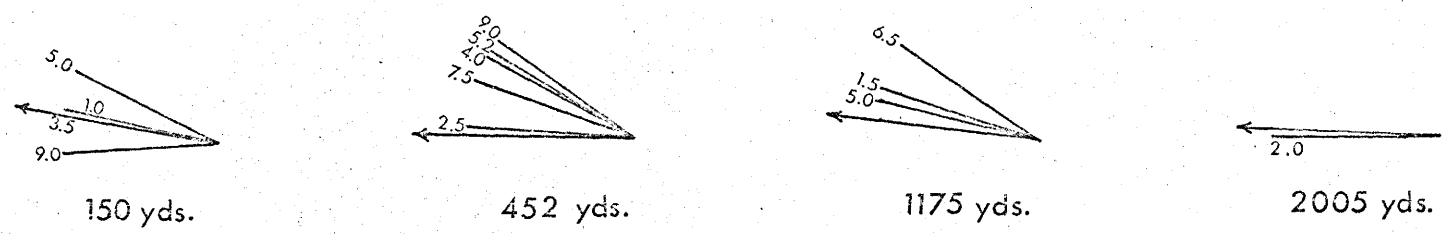
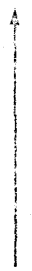


Fig. 2.2f



BED G-49

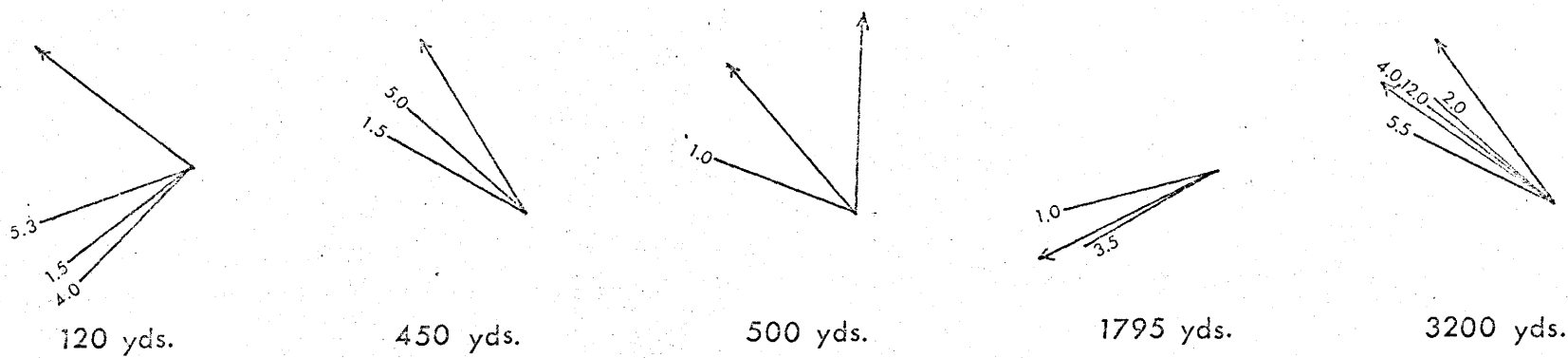


Fig. 2.2g

Fig. 2.3a-2.3h - Rose diagrams for sole mark directions for the eight beds.

— Vector mean

BED G-68

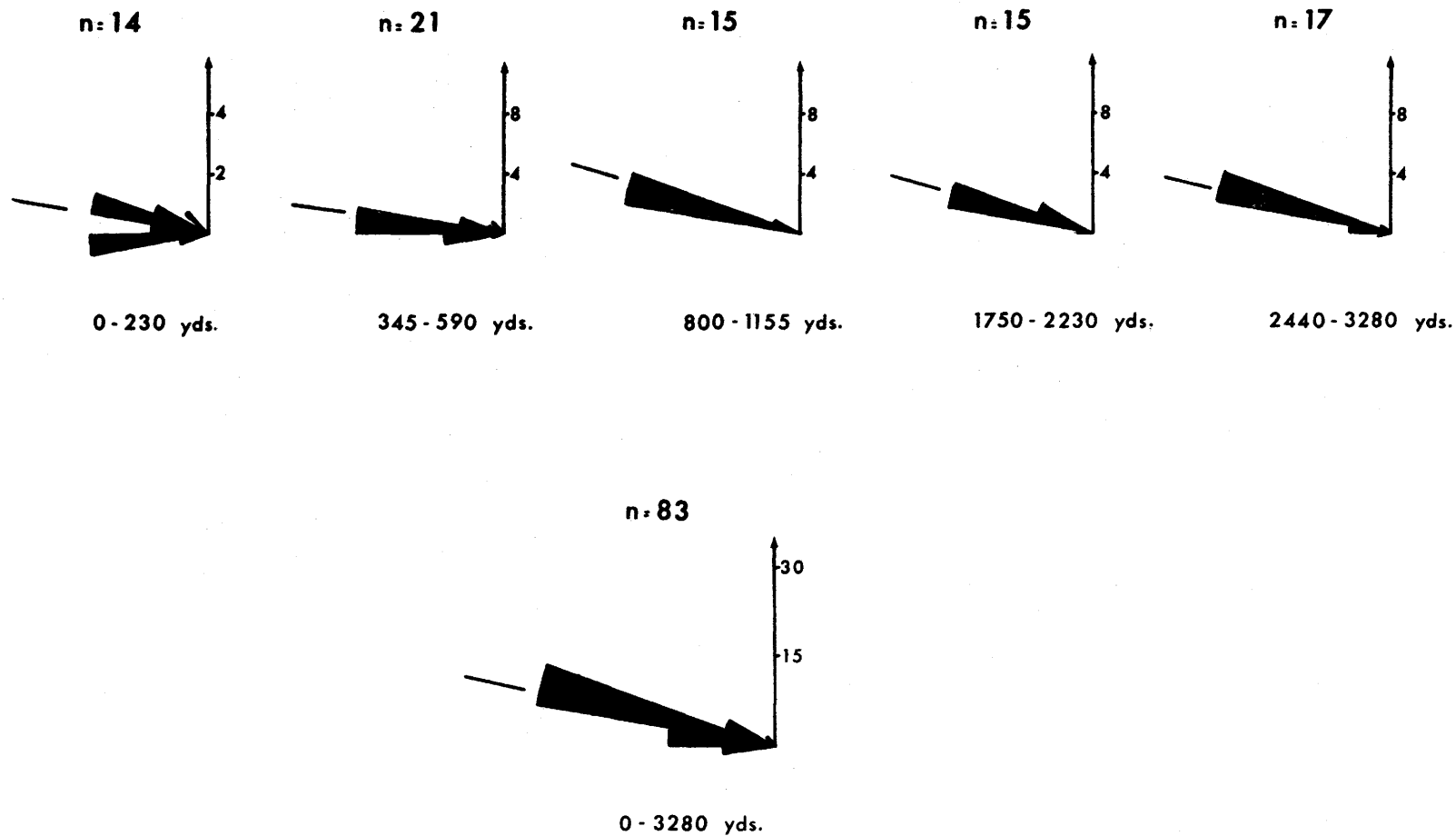


Fig. 2.3 a

BED G-67

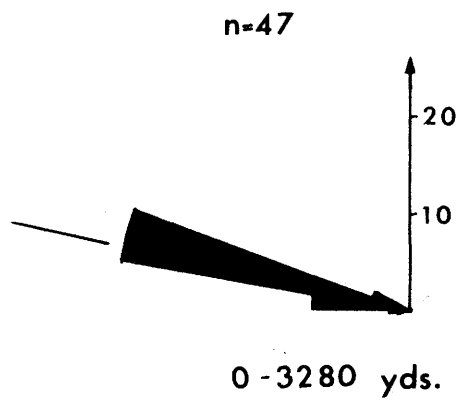
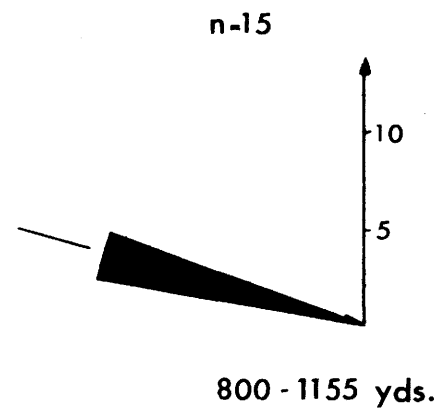
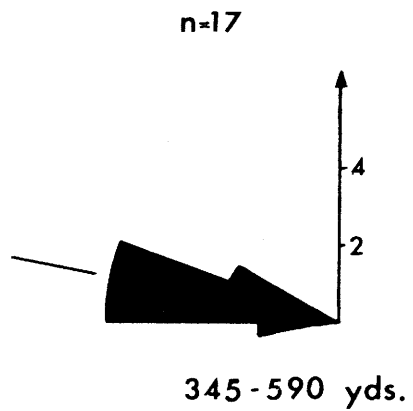
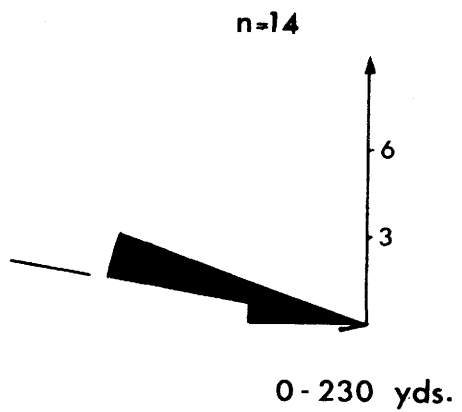


Fig. 2.3b

BED G-66

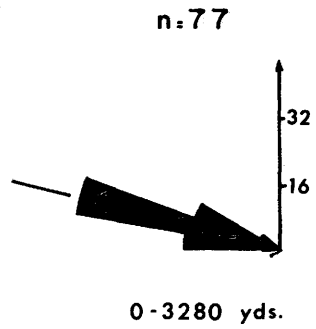
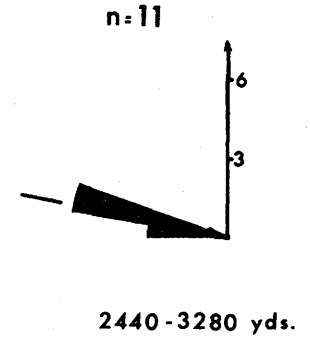
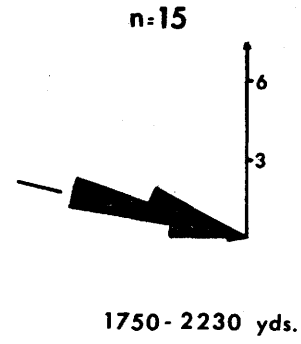
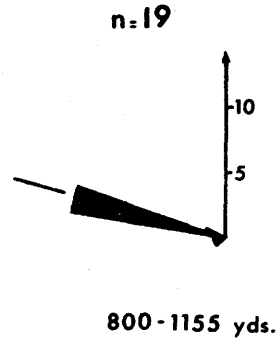
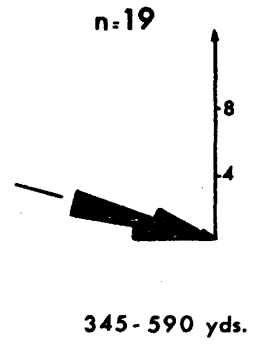
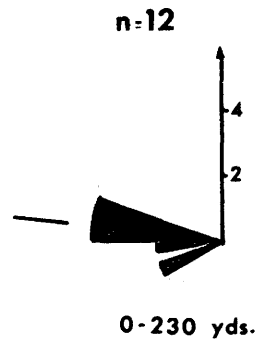


Fig. 2.3c

BED G-65A

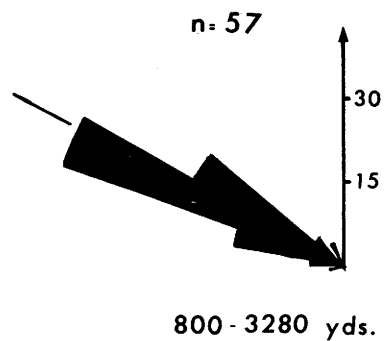
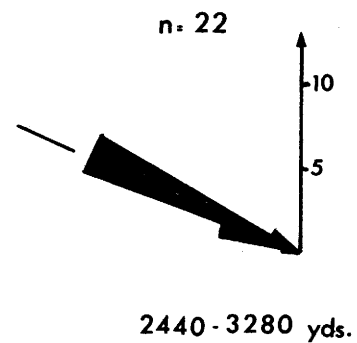
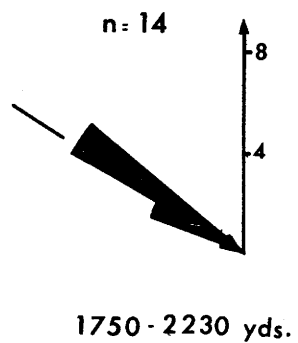
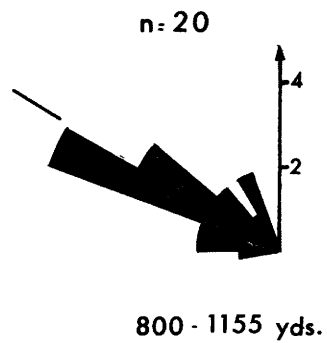


Fig. 2.3d

BED G-65

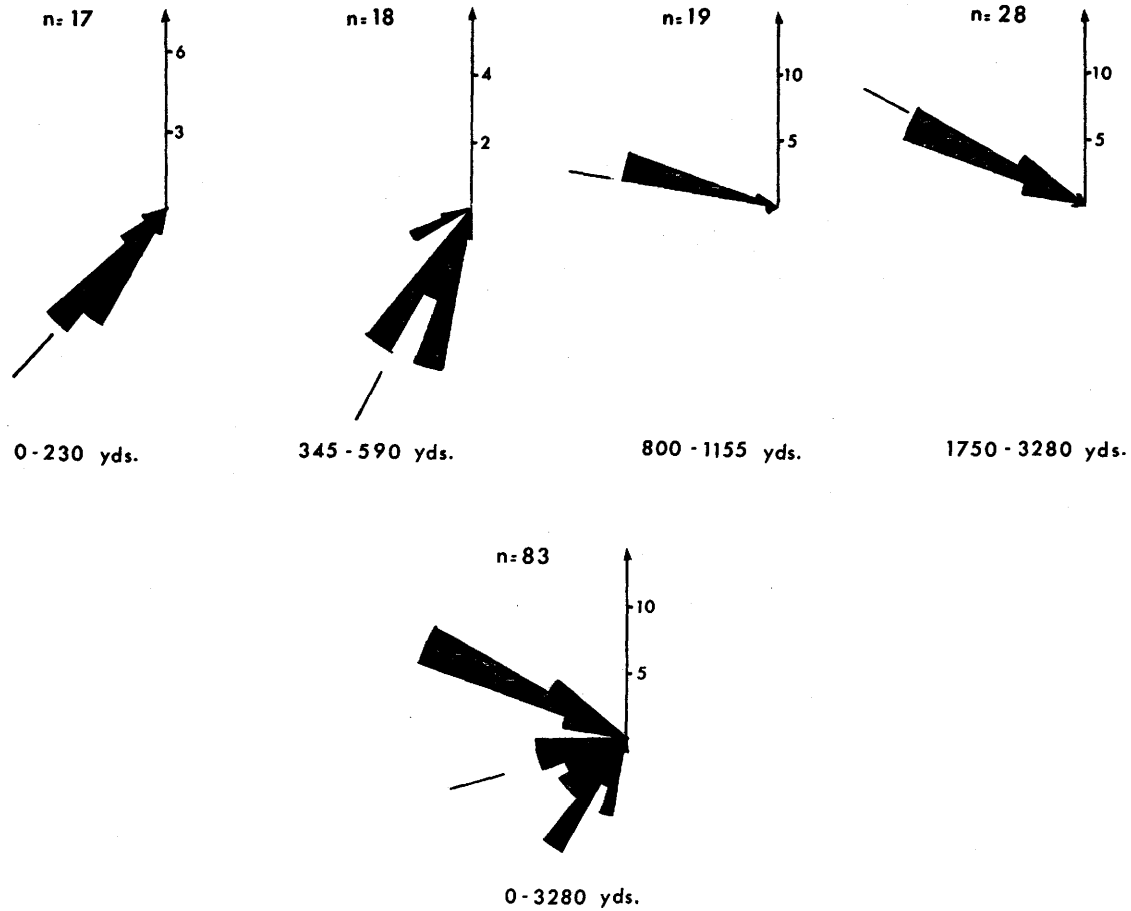


Fig. 2.3e

BED G-58

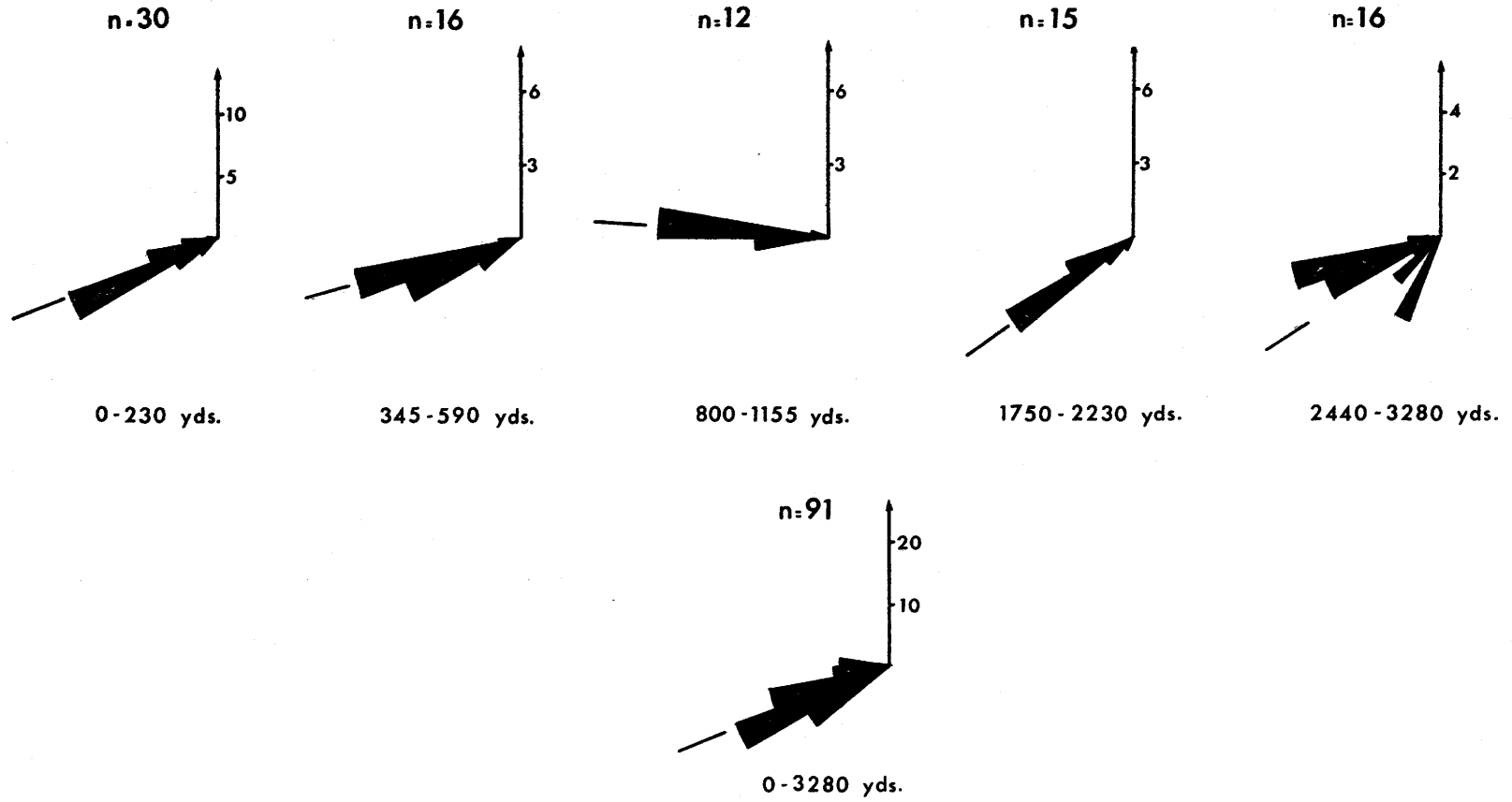


Fig. 2.3f

BED G-50

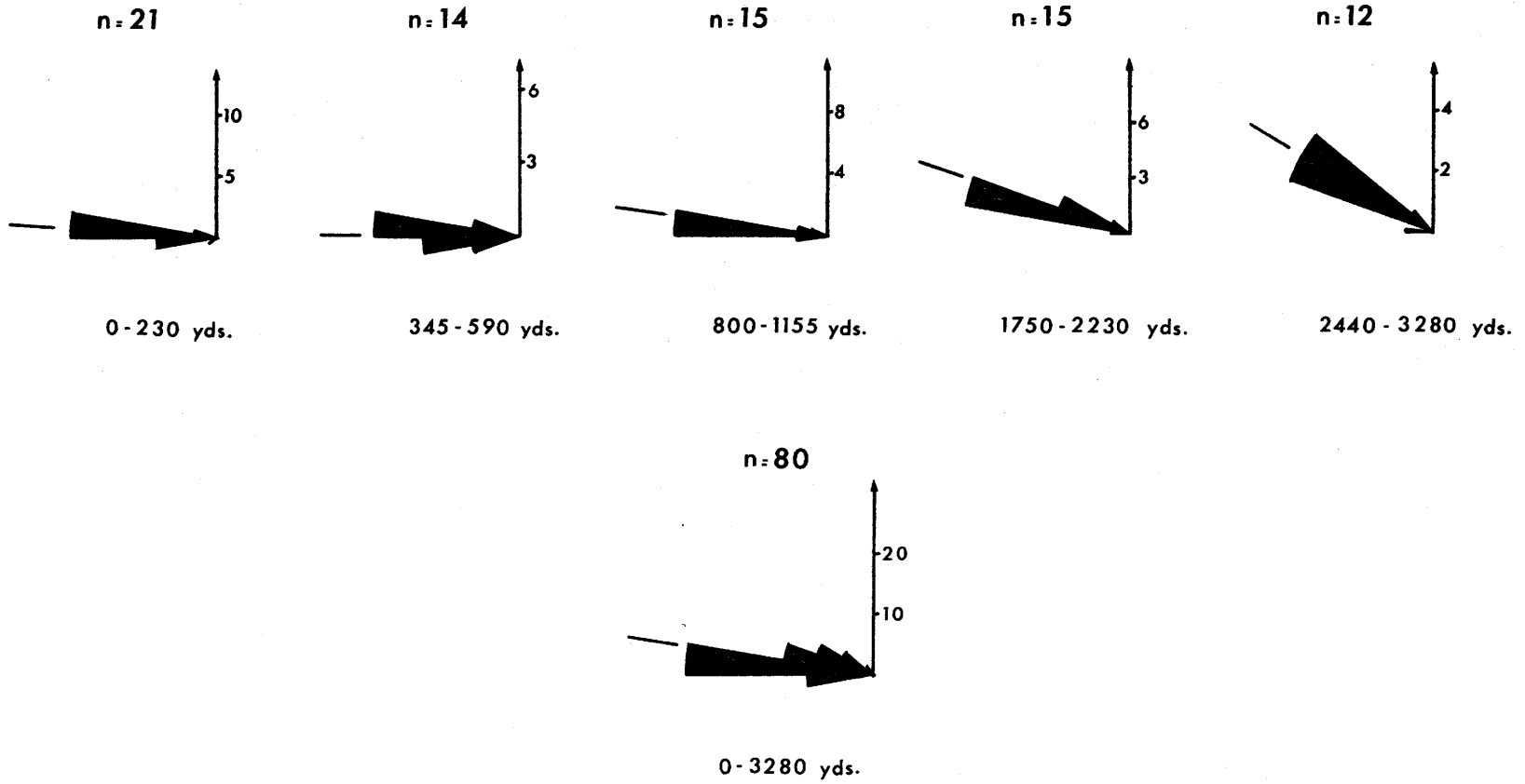


Fig. 2.3g

BED G-49

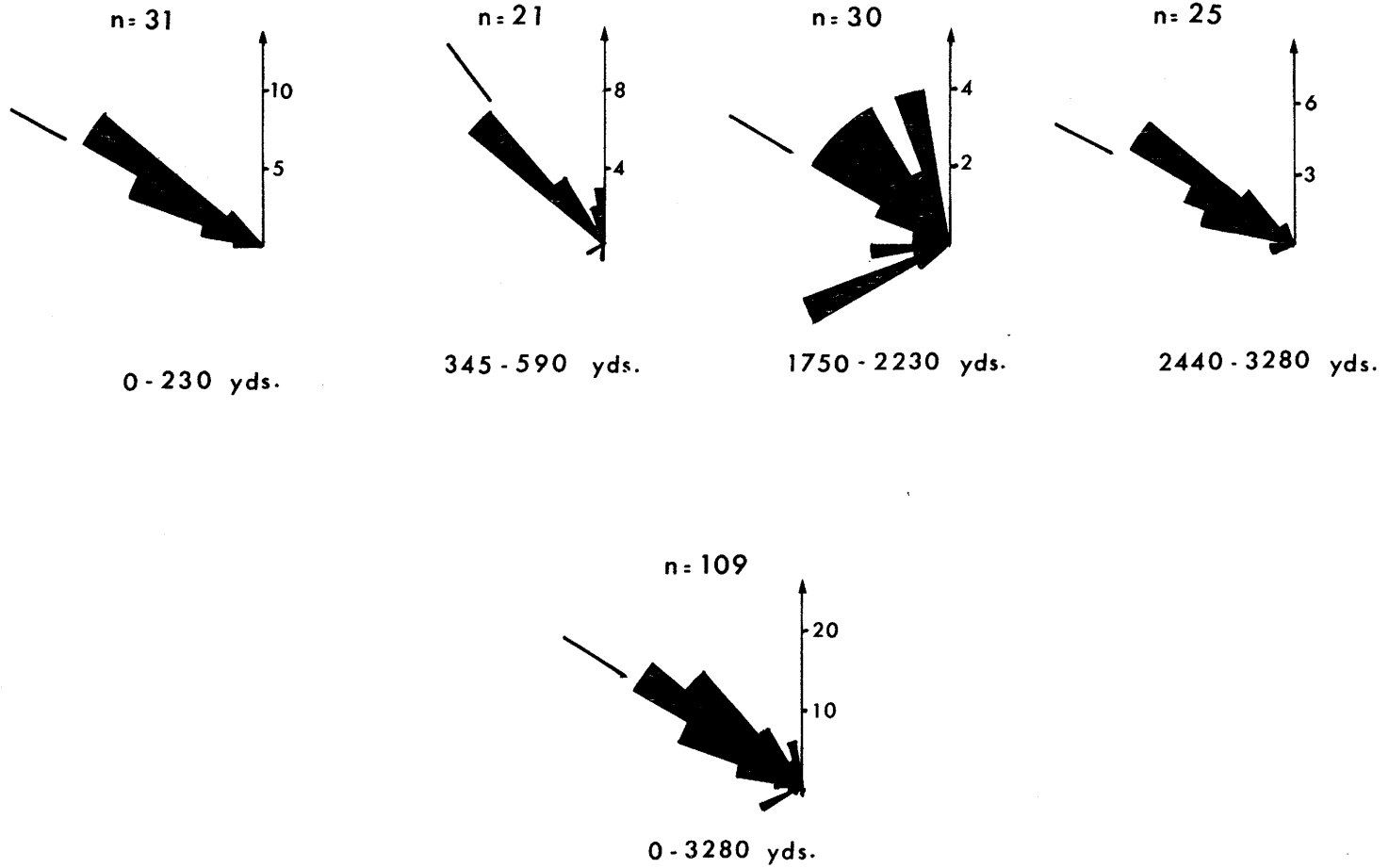


Fig. 2.3h

and Hubert and others (1966). The lineation consists of very fine striae at the joint. The direction of lineation may differ from that of the sole by as much as 40° . In many examples, graptolites are aligned along the intrabed lineation. In a few examples, at the downstream end of the lineation, tools such as argillite fragments are observed.

The base of beds shows moulds of tool marks such as grooves, prod marks and bounce marks and current marks e.g., longitudinal ridges (L-ridges) and flutes. Excellent descriptions of these sole structures are available in literature (Dzulynski and Walton, 1965). The bottom of the bed may show mould of a knobby pattern with convex side of knobs towards the bottom (figs. 2.9, 2.17, 2.31, 2.35). Similar knobby structures have been variously called as cushion-like marks (Dzulynski, 1965, p.203), polygonal ridges (Dzulynski, 1966, p.292; Dzulynski and Simpson, 1966, a, b) and scaly structures (Dzulynski and Walton, 1965, p.207). Different sole structures have been modified by load casting in bed G-58.

Longitudinal ridges are intimately associated with flute marks. L-ridges may pass laterally into flute marks. At places, bars with convex side upstream cross longitudinal ridges giving the impression of flutes overlapping longitudinal ridges. The cusped crossing bars may be from indistinct to very well developed. Thus it seems that all

gradations exist between L-ridges and flutes and the following terms are used to describe the gradational structures between the two end members: (i) longitudinal ridges (figs. 2.10, 2.11), (ii) longitudinal ridges with cusped crossing bars (figs. 2.21, 2.37, 2.38), (iii) longitudinal ridges with overlapping flutes (base of bed G-66 in fig. 2.12) and (iv) flutes (fig. 2.36). In a few cases, a similar relationship between longitudinal ridges and scaly structures was observed.

The eight beds are described below in the stratigraphic order from the oldest to the youngest bed. The beds are illustrated in figures 2.4 - 2.44. Right, left, top and bottom of the figures showing the side view of the beds correspond to east, west, north and south respectively and tops of the beds are towards north. In figures showing the sole marks, the right and left side of the figure are east and west respectively.

Bed G-68

Bed G-68 persists throughout the area of study except between the 2300 and 2560 yard points, where it seems to have been eroded completely by the current depositing the overlying bed G-67 (fig. 2.1). Except for small patches where the whole thickness of the bed along with thin argillite at the top is preserved (fig. 2.5), an unknown thickness of the bed has been eroded away between the

- Fig. 2.4: Beds G-68, G-67 and G-66. Two parts of a bed separated by a bedding joint can be made out in beds G-68 and G-67. 3250 yard point.
- Fig. 2.5: Beds G-68, G-67 and G-66. Beds G-68 and G-67 are amalgamated to the east (right), but the whole thickness of the bed G-68 along with some overlying argillite is preserved for a distance of a few yards in the west. 3200 yard point.
- Fig. 2.6: Beds G-68, G-67 and G-66. Upper laminated part of bed G-67 shows slight convolution. Poorly developed plane laminations are present in the lower part of bed G-66. 2580 yard point.
- Fig. 2.7: Beds G-68, G-67 and G-66. The bed G-67 contains a large argillite fragment nearly 5 feet in length in the upper part. 500 yard point.



Fig. 2.4



Fig. 2.5

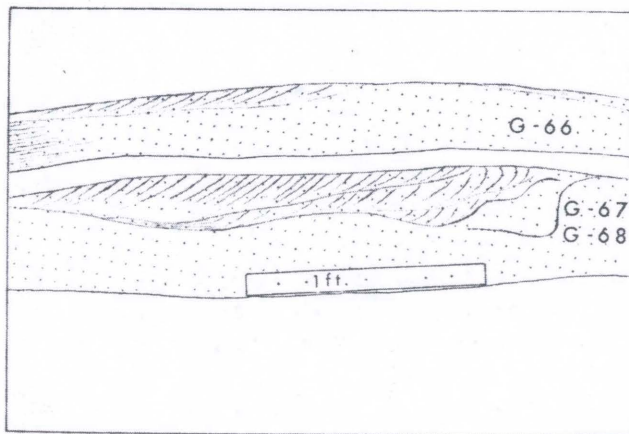


Fig. 2.6

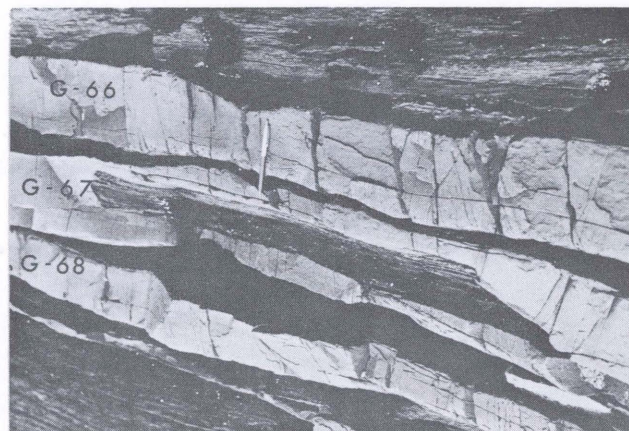


Fig. 2.7

1750 - 2300 and 2560 - 3240 yard points. A study of the whole thickness of the bed, where it has not been eroded, gives a picture of its general increase in thickness from east to west.

Changes in sole structures from east to west are very conspicuous. In the east, the bottom is smooth and grooved at places. West of the 2600 yard point, the bed has very fine, delicate L-ridges which, pass into well developed longitudinal ridges with occasional large grooves (figs. 2.8 - 2.10). At places near the 1100 yard point, some load structures (figs. 2.11, 2.12) are observed. Further west, the bed has poorly developed, shallow longitudinal ridges with occasional cusped 'crossing bars' (fig. 2.13). In the westernmost region, the base is smooth with occasional grooves.

The mean orientation direction of the sole marks seems to be fairly constant with a very small variance in the east. However, the variance about the mean increases west of the 600 yard point. The readings selected to show the maximum variation in the sole mark directions plotted in figure 2.1 confirms this observation. Cumulative frequency histograms in figure 2.3a and vector magnitude percent values (Curry, 1956) in table 2.1 for the five tidal platforms also demonstrate a higher variance in the sole mark directions in the west than in the east.

Fig. 2.8: Smooth base with curving grooves, bed G-68, 3250 yard point.

Fig. 2.9: Delicate longitudinal ridges and 'scaly' marks in the lower right side, bed G-68, 2662 yard point. Current to left.

Fig. 2.10: Longitudinal ridges at the base of bed G-68, 1905 yard point.

Fig. 2.11: Longitudinal ridges and load structures due to differential sinking of the bed into substratum at the base of the bed G-68, near 1100 yard point.

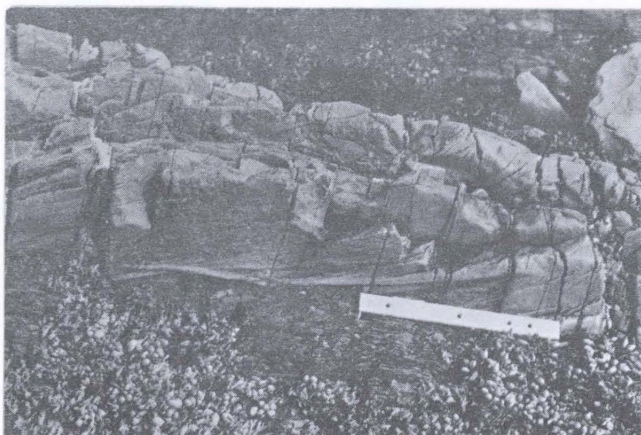


Fig. 2.8

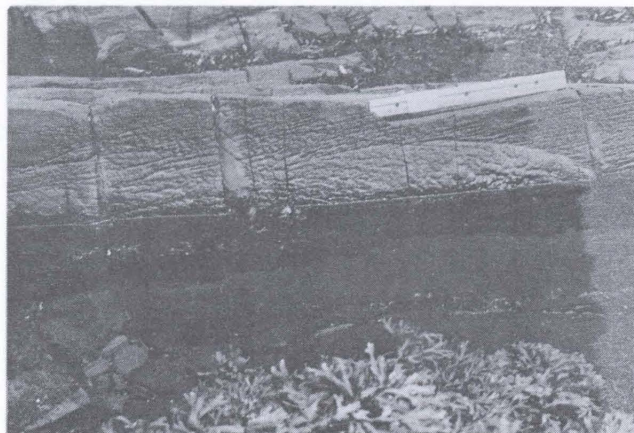


Fig. 2.9

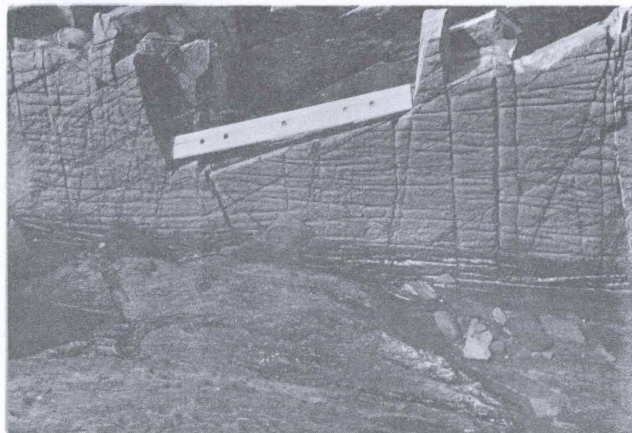


Fig. 2.10



Fig. 2.11

- Fig. 2.12: Longitudinal ridges are present at the base of beds G-68, G-67 and G-66. Also, small load cast structures are present at the base of the bed G-68 and flutes overlap longitudinal ridges at the base of the bed G-66, near 1100 yard point.
- Fig. 2.13: Poorly developed longitudinal ridges at the base of bed G-68. 400 yard point.
- Fig. 2.14: Small scale 'dish structure' in bed G-67. The lines on the side surface of the bed form an anastomosing pattern and are slightly curved up. Near 1140 yard point.
- Fig. 2.15: Small scale 'dish structure' in the bed G-67. The lines on the side surface of the bed form an anastomosing pattern. Near 1140 yard point.

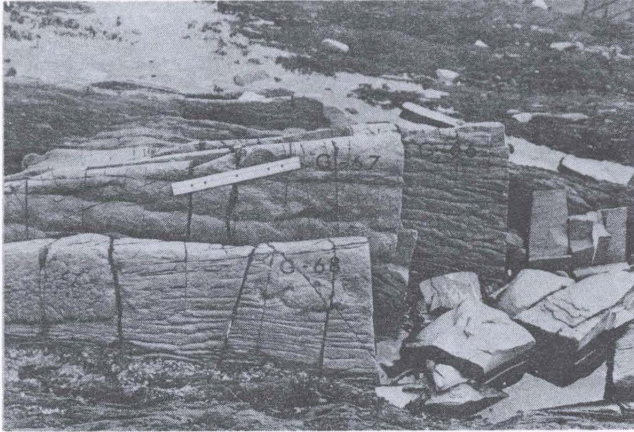


Fig. 2.12

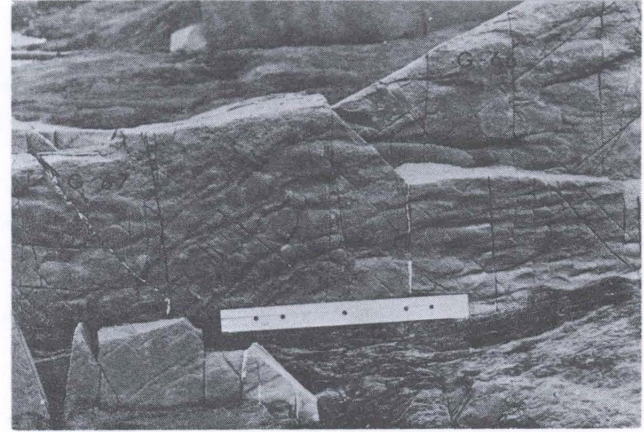


Fig. 2.13

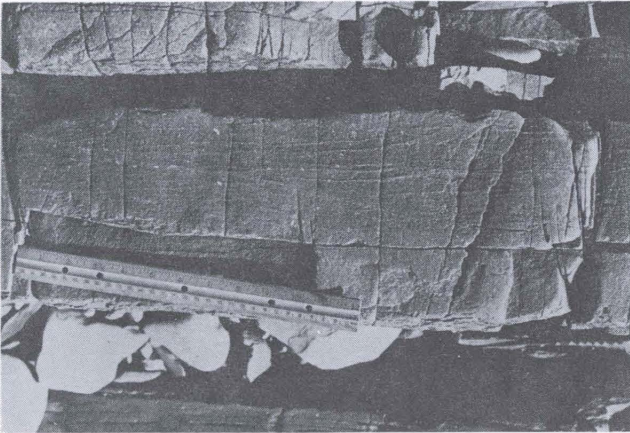


Fig. 2.14

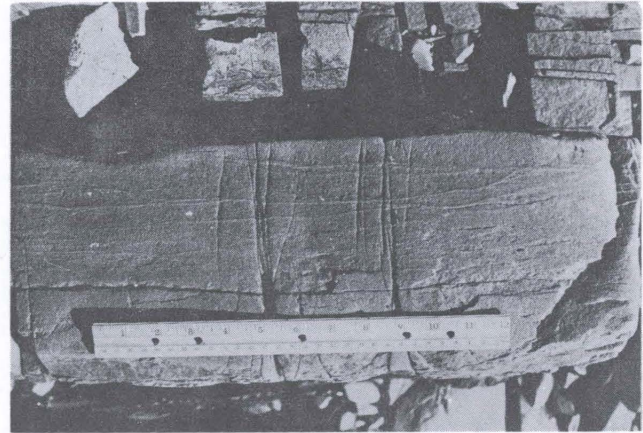


Fig. 2.15

Deviations of graptolite directions in the bed from that of the sole marks is small in most exposures, but may be as high as 70° near the top of the bed in the western region (fig. 2.2a). Deviation is always clockwise.

Bed G-67

Bed G-67 is the thickest bed studied and the maximum thickness observed is 23 cm. It shows an increase in thickness from east to west. Two parts of the bed can be recognized at all places except between the 1750 and 3260 yard points, where the bed consists of only one part. Also, the line marking the position of the joint in the last 100 yards in the westernmost region in figure 2.1 is arbitrary, as at places, the position of the joint is not clear and the bed is massive throughout with no recognizable grain size break.

In the eastern region, where the bed consists of only one part, the massive division at the bottom passes up into cross-laminated division, at many locations through a poorly developed plane laminated division. A large number of argillite fragments are plastered at the top of the bed. Between the 2300 and 2600 yard points, the thickness of the bed is quite variable. In areas with very small thickness, the bed starts with plane-laminated division and passes up into cross-laminated division. The

laminae in the plane-laminated division are slightly wavy and probably reflect slight irregularities of the bottom at the time of deposition of the bed. At places, the cross-laminated division of the bed exhibits slight convolution (fig. 2.6). The cross-laminated division is a single set of cross-laminae except at one place where two sets of cross-laminae could be detected.

The bed shows small scale 'dish structure' (figs. 2.14, 2.15) between the 1100 and 1180 yard points (cf. Stauffer, 1967, p.493). Especially in the upper part of the bed, weathering has brought out a number of lines consisting of slightly coarser grains than the surrounding material along the side of the bed. These lines at places form an anastomosing pattern. The lines are usually parallel to the bedding plane or slightly curved upwards. The structure disappears upwards as well as downwards almost abruptly. There are a number of differences between the observed structure and that described by Stauffer (1967). The thickness of the bed in the present case is only 23 cms, which is just a fraction of thickness of the thinnest bed showing 'dish structure' described by Stauffer. Also the bed is devoid of any rock fragments in this region in contrast with the beds with large scale 'dish structure'.

The bottom of the bed is not well exposed in the

- Fig. 2.16: Sharp nosed flute marks and some tool marks (e.g., bounce marks on the extreme left) on the smooth base of bed G-67. 2550 yard point. Current to left.
- Fig. 2.17: Small 'scaly' structures filled with coarse grains on the smooth bottom of bed G-67. 2495 yard point.
- Fig. 2.18: Mould of wrinkled mud bottom. Wrinkling of mud bottom was caused by dragging of a tool at the bottom. Bed G-67. 1850 yard point.
- Fig. 2.19: Longitudinal ridges with overlapping 'scaly' structures. Bed G-67. Near 1100 yard point.

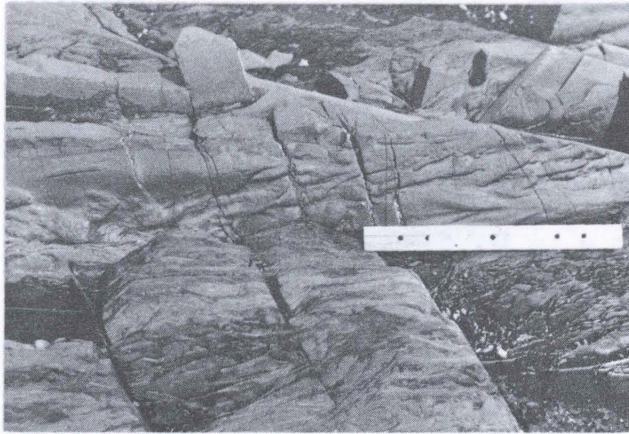


Fig. 2.16

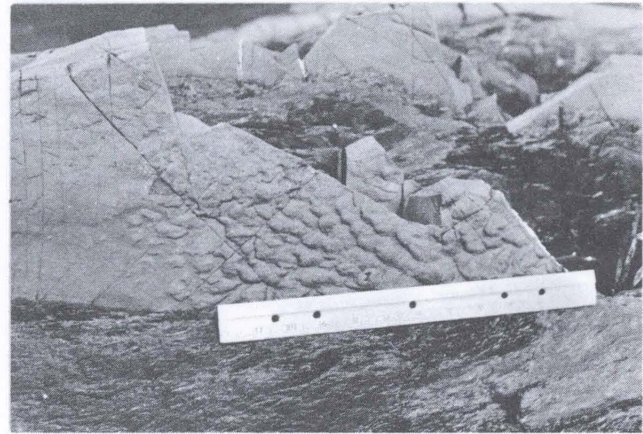


Fig. 2.17

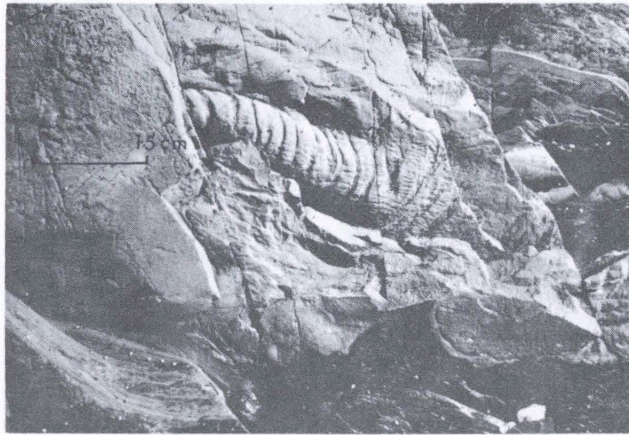


Fig. 2.18

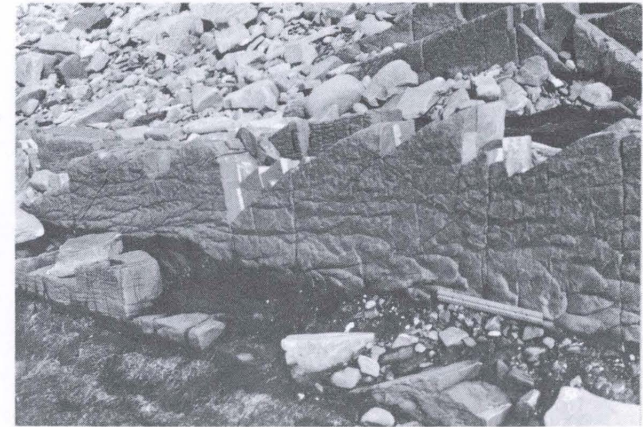


Fig. 2.19

- Fig. 2.20: Fan shaped flute marks filled with coarse grains, bed G-67, near 1100 yard point. Current to left.
- Fig. 2.21: Shallow longitudinal ridges with crossing cusped bars at the base of the bed G-67. 135 yard point.
- Fig. 2.22: Poorly developed longitudinal ridges at the base of bed G-67, 125 yard point.
- Fig. 2.23: Grooves at the base of beds G-67 and G-66. The bottom of bed G-66 is rough probably due to poorly developed longitudinal ridges (trending right to left) at an earlier stage before the formation of the groove mark. 80 yard point.

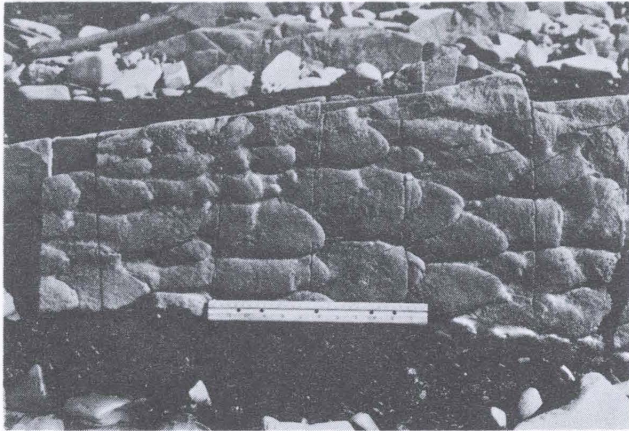


Fig. 2.20

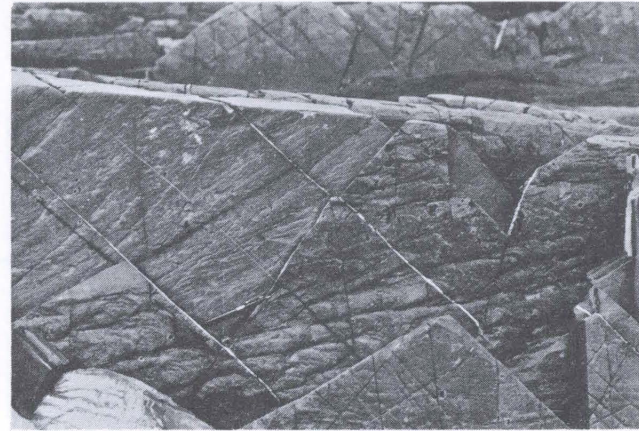


Fig. 2.21

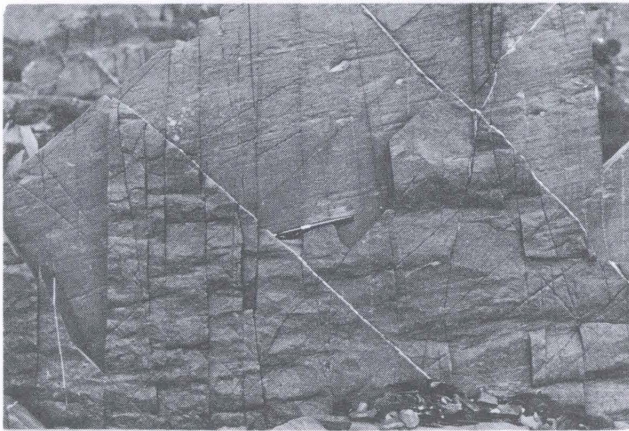


Fig. 2.22

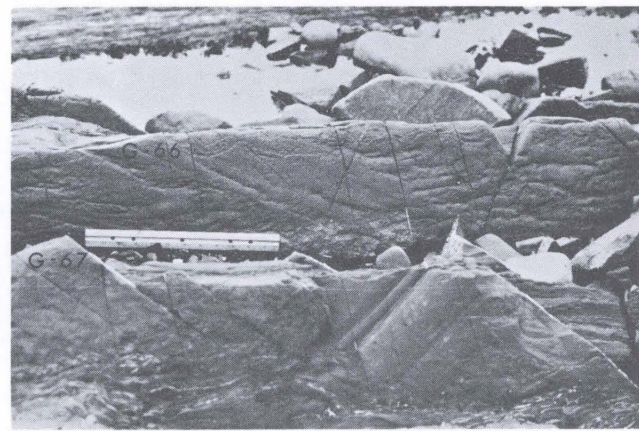


Fig. 2.23

eastern region due to amalgamation with the underlying bed G-68. Between the 2350 and 2560 yard points, the exposed bottom shows a smooth surface occasionally marked by isolated flute marks, tool marks and scaly structures which may be filled with coarse grains (figs. 2.17). At about the 1850 yard point, the bed shows a mould of the wrinkled mud bottom (fig. 2.18). The wrinkling may have been caused by dragging of a tool over a cohesive mud bottom. Further west, the bed has L-ridges with flutes lying side by side or overlapping the L-ridges (figs. 2.20 - 2.22), which pass into smooth base with grooves at places (fig. 2.23) through poorly developed L-ridges with occasional cusped crossing bars.

Except between the 2330 and 2640 yard points, the bed contains substantial number of argillite and calcisiltite fragments. The fragments are usually confined to the upper part of the bed and are as large as 5 feet in length (fig. 2.7). Probably these fragments have been dragged over the already deposited lower part of the bed and thus have served as tools for the formation of intrabed lineation present at the joint.

A very good exposure at the 425 yard point allows a comparison of directions of sole mark, graptolites and intrabed lineation at the joint and long axis of the argillite fragments (fig. 2.24). Graptolites with a mean

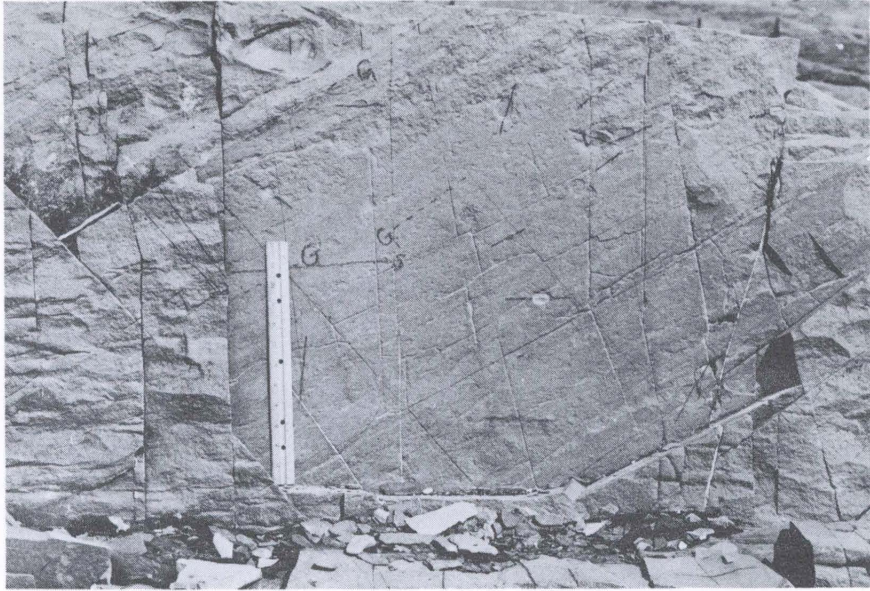


Fig. 2.24a:- Photograph of the base of bed G-67. The bed has poorly developed longitudinal ridges (left side of foot rule). Graptolites (G), argillite fragments (marked by short dark lines) and intra-bed lination (top left) are exposed along the bedding joint. 425 yard point.

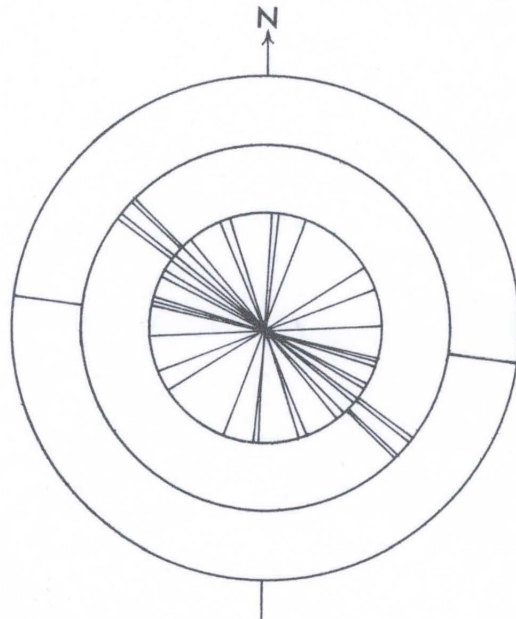


Fig. 2.24b:- Relationship between orientation of long axis of argillite fragments (inner circle), graptolites (second circle) and sole mark (third circle) in bed G-67. 425 yard point.

direction of 302° are nearly parallel to the intrabed lineation. Argillite fragments have a very wide range of orientation directions with a mean direction of 287° lying between the sole direction of 277° and the mean graptolite direction of 302° .

The mean direction of sole marks is fairly constant and the variance of sole mark directions is very small all along the outcrop. Inclusion of intrabed lineation directions increases the dispersion of sole directions significantly between the 0 and 600 yard points (table 2.1). This is due to the fact that intrabed lineation direction deviates from the sole by a large angle in this region.

Orientation of graptolites within the bed was studied only at two points (fig. 2.3b). Maximum deviation of graptolite orientation direction from the sole mark direction observed is 37° .

Bed G-66

This bed is very similar to beds G-68 and G-67 in most of its characteristics. The bed is quite variable in thickness. In the eastern region, it is quite thin and has fairly well developed, slightly wavy, plane lamination.

The bed has grooves and prod marks as sole marks in

the eastern region, which are replaced by longitudinal ridges with occasional overlapping flutes to the west. West of the 600 yard point, poorly developed L-ridges with cusped crossing bars appear. In the western region, the base of the bed is smooth and grooved at places (fig. 2.23).

Variance of sole mark orientation directions increases from east to west. (figs. 2.1, 2.3c; table 2.1).

Graptolite orientation was observed at four places west of the 2000 yard point. Deviations of graptolite directions from the sole are very large and show a systematic increase from bottom to top. The maximum deviation remains the same in all the cases. Deviation is everywhere clockwise from the sole.

Beds G-65A and G-65

Beds G-65A and G-65 occur close to each other in the stratigraphic column, separated only by a thin argillite layer (fig. 2.26) and thus form an easily traceable duplet.

The bed G-65A vanishes west of the 800 yard point. It consists of two parts except between 1800 and 2500 yard points, where it consists of only one part and exhibits plane lamination in some places. The bed has a fairly constant mean sole direction throughout (figs. 2.1, 2.3d). There is a slight increase in variance of sole mark directions

- Fig. 2.25: A large groove with striated trough and with coarse grains, bed G-66, 2659 yard point.
- Fig. 2.26: Beds G-65A and G-65. Argillite fragments in the upper part of the bed G-65 show slight imbrication in the upstream direction (right). 3180 yard point.
- Fig. 2.27: Bed G-65A. The bed has a groove with striated trough on a rough bottom with incipient development of flutes marks. Two sets of intrabed lineations at different levels in the bed are also exposed. 3190 yard point.
- Fig. 2.28: Bed G-65. Direction of intrabed lineation and graptolites at the bedding joint deviate from the direction of groove at the base by 30° . 430 yard point.

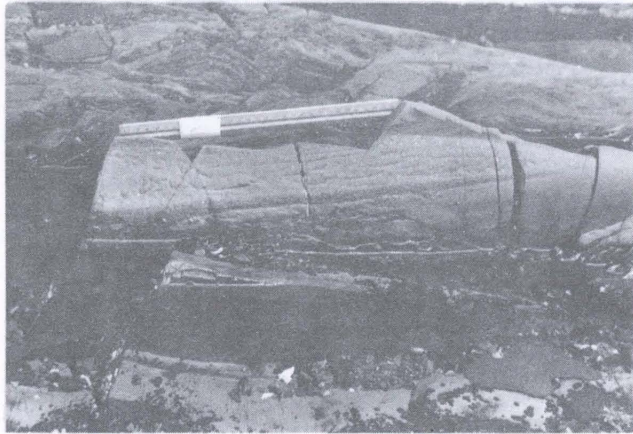


Fig. 2.25

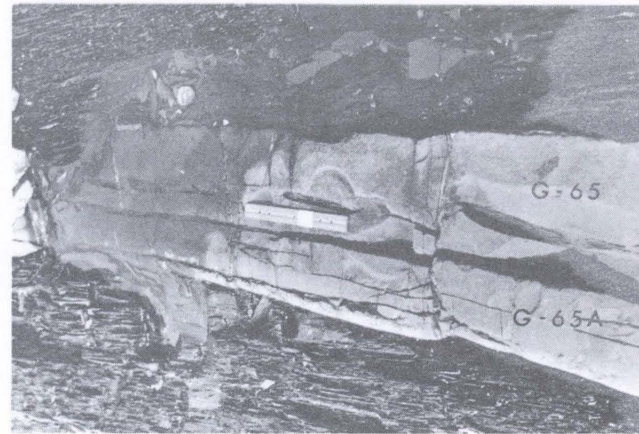


Fig. 2.26

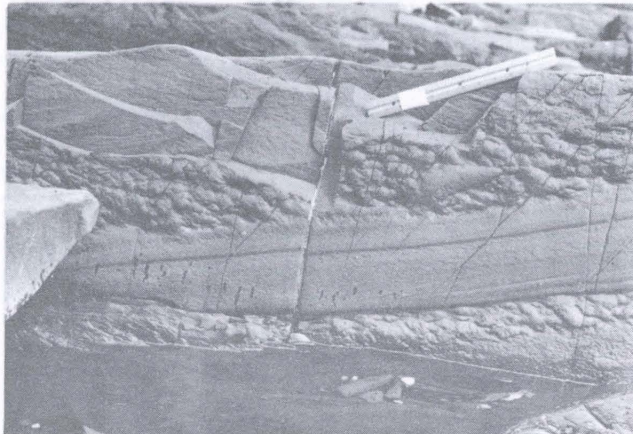


Fig. 2.27

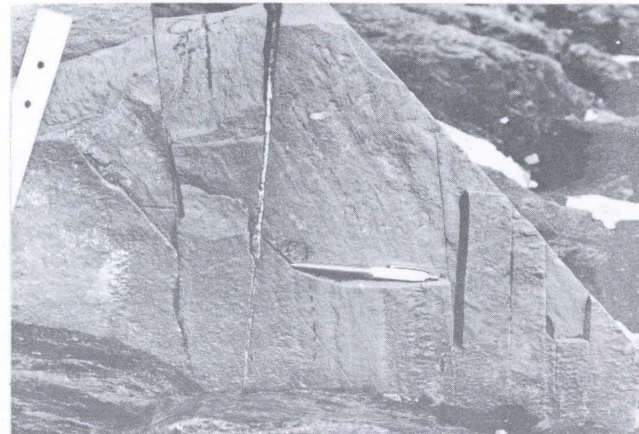


Fig. 2.28

from east to west (fig. 2.3d). The bed has a very rough bottom in the east (fig. 2.27), which may be due to the presence of a soft mud bottom at the time of deposition of the bed and incipient development of flutes. Also grooves with striated bottom are present (fig. 2.27). At about the 1970 yard point, the bed has longitudinal ridges and further west only grooves are present.

A sequence of sole structures from east to west similar to G-65A is shown by G-65. Another joint at a height of 1 - 2 cm above the joint not marked in the figure 2.1 is present at places. It also exhibits small scale 'dish structure' similar to that of bed G-67 in the region near the 1100 yard point. The direction of sole marks changes from NW to SW as the bed is traced from east to west. It is interesting to note that between the 1800 and 2300 yard points, both sole marks and intrabed lineation have NW direction. Further west between the 870 and 1100 yard points, intrabed lineation continues to have NW direction, whereas the sole marks tend to have SWW direction (fig. 2.1). Graptolite orientations show both clockwise and anticlockwise deviations from the sole direction (fig. 2.2e).

Bed G-58

Bed G-58 is continuous all along the exposure and

shows little variation in thickness. It shows two parts only for a short distance in the east. At section II₆, one can distinguish plane laminations towards the top (fig. 2.29). The plane laminations are slightly different from the usually described plane laminations. The bed does not split along these laminations, neither does weathering bring out micro furrows and ridges on the side surface.

The sole marks are irregular grooves, 'scaly' structures, L-ridges and flutes (figs. 2.30, 2.31). It seems that all the sole marks are modified to some extent by load casting. The underlying greywacke beds G-59, G-60 and G-60A (fig. 1.4) also exhibit load cast structures. Argillite between beds G-60A and G-60B contains many volcanic ash fragments. Volcanic ash may impart a highly hydroplastic nature to argillite. Thus the presence of volcanic material in various amounts in argillite between these beds may have been a factor in load deformation in the present case, but it is not always the necessary condition for the formation of load structures.

The sole direction is quite constant in the eastern region up to the 1770 yard point. Further west, it is very variable (fig. 2.1). All the observed grooves at the bottom of bed G-58 between the 1770 and 3170 yard points have a constantly south-westerly direction making an average angle of 39.6° with the strike. It may therefore be calculated

- Fig. 2.29: Bed G-58 with faintly developed plane laminations towards the top, 1840 yard point.
- Fig. 2.30: Large irregular grooves modified by load casting at the base of the bed G-58, 1800 yard point.
- Fig. 2.31: "Scaly" structures at the base of bed G-58, 80 yard point.
- Fig. 2.32: Lobate structure just below the bedding joint, bed G-50, near 1100 yard point.

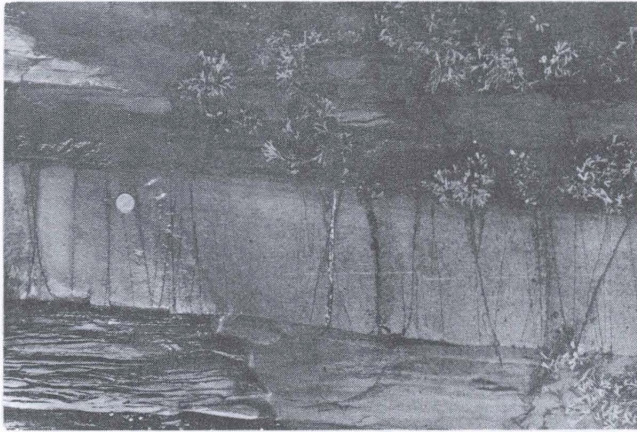


Fig. 2.29

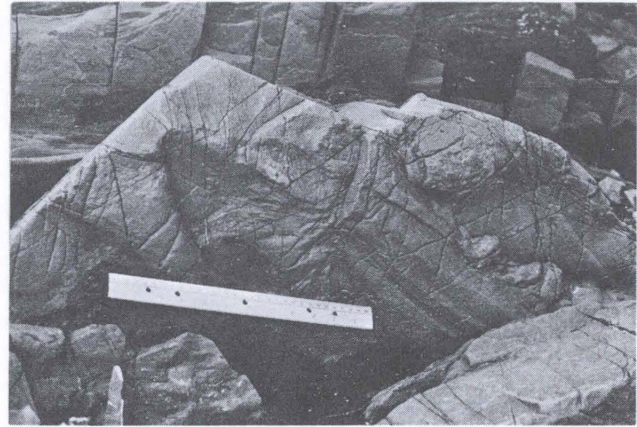


Fig. 2.30



Fig. 2.31

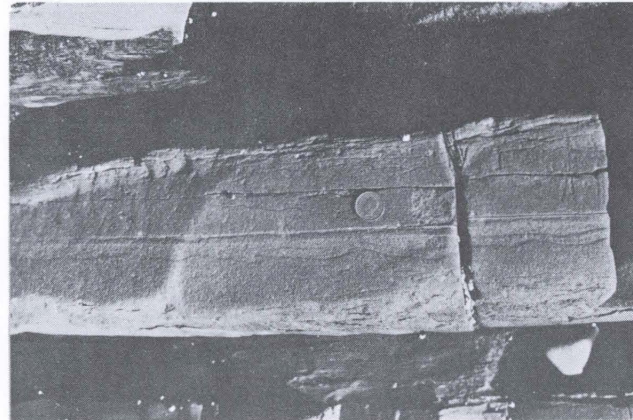


Fig. 2.32

that the current depositing the bed had a minimum width of 892 yards. In most other beds, the current direction as deduced from sole marks is nearly parallel to the strike direction, so that it is difficult to get any idea about the width of the depositing current.

In the eastern region, the bed has a very large number of rock fragments and is very argillaceous in nature.

Bed G-50

Changes in internal structures along the exposure are plotted in fig. 2.1. At places, the bed has lobes of yellowish material just below the bedding joint in the lower part of the bed. The grain size of these lobes may be slightly coarser than the surrounding material. The lobes are rounded from below and are truncated at the joint (figs. 2.32 - 2.34). Thus they can be used for top and bottom criterion in beds which lack other indications. Also, the lobes are overturned in the downcurrent direction. When traced laterally, the lobes may be represented simply by a layer 1 cm or less in thickness parallel to the bedding just below the joint. The yellowish color may be due to the presence of calcisiltite.

At places, weathering has brought out small irregular patterns with a yellowish weathering color in the middle of the bed (fig. 2.40). These may represent some inclusions in the depositing current not readily miscible with the

Fig. 2.33: Lobate structure just below the bedding joint, bed G-50, near 1100 yard point.

Fig. 2.34: Lobate structure just below the bedding joint, bed G-50, near 550 yard point.

Fig. 2.35: "Scaly" structures at the right pass into longitudinal ridges, which further pass into "scaly" structures, bed G-50, near 1800 yard point.

Fig. 2.36: Closely spaced flute marks, bed G-50, 1150 yard point.

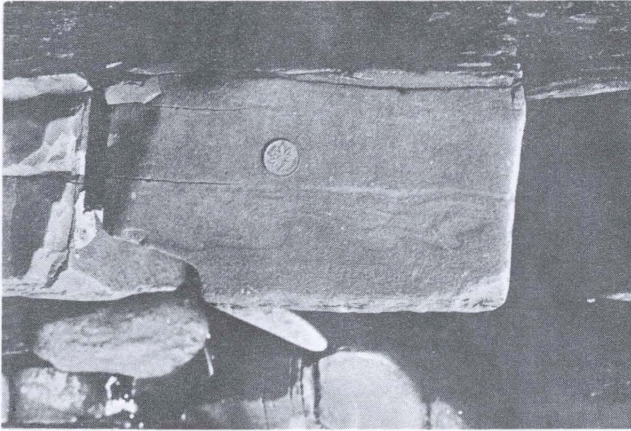


Fig. 2.33



Fig. 2.34

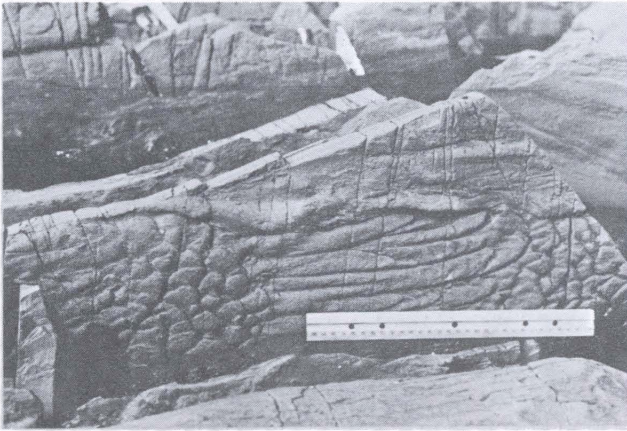


Fig. 2.35

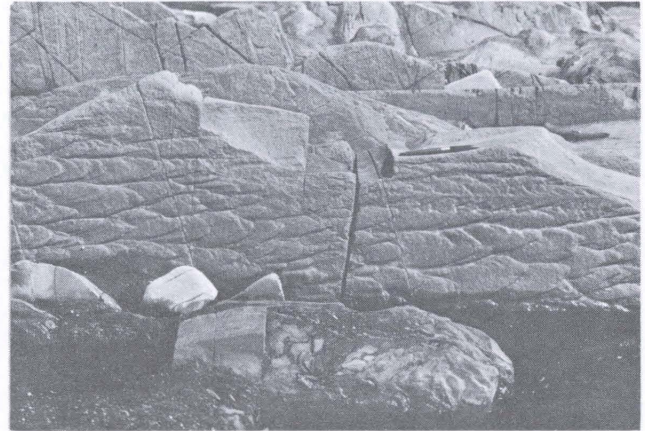


Fig. 2.36

- Fig. 2.37: Longitudinal ridges with crossing cusped bars, bed G-50 1115 yard point.
- Fig. 2.38. Shallow longitudinal ridges with cusped crossing bars, bed G-50, 30 yard point.
- Fig. 2.39: Bed G-50. Coarse grains are scattered throughout the lower part of the argillite overlying the sandy portion of the bed and argillite is topped by cross-laminated calcisiltite less than 1 cm thick, 100 yard point.
- Fig. 2.40: Bed G-50. The topmost part of the bed (z) is very sandy and is equivalent to argillite elsewhere. It has a well defined lower boundary and is bounded at the top by 0.5 cm thick cross-laminated calcisiltite. The bed shows small irregular patterns of yellowish color in the middle part. The bed is nearly 16 cm thick. 450 yard point.

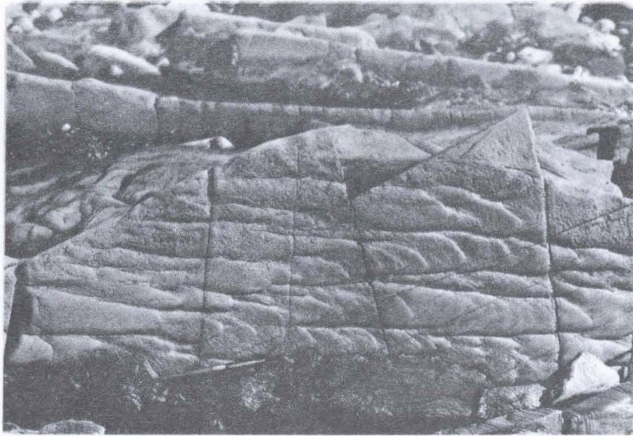


Fig. 2.37

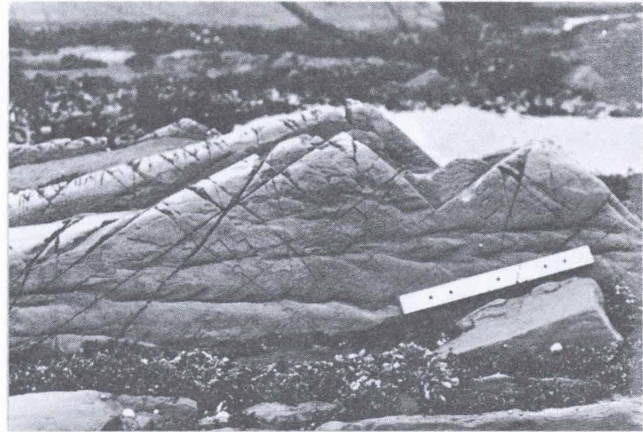


Fig. 2.38



Fig. 2.39

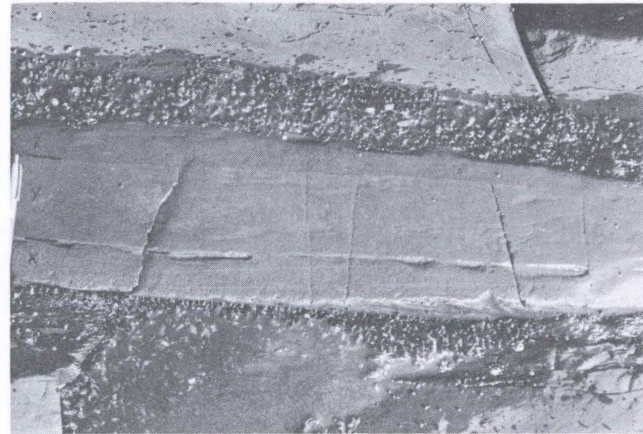


Fig. 2.40

rest of the suspended material.

The bed has grooves as sole marks in the eastern region, which are replaced by L-ridges, flute marks and cushion marks lying side by side or overlapping each other (figs. 2.35 - 2.38). In the westernmost region, grooves start appearing. The mean sole direction of E-W remains fairly constant throughout the area with one exception. In the eastern region, two anomalous directions trending N-S are observed. These two readings have been excluded in computation of the mean and variance of sole directions given in table 2.1.

The orientation of graptolites within the bed is very close to the sole mark (fig. 2.3f). Deviation of graptolite orientation from the sole is less than 35° .

Bed G-49

Bed G-49 is quite variable in thickness and is absent between the 900 and 1250 yard points. Since the bed is not amalgamated on to any other bed, most probably it was not deposited in this area.

Throughout the outcrop the bed has grooves as sole marks (figs. 2.43, 2.44). At many places, the bed has two sets of crossing grooves (fig. 2.43), and the intra-bed lineation is parallel to one of the sets. Maximum depth of the grooves in the eastern region where the bed is thick is greater than that in the western

- Fig. 2.41: Beds G-50 and G-49. Both the beds are traversed by bedding joints dividing them into two distinct parts. 2600 yard point.
- Fig. 2.42: Beds G-50 and G-49. The bed G-49 is very thin and at this place the lower part of the bed is represented by a lens (below the foot rule) only. 2410 yard point.
- Fig. 2.43: Bed G-49. Intrabed lineation is parallel to one of the two sets of crossing grooves at the base of the bed. 3130 yard point.
- Fig. 2.44: Bed G-49. A large groove and a tool at the base of the bed. The tool is oriented with its axis nearly perpendicular to the groove direction. 2425 yard point.

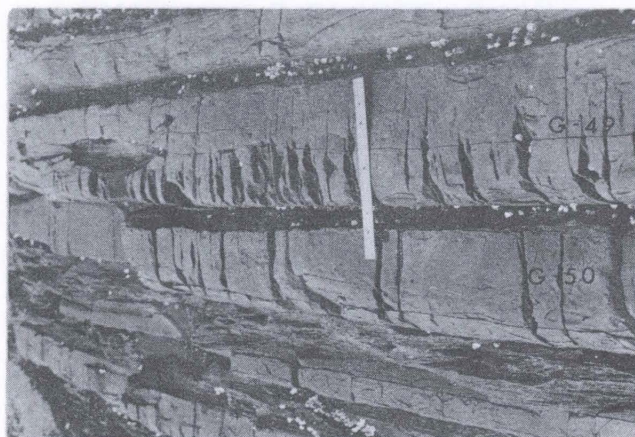


Fig. 2.41

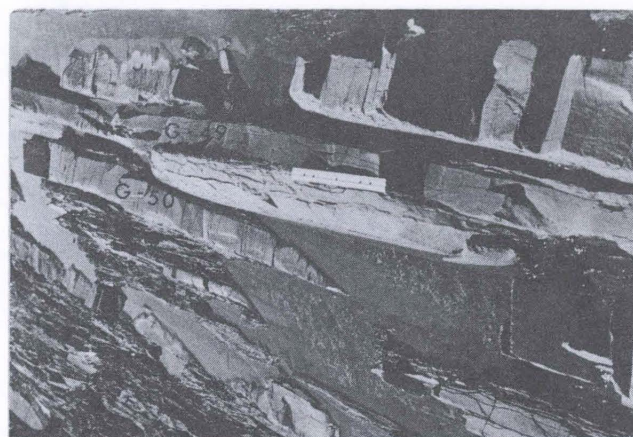


Fig. 2.42



Fig. 2.43



Fig. 2.44

region where the bed is thin. At about the 2430 yard point, a decrease in thickness takes place from east to west and is accompanied by a change in sole direction of more than 50° . As the lower part is represented at one or two places in the west as lenses (fig. 2.42), the thin bed in the western area corresponds to the upper part of the bed in the east.

The sole mark orientation is variable and the graptolites in the bed exhibit orientation directions deviating from that of the sole in clockwise as well as anti-clockwise direction (fig. 2.2g).

Conclusions

Great caution should be exercised in interpreting the observations. Because only a cross section of the beds can be seen (i.e., the beds are exposed along the strike direction 274° - 278°) only the beds with sole direction nearly parallel to the strike should be studied for changes along the path of the depositing current. Changes in beds with wide divergence of sole direction from the strike may simply reflect irregular topography of the cross section of the path of current. A quick study shows that beds G-68, G-67, G-66 and G-50 satisfy the requirements to a fair degree. Each of the beds shows parallelism of sole marks with the strike at least

in the eastern region. Another proof comes from the fact that these beds gradually grade to argillaceous beds in the west. In experimental turbidites deposited by fast currents, segregation of muddy material has been observed in the downcurrent direction (Dzulynski and Walton, 1965, p.200). Thus sedimentologic changes along the strike of these four beds represent to a great extent the variation in the beds along the path of the depositing currents.

The results of this section are summarized as follows:

(i) Two parts of a bed - Bouma (1962, p. 50)

first reported that a graded bed could be divided into two parts: the lower coarse grained graded part and the upper fine grained graded part. These two parts were found to be separated by a well-defined grain size discontinuity. Later Enos (1965) and Hubert and others (1966) found that the intrabed lineation at the discontinuity may have a direction different from that of the sole by as much as 40° . Hubert and others (1966) reported a grain orientation from the lower part of the bed parallel to the sole and from the upper part close to the intrabed lineation direction.

In the beds under study, a grain size break at the bedding joint separating the two parts was recognized in the field. Also, the intrabed lineation differed from the sole by as much as 40° . Graptolite orientation from

the lower part was found to be very closely parallel to the sole and that from the upper part was more variable, but closer to the intrabed lineation. Variance of sole mark and intrabed lineation directions taken together is higher than that of sole mark directions alone.

(ii) Changes in internal structure - A change of poorly graded bed in proximal regions to well graded beds in the distal regions has been observed experimentally by Kuenen and Migliorini (1950), Kuenen and Menard (1952), Dzulynski and Walton (1965) and Middleton (1967a). Experiments by Dzulynski and Walton showed not only a lack of grading, but also the development of a crude stratification in the proximal area. Further downcurrent, grading appeared with finer wavy lamination which passed into crude lamination. Combining the results of all these experiments, Dzulynski and Walton (1965, p.238) gave the following lateral and vertical sequence to be expected in a single turbidite sequence as it is traced away from the source:

(a) coarse grained thick deposit with large erosion structures

(b) coarse grained beds with multiple grading

(c) laminated interval underlain by medium grained graded interval

(d) wavy lamination in places convoluted overlying

the fine grained laminated bed

(e) silts and shales

Bouma (1962, p.48) first defined a complete vertical sequence as one which contains a graded division (A), Lower division of parallel lamination (B), division of current ripple lamination (C), an upper division of parallel lamination (D), and pelitic division (E) and thought that a slowing down current will give rise to such a sequence. Bouma (1962, p.98) also noted that in distal regions, the upper divisions are more abundant. Hubert (1966) observed the presence of large scale cross-beds below the current ripple lamination division C of Bouma (1962) in the upper Ordovician geosynclinal rocks of Scotland.

In the present study, it seems that when the bed is thin, it is also laminated in case of beds G-67, G-66 and G-50. However, this is true only in the proximal area. In the distal areas, the thinner parts of the bed are also massive, e.g., bed G-66 between the 0 and 300 yard points.

(iii) Variation in sole markings - Dzulynski and Walton (1963, 1965) and Costello (1968) observed a lateral variation in sole marks of experimentally deposited turbidites. Flutes in the proximal area were replaced downcurrent by longitudinal ridges, which in turn gave way to dendritic ridges. The longitudinal ridges may be associated with tool marks. Later experiments by Dzulynski

and Simpson (1966a) suggest that space between the proximal flutes and discharge may be occupied by longitudinal ridges and small scour marks. The most distal part shows smooth bottom with occasional tool marks.

Also Dzulynski and Walton (1963, p.298) observed that longitudinal ridges occupied a relatively large area in the experimentally deposited turbidites and noted that the natural occurrences do not show any abundance of longitudinal ridges over flutes and other sole marks.

Enos (1965, p.86) found a slight increase in number of flutes in the downcurrent direction by measuring the same stratigraphic interval at several points and noted that flutes do not tend to be associated with thick beds or with the thinner parts of the beds with variable thickness or with coarser grained beds. Of course, flutes are found to be rare in type 2 greywacke beds.

In the present study, irrespective of the internal structure of the beds, the following general change of sole marks from the proximal to distal region is observed: (1) smooth bottom with tool marks such as prod marks, grooves, etc., and some isolated flute marks, to (2) longitudinal ridges, longitudinal ridges with overlapping flutes and closely spaced flutes, to (3) poorly developed, shallow longitudinal ridges with occasional cusped crossing bars. to (4) smooth bottom with occasional groove

marks. Longitudinal ridges and associated sole structures are present for distances of about 2300, 2000 and 1600 yards along the outcrop in beds G-68, G-66 and G-50 respectively.

(iv) Lateral changes in sole mark direction - Enos (1965) found that variance of current direction measurements for a number of stratigraphic intervals compared with that of current directions measured for the same stratigraphic intervals at distances of 1.8 to 8 miles indicates no general trend towards an increase in variance in the down-current direction. Scott (1967) observed that in a single stratigraphic section, thicker beds tend to have a sole direction deviating from the mean in an anticlockwise direction and that the opposite was true for thinner beds. In the present study, an increase in variance of sole mark directions can be detected in the downcurrent direction for beds G-68, G-66 and G-50 without large change in the mean direction. A change of nearly 90° in the sole direction is observed in bed G-65, as the bed is traced from east to west. Also, there does not seem to be any fixed trend in the deflection of the sole mark directions (i.e., clockwise or anticlockwise) in the distal regions.

(v) Graptolite orientation in the beds - In the beds under study, graptolites may have an orientation nearly normal to the sole mark. The deviation of graptolites orientation from the sole mark increases from bottom to top of the bed.

The maximum deviation may increase in the downcurrent direction. Deviation of graptolite orientation from the sole mark direction is both clockwise and anticlockwise.

Graptolite orientation will be further discussed in conjunction with grain orientation results.

CHAPTER III

GRAIN ORIENTATION STUDY

Appositional fabric from turbidites has been studied by numerous workers in recent years, usually to find out whether it can be used as a paleocurrent indicator, in cases where other paleocurrent indicators are not available (see Potter and Pettijohn, 1963; Middleton, 1965; Dzulynski and Walton, 1965). However, the primary fabric of turbidites (in fact of all the sedimentary rocks) is controlled by depositional processes and the study of fabric combined with other textural studies such as grain size, shape, etc., could lead to the understanding of the depositional processes involved. So a detailed study of the appositional fabric of the beds under investigation was undertaken.

Experimental Details

Cores with a diameter of 0.8 inch were drilled in a direction normal to the bedding from the oriented specimens and thin sections parallel to the bedding were cut at intervals of one to three cms. The detailed methodology for preparing oriented thin sections is described by Onions (1965) and Martini (1965). Thin sections from a hand specimen.

(say II_6-50) are numbered from bottom to top (e.g., II_6-50-1 , II_6-50-2 , etc.).

As a number of thin sections were to be cut from the same core, it was found convenient to mark the strike and dip at the top and bottom of the core and straight lines marking the vertical plane through the strike direction were drawn on the sides of the core with the help of a steel cylinder. The diameter of the steel cylinder was slightly greater than that of the core so that it can just slip around the core. It had a slit on the side parallel to its axis.

The grain orientation measurements in this study were made with a petrographic microscope, equipped with mechanical point counter. The N-S cross hair of the ocular was used as a reference direction. Only quartz grains were studied to keep the hydrodynamic conditions uniform. The orientation was measured of the 'least projection elongation' direction, which is defined as the direction of two parallel lines with minimum separation that can be drawn tangent to the grain boundary (Dapples and Rominger, 1945). The largest intercept parallel to these lines is defined as 'a' axis and the distance between the two lines as 'b' axis. Only those grains with 'a' axis greater than 0.1 mm and elongation ratio, b/a , less than 0.7 were measured. The size and elongation ratio were estimated

visually. The grains measured were selected by traversing across the thin section with a point counter. Only those grains that fall under cross hairs were measured (Glagolev Procedure), so that the resulting frequencies were frequencies weighted by the volume of the grains.

One hundred grains or the maximum number of grains available (if fewer than 100) were studied in each thin section. Rose diagrams were prepared by plotting percentage of measurements in each 20 degree class at the centre of that class. The orientation direction and degree of preferred orientation for individual thin sections were computed using a two dimensional vector analysis technique described by Curray (1956). The degree of preferred orientation was tested by the Rayleigh test (Rayleigh, 1884; in Potter and Pettijohn, 1963, p.266). The orientation was considered significant at a 90% confidence level.

Number of Measurements per Thin Section

Raup and Miesch (1957) describe a method to find the number of measurements of cross-strata dip directions necessary in order to obtain a significant average direction for the area. This is based on the fact that the number of measurements needed is proportional to their standard deviation. Another method of calculating the minimum

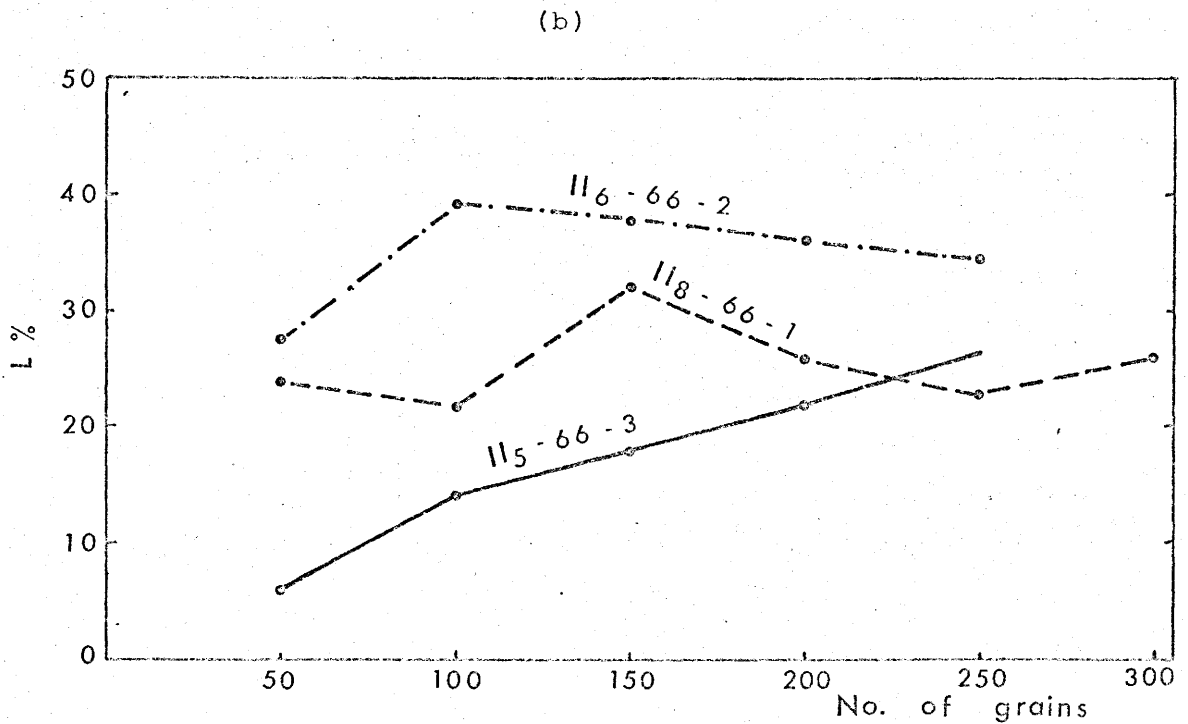
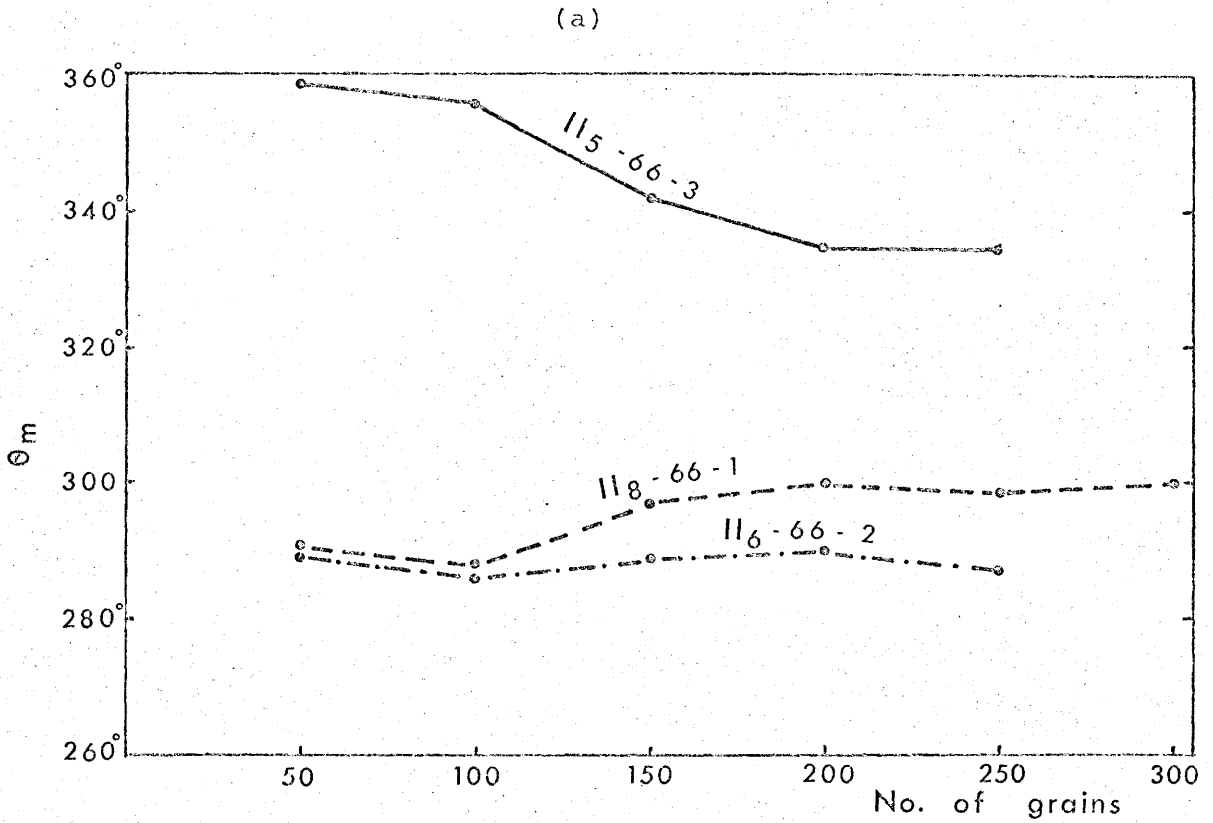


Fig. 3.1 - Variation in vector mean (a) and vector magnitude per cent (b) of grain orientations with increase in number of measurements.

number of measurements needed is to measure the grains in successive groups of 50 grains, add these to the previously measured ones and calculate the vector mean. At a certain stage, addition of more measurements does not change the vector mean significantly. Then the flatness point is said to be reached. The flatness point indicates the minimum number of grains required for study.

In the present study, the maximum standard deviation is 52° . From the table of Raup and Miesch (1957), the minimum number of measurements required for study is 96. Also the vector mean and vector magnitude percentage are plotted against number of measurements for three thin sections in figures 3.1a and 3.1b and the data is summarized in table 3.1. For thin sections II₈-66-1 and II₆-66-2, the vector mean obtained from 50 grains is essentially satisfactory. For thin section II₅-66-3, the flatness point is reached at 200 grains. This is perhaps due to the inhomogeneity of the thin section and high dispersion. As a general rule, one hundred measurements per thin section are considered to be sufficient.

Dispersion varies irregularly with increase in number of measurements. In thin section II₅-66-3, there is a decrease in dispersion with increase in the number of measurements. Dispersion varies irregularly in thin section II₈-66-1. But in thin section II₆-66-2, after 100

grains additional measurements tend to increase cumulative dispersion.

Table 3.1

Determination of 'flatness' point

No. of grains	II ₆ -66-2		II ₈ -66-1		II ₅ -66-3	
	θ_m	L%	θ_m	L%	θ_m	L%
50	289.9	27.67	291.5	23.78	359.5	5.7
100	286.1	38.96	287.7	21.82	355.3	14.07
150	288.5	37.43	297.0	31.91	342.5	18.06
200	289.6	35.75	299.1	25.68	334.5	21.75
250	287.5	34.34	297.1	22.73	335.2	25.42
300			300.9	25.84		

Accuracy and Consistency of Measurements

Smoor (1960), Onions (1965) and Martini (1965) have shown that in grain orientation measurements, accuracy is quite high. So, only a consistency test was run. Five thin sections were selected from all those cut from bed G-66 and the orientation measurements were duplicated after a period of 4 weeks. The resulting data is given in table 3.2. The orientation distributions are plotted in figure 3.2. Figure 3.3 shows vector mean and dispersion plotted against each thin section for the two point counts.

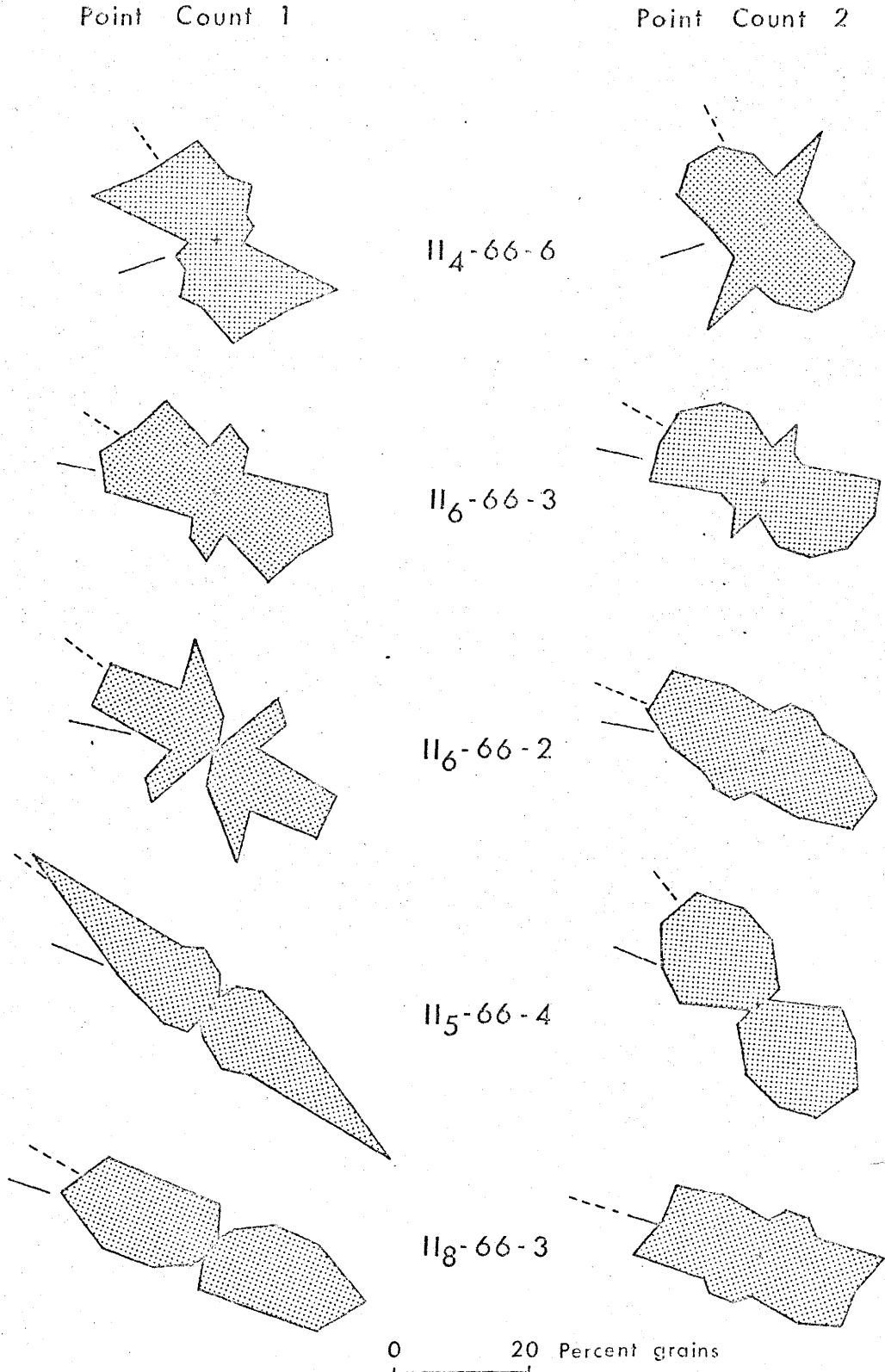


Fig. 3.2 - Grain orientation frequency distributions in operator experiment. Solid line represents direction of sole mark and dotted line marks the direction of vector mean.

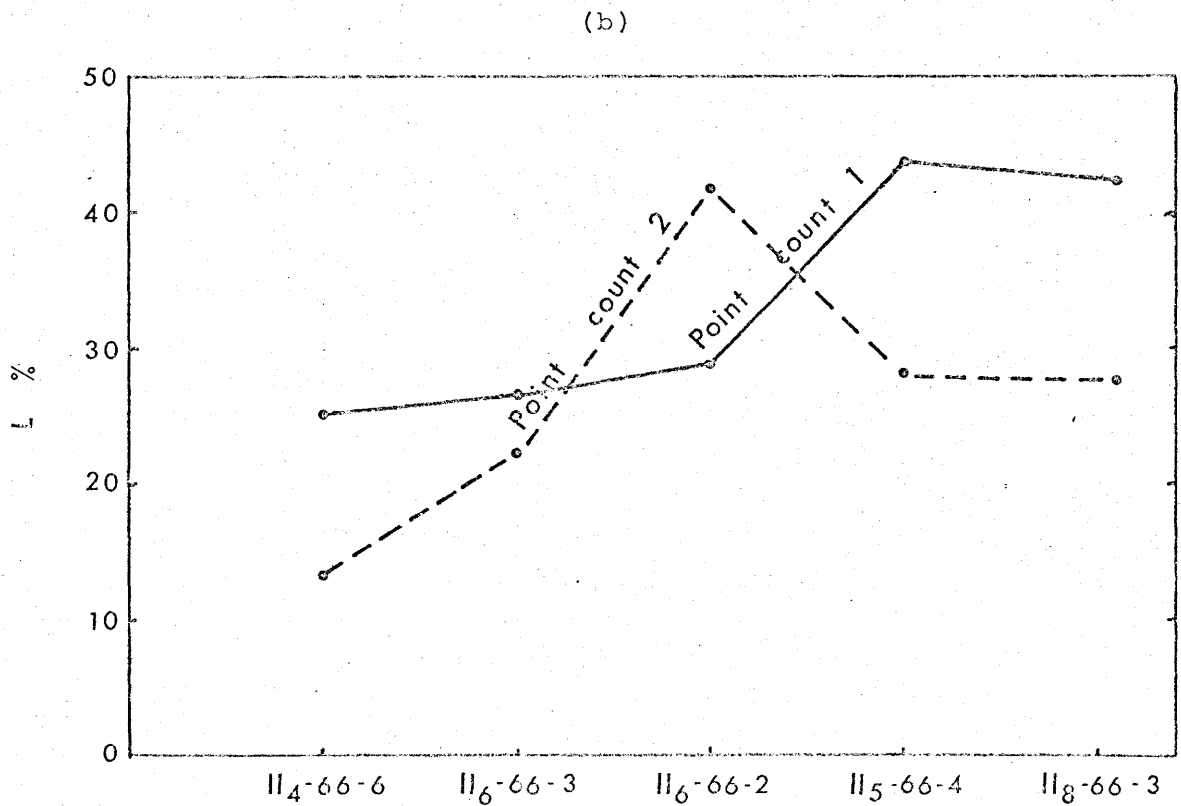
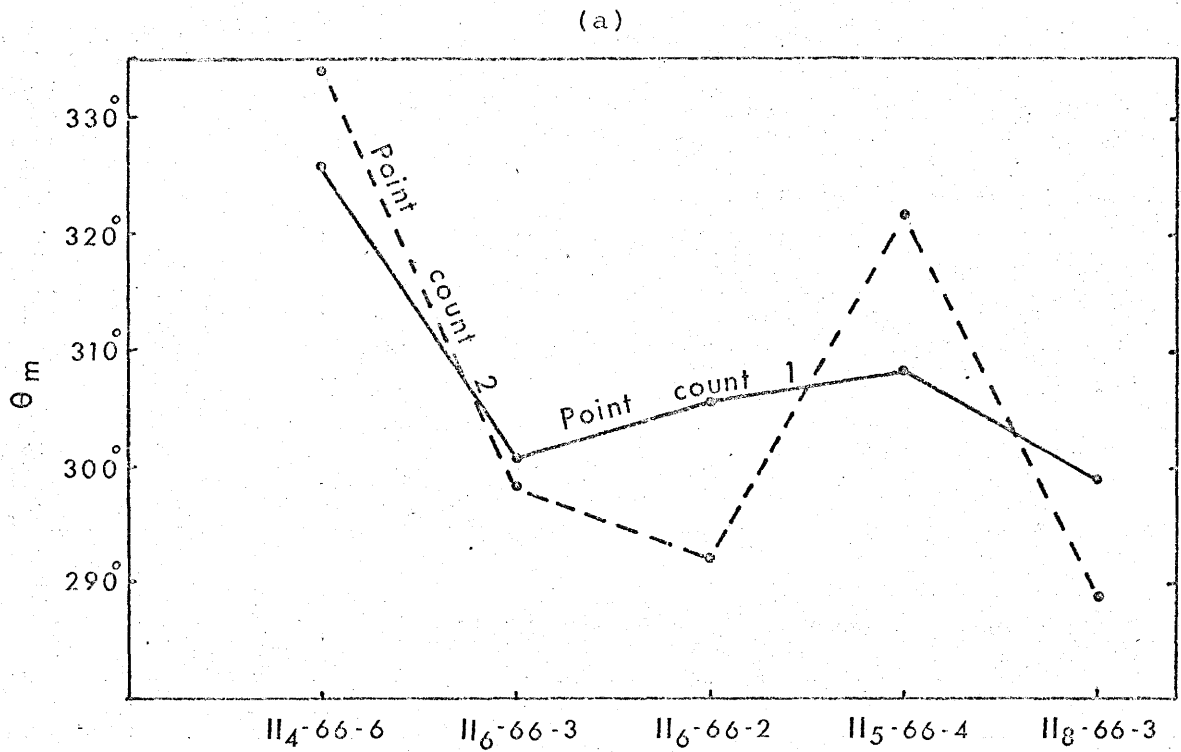


Fig. 3.3 - Vector mean (a) and vector magnitude per cent (b) in five thin sections in operator experiment.

Table 3.2

Summary statistics: operator experiment - vector mean

Thin section	Point count 1		Point count 2	
	θ_m	L%	θ_m	L%
II ₄ -66-6	325.7	25.00	333.9	13.08
II ₆ -66-3	301.0	26.50	298.3	24.07
II ₆ -66-2	305.6	29.10	292.3	42.53
II ₅ -66-4	308.0	43.88	321.9	27.44
II ₈ -66-3	298.7	42.57	288.6	27.09

A t-test for paired observations (Snedcor, 1956, p.50) was run on the data. The computed value of t is 0.769 and the value of $t_{4,0.95}$ from the tables is 2.776. Therefore, the hypothesis that means are equal is accepted. The 95% confidence limits for the experiment are $\pm 14.4^\circ$ and are calculated by the formula

$$\theta_m \pm t(N-1)(1-\alpha/2) \frac{S}{\sqrt{N}}$$

where N = the number of thin sections, and S = the standard deviation.

The data were also subjected to an analysis of variance (table 3.3). This indicates that operator error is negligibly small and is in agreement with the results obtained from the t-test.

Table 3.3

Analysis of variance: operator experiment - vector mean

Source of variation	d.f.	SS	MS	F	F _{0.95}
Between point counts	1	1.60	1.60	0.02	7.71
Between thin sections	4	1759.08	439.77	6.48	6.39
Error	4	271.22	67.81		
Total	9	2031.90			

Relationship Between Grain Orientation and Graptolite Orientation within a Hand Specimen

Since the greywacke beds contain abundant graptolites, an experiment was run to study the relationship between graptolite and grain orientation. An oriented sample of bed G-50 containing abundant graptolites was obtained at section II_g. The specimen consists of two parts and has longitudinal ridges as sole marks with a direction of 277°. Graptolites from the lower part tend to be close to this direction, whereas graptolites from the upper part have an orientation closer to the intrabed lineation direction of 312°. Five thin sections were cut at different levels from the specimen. Figure 3.4 shows the grain orientation distributions and orientation statistics is listed in table 3.4. In the lower part of the specimen, all the three grain orientations differ from the sole by less than

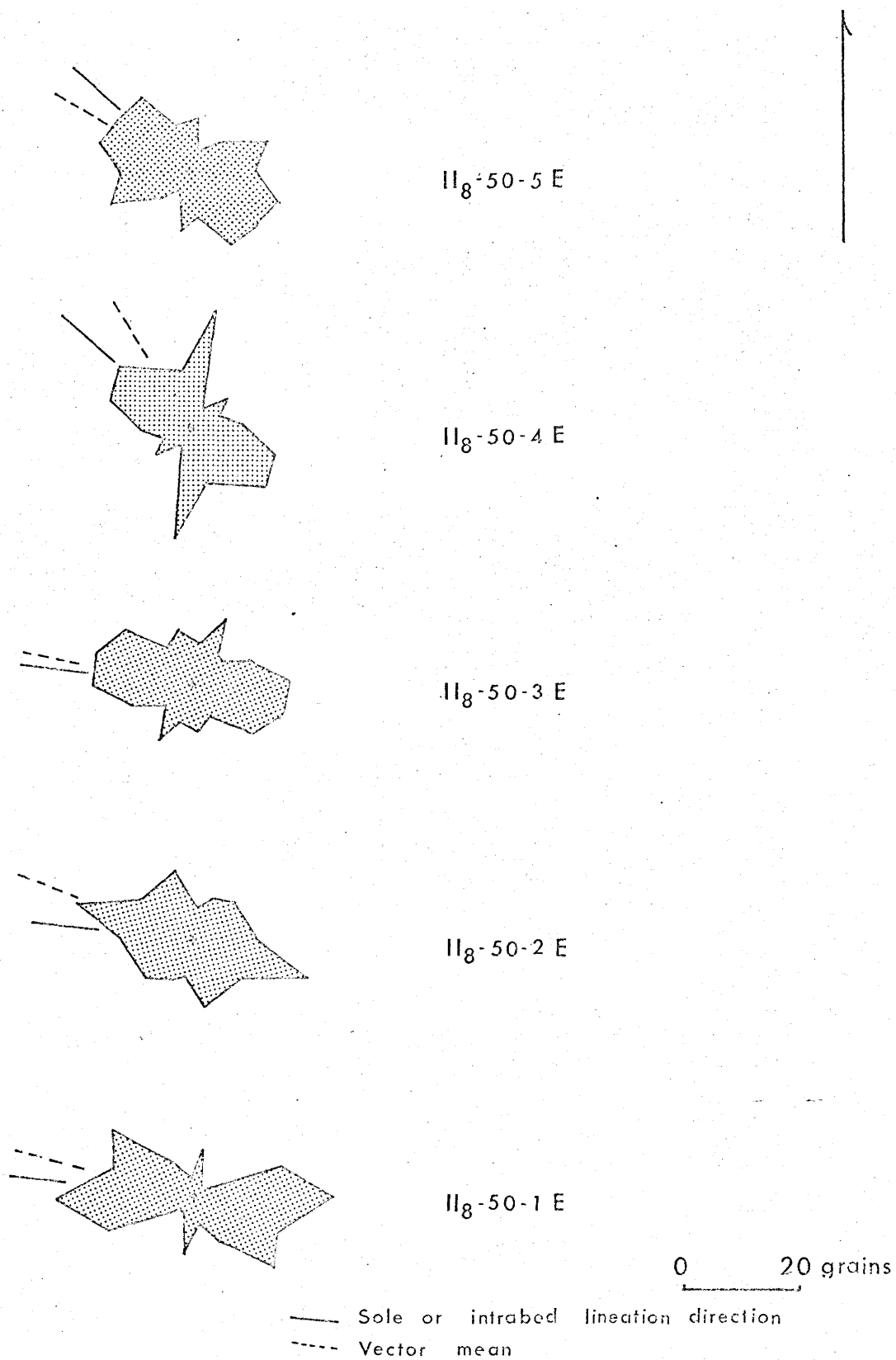


Fig. 3.4 - Orientation frequency distributions in the specimen with large number of graptolites.

Table 3.4

Experiment on relationship between graptolite and grain orientation in a hand specimen

Thin Section Number	Ht. above the base (cms)	Sole or intrabed lineation direction	Grain orientation			statistics		
			No. of measure- ments	Vector mean	Deviation from sole or intra- bed line- ation	Rayleigh Probability	Vector Magni- tude per cent	95% Confi- dence inter- val
II ₈ -50-5E	9.0	312°	100	303.1°	8.9° _a	0.039 **	21.07	± 8.72°
II ₈ -50-4E	6.0	312°	100	329.3°	17.3° _c	0.02 **	22.25	± 8.70°
		Bedding	Joint	at	a height	of	5.6 cm	
II ₈ -50-3E	5.3	277°	100	280.5°	3.5° _c	0.018 **	20.06	± 8.89°
II ₈ -50-2E	2.8	277°	100	291.6°	14.6° _c	0.05 **	17.24	± 9.10°
II ₈ -50-1E	0.3	277°	100	285.0°	8.0° _c	0.000 **	38.81	± 7.45°

a deviation of vector mean from the sole in anticlockwise direction

c deviation of vector mean from the sole in clockwise direction

** indicates significance at 95% level

15° and deviate from the sole clockwise. Thin section II₈-50-4E has a vector mean deviating clockwise from intrabed lineation by 17.3° , though a strong primary mode is at 310° , close to the graptolite orientation. The large deviation of the mean from this mode is caused by the presence of another mode nearly at 60° to the first mode. Thin section II₆-50-5E from the upper part shows grain orientation deviating from the intrabed lineation by only 9.0° anticlockwise.

Thus it seems that there is a good correspondence between graptolite and grain orientation, though deviations of the grain orientation vector mean from graptolite orientation as large as 17° may occur. The vector mean is not a good indicator of general current direction for orientation distributions with two strong modes. Similar agreement between grain orientation and plant orientation directions is reported by Henningsen (1968) from Paleozoic turbidites of Ehenish Schiefergebirge in Germany.

It should be emphasized that graptolite orientations are studied over slabs of 300 square cm or larger size, so that they are a better sample of the average fabric characteristics of the rock than the grain orientation which is measured in thin sections which cover an area of only approximately 4 square cm. However,

graptolite studies are limited only to those parts of the beds which contain graptolites and can be split, and it is more difficult to obtain objective average directions and measures of dispersion.

It seems that tectonism or soft sediment deformation has not disturbed the primary fabric of these rocks to any significant extent. The effect of tectonism or soft sediment deformation will be to homogenize the fabric over small volumes of rock. Thus if tectonism or soft sediment deformation had affected these rocks, the two parts of the bed would show a similar fabric. The difference in the fabric from the two parts of the bed, the alignment of the fabric with the current direction indicators (sole mark and intrabed lineation) and the agreement between graptolites and grain orientation strongly support the idea that the fabric is primary in nature.

Homogeneity of Samples

An attempt was made to study the homogeneity of grain orientation in a hand specimen. A specimen was selected at random (II₆-49) and two sets of cores were drilled from the specimen. Four thin sections were cut from each set of cores at approximately the same levels, and each thin section was replicated for grain orientation after a period of 4 weeks. An analysis of variance

Table 3.5
Homogeneity of grain fabric in a hand specimen
A. Data

Thin Section	Point Count 1				Point Count 2			
	Core I		Core II		Core I		Core II	
	Vector mean	Vector magnitude %	Vector mean	Vector magnitude %	Vector mean	Vector magnitude %	Vector mean	Vector magnitude %
4	297.7	38.56	303.7	26.83	295.9	38.45	310.0	3.44
3	312.0	11.26	301.0	37.53	301.7	17.63	304.4	26.33
2	298.0	11.84	301.1	33.46	312.7	14.24	293.4	30.56
1	300.5	25.41	287.5	39.42	309.3	35.4	280.8	20.08

Table 3.5

B. Analysis of variance

Source of variation	d.f.	SS	MS	F ratio	
				Type I model	Type II model
Between cores	1	131.676	131.676	2.78 N.S.	0.82 N.S.
Between thin sections	3	225.308	75.103	1.59 N.S.	0.46 N.S.
Interaction	3	483.721	161.240	3.42 N.S.	
Sub total	7	840.705			
Between point counts	8	378.145	47.268		
Total	15	1118.85			

N.S. - Not significant at 95% level.

utilizing 'two way cross mode' (Middleton, 1966) is used to analyse the data (table 3.5).

The results indicate that interaction is not significant. Variations between thin sections and between cores are negligible, which goes to show that this particular hand specimen has a very homogeneous fabric developed throughout, laterally as well as vertically.

It will be seen later, however, that grain orientation may change quite drastically from bottom to top of a specimen.

Degree of Preferred Orientation and Deviation of Grain Orientation from the Sole

Most of the grain orientation studies from turbidite beds have been reported to have statistically significant preferred orientation. Scott (1966, p.85) reported one non-significant preferred orientation from a very well graded unit from the Cretaceous flysch sequence of Chile. Onions (1965) and Onions and Middleton (1968) found that 15% of all the thin sections studied from the Normanskill Formation had non-significant preferred orientation. Rukavina (1965) noted the presence of non-significant preferred orientations, current normal or bimodal orientation distributions towards the top of the bed and away from the source in experimentally deposited

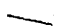
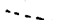
turbidites.

Different workers have obtained different results regarding the relationship of grain orientation and sole structures. Parallelism of sand grains and associated sole structures has been reported by Kopstein (1954), ten Haaf (1959), Smoor (1960), McIver (1961) and McBride (1962). Preferred orientation perpendicular (Basset and Walton, 1960, Bouma, 1962, Ballance, 1964) and oblique (Spotts, 1964, Spotts and Weser, 1964, Scott, 1967) to the sole mark also have been reported. Also there is some evidence of both sole-parallel and sole-normal preferred orientation at different levels within the same bed (Hand, 1961; Stanley, 1963; Rukavina, 1965). Onions (1965), Onions and Middleton (1968) and Colburn (1968) observed that there is only a slight tendency for grain orientation to be parallel to the sole and grain orientation deviates from the sole very irregularly with height above the base of the bed.

Grain orientation distributions obtained in this study are plotted in figures 3.5 - 3.12 and the orientation statistics are summarized in Appendix I. Vector means and sole directions are separately plotted in figure 3.13. The height of each grain orientation from the base in cm is shown along each direction. Significant preferred orientations are shown by solid lines and non-significant

Figs. 3.5-3.12 - Grain orientation frequency distributions in different beds.

The following notations are used in these figures -

- (i)  indicates sole mark direction
 indicates vector mean direction

- (ii) Vertical lines in block diagrams refer to N-S direction and horizontal lines at the top of diagrams indicate E-W direction.

- (iii) For thin sections cut parallel to the bedding plane -
Dark pattern (checkered) indicates significant preferred orientation at $\alpha = 0.10$.
Light pattern (horizontal lines) indicates non-significant preferred orientation at $\alpha = 0.10$.

For thin section studied for grain imbrication -

Dark pattern (checkered) indicates imbrication value different from zero at $\alpha = 0.05$.

Light pattern (dotted) indicates imbrication value not different from zero at $\alpha = 0.05$.

- (iv) Numerals on the right side of rose diagrams refer to the last figure in thin section numbers.

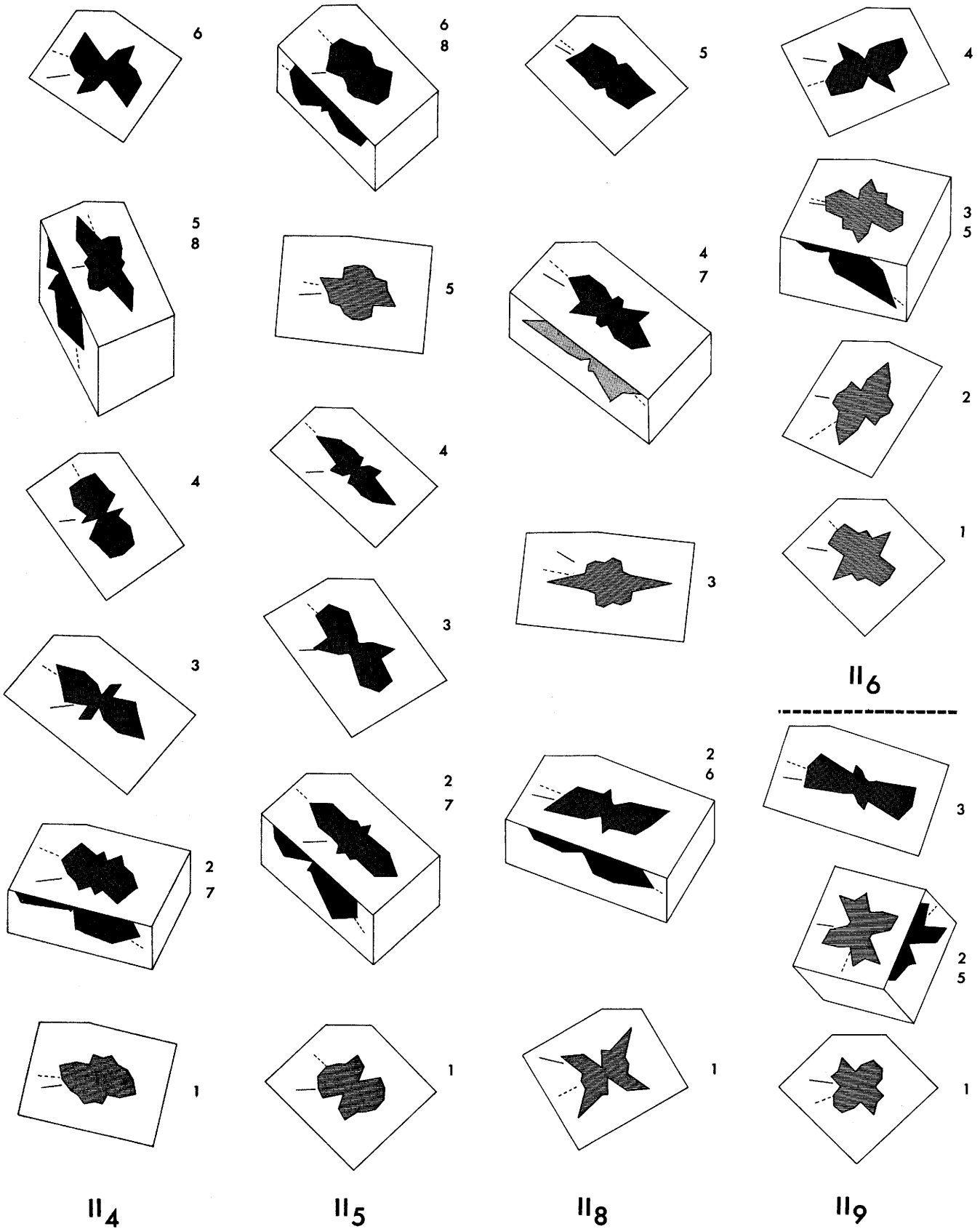


Fig. 3.5 - Grain orientation frequency distributions in bed G-68.

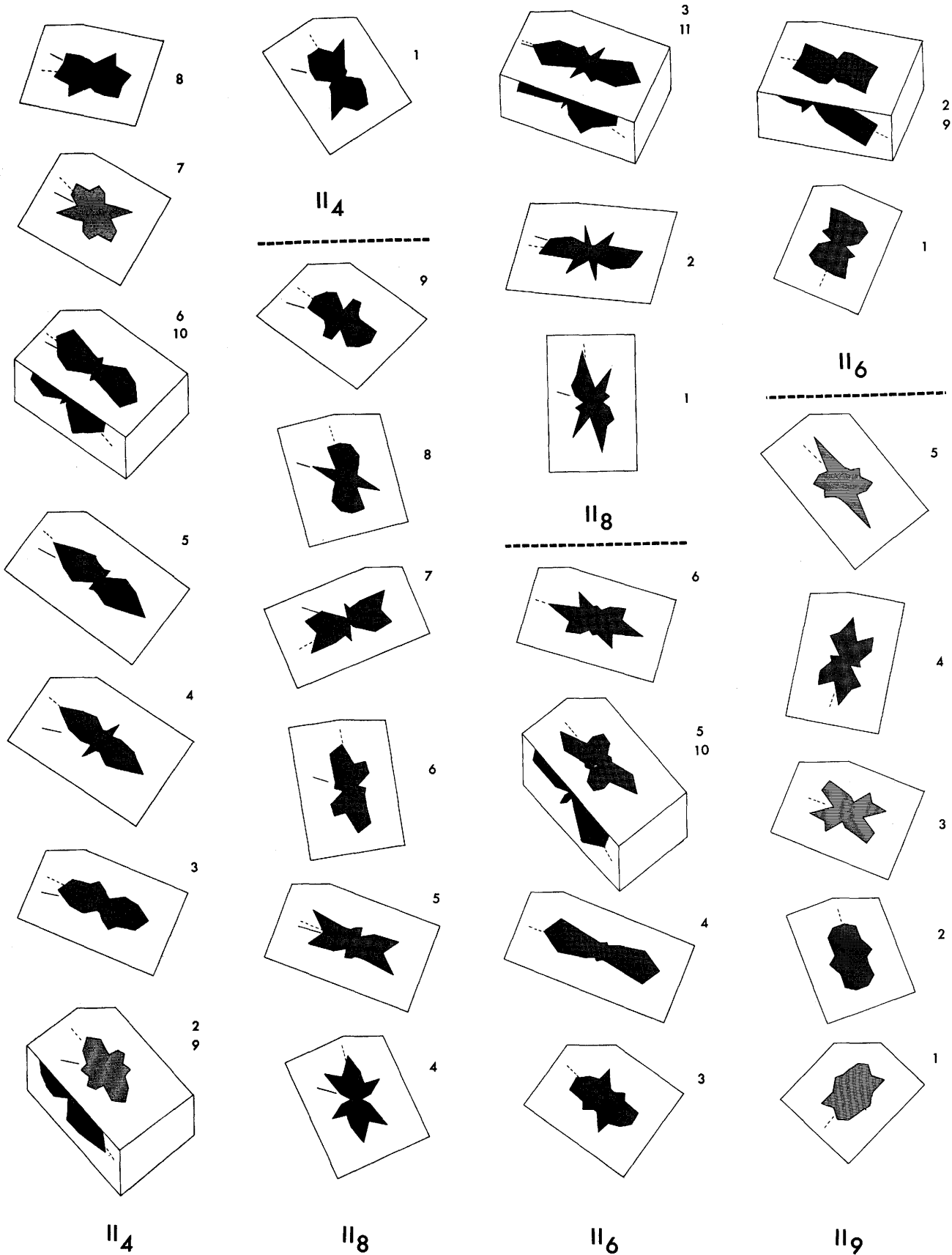


Fig. 3.6 - Grain orientation frequency distributions in bed G-67.

0 20 40 PERCENT GRAINS

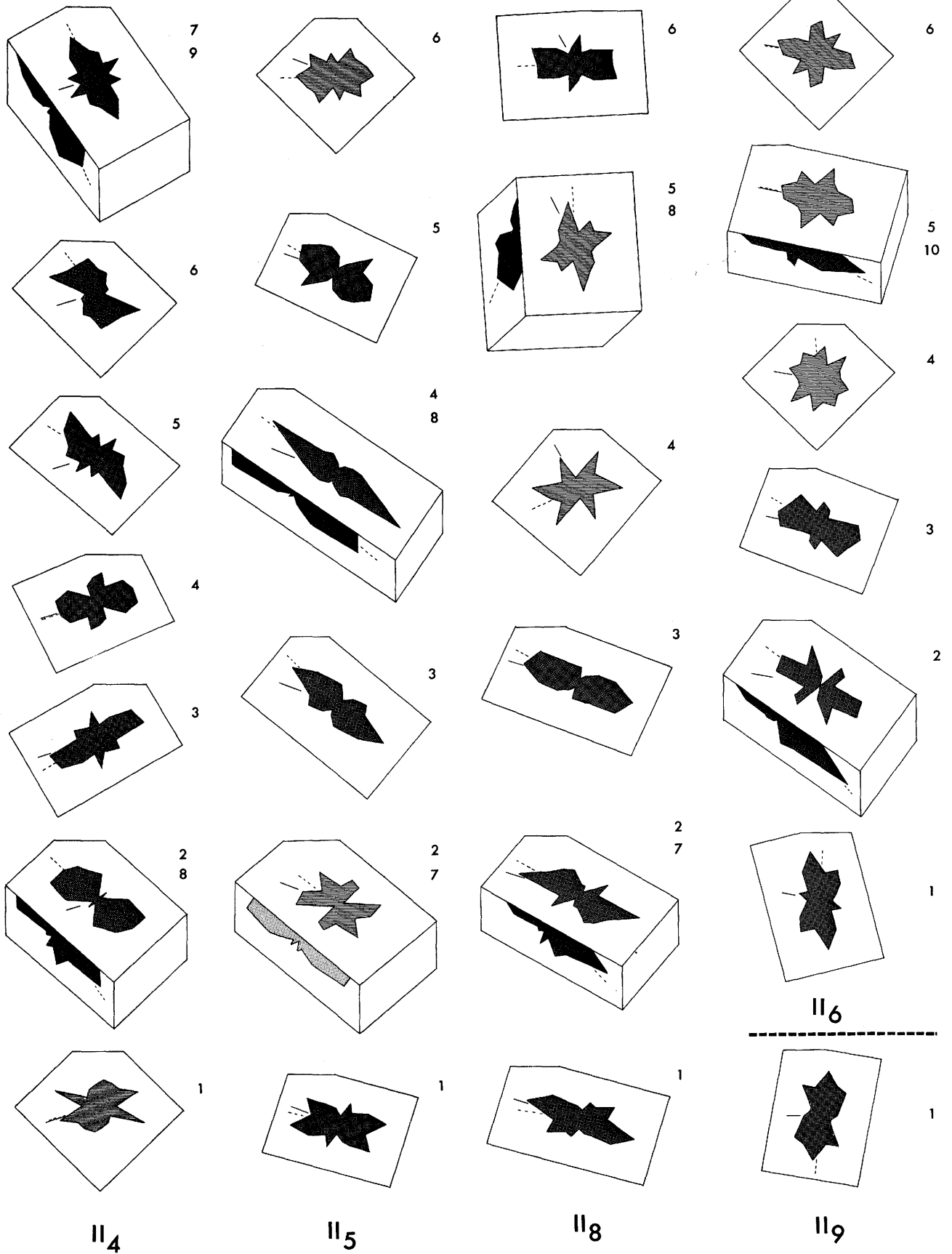


Fig. 3.7 - Grain orientation frequency distributions in bed G-66.

0 20 40 PERCENT GRAINS

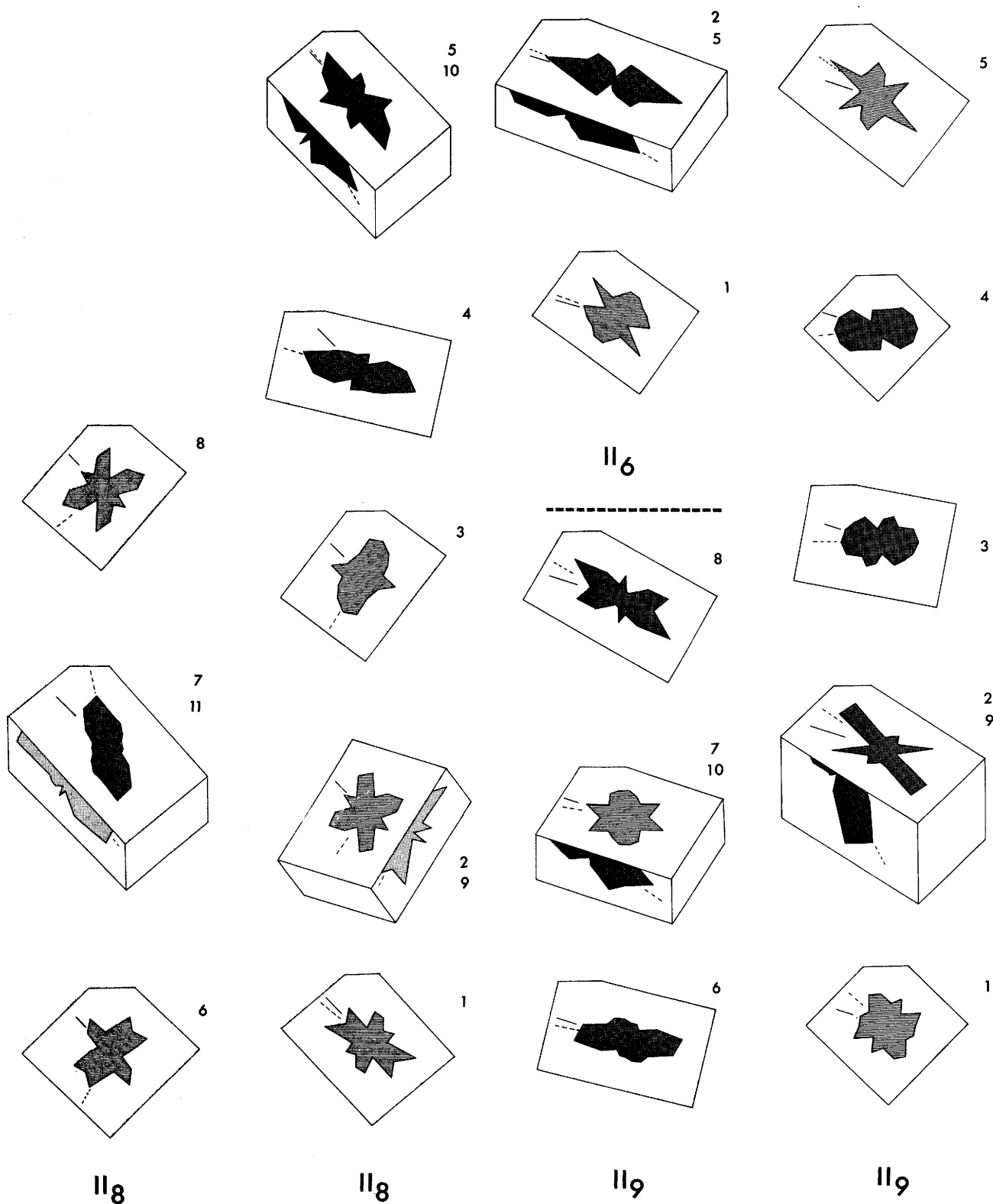


Fig. 3.8 - Grain orientation frequency distributions in bed G-65A.

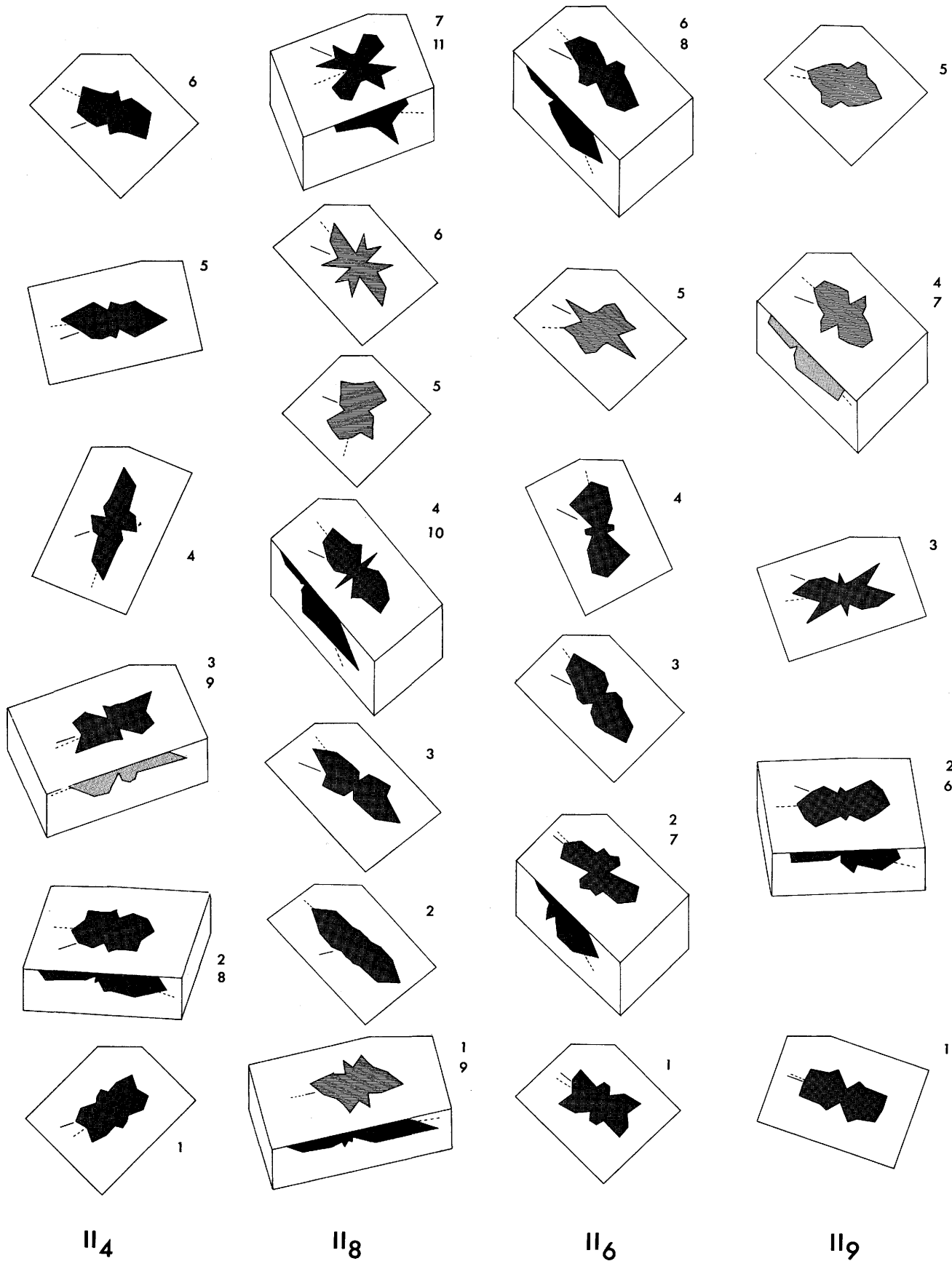


Fig. 3.9 - Grain orientation frequency distributions in bed G-65.

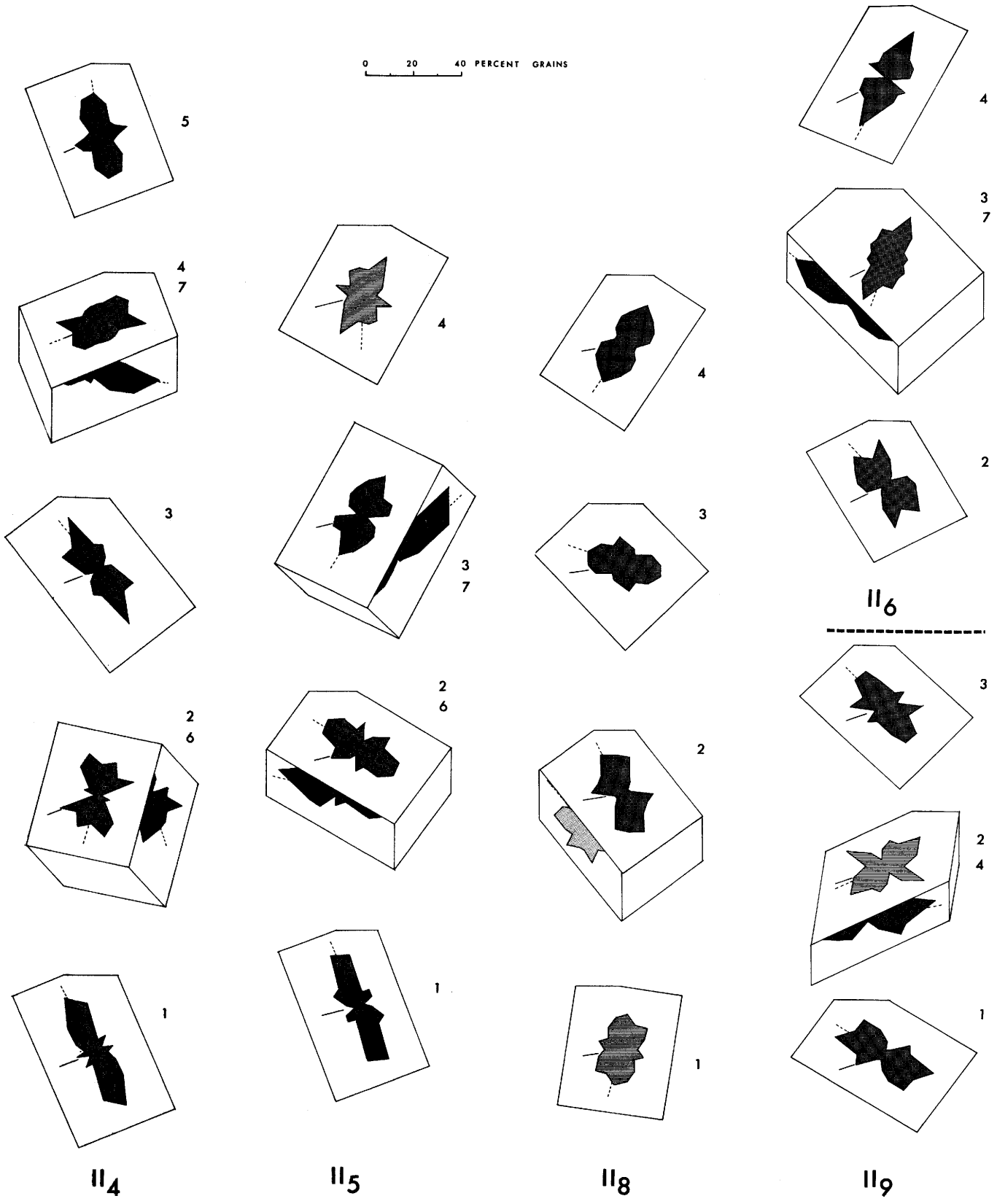


Fig. 3.10 - Grain orientation frequency distributions in bed G-58.

0 20 40 PERCENT GRAINS

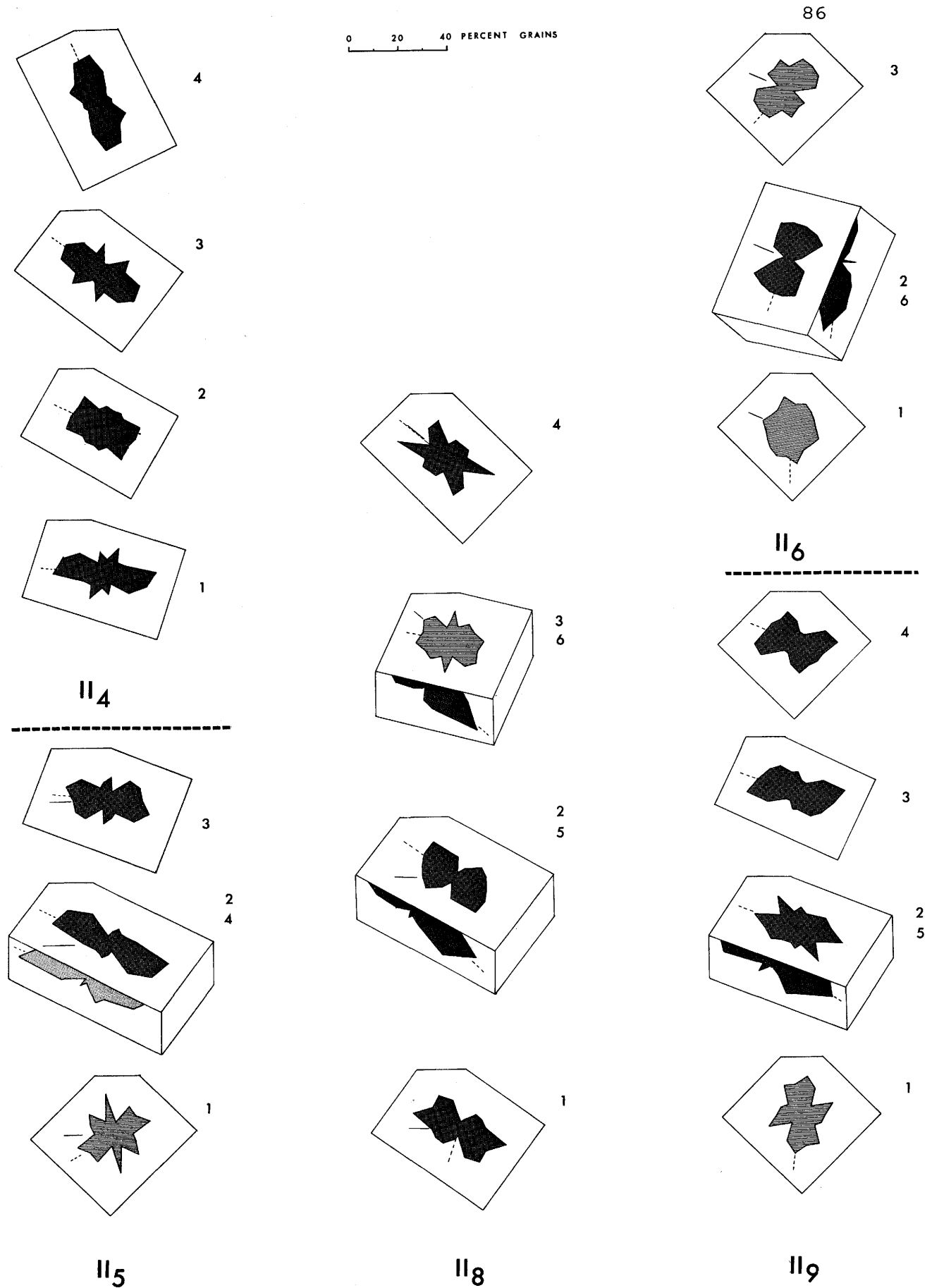


Fig. 3.11 - Grain orientation frequency distributions in bed G-50.

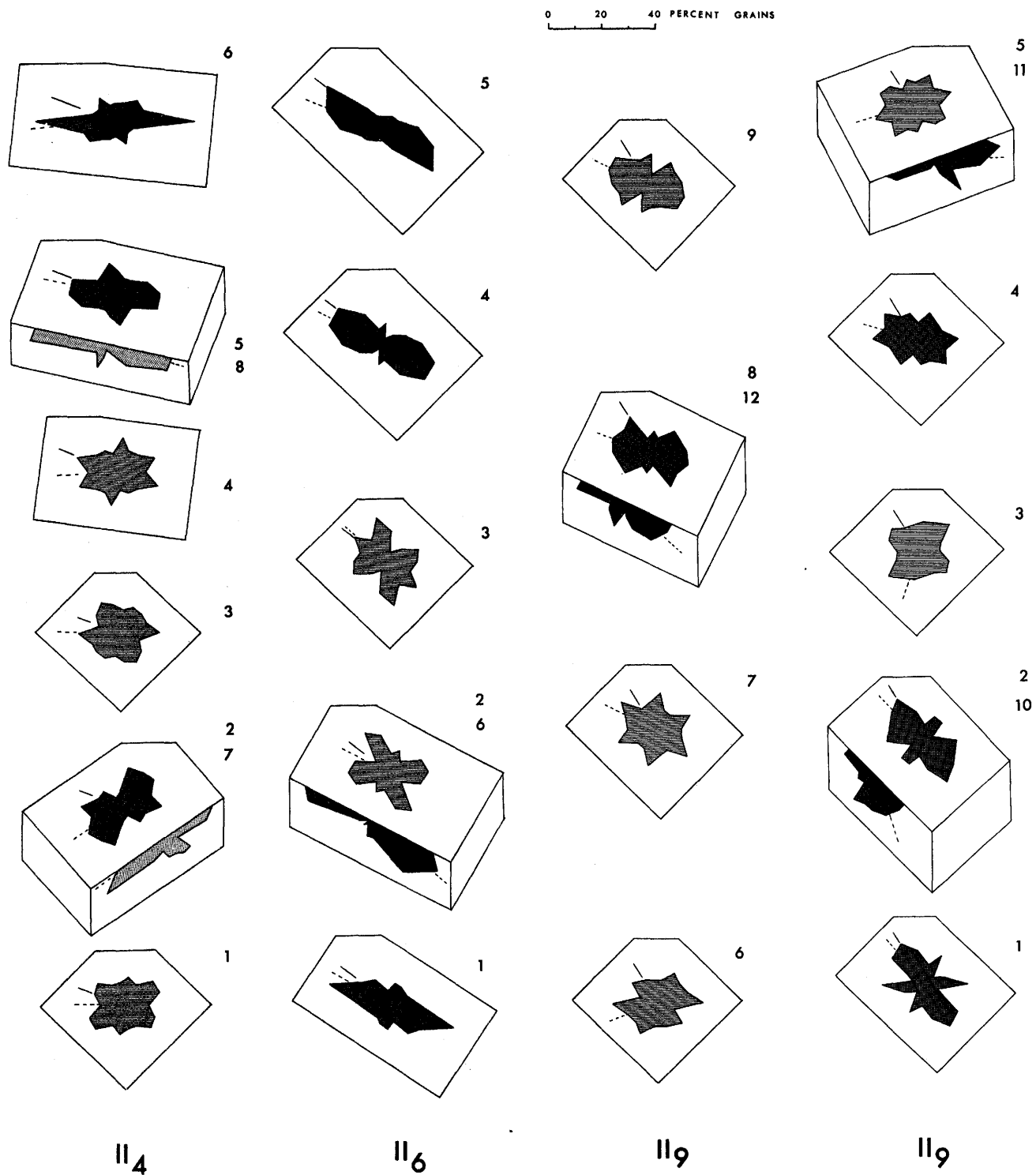
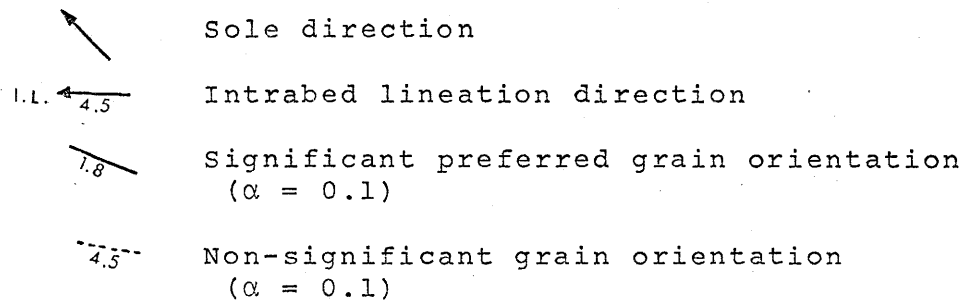


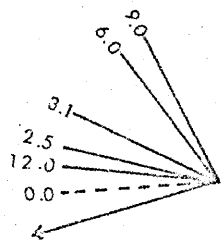
Fig. 3.12 - Grain orientation frequency distributions in bed G-49.

Fig. 3.13a-3.13h - Relation between vector mean directions of grain orientation distributions and sole directions for different beds.

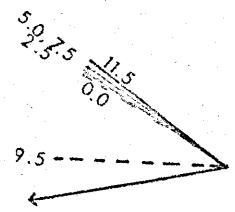


Figures along the marked directions indicate height in centimeters above the base of the bed.

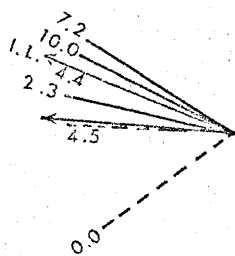
BED G-68



114

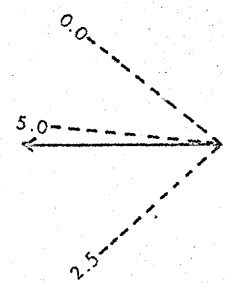


115

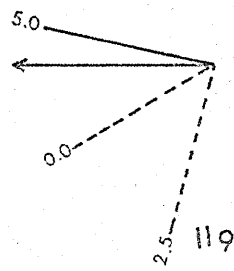


118

Fig. 3.13a

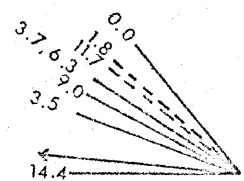


116

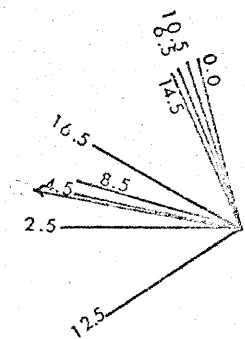


119

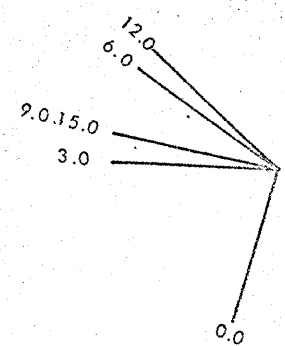
BED G-67



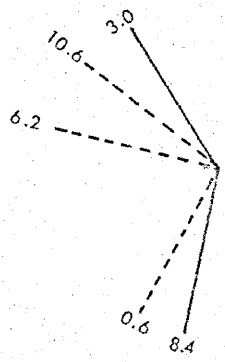
114



118



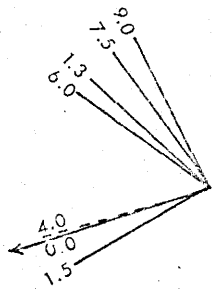
116



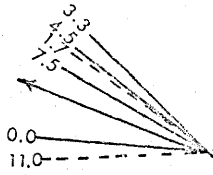
119

Fig. 3.13b

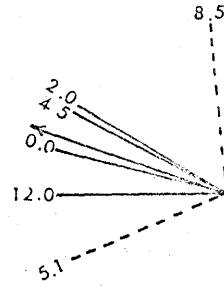
BED G-66



II4

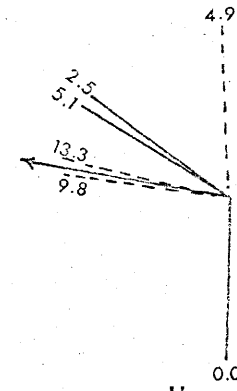


II5

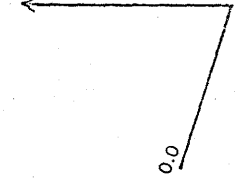


II8

Fig. 3.13c

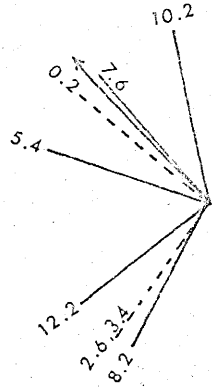


II6

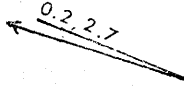


II9

BED G-65A

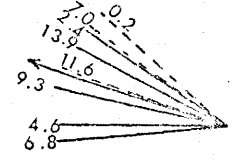


II8

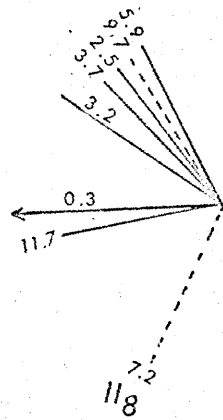
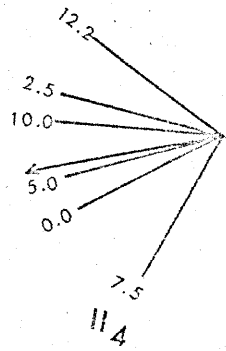


II6

Fig. 3.13d



II9



BED G-65

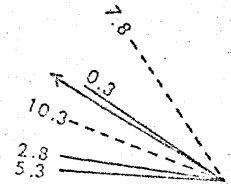
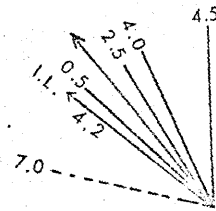
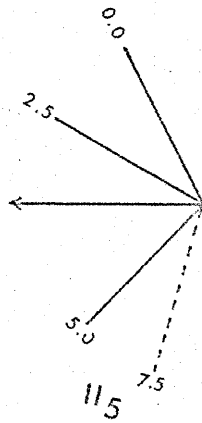
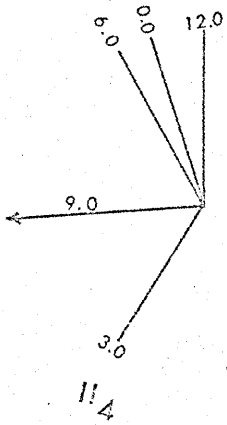


Fig. 3.13e



BED G-58

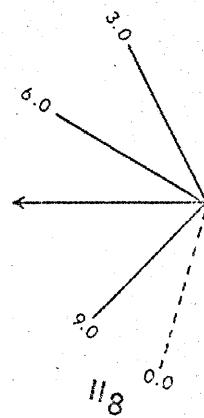
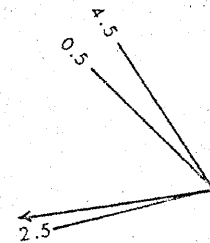
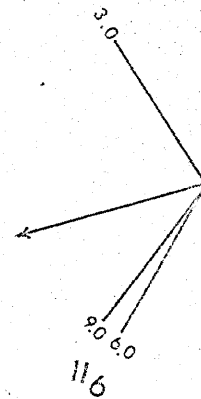
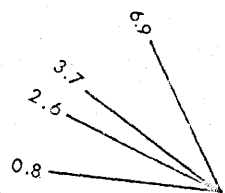
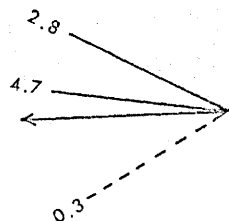


Fig. 3.13f



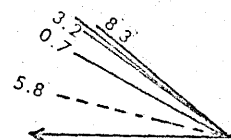


II4



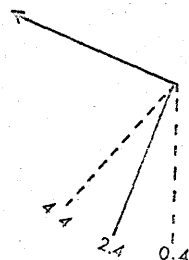
II5

BED G-50

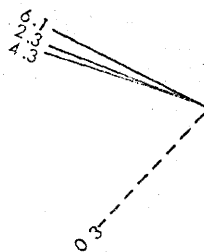


II8

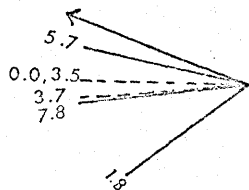
Fig. 3.13g



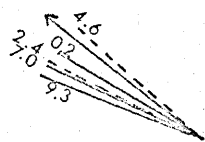
II6



II9



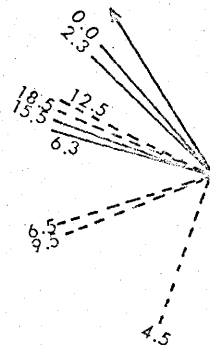
II4



II6

BED G-49

Fig. 3.13h



II9

orientations are marked by dotted lines.

Of 175 thin sections studied for grain orientation, 120 thin sections have statistically significant preferred orientations (table 3.6). The beds G-68, G-67, G-66 and G-50 have directed sole structures over part of the outcrop and the sense of direction (versus) of the current is known. The current was assumed to be from E or SE for the rest of beds with groove marks. The justification for such an assumption will be obvious after the discussion of imbrication. Figure 3.14 shows the deviations of grain orientation as related to sole marks. Most of the orientations are concentrated around the sole marks, and secondary modes at angles of nearly 60 degrees from the sole marks can be detected. Out of 110 thin sections with significant preferred grain orientations and from specimens with known sole directions, 34 thin sections have grain orientation directions which are not significantly different from sole directions within experimental error ($\pm 14.4^\circ$) at the 95% confidence level, 46 thin sections exhibit significant clockwise deviation from the sole and 30 thin sections show significant anticlockwise deviation from the sole. 55.5% of thin sections have deviation of less than 30° from the sole.

Variation of grain orientation and degree of preferred orientation in each bed are described below,

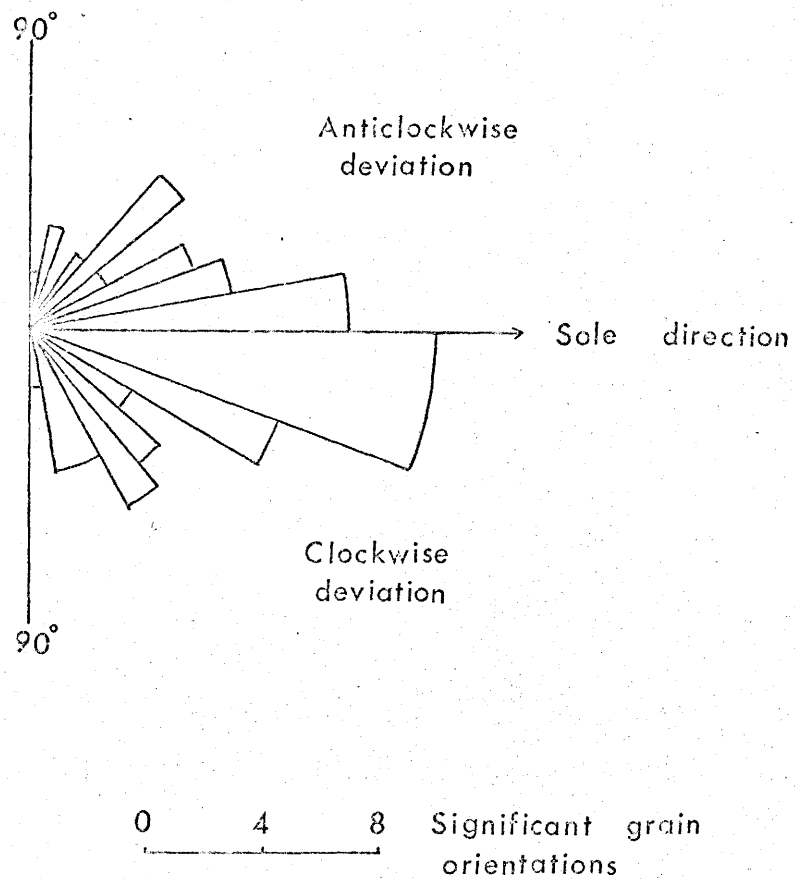


Fig. 3.14 - Frequency distribution of deviations of significant grain orientations from the sole direction.

Table 3.6

Summary statistics of grain orientation study

Bed no.	For thin sections cut parallel to bedding plane				For thin sections cut normal to bedding plane (for imbrication)	
	No. of thin sections studied	No. of significant preferred orientations	No. of significant bimodal orientations	No. of non-significant orientations	No. of significant orientations	Imbrication values different from zero
G-68	23	13	4	6	8	7
G-67	28	23	1	4	6	6
G-66	26	18		8	8	7
G-65A	23	17	1	5	6	4
G-65	18	9	2	7	9	6
G-58	19	17		2	6	6
G-50	18	13		5	5	4
G-49	20	10		10	6	4
Total	175	120	8	47	54	44

and significant grain orientations are compared with graptolite orientations observed in the field.

(i) Bed G-68 - In the bed G-68, two thin sections from section II₉ and all three thin sections from section II₆ have non-significant preferred orientation (figs. 3.5, 3.13). Two thin sections from each of sections II₈ and II₅ show non-significant orientation. Thus there is a slight indication that grain orientations tend to be non-significant more often in the eastern regions than in the western region. Also, all thin sections cut close to the base of the bed demonstrate a non-significant preferred orientation.

All significant preferred orientations are close to the sole or deviate from it by a small angle from section II₉ to II₈. At section II₅, there is a constant clockwise shift of nearly 45° from the sole. At section II₄, there is a gradual shift from sole parallel to nearly sole normal position from the bottom towards the top of the bed. At the top again, the preferred orientation reverts back closer to the sole mark.

Thin section II₆-68-4 seems to have come from the lower part of the overlying bed as shown by its preferred orientation, high percentage of matrix, poor sorting and coarse grain size. It was included in the bed G-66 by mistake, as it was not possible to locate

the contact clearly between the two beds in the specimen. So it has been left out of consideration in all the discussion.

Graptolite orientations between the 350 and 1200 yard points are close to the sole, but at the 130 yard point (close to the section II₄), a gradual change from sole parallel position at the base of the bed to nearly a 60° clockwise shift from the sole towards the top of the bed is noticed. Thus, there is close agreement between the graptolite and grain orientation results.

(ii) Bed G-67 - The bed G-67 has three non-significant orientations at section II₉ and two non-significant orientations at section II₄ (fig. 3.6). Because of amalgamation at the bottom at sections II₉ and II₆, no sole directions are available for comparison with grain orientations. From the few sole directions which are available in this region, it can be assumed that sole directions are usually from east to west or a few degrees north of west. This will lead to the conclusion that significant grain orientations are nearly normal to the sole direction at section II₉ and all grain orientations from section II₆, except the basal one, are probably parallel to the sole direction.

At section II₈, all the grain orientations are either parallel or normal to the sole. Though the specimen

II₈-67 does not show any apparent internal structure, it comes from a region, where the bed shows the development of small scale 'dish' structure. At section II₄, grain orientations are rather variable. However, a tendency of grain orientations to have a clockwise deviation of $\sim 35^\circ$ can be recognized.

Graptolite orientations studied at the 120 and 425 yard points have large clockwise deviations from the sole. Grain orientations from section II₄ from this region are in conformity with graptolite orientations.

(iii) Bed G-66 - In the bed G-66 at section II₆, all three thin sections from the upper part show non-significant grain orientations. Further west at section II₈, only two out of 6 thin sections show non-significant orientation. One thin section from each of sections II₅ and II₄ has a non-significant preferred orientation (figs. 3.7, 3.13). Thus a trend of non-significant to significant preferred orientations from east to west may exist in the bed G-66. It may be noted that non-significant orientations are from the upper part of the bed at sections II₆ and II₈.

From section II₉ to II₅, all the thin sections showing significant orientation with a few exceptions have grain orientations parallel to the sole mark. Thin sections II₆-66-1 and II₉-66-1, which come from very close

to the bottom of the bed show large deviations from the sole. Thin section II₅-66-3 has a clockwise deviation of 23°, and it has a secondary mode parallel to the sole. At section II₄, thin section II₄-66-2 from just below the joint shows a large deviation from the sole. In the upper part, there is a gradual shift of preferred grain orientations from a position of parallel to the sole direction at the base of the bed to that nearly normal to it towards the top of the bed.

Graptolites show consistently large clockwise deviations from the sole west of the 1975 yard point. In contrast, grain orientations show large deviations from the sole only at section II₄. A more detailed examination shows that the two studies are not as contradictory as they appear to be. High deviations of graptolite orientations from the sole at the 445 yard point occur above 15 cm from the base of the bed. Grain orientations at nearby section II₅ up to 12 cm above the base of the bed are in complete conformity with those of graptolites. Also large deviations of graptolites from the sole at the 1145 and 1970 yard points are in the upper part of the bed. It is suggested that these large graptolite deviations are related to non-significant grain orientations observed in this region (sections II₈ and II₆) from the upper part of the bed. It should be noted that some non-

significant preferred grain orientations have vector means normal to the sole.

(iv) Bed G-65A - Three thin sections from section II₉ and five thin sections from section II₈ show non-significant grain orientations. All the significant grain orientations at section II₉ exhibit a deviation of less than 25° from the sole. Grain orientations are very close to the sole at section II₆. At section II₈, the bed is divided into three parts by two bedding joints. The topmost and lowermost parts of the bed have non-significant or bimodal grain orientations and the middle part has mostly significant orientations. Non-significant grain orientations from the uppermost part have vector means nearly normal to the sole direction. Significant grain orientations are roughly parallel to the sole direction.

Graptolite orientations were studied only at two places. Graptolite orientations at the 3185 yard point are similar to grain orientations at section II₉ in the fact that usually deviations from the sole are small and deviations are both clockwise and anticlockwise from the sole. Large deviations of graptolites from the sole are observed at the 1135 yard point. In contrast at a nearby section II₈, grain orientations are either parallel to the sole or normal to it.

(v) Bed G-65 - Non-significant preferred grain

orientations occur towards the top of the bed at sections II₉ and II₈. Deviations of grain orientation from the sole are less than 30° at section II₉. The same is true of grain orientations at section II₆, except that the grain orientation just above the lower joint shows a high deviation from the sole. At section II₈, there is tendency to have a clockwise shift of nearly 60° from the sole. Grain orientation directions are variable at section II₄, and probably deviations of grain orientation from the sole are higher in the upper part of the bed than in the lower part of the bed (figs. 3.9, 3.13).

Since the bed shows large variation of both sole mark and graptolite directions over short distances, it is difficult to compare grain orientations and graptolite orientations. Generally angles of deviation from the sole and sense of deviation from the sole of grain orientations are comparable to those of graptolites.

(vi) Bed G-58 - One thin section each from sections II₅ and II₈ has non-significant grain orientation. Generally grain orientations tend to have a direction normal to the sole or make a wide angle with the sole direction (figs. 3.10, 3.13). Bed G-58 could not be split in the field, so no graptolite orientations were observed from this bed.

(vii) Bed G-50 - The bed G-50 has a general trend

of sole directions nearly E-W in the eastern region, except for two anomalous sole directions trending nearly in the N-S direction (fig. 2.1). Three grain orientations from the eastern section II₉ again give an E-W direction (figs. 3.11, 3.13). The basal thin section from section II₉ has non-significant preferred grain orientation and a vector mean nearly normal to general sole direction. At section II₆, all three thin sections have grain orientation direction normal to the sole direction. It should be noted that the bed shows poorly developed plane laminations at section II₆. The grain orientations are nearly parallel to the sole at sections II₈ and II₅. At section II₄, grain orientations have E-W direction at the base of bed and shift in clockwise direction towards the top of the bed by more than 50°.

Grain orientations conform to the observed sole parallel to graptolite orientations between the 400 and 2005 yard points, except that grain orientations are nearly normal to the sole at section II₆ where there are also poorly developed plane laminations.

(viii) Bed G-49 - The bed was studied for grain orientation only at sections II₉, II₆ and II₄ (figs. 3.12, 3.13). The bed has a large number of non-significant grain orientations distributed throughout the bed at the three sections. At section II₉, irrespective of the degree

of preferred grain orientation, there is a definite trend in the deviation of vector means from the sole. All grain orientations deviate from the sole in an anticlockwise direction in the lower part of the bed. Deviations increase from 9° at the base to nearly 40° towards the top of the lower part of the bed. Again the topmost three thin sections show anti-clockwise deviations between 30° to 40° from the sole. At section II₆, all vector means deviate less than 20° from the sole. Grain orientations are more variable at section II₄ and usually they have deviations from the sole less than 30 degrees.

Anticlockwise deviations of graptolites from the sole at the 120, 450 and 500 yard points are duplicated by grain orientations at section II₄. Graptolite orientations nearly parallel to the sole at the 1795 yard point are matched by similar grain orientations at nearby section II₆. At the 3170 yard point, graptolite orientations are close to sole direction, but it is noted that intrabed lination directions deviate from the sole from 5° to 30° in the anticlockwise direction in this region (fig. 2.1). A gradual shift of grain orientation from sole parallel to 40 degrees in the anticlockwise direction from the sole in the middle of the bed is in conformity with it.

Composite rose diagrams for each bed are obtained by adding the orientation frequency in each 20 degree

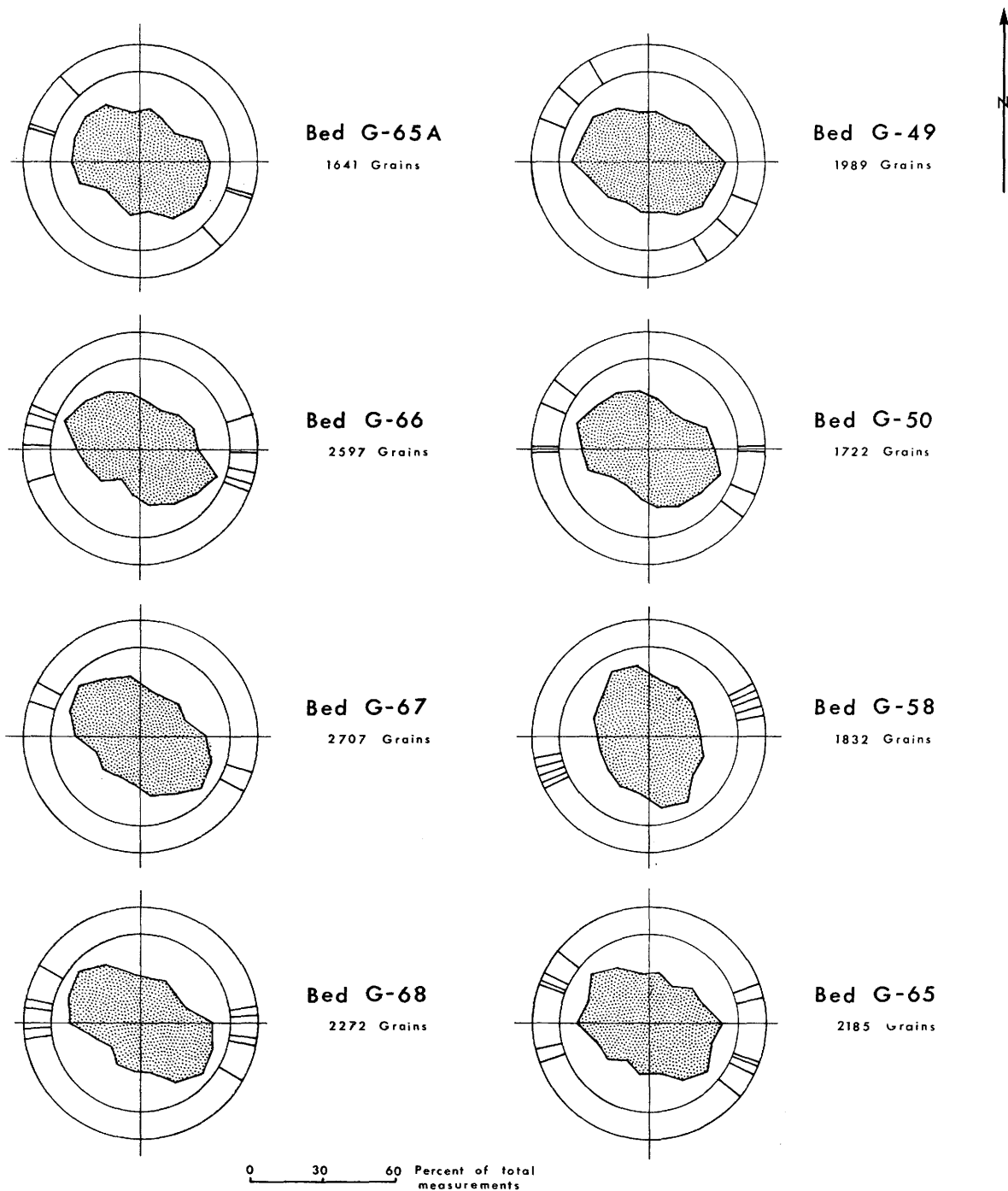


Fig. 3.15 - Composite grain orientation frequency distributions (inner circles) and sole mark directions (outer circles) for different beds.

class for all the thin sections for the bed and are plotted in the figure 3.15. Also, the sole mark directions for all the specimens studied for grain orientation are marked in the outer circle of the diagrams. Generally the grain orientation distributions and sole directions are in fair agreement. Beds G-66, G-67 and G-68 show an average clockwise deviation of grain orientations from sole marks and bed G-49 shows an average anticlockwise deviation. The sole normal grain orientations for bed G-58 are very well brought out.

Secondary Modes

Fifty-seven thin sections which showed no significant preferred grain orientation at the 90% level of confidence were further examined for bimodality. The line of movement data showing non-significant unimodes was multiplied by 4. If the resultant distribution tended to be unimodal with Raleigh Probability within the significant range (i.e., $\alpha = 0.1$), the sample was considered to exhibit two modes 90 degrees apart, otherwise the orientation distribution was taken to be uniform. The results are summarized in Appendix I under the bimodal test. Since there is no statistical procedure known for testing for the bimodal distribution other than 90° apart modes or for testing for polymodal distribution, the arbitrary method of visual

estimation of the type of grain orientation distribution as seen in the rose diagrams was employed.

Only eight of the observations with non-significant unimodes show statistically significant modes 90° apart. In all of these thin sections except one, visual examination of orientation distributions confirms this; but in the case of thin section II_8-66-3 , a unimode at the 85% level of confidence would have been a better decision. Of the thin sections with bimodal distributions, two thin sections (II_6-68-1 , II_8-68-1) come from very close to the bottom of the bed. Thin section II_9-67-5 belongs to a specimen which has mostly sole normal or non-significant grain orientations. Two other thin sections ($II_8-65A-6$ and $II_8-65A-8$) come from the topmost part of the bed.

It has been found that visual examination is a powerful tool for finding the type of orientation (Martini, 1965, p.175), so all the rose diagrams were examined irrespective of their statistical significant of preferred orientation. Visual examination brings out some interesting features -

(i) In some of the basal thin sections (e.g., II_8-66-1 , II_4-49-1 , $II_6-65A-1$, II_4-66-1), there are two distinct modes. One of the two modes is parallel to the sole and the other is oblique to the sole. This could be due to the fact that local irregularities at the bottom are influencing

the orientation of particles to some extent and may produce a mode at an angle to the direction of the current.

(ii) Some of the thin sections, classified as having uniform distribution by the procedure described above, show recognizable secondary modes approximately normal to the observed primary modes. These include 8 thin sections (II₆-68-3, II₉-67-3, II₆-66-5, II₆-66-6, II₈-65A-2, II₈-66-5, II₉-50-1) which would be classified as having bimodal distributions with 90° apart modes if the confidence limits were lowered to $\alpha = 0.25$.

Imbrication

To study three dimensional orientation of quartz grains, 55 thin sections were cut parallel to the bedding plane vector mean and perpendicular to the bedding plane and studied for grain orientation. The angle between the vector mean of these thin sections and the horizontal (or the bedding plane) is called the angle of imbrication or simply imbrication. The orientation frequency diagrams for the imbrication study are plotted along the appropriate orientation frequency diagrams of thin sections cut parallel to the bedding plane and orientation statistics are summarized in Appendix II.

Fifty-four thin sections show a significant preferred orientation at the 90% level of confidence. 44 thin sections

have imbrication values significantly different from zero at the 95% level of confidence. 20% of the thin sections studied for imbrication have an angle of imbrication less than 5 degrees and 87.2% of the thin sections have imbrications less than 20 degrees. In the case of bed G-68, G-66 and G-50, which have directed sole structures over part of the outcrop so that upcurrent and downcurrent directions can be determined with certainty, 20 thin sections out of 21 which were cut nearly parallel to the sole structures and have imbrication values different from zero, exhibit upcurrent imbrication.

Other points of interest are:

(i) There is a reversal in imbrication direction from the lower to the upper part of the bed for specimen II₅-68 and change of imbrication direction is from upcurrent to downcurrent direction. This suggests that imbrication values from close to the base of the bed are more reliable than from the upper portions for determining the sense of current direction.

(ii) Specimens II₈-67 and II₈-65A demonstrate a larger imbrication parallel to the sole direction than in a direction nearly normal to the sole.

(iii) The angle of imbrication for 40 thin sections which are cut parallel to or at small angles to the sole direction is plotted against grain size in figure 3.16.

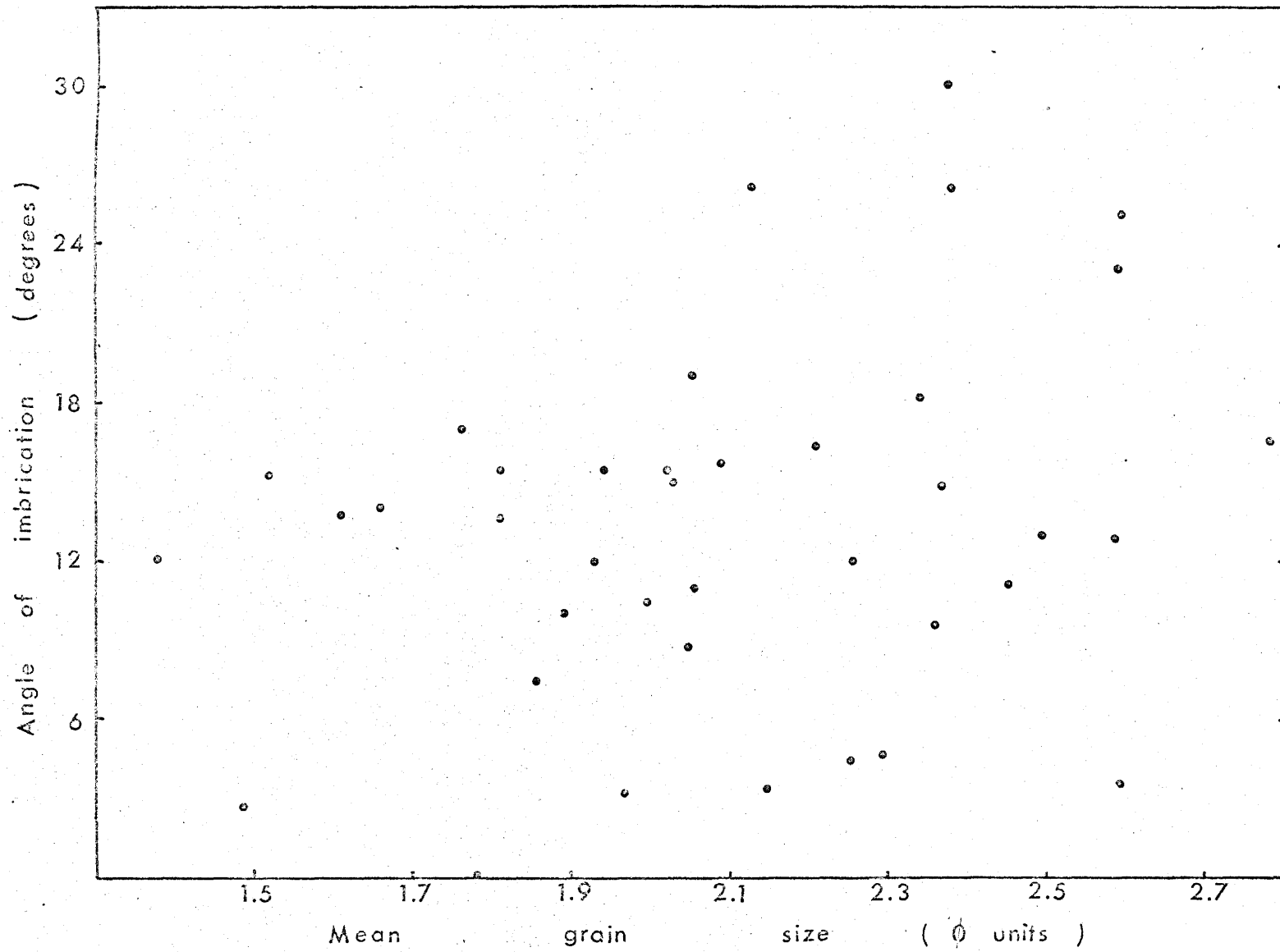


Fig. 3.16 - Plot of angle of imbrication vs. mean grain size.

There is no apparent relationship between grain size and imbrication values, except that imbrication angles greater than 18° are confined to grain sizes smaller than 2.0 phi.

Similarly it is not possible to detect any correlation between the value of imbrication and degree of preferred grain orientation parallel to the bedding plane.

(iv) Figure 3.17 shows polar plot of all the imbrication values. Most of imbrications have a dip direction between $N0^{\circ}$ and $N180^{\circ}$. Extensive measurements of sole directions by Enos (1965, table 9) show an easterly source of the depositing currents and therefore most of the imbrications are interpreted to dip in the upcurrent direction.

In contrast to the present results, Kopstein (1954) reported a predominantly downcurrent imbrication in coarse grained massive beds and absence of distinctly preferred orientation in finer material. Bassett and Walton (1960), however, claimed that the grain orientations recorded by Kopstein were mainly a result of metamorphism. Smoor (1960) found a significant upcurrent imbrication in grey-wackes from the Normanskill Formation. Bouma (1962, p.85), Dzulynski and Slacka (1958; in Bouma, 1962, p.85) and Colburn (1968) noted that in samples near the base of the bed, elongate grains dipped upcurrent, but in higher levels

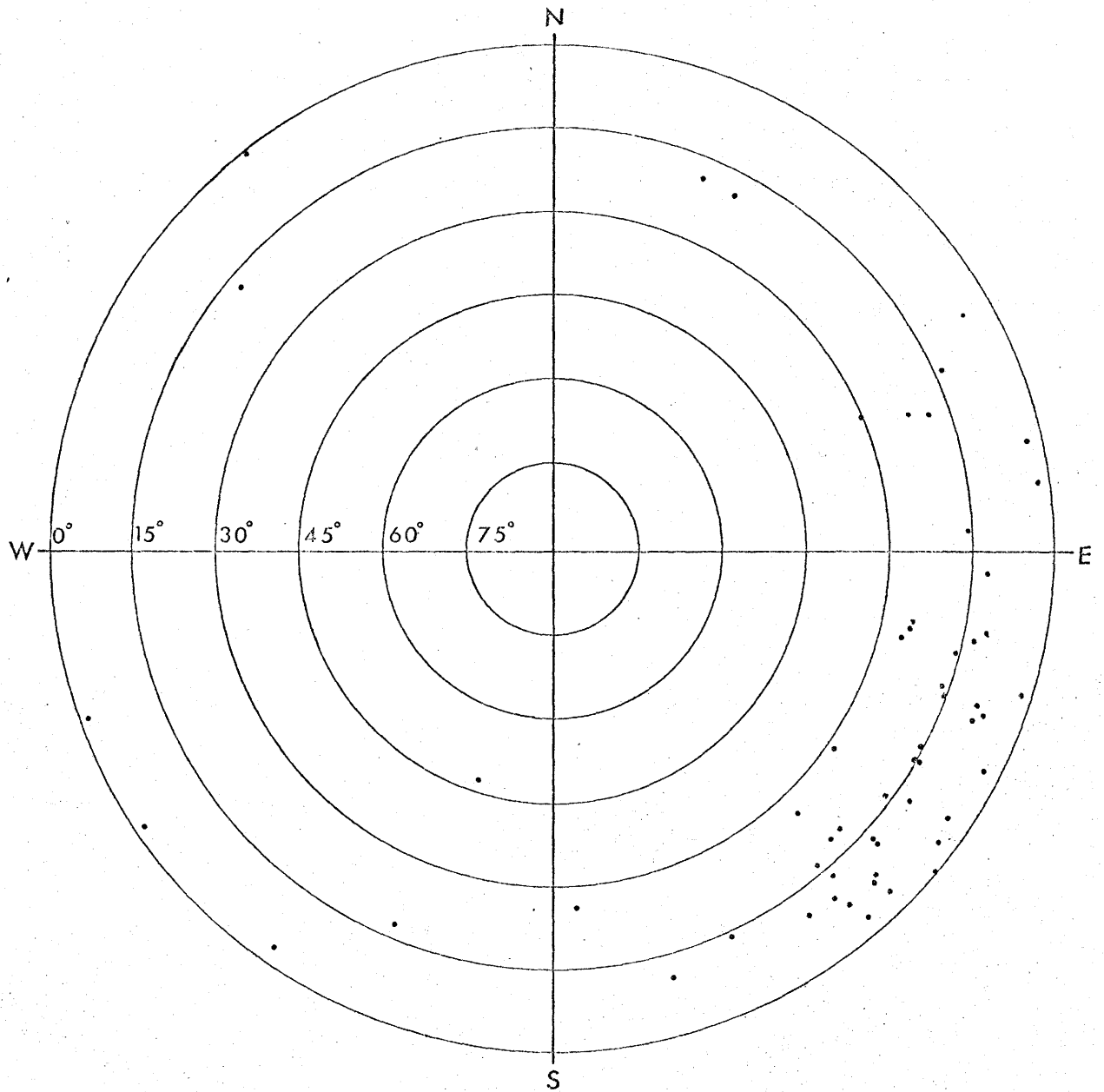


Fig. 3.17 - Polar plot of grain imbrications. The lower hemisphere is used to project grain imbrications onto the horizontal plane.

they dipped downcurrent. Sestini and Pranzini (1965), Henningsen (1968) and Onions and Middleton (1968) found mostly upcurrent imbrications. Sestini and Pranzini (1965) observed imbrication values other than zero in a direction normal to the sole. Also, Onions and Middleton (1968) noted that eighty percent of thin sections studied showed an average imbrication of 15° to 25° from the horizontal.

Since it has been demonstrated that grain imbrication is commonly upcurrent, this may be used as a criterion for determining the sense of direction of the depositing currents for beds with grooves as sole marks. Using this criterion for beds G-49, G-58, G-65 and G-65A yields the following results.

(a) Most of the imbrication directions for bed G-65A indicate that the depositing current was from SE and not from the reverse direction.

(b) As the bed G-65 is traced from east to west along the outcrop, the grooves at the base of the bed show a gradual change in direction from NW to W to SW. Two interpretations are possible: (i) the depositing current originated somewhere in the eastern region and flowed towards directions given above, and (ii) the current originated in the western region and flowed in the reverse direction, i.e., NE to E to SE. The first alternative is more probable on the basis of imbrication directions.

(c) Grain orientations are either parallel to the sole or nearly normal to the sole for bed G-58 and imbrication directions are variable. It is difficult to postulate a definite direction of the depositing current from imbrication directions.

(d) Imbrications dip due SE for the bed G-49 at sections II₆ and II₉ and current was probably from SE in this region. Two thin sections for imbrication study from section II₄ cut at large angles to each other at different levels in the bed show imbrication values close to zero, so it is difficult to assess the versus of direction of the current in this region.

Conclusions

(i) Quartz grains and graptolites show similar patterns of orientation within individual beds. Also, grain orientations and graptolite orientations are not local features, but exhibit certain regular variation in the individual beds all along the outcrop.

(ii) In the beds G-68, G-67 and G-66, there is a slight tendency for non-significant preferred grain orientations to occur in the eastern sections more often than in the western sections. In the bed G-67 (at section II₉), non-significant grain orientations are associated with sole normal orientations or bimodal orientations. In

the bed G-66, the non-significant grain orientations occur only in the upper part of the bed and some of these grain orientation distributions may be bimodal.

(iii) Deviations of significant grain orientations from the sole directions are mostly small in the eastern sections for beds G-68, G-67, G-66 and G-50 and are large in the western regions. Bed G-67 at section II₈ and bed G-50 at section II₆ have grain orientations nearly normal to the sole associated with the presence of small scale 'dish' structure and plane laminations respectively. There may be a gradual change in the direction of grain orientation at the westernmost section from the sole parallel position at the base of the bed to nearly sole-normal orientation towards the top of the bed. An almost similar pattern is shown by bed G-65.

Bed G-58 has a variable grain orientation. Most grain orientations make a large angle with the sole direction.

Significant preferred grain orientations show both clockwise and anticlockwise deviations from the sole. There is no definite preference for either deviation.

(iv) Many thin sections from close to the base of the bed have non-significant orientation, significant preferred orientation with a direction normal to the sole, or even bimodal orientation.

(v) A few thin sections from close to the

bedding joint show sole normal orientations.

(vi) Quartz grains in most samples show upcurrent imbrication.

CHAPTER IV

GRAIN SIZE AND SHAPE STUDY

The objective of this chapter is to supplement the grain orientation observations with grain size and shape data, since grain fabric is affected greatly by these two textural parameters. Also, grading characteristics may provide significant clues to size distribution in the depositing currents as theoretically demonstrated by Scheidegger and Potter (1965).

Experimental Details

The size and sphericity of grains were studied on a Shadowmaster. The grains were selected in a similar manner as for grain orientation study with the help of a point counter. The two axes 'a' and 'b' for each grain are defined in the same way as for the orientation experiments. The size of grains in ϕ units is given by the formula

$$\phi = - \log_2 k\sqrt{ab}$$

where k is the factor to reduce the measured size of axes 'a' and 'b' on the Shadowmaster screen to millimeters.

The study was confined to quartz grains and grains

with size less than 0.05 mm were not measured.

As the purpose of the present study is mainly to examine the variation between samples, an experiment was run to study whether the measurements of only the longest axis instead of the two axes could be used as a size parameter of the grains. The cumulative curves of size distribution as determined from measurement of the two axes of grains for five thin sections from the bed G-66 at section II₆ are plotted in figure 4.1. Comparison of figure 4.1 with size distribution curves determined by measuring only the longest intercept in figure 4.2 shows that the mutual relationship between the different plots is the same in both cases. Thus the measurement of the longest axis of the grains seems to be an adequate measure of size for the purposes of comparison.

Thus only the 'a' axis was measured for all the thin sections and cumulative frequency distribution of quartz grains against size in ϕ units for different beds are plotted on probability paper in figures 4.4 - 4.11. Most of these plots are approximations to straight lines, thus showing that quartz grain size distributions are roughly log-normal.

Since no grains with size less than 0.05 mm were measured it might lead to an over-estimation of the mean size. However, Middleton (1962, p.730) found that

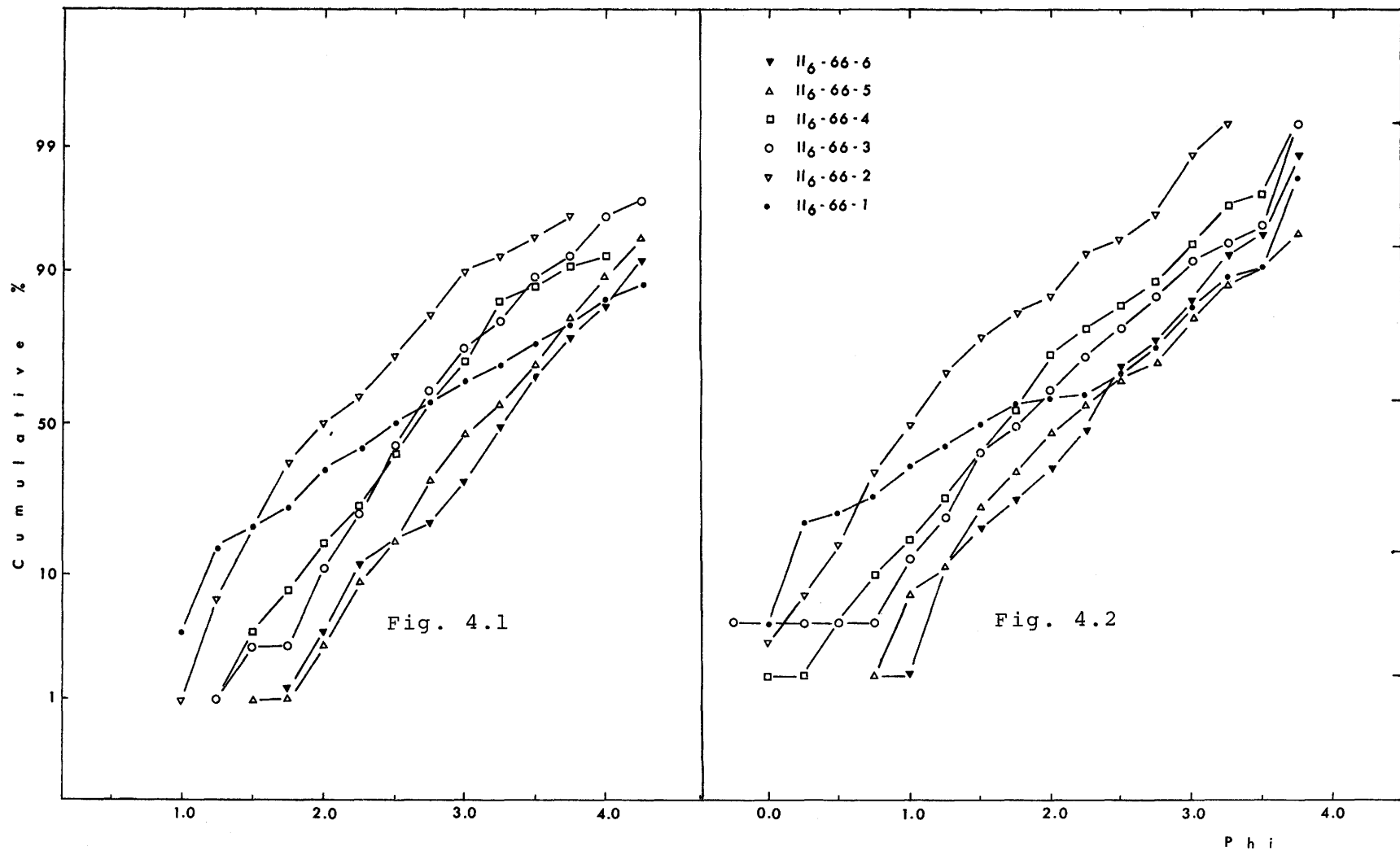


Fig. 4.1-4.2 - Cumulative curves of size distribution as determined by measuring two axes a and b (fig. 4.1) and by measuring only the longest axis (fig. 4.2) for bed G-66 at section II₆.

the effect of censoring the grain size population was quite small, so no correction was applied for sample truncation.

The variance and higher moments about the mean size of quartz grains, i.e., m_2 , m_3 , m_4 and Fisher's k_2 , k_3 , k_4 , g_1 and g_2 statistics, were computed using I.B.M. 7040 computer (see the author's Tech. Memo. 68-2) and are listed in Appendix III. The formulae for calculating the different statistics are given by Yule and Kendall (1950, p.151-161). The variance is given by m_2 and k_2 statistics and these are measures of sorting of quartz grains. Statistics m_3 , k_3 and g_1 are measures of skewness. Kurtosis is estimated by calculating m_4 , k_4 and g_2 . The expected values of k_3 , k_4 , g_1 and g_2 for a normal population are zero.

Operator consistency in determining mean size was estimated by running a replicate experiment. Ten thin sections selected randomly from all those available were duplicated after a time interval of 4 weeks. The results are plotted in figure 4.3. Grain size statistics are given in table 4.1. A t -test for paired observations was applied to the data on mean size. The calculated value of t is 0.251 and value of $t_{9,0.95}$ from tables is 2.262. So the hypothesis that there is no difference in

the mean size of different thin sections between first and second counts is accepted.

The 95% confidence limits for the above experiment are $\pm 0.176 \phi$, which include the operator error and some sampling error due to the fact that the traverses made in selecting the grains were not the same in the second count as in the first count.

An analysis of variance was made to determine the amount of error which might be introduced by the operator in the mean size determination. The results are shown in table 4.2. The F-test shows that the operator error is non-significant. Variance component due to inconsistency of the operator is negligibly small and most of the variance is contributed by differences in the mean size of the different thin sections.

Table 4.1

Summary statistics: operator experiment - mean size

Thin section	Point count 1		Point count 2	
	k_1	k_2	k_1	k_2
II ₄ -50-4	2.326	0.438	2.268	0.418
II ₈ -65A-1	1.918	0.342	2.025	0.405
II ₈ -66-6	2.325	0.684	2.404	0.775
II ₆ -50-2	2.319	0.553	2.377	0.521
II ₉ -67-3	1.772	0.436	1.827	0.473
II ₆ -66-3	2.104	0.723	2.172	0.761
II ₉ -65-3	2.164	0.653	2.216	0.725
II ₄ -58-2	1.872	0.567	1.812	0.737
II ₉ -49-3	2.032	0.488	2.085	0.464
II ₈ -67-2	1.959	0.601	1.904	0.884

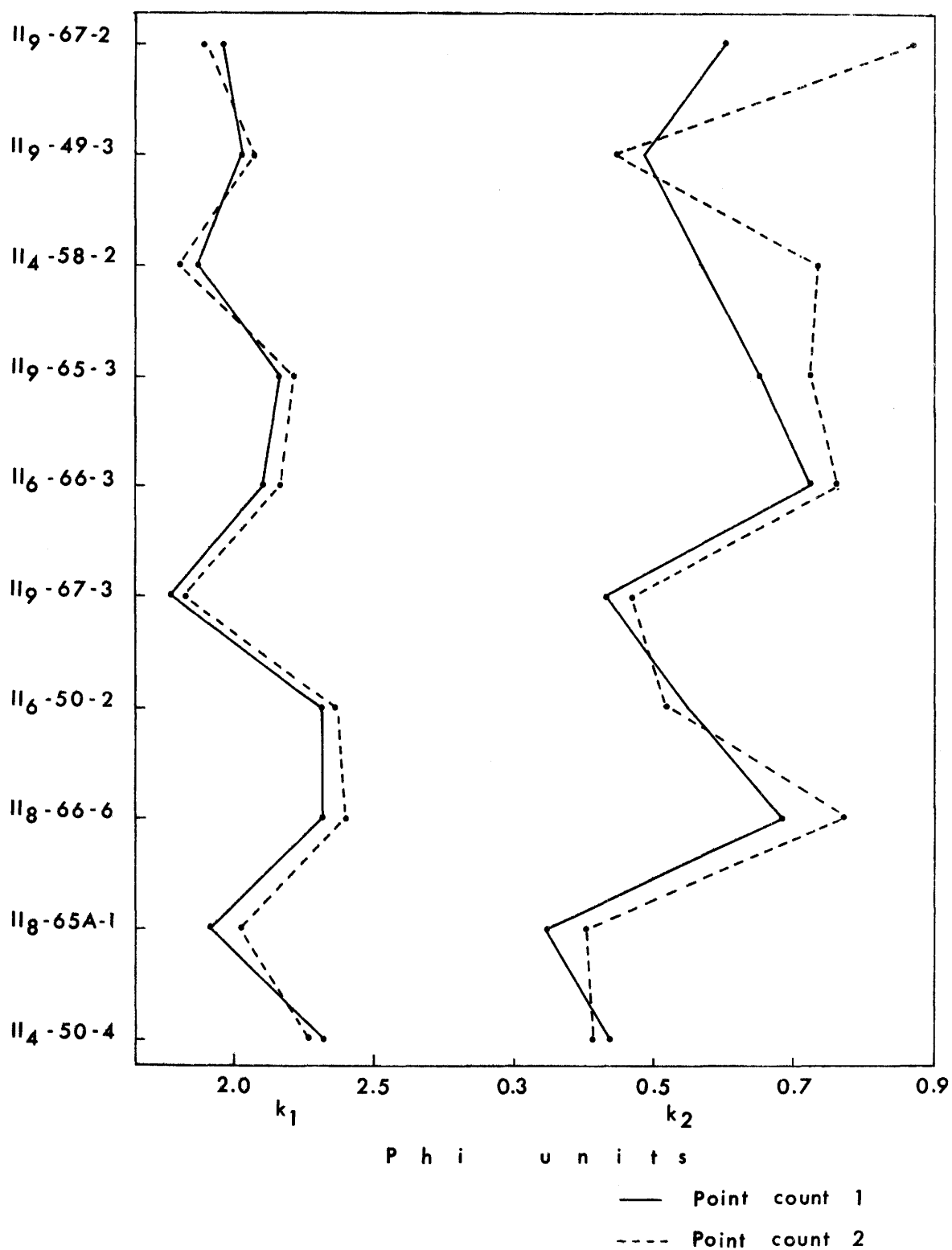


Fig. 4.3 - Operator consistency in determination of the mean grain size and sorting.

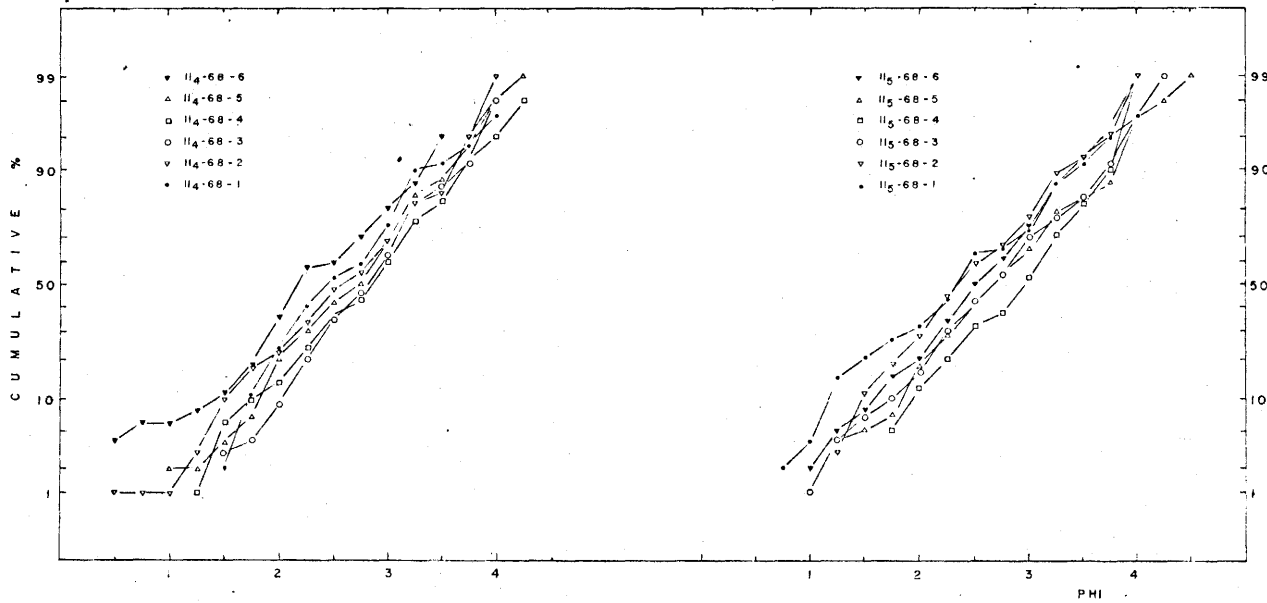
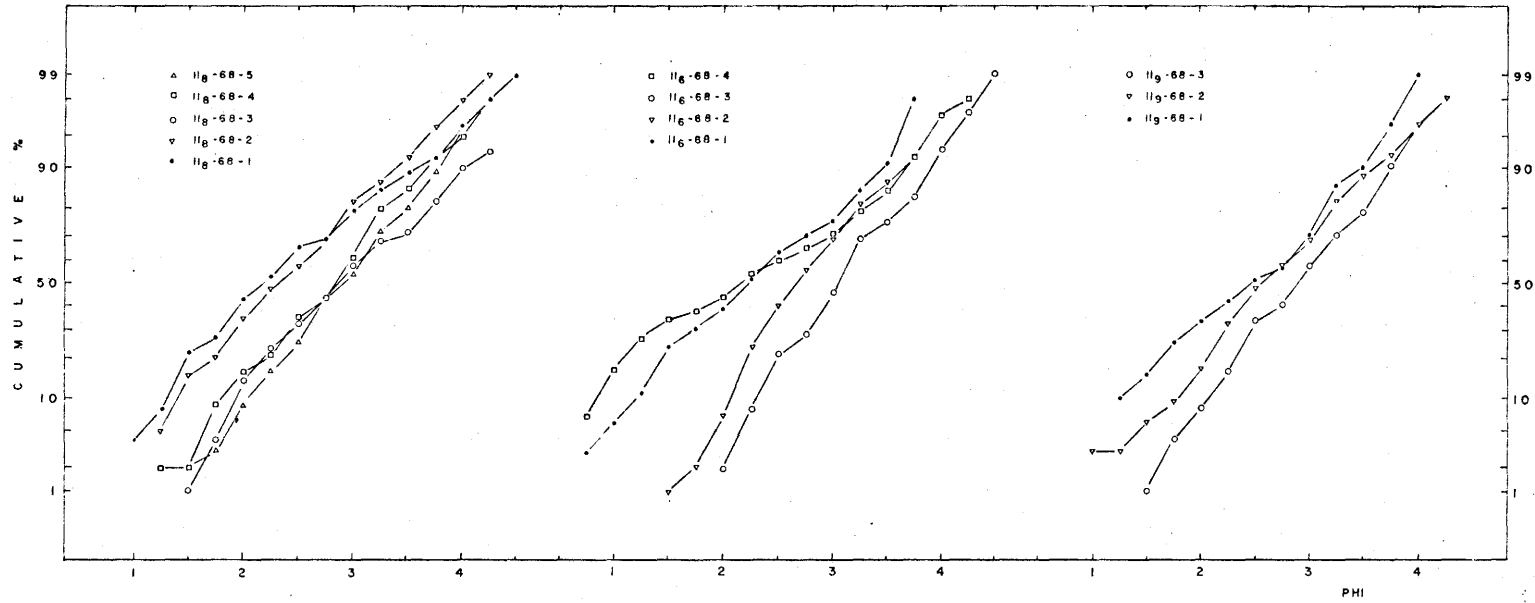


FIG. 4.4: CUMULATIVE GRAIN SIZE DISTRIBUTION CURVES FOR BED G-68

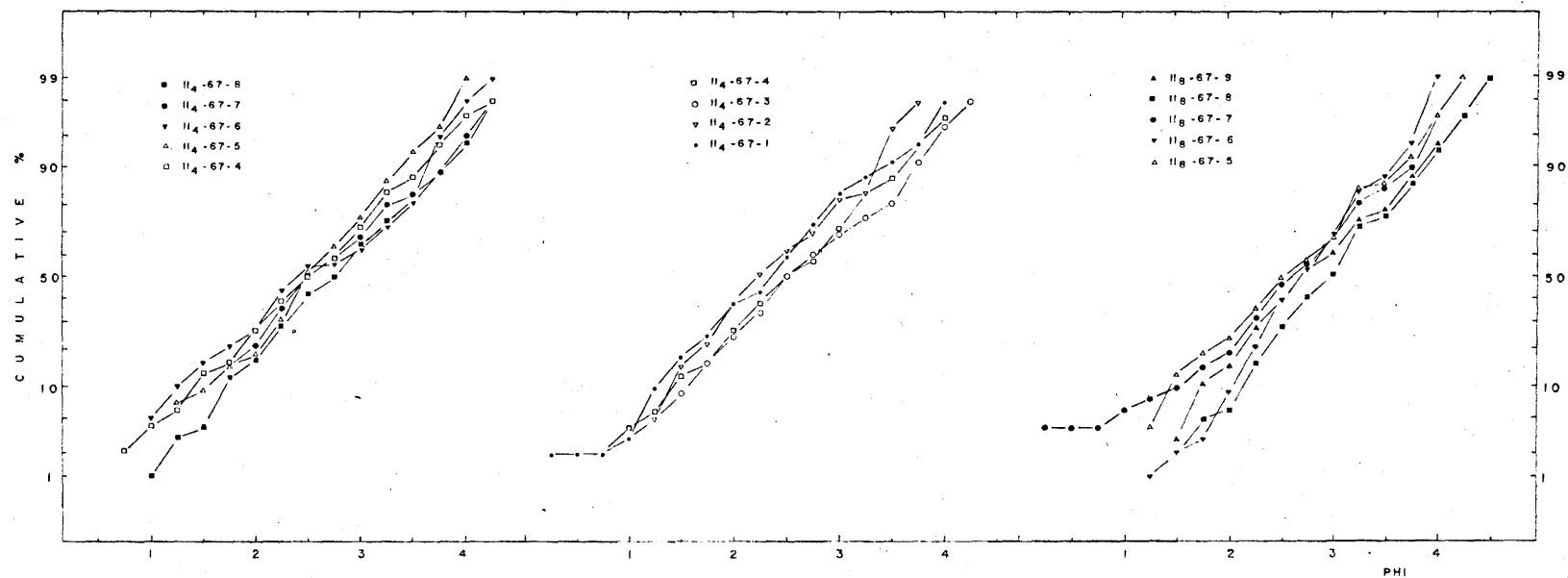
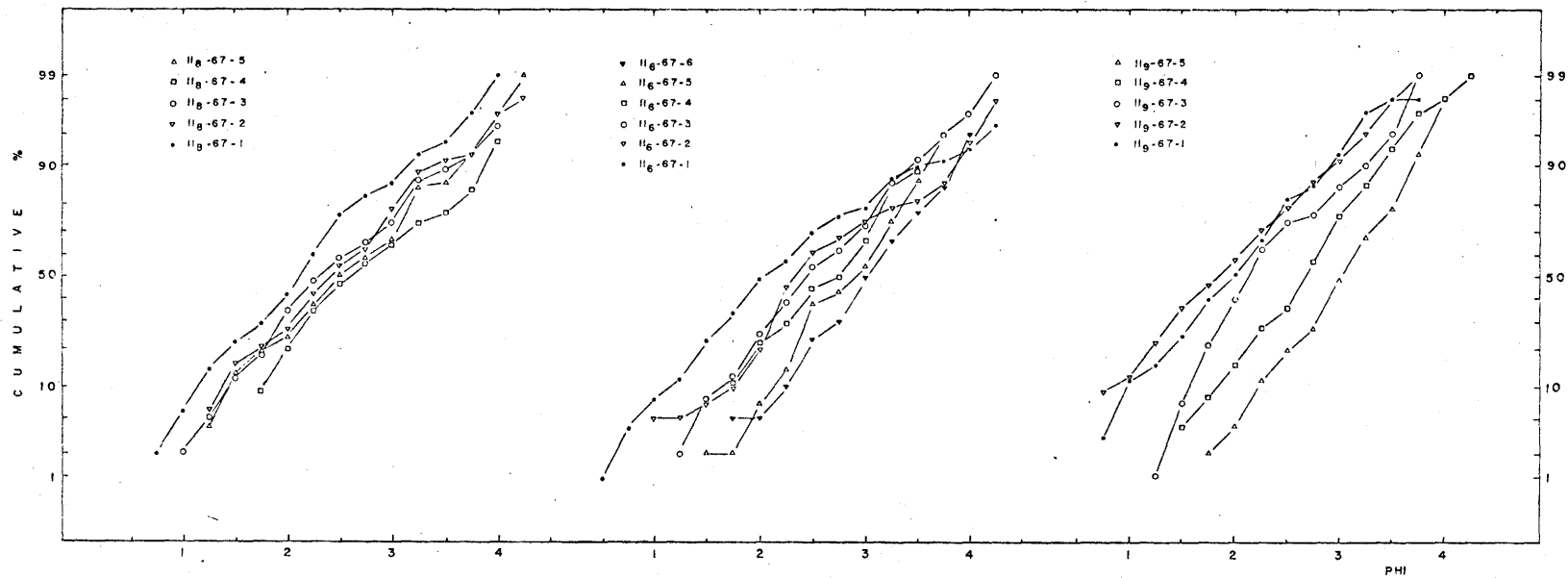


FIG. 4.5: CUMULATIVE GRAIN SIZE DISTRIBUTION CURVES FOR BED G-67

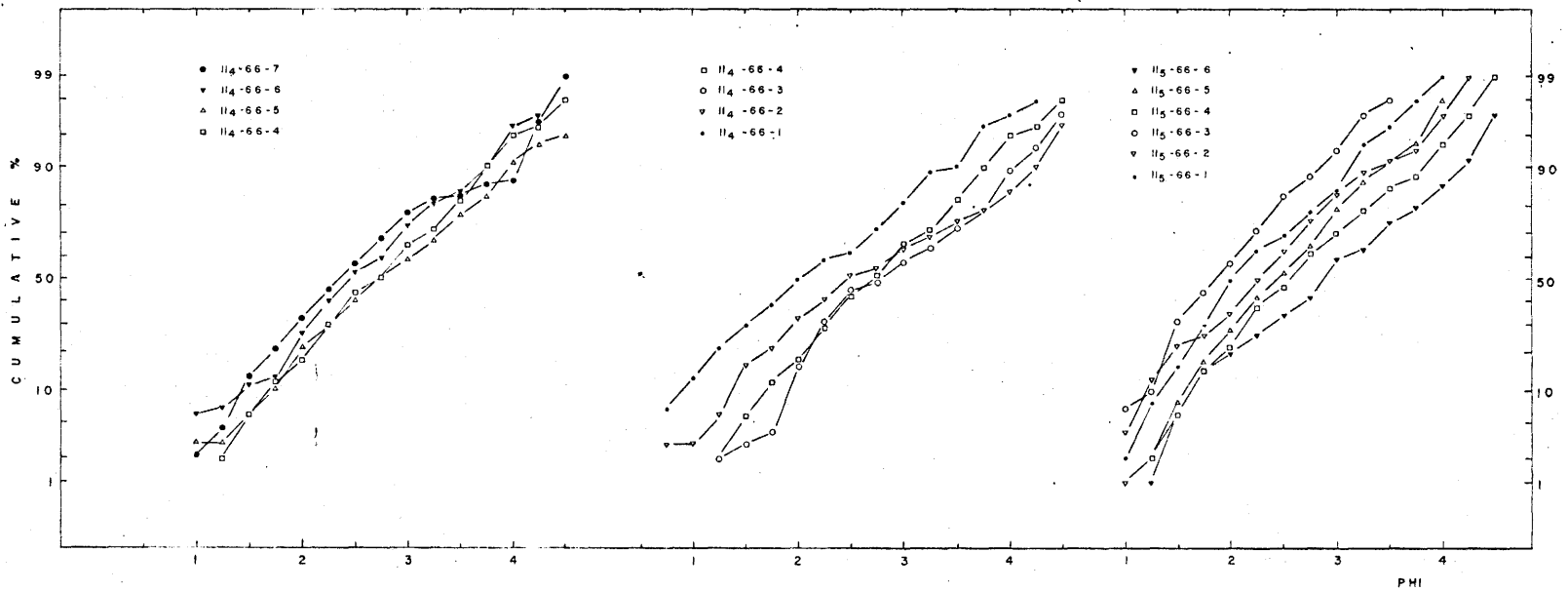
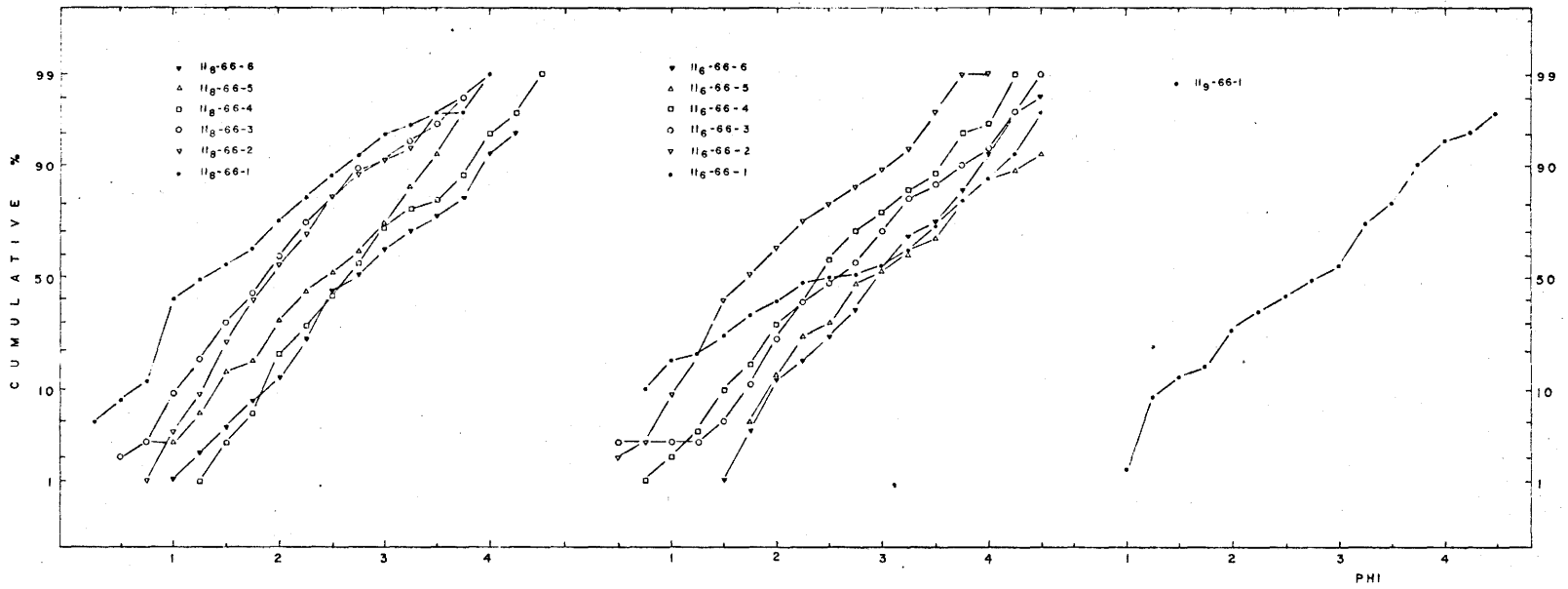


FIG. 4.6: CUMULATIVE GRAIN SIZE DISTRIBUTION CURVES FOR BED G-66

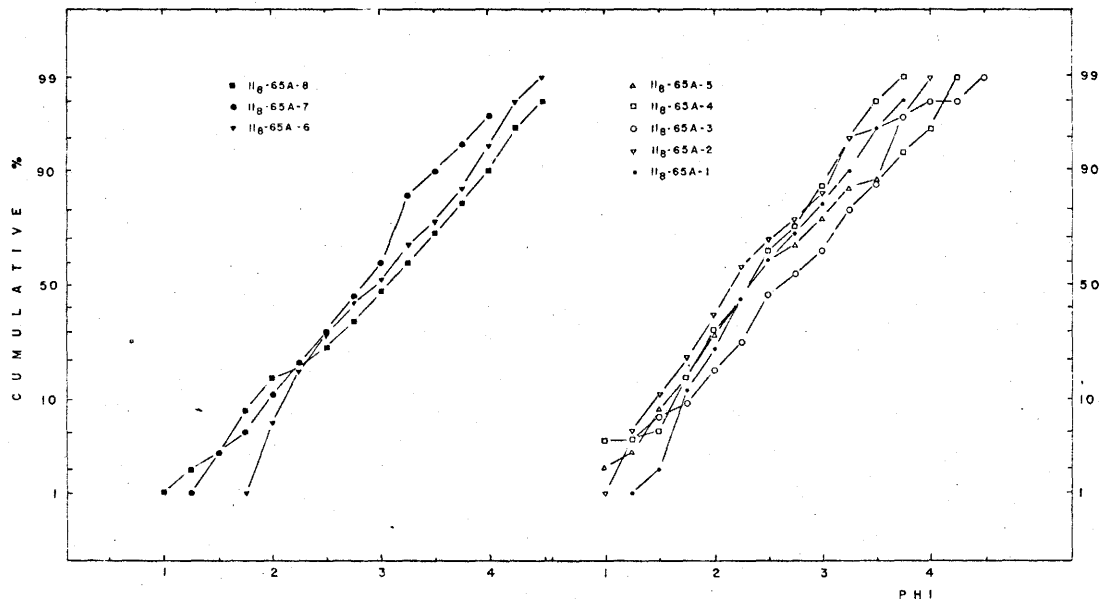
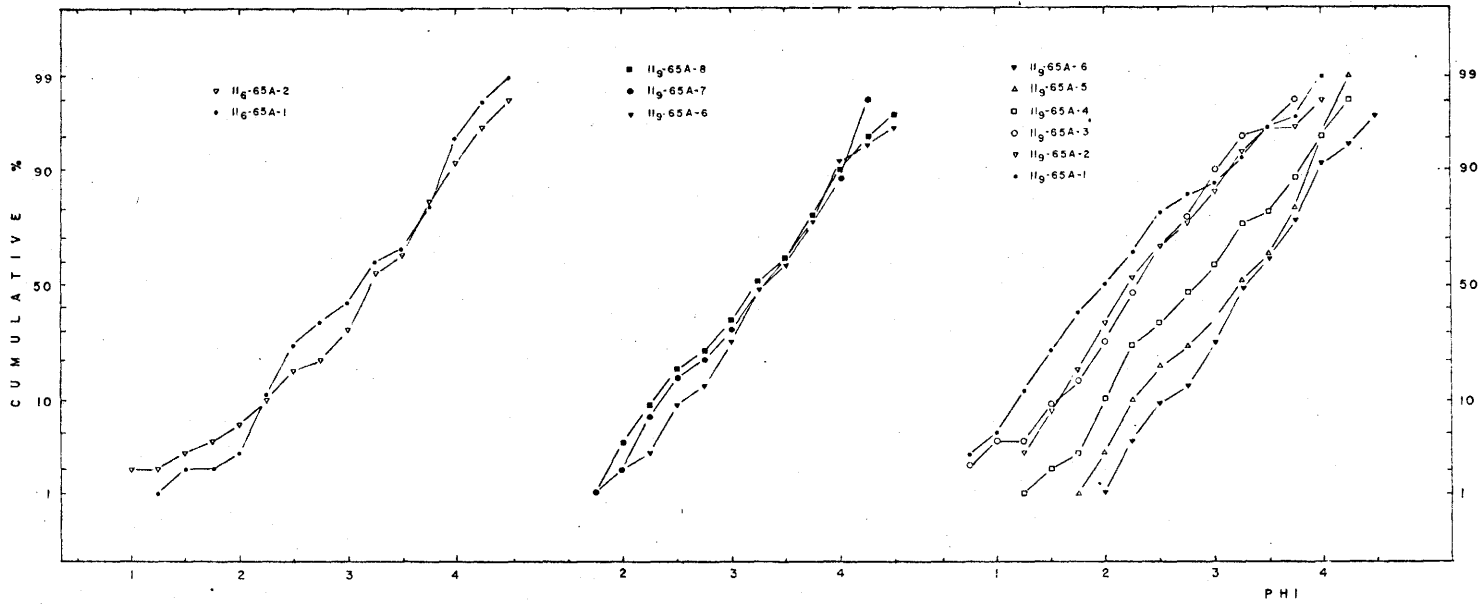


FIG. 4.7: CUMULATIVE GRAIN SIZE DISTRIBUTION CURVES FOR BED G-65A

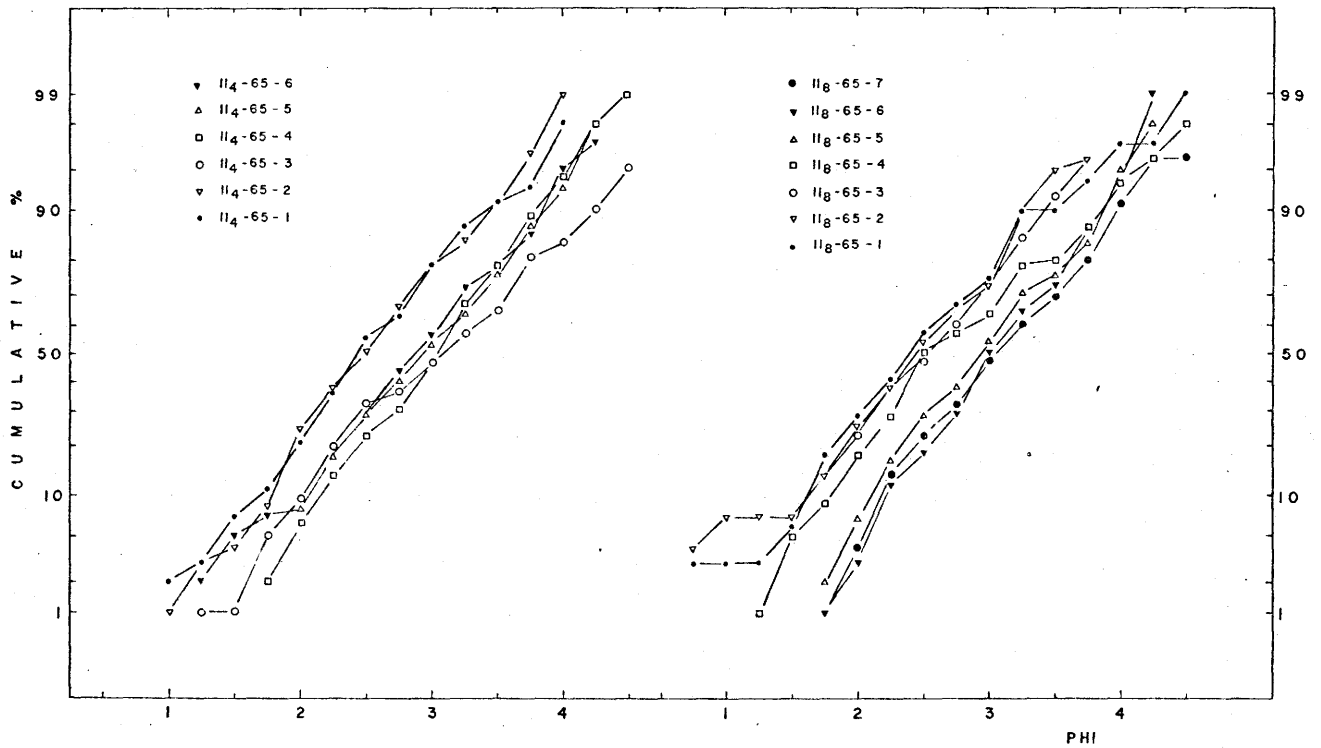
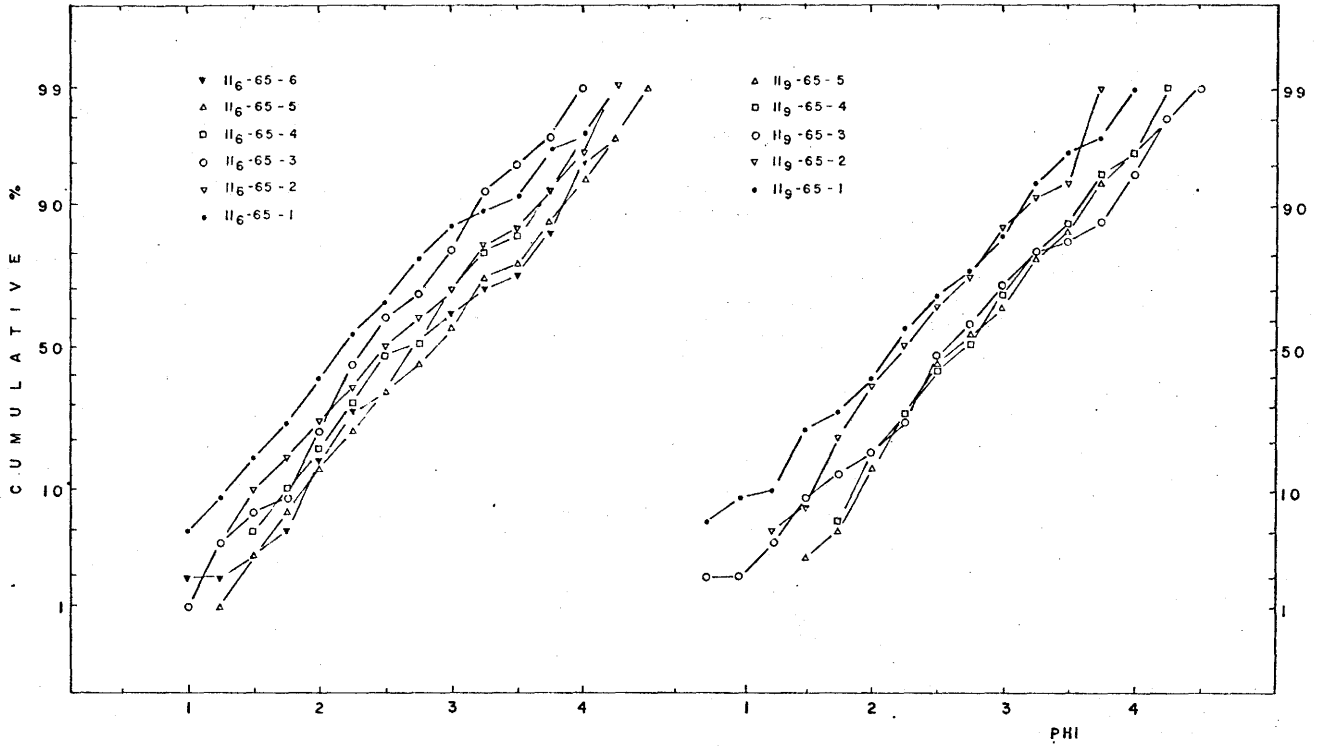


FIG. 4.8: CUMULATIVE GRAIN SIZE DISTRIBUTION CURVES FOR BED G-65

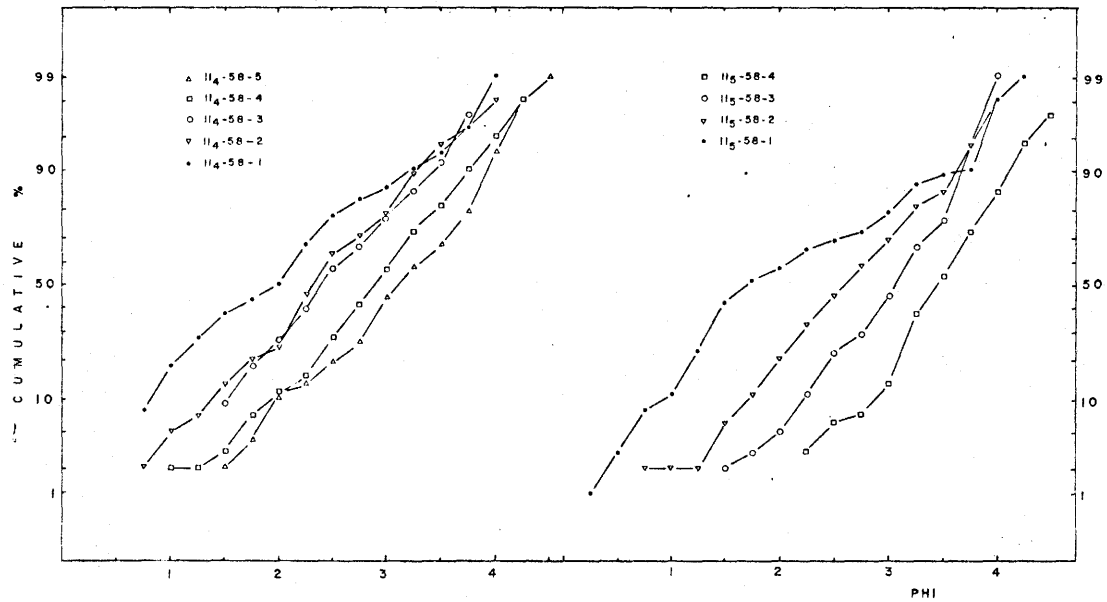
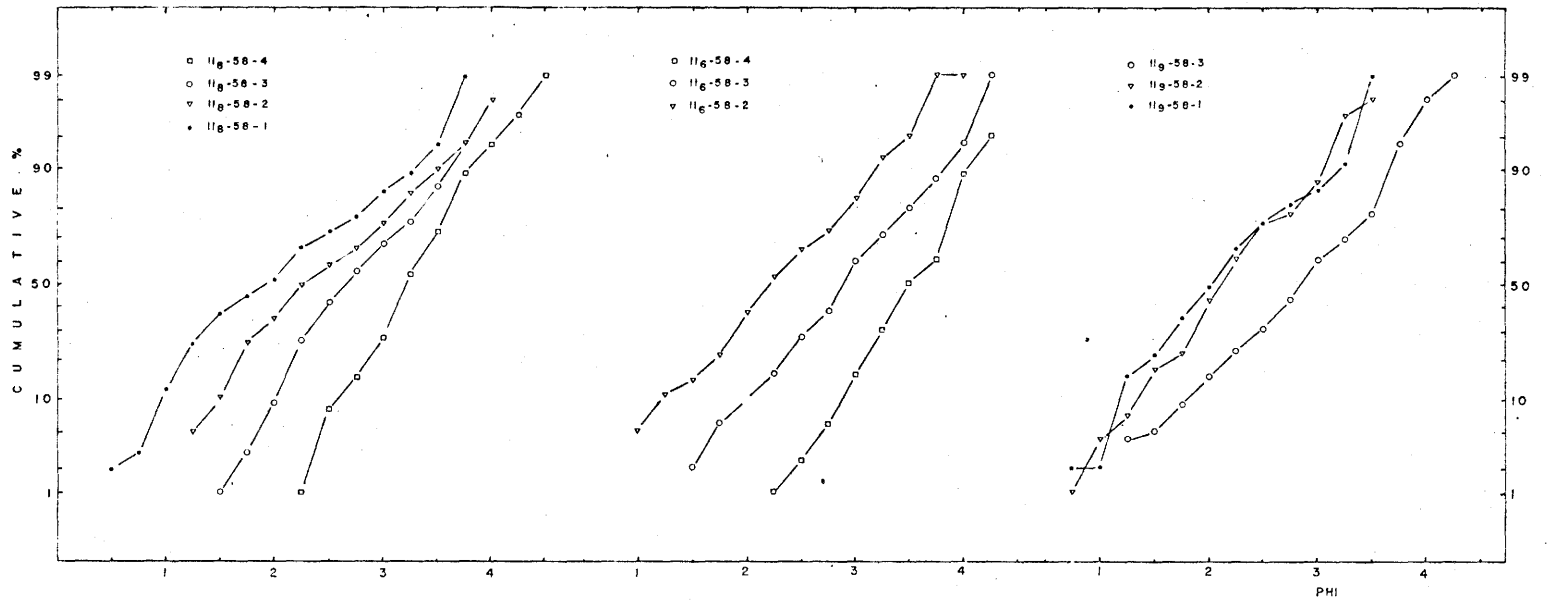


FIG. 4.9: CUMULATIVE GRAIN SIZE DISTRIBUTION CURVES FOR BED G-58

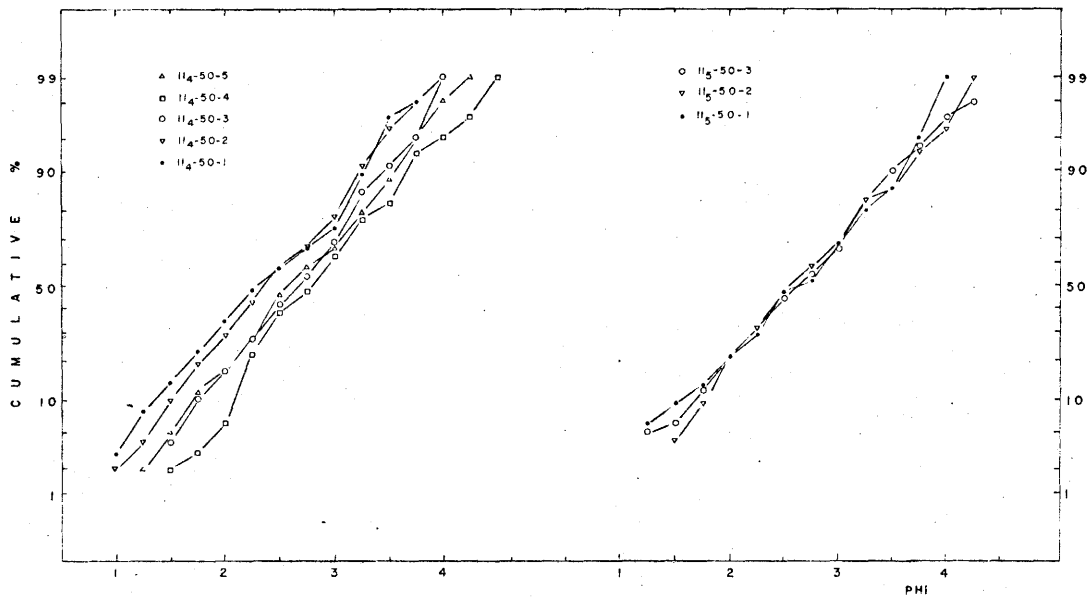
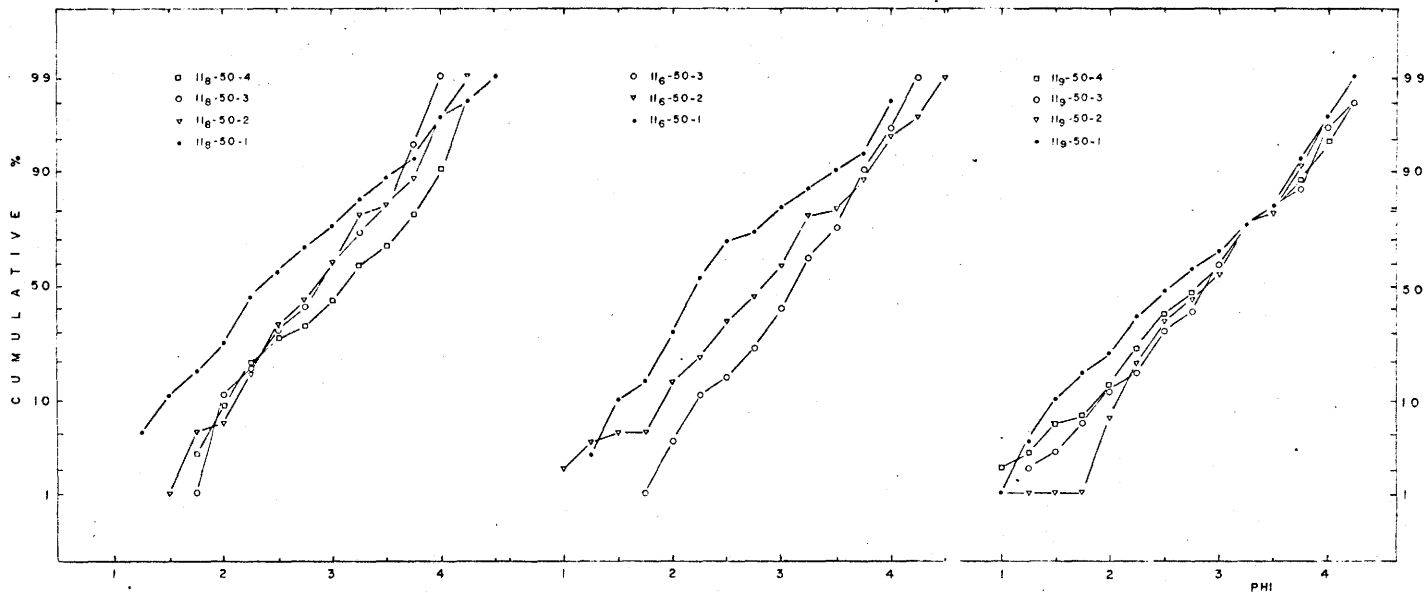


FIG. 4.10: CUMULATIVE GRAIN SIZE DISTRIBUTION CURVES FOR BED G-50

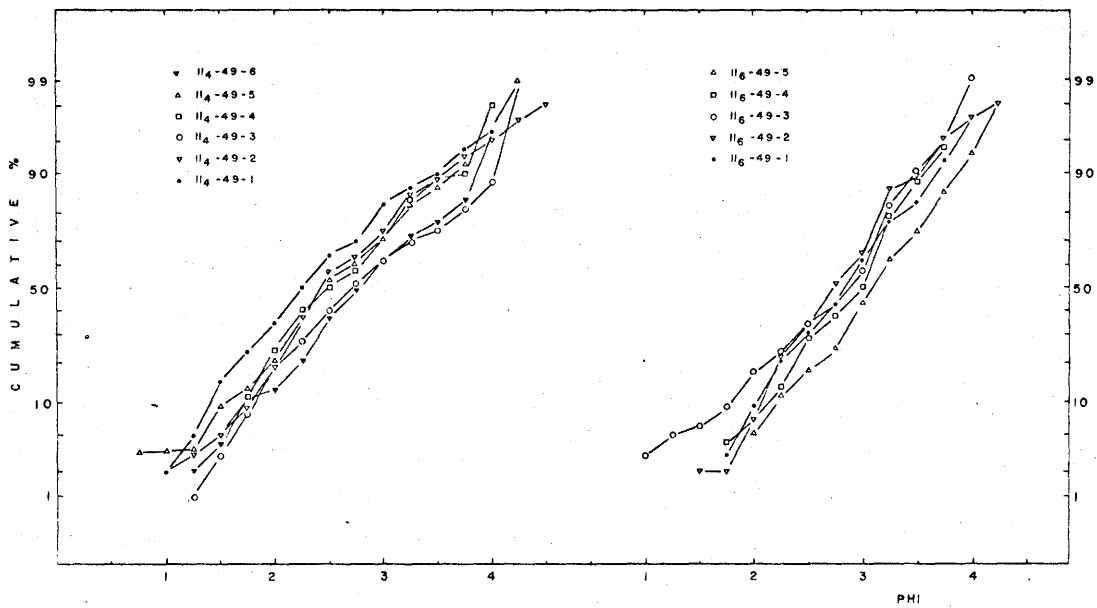
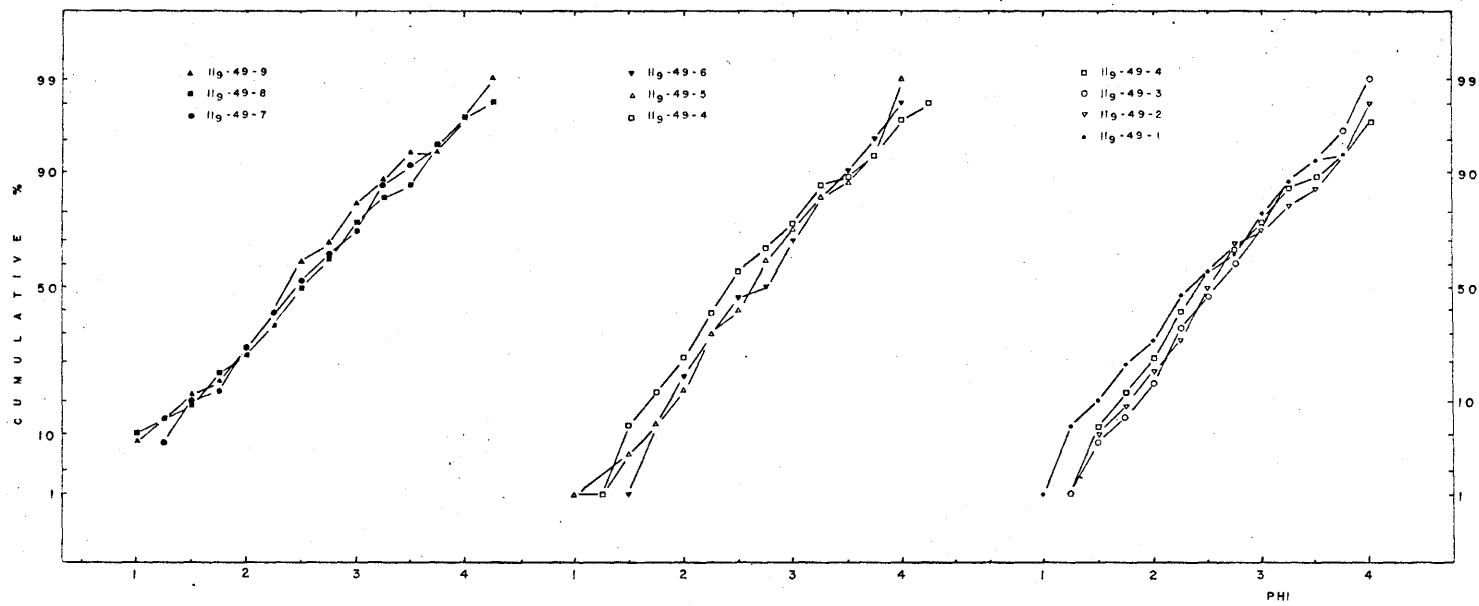


FIG. 4.11: CUMULATIVE GRAIN SIZE DISTRIBUTION CURVES FOR BED G-49

Table 4.2

Analysis of variance: operator experiment - mean size

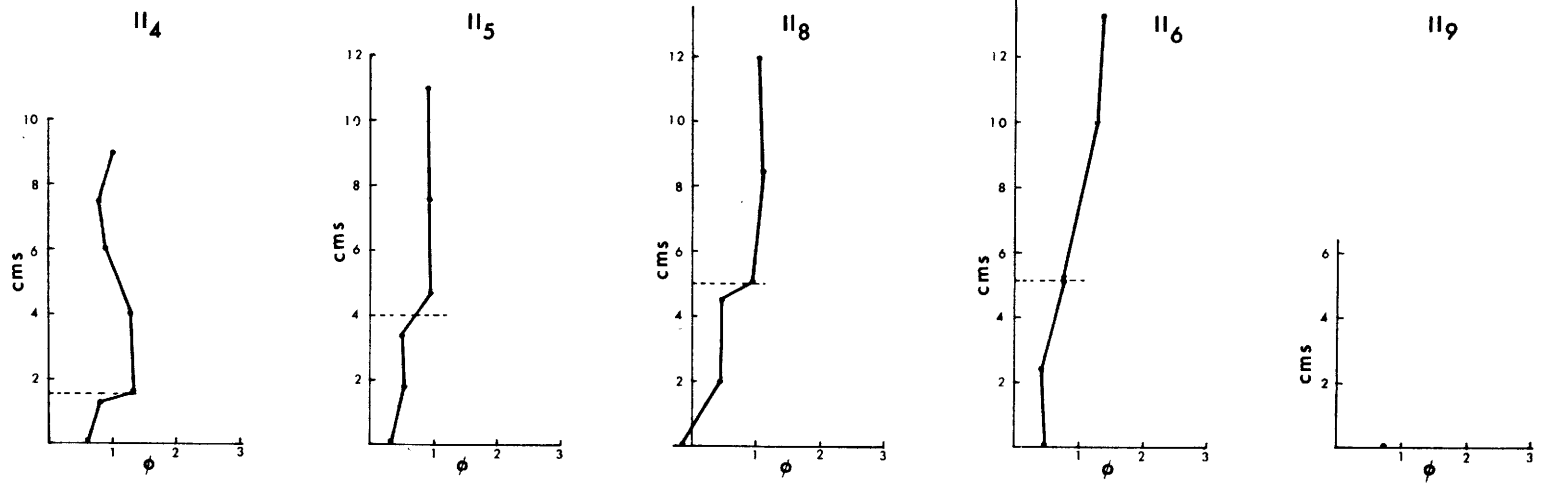
Source of variation	d.f.	SS	MS	F	F _{0.95}
Between thin sections	9	0.7659	0.0851	4.34	3.18
Between point counts	1	0.0045	0.0045	2.28	5.12
Error	9	0.0176	0.0019		
Total	17	0.7880			

Comparison of variance of size distribution given by statistics k_2 between the two point counts (table 4.1) shows that these values are highly reproducible.

Relationship Between Mean Size and Maximum Size

Middleton (1962, 1967a) and Passega (1957) and Scheidegger and Potter (1965) have emphasized the importance of the study of the maximum size in the turbidite beds. So the maximum size was determined by measuring the largest intercept of ten largest quartz grains and calculating their mean. Changes in the maximum size with distance from the base for beds G-68 and G-66 are portrayed in the figure 4.12 and data are given in table 4.3. The maximum size values emphasize the grading characteristics of the beds as shown by the mean size (fig. 4.13) with a few exceptions. In bed G-68, at section II₈ the mean size

BED G-66



BED G-68

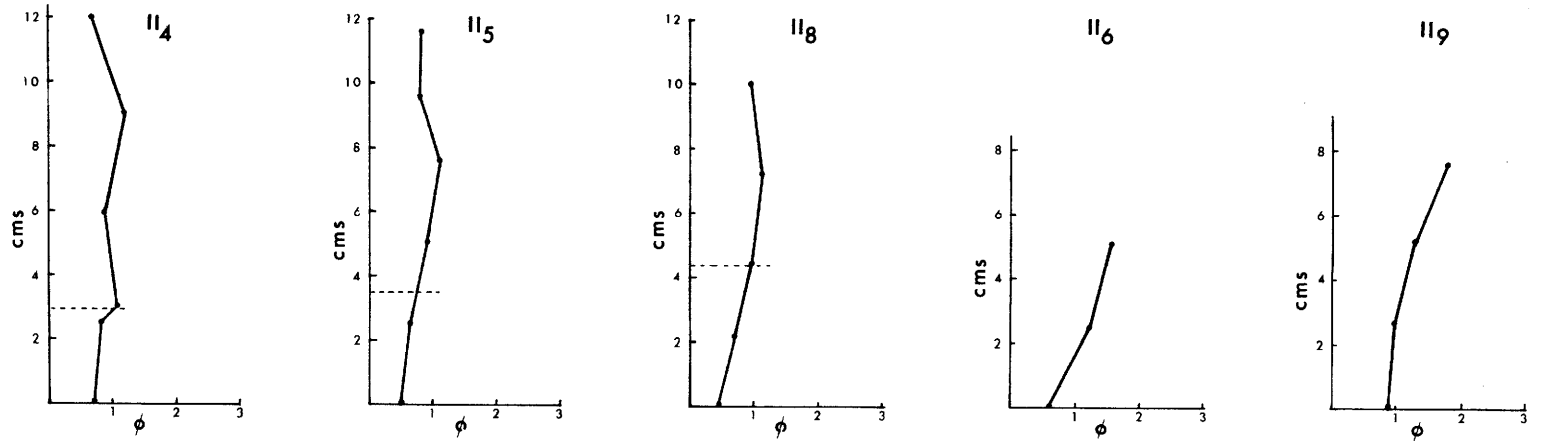


Fig. 4.12 - Variation of the maximum grain size with the height above the base in beds G-68 and G-66.

Table 4.3

Maximum grain size and matrix percentage in thin sections from beds G-68 and G-66

Thin Section	Max. size (ϕ units)	Per Cent Matrix (<0.03 mm)	Thin Section	Max. size (ϕ units)	Per Cent Matrix (<0.03 mm)
II ₉ -68-4	1.766	86	II ₉ -66-1	0.749	80
II ₉ -68-3	1.210	74			
II ₉ -68-2	0.986	76	II ₆ -66-6	1.344	76
II ₉ -68-1	0.896	80	II ₆ -66-5	1.269	65
			II ₆ -66-4	0.759	58
II ₆ -68-4	0.560	90	II ₆ -66-3	0.759	60
II ₆ -68-3	1.548	75	II ₆ -66-2	0.446	59
II ₆ -68-2	1.234	76	II ₆ -66-1	0.462	62
II ₆ -68-1	0.588	64			
			II ₈ -66-6	1.056	83
II ₈ -68-5	0.968	85	II ₈ -66-5	1.104	67
II ₈ -68-4	1.138	83	II ₈ -66-4	0.969	62
II ₈ -68-3	0.986	76	II ₈ -66-3	0.460	44
II ₈ -68-2	0.766	76	II ₈ -66-2	0.458	53
II ₈ -68-1	0.448	68	II ₈ -66-1	0.170	45
II ₅ -68-6	0.806	72	II ₅ -66-6	0.941	68
II ₅ -68-5	0.804	81	II ₅ -66-5	0.949	60
II ₅ -68-4	1.096	89	II ₅ -66-4	0.941	72
II ₅ -68-3	0.934	79	II ₅ -66-3	0.492	52
II ₅ -68-2	0.676	65	II ₅ -66-2	0.589	43
II ₅ -68-1	0.511	67	II ₅ -66-1	0.386	54
II ₄ -68-6	0.662	82	II ₄ -66-7	1.040	63
II ₄ -68-5	1.119	78	II ₄ -66-6	0.806	70
II ₄ -68-4	0.876	81	II ₄ -66-5	0.922	71
II ₄ -68-3	1.090	86	II ₄ -66-4	1.288	75
II ₄ -68-2	0.801	73	II ₄ -66-3	1.355	60
II ₄ -68-1	0.702	75	II ₄ -66-2	0.805	52
			II ₄ -66-1	0.606	56

can be interpreted as slightly graded in the upper portion of the bed, but the maximum size values indicate reverse grading.

Sphericity

Sphericity measurements were made to see if there was any significant difference in the sphericity of quartz grains in the different parts of a bed. Sphericity was measured by the ratio b/a , where a and b are the two axes of quartz grains as already defined. This measure is reciprocal of Bokman's (1952) 'elongation quotient' and has been used by Middleton (1962), Griffith (1967) and coworkers in study of the shape of quartz grains.

In a preliminary experiment, sphericity was determined for five thin sections randomly selected from the bed G-66 and experiment was replicated after 8 weeks (table 4.4). An analysis of variance on the data (table 4.5) shows that variance due to difference in the mean sphericity between thin sections is nearly equal to that contributed by the operator error. The F-test shows that both the variances due to the difference between thin sections and the operator error are non-significant as compared to error term which includes operator-thin section interaction. Thus it is not possible to distinguish between the average sphericity of the different thin

sections and so the further study of sphericity was abandoned.

The value of sphericity of quartz grains from different rock types by different workers (Middleton, 1962, Griffith, 1967, and coworkers) lies within a very small range of 0.589 to 0.682. Thus the similarity of values of sphericity from thin sections from the same bed should not be surprising.

Table 4.4

Replicate sphericity determinations in operator experiment

Thin section	Point count 1		Point count 2	
	Mean	Variance	Mean	Variance
II ₆ -66-5	0.616	0.037	0.630	0.035
II ₄ -66-4	0.601	0.027	0.651	0.035
II ₅ -66-2	0.625	0.32	0.626	0.029
II ₈ -66-2	0.652	0.036	0.627	0.035
II ₅ -66-5	0.644	0.034	0.656	0.035

Table 4.5

Analysis of variance of sphericity determinations
in operator experiment

Source of variation	d.f.	SS	MS	F	F _{0.95}
Between point counts	1	0.00027	0.00027	0.729	7.71
Between thin sections	4	0.00105	0.00026	0.719	6.39
Error	4	0.00148	0.00037		
Total	9	0.00280			

Vertical Grading

In Kuenen's experiments (Kuenen and Migliorini, 1950; Kuenen and Menard, 1952), a change from a poorly graded bed in the proximal region to a graded bed in the distal region was clear. Similar results were obtained by Dzulynski and Walton (1965, p.198) in their experiments. Middleton (1967a) recognized two types of grading - 'distribution' grading and 'coarse-tail' grading in the experimentally deposited turbidites. In distribution grading, there is a progressive shift towards the finer grain sizes for all the percentiles of the distribution as the distance from the base of the bed increases, whereas in the coarse-tail grading, only the coarse tail (1-5%) of the distribution shows a progressive shift towards finer sizes from the base to the top of the bed. Coarse-tail grading may pass towards the top of the bed and in the downcurrent direction into distribution grading.

A systematic decrease in mean size from the base to the top of turbidite beds has been noted by many workers (Radomski, 1958, 1960, in Enos, 1965; Webby, 1959; Shiki, 1961). An examination of Webby's and Shiki's diagrams shows that in the upper part of some of the beds, the decrease in grain size is very small and beds

are almost ungraded. Middleton (1962) found no regular variation in the mean size from bottom to top of turbidite beds from Normanskill and Charny Formations.

The mean size vs. height above the base are plotted in figure 4.13 for the different beds. The following features are noteworthy:

(i) Beds G-68, G-67, G-66 and G-50 show very good grading in the proximal eastern regions and become ungraded or slightly reverse graded in the upper portion of the bed in the western regions.

(ii) Bed G-58 is graded at all the sections examined.

(iii) Beds G-65A and G-65 are graded in the lower part and ungraded in the upper part at all sections except that the bed G-65A is reverse graded in the upper portion at the westernmost section II₄.

(iv) Bed G-49 is ungraded in the east and becomes graded in the west.

Except for the bed G-58, all the beds show an ungraded character in at least part of the bed at one or more sections studied. An average of the mean sizes of thin sections cut close to one another and having mean sizes within experimental error was calculated. The value of mean size at which the beds become ungraded varies from 1.8 ϕ to 2.7 ϕ . However, the beds tend to be ungraded for mean sizes of 2.2 ϕ or smaller sizes.

Fig. 4.13a-4.13h - Variation of the mean grain size with the height above the base in the eight beds.

----- Bedding joint

BED G-68

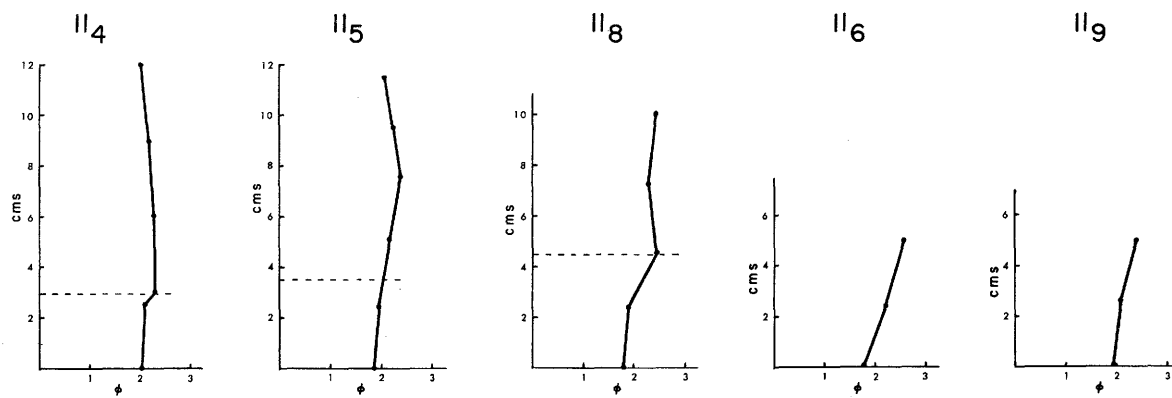


Fig. 4.13a

BED G-67

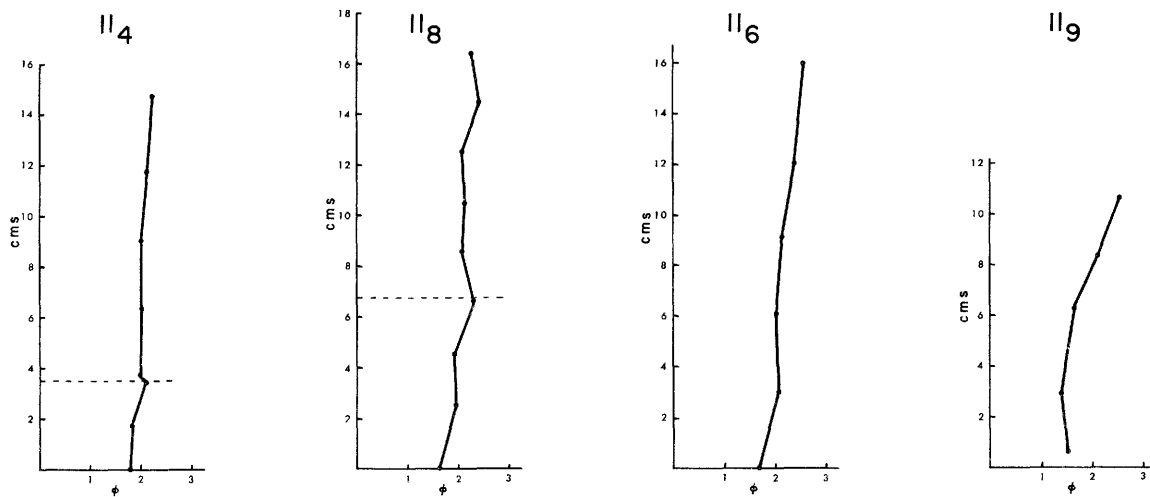


Fig. 4.13b

BED G-66

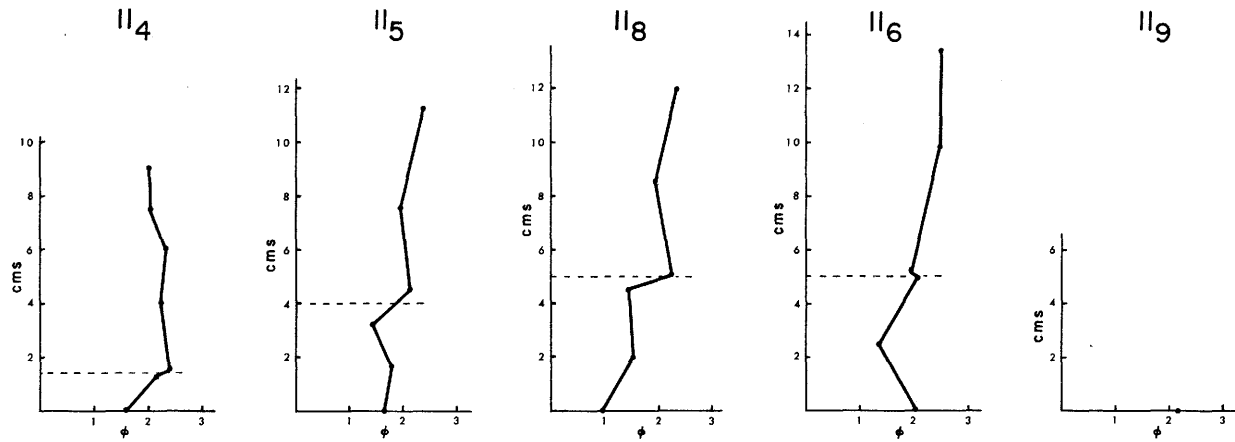


Fig. 4.13c

BED G-65A

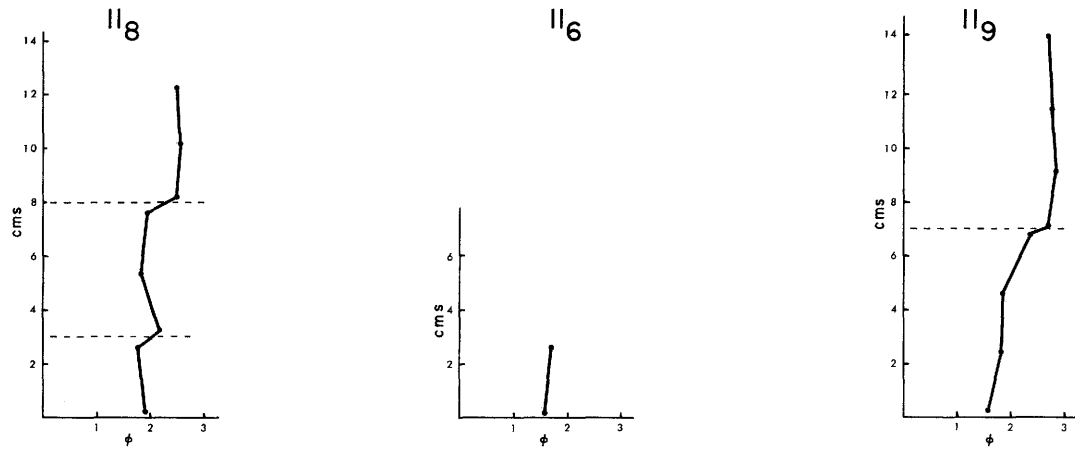


Fig. 4.13d

BED G-65

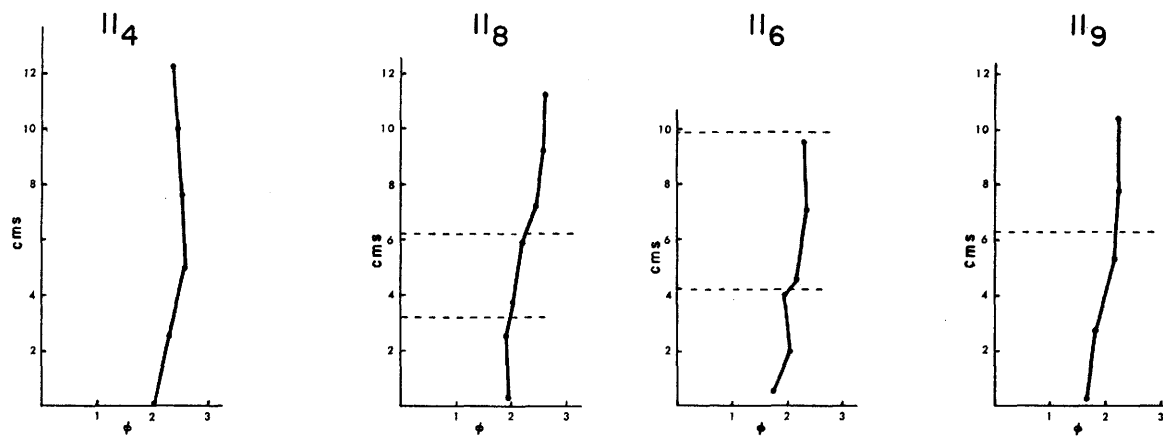


Fig. 4.13e

BED G-58

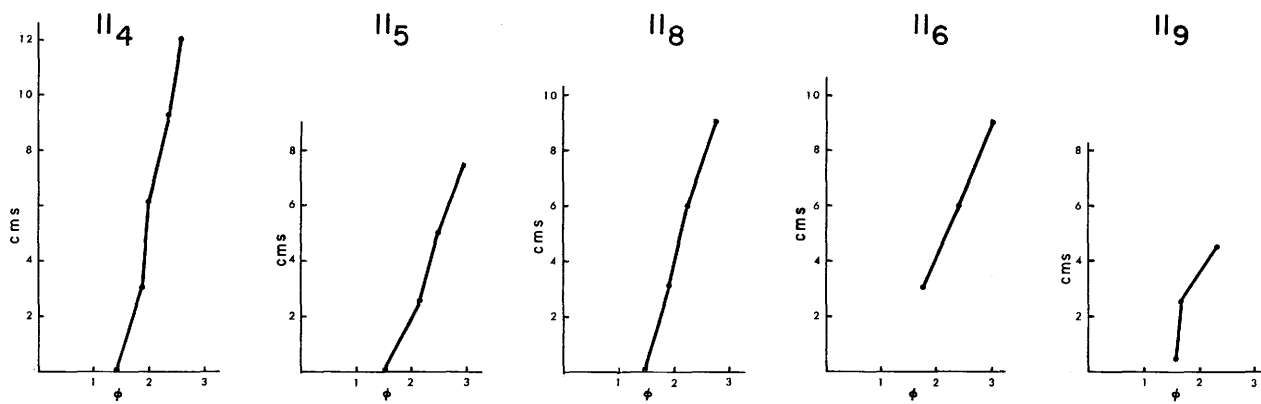


Fig. 4.13f

BED G-50

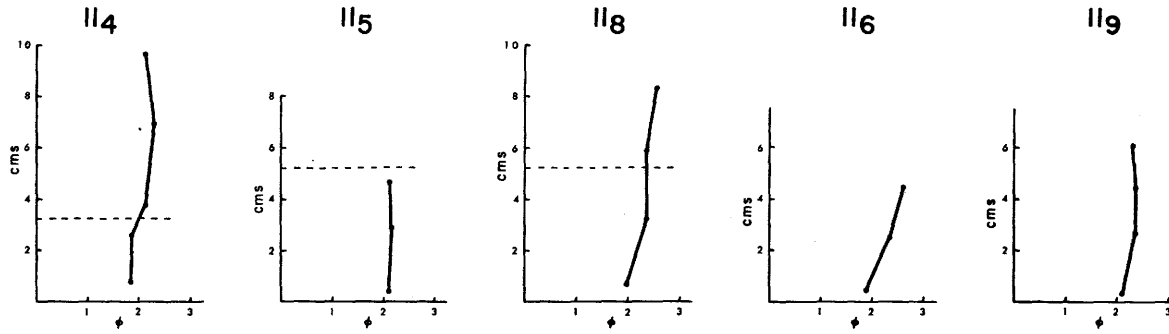


Fig. 4.13g

BED G-49

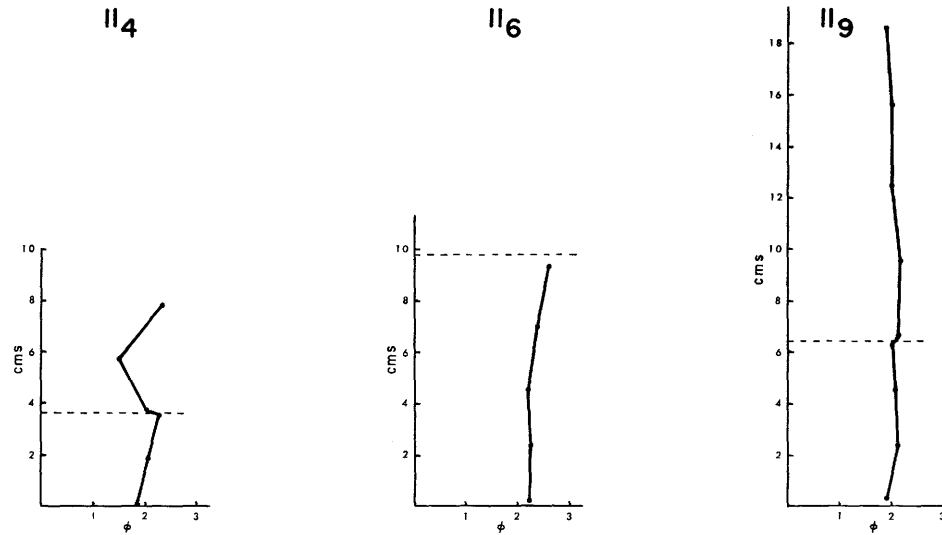


Fig. 4.13h

The bedding joint marks a great discontinuity between the two parts of the bed. Frequently the bedding joint is exactly at the place where the two parts of the bed have a break in grading characteristics, e.g., the part of the bed below the joint is graded and the part above the joint is ungraded (specimens II₄-67, II₈-65, II₉-65A, II₉-65) or even slightly reverse graded (specimens II₄-66, II₄-68). Also, there is a marked contrast in grain size across the joint (specimens II₈-66, II₄-66, II₄-68, II₄-67, II₈-65A, II₉-65A, II₄-49, II₆-65). At some localities, the lower part is reverse graded just below the joint (specimens II₈-68, II₆-65). This may be comparable to reverse grading observed in the upper part of some beds in the western sections. A grain size break across the joint is small in the eastern sections for beds G-68, G-67, G-66, G-50 and G-49, but it becomes very large in the western sections.

Scheidegger and Potter (1965) have distinguished three types of size-decline curves in turbidites - convex-side up, concave-side up and uniform size decline curves. It is frequently difficult to assign a curve to the whole thickness of the bed due to change in grading characteristics of the bed across the joint. When the bed consists of only one part, the size decline curves are convex-side up (specimens II₉-67, II₉-66, II₉-58), concave-side up

(specimen II₉-50) or uniform size decline curves (II₆-58, II₄-58). The convex-side up curves occur only in the eastern region. It should be noted that size decline curves are plotted using ϕ units instead of actual size as in the case of Scheidegger and Potter (1965).

Grading Characteristics and Grain Orientation

In the case of beds G-68, G-67 and G-66, the maximum number of non-significant preferred orientations occur in the eastern region and also these beds show good grading in this region. This observation is similar to that of Scott (1966), who noted a non-significant grain orientation from a well graded bed. However, non-significant orientations also occur in ungraded beds. Bed G-49 is ungraded at section II₉ and shows mostly non-significant preferred grain orientations. Also, the top ungraded portions of beds G-65 and G-65A at sections II₉ and II₈ show mostly non-significant or bimodal orientation distributions.

Reverse grading is accompanied by large deviations of grain orientations from the sole in beds G-66 and G-68 at section II₄. An attempt was made to see whether it is universally true. Most of the thin sections in the bed G-68 at section II₅ show a deviation of 45° from the sole and reverse grading is confined to the upper part. In

contrast, the bed G-67 at section II₈, and bed G-58 at sections II₄ show large deviations from the sole direction without being accompanied by reverse grading. Only in the bed G-65 at section II₄ large deviations of grain orientation occur in conjunction with reverse grading. It seems that the reverse grading and large deviations of grain orientation from the sole may occur independently.

In beds G-67 and G-50 (?), large deviations of grain orientation from the sole are associated with the ungraded nature of the bed at section II₄.

Lateral Grading

A lateral decrease in grain size away from the source within a thick turbidite sequence is commonly observed (Stanley, 1961; ten Haaf, 1959). A general decrease in maximum grain size down the paleoslope was observed by Carozzi (1957) in a few microbreccia and conglomerate beds of Alpine flysch correlated in sections 2 to 19 kms apart over a distance of 40 kms. However, in some beds, the maximum size occurred some distance down-current rather than in the most proximal area. Enos (1965) made a detailed field study of changes in the maximum size in individual beds in the area under investigation. Enos (1965) noted a significant decrease in grain

size in 37 beds out of 166 and 5 beds showed a significant increase in the downcurrent direction. Middleton (1967a) found a very good lateral gradation in experimental turbidite beds deposited by 'low concentration' flows, but only a poorly defined decrease in grain size away from the source could be detected in beds deposited by 'high concentration' flows.

Lateral gradation in the beds under consideration was studied by comparing the mean size of quartz grains at the base of beds at different localities. In most cases, the basal thin sections were cut very close to the base. However, in other cases, it was slightly above the base and grain size at the base was determined by projecting grain size decline curve to the base of the bed. A similar procedure was adopted in cases, where the basal thin section happened to be exceptionally fine grained. Lateral changes in mean grain size along the strike are plotted in figure 4.14. For the bed G-66, the largest mean size occurs in the central region of the outcrop and grain size decreases eastwards and westwards from that point. A decrease in grain size from east to west is noted for the beds G-67 and G-65. Beds G-65A and G-49 have a minimum grain size in the middle and grain size increases on both sides of it along the outcrop. Beds G--6, G-58 and G-50 show very small variation in

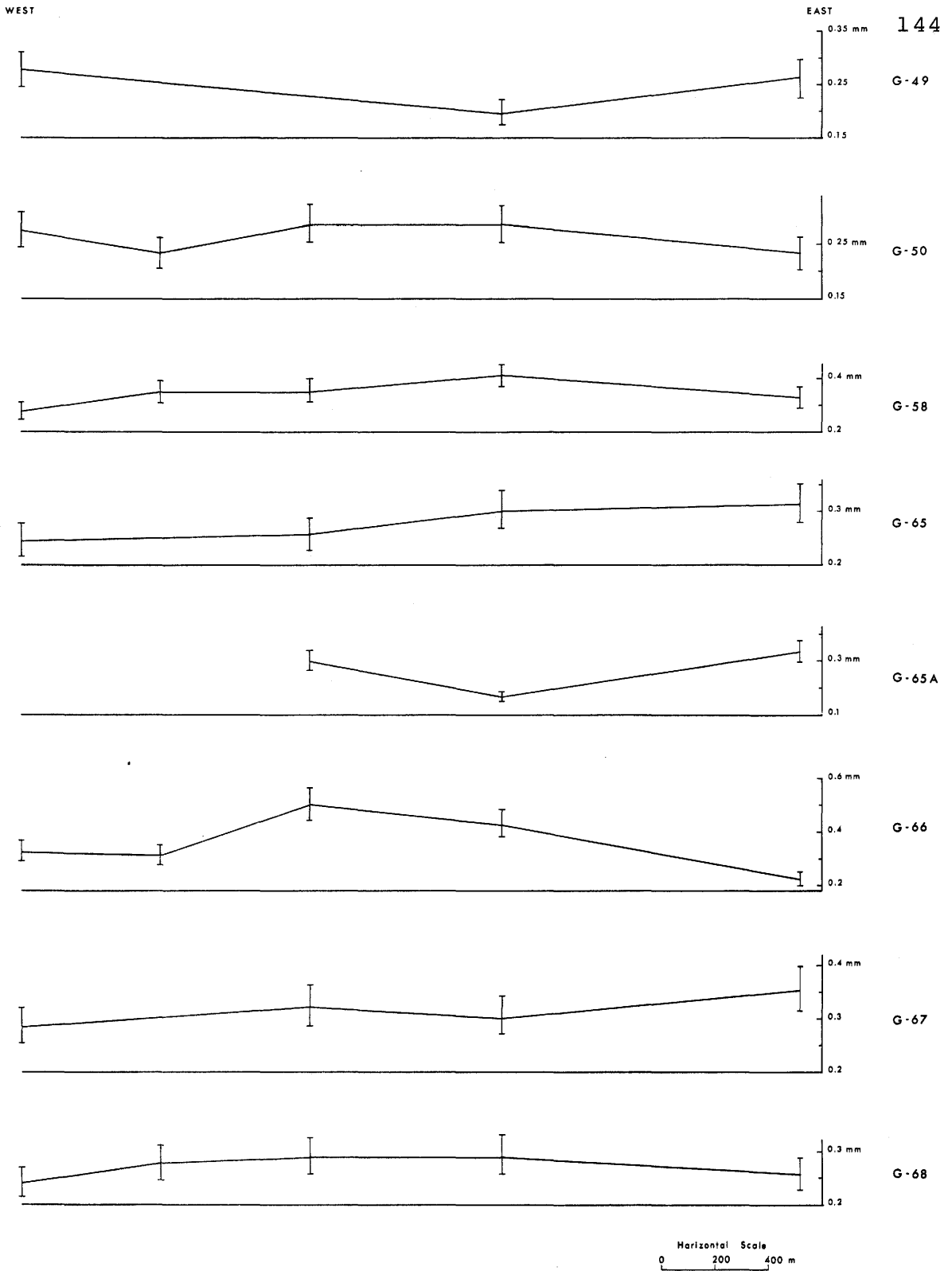


Fig. 4.14 - Variation of the mean grain size at the base of the bed along the strike. 95% confidence limits for each grain size determination are indicated by vertical lines (I) in the figure.

grain size along the strike.

Sorting

Sorting is inversely related to dispersion of grain size distributions and is measured by statistics m_2 and k_2 . Some of the basal thin sections (II₆-66-1, II₅-58-1) have extremely high variance and thus have a poor sorting. This may be due to rapid deposition from within or behind the head of the depositing current at an early stage of deposition (Middleton, 1967a, p.489). Also, some specimens (II₉-67, II₆-67, II₉-68, II₆-68, II₅-58, II₈-58) show an improvement of sorting (decrease in value of k_2) from bottom to top of the bed. It should be noted that these specimens show good grading too.

An attempt was made to study variation of sorting with grain size for each bed. A significant negative correlation at 95% level of confidence was obtained between k_2 and k_1 values for the beds G-68, G-67, G-58 and G-50 showing thereby that sorting improves with decrease in grain size for these beds (fig. 4.15, table 4.6). A non-significant positive correlation exists for the beds G-66 and G-49 between k_2 and k_1 values.

Improvement of sorting from bottom to top of

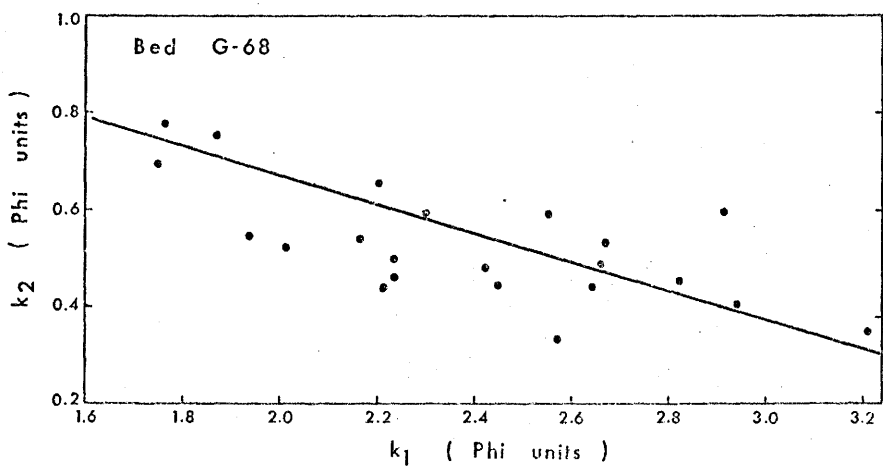
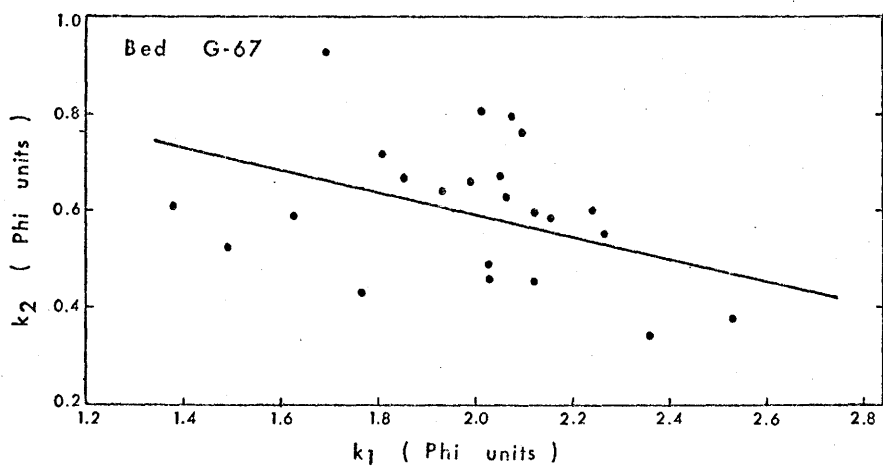
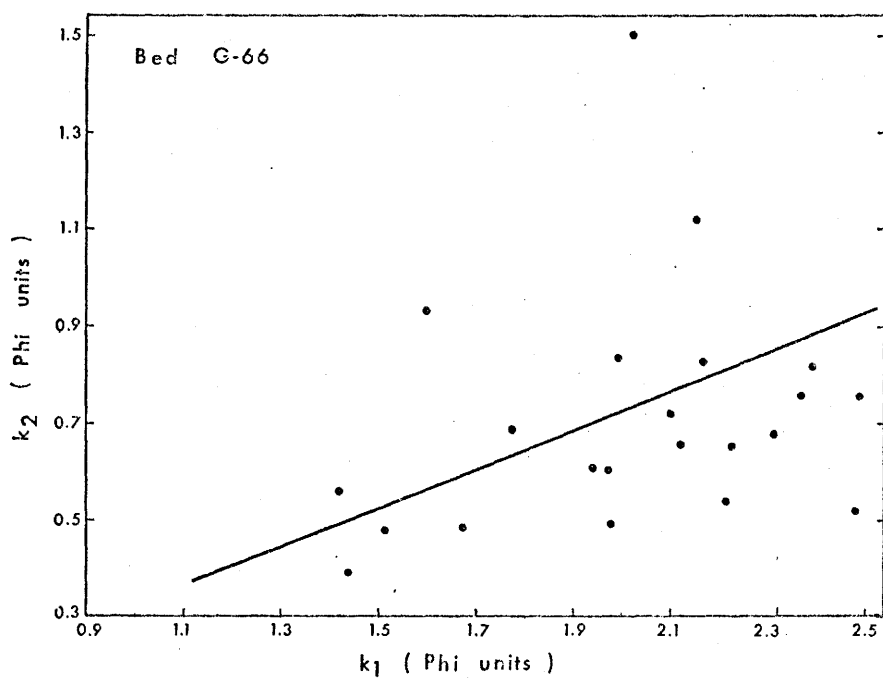


Fig. 4.15 - Plots of the dispersion (k_2) vs. the mean grain size for beds G-68, G-67 and G-66.

Table 4.6

Linear regression equations and correlation coefficients
for relationship between k_1 and k_2

Bed no.	Regression equation	No. of measurements	Correlation Coeff. r
G-68	$k_2 = 1.691 - 0.530 k_1$	24	- 0.741 *
G-67	$k_2 = 1.051 - 0.230 k_1$	28	- 0.440 *
G-66	$k_2 = 0.457 + 0.131 k_1$	26	+ 0.220 N.S.
G-65A	$k_2 = 0.475 - 0.013 k_1$	18	- 0.065 N.S.
G-65	$k_2 = 0.679 - 0.075 k_1$	24	- 0.217 N.S.
G-58	$k_2 = 1.205 - 0.323 k_1$	19	- 0.795 *
G-50	$k_2 = 0.893 - 0.180 k_1$	19	- 0.443 *
G-49	$k_2 = 0.145 + 0.206 k_1$	20	+ 0.100 N.S.

* Significant at 95% confidence level

N.S. Non-significant at 95% confidence level

turbidite beds was found by Mizutani (1957), Middleton (1962) and Okada (1966). Similar results were obtained for experimental turbidites by Middleton (1967a). Folk and Ward (1957) found that the best sorting coincided with gravel, medium- to fine sand and clay modes following an M-shaped trend in a Brazos river bar. Later studies of variation of sorting with grain size from turbidite beds tend to give similar results (Mizutani, 1957; Kelling, 1962; Unrug, 1963; Okada, 1966; Hubert, 1967).

Skewness and Kurtosis

Skewness is estimated by statistics m_3 , k_3 and g_1 . A fair idea about the skewness can be obtained by looking at the cumulative size distribution plots. Size distribution curves with convex-side up are positively skewed, curves with concave-side up are negatively skewed and those curves which approximate straight lines represent normal distributions. It is obvious that most of the plots tend to be straight lines and it is confirmed by the fact that most of g_1 values are not significantly different from zero. In some beds, the curves are either convex side up or straight lines for thin sections from bottom of the bed and change to concave-side up towards the top of the bed (specimens

II₆-65, II₄-65, II₉-58, II₆-58, II₈-58, II₅-58, II₉-67, II₈-50, II₆-50, II₈-68, II₆-67, II₆-68). Values of g_1 change from positive to negative from bottom to top of these specimens. Also, generally significant positive values occur in the lower part of the bed and significant negative values occur in the upper part of the bed. The change of positive to negative values of g_1 is very well demonstrated in graded beds.

Grain size distributions are positively skewed in turbidites of Permian of Japan (Mizutani, 1957) and negatively skewed in Scottish Ordovician greywackes (Kelling, 1962). Middleton (1962) observed a change of positive skewness at the base to zero or negative skewness at the top of turbidites from Charny and Normanskill Formations. Middleton (1967a) noted that maximum skewness values occurred in the middle and these values decreased towards top and bottom of the experimentally deposited turbidites. Hubert (1967) reported that medium- to fine sands were nearly symmetrical in skewness and silt beds were characterized by finer skewed frequency distributions in the Prealpine Flysch sequences of Switzerland. Ericson et al (1961) found that most of cores of deep sea sands from Atlantic ocean had positively skewed size distributions.

Kurtosis is given by statistics m_4 , k_4 and g_2 .

In general, g_2 values are negative indicating that quartz grain size distributions are platykurtic. Similar results were reported from Normanskill and Charny Formations (Middleton, 1962).

Matrix

Percentage of matrix was also estimated with the help of Shadowmaster by measuring one hundred grains and using a magnification of $\times 100$. All the grains with maximum diameter less than 0.03 mm were also included in matrix. Determinations were made only for beds G-68 and G-66 and values are listed in table 4.3. Percentage of matrix is plotted against grain size in ϕ units in figure 4.16 and a positive correlation clearly emerges between the two. The linear equations representing the relationship between the matrix percentage and mean size for the two beds are as follows:

Bed	Linear Equation	Correlation Coefficient	Coefficient of Determination
G-66	Matrix = $23.01 - 19.76 k_1$	0.715	51.2
G-68	Matrix = $37.37 - 18.21 k_1$	0.618	38.3

Similar results have been reported by a number of other workers (Walton, 1955; Kuenen and Migliorini, 1950; Kelling, 1962; Allen, 1962; Okada, 1966). It may be noted that parts of the beds having same grain size also contain

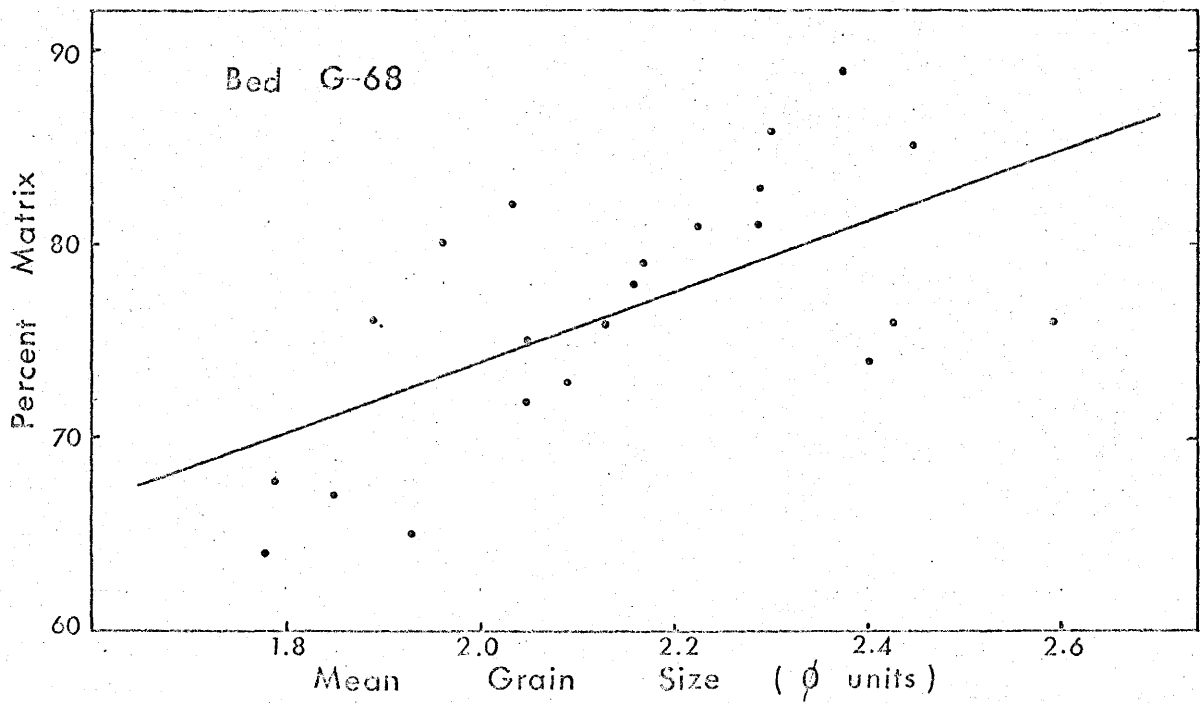
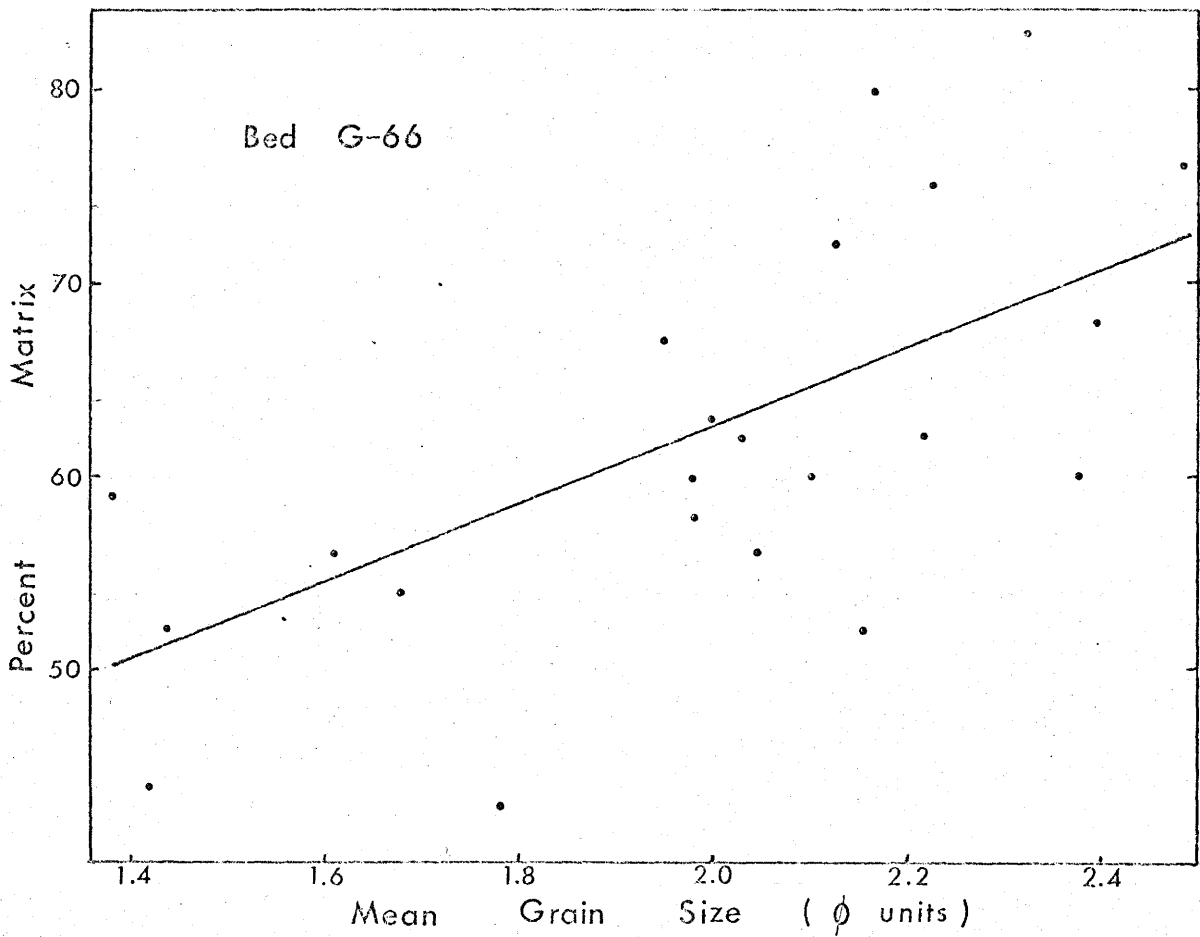


Fig. 4.16 - Relationship between percentage of matrix and the mean size of quartz grains in beds G-68 and G-66.

similar amounts of matrix, and thus these parts of the beds are completely ungraded. Also, the bed G-68 contains a very high percentage of matrix (65% - 90%).

Conclusions

(i) Since the beds G-68, G-67, G-66 and G-50 have their sole directions nearly parallel to the strike, their changes along the strike can be regarded as those taking place in the direction of the current. Also, these beds show similar variation in some respects. The changes in grading characteristics of these beds from the proximal to the distal region are:

(a) The beds show good grading in the proximal region and become ungraded or slightly reverse graded in the upper part of the beds in the distal region.

These grading characteristics are exhibited by both the mean and maximum grain size of quartz grains.

(b) The break in grain size across the bedding joint is small in the proximal region and it becomes large in the distal region.

(c) The largest mean size at the base of the bed does not occur in the most proximal region, but some distance downcurrent; the grain size decreases from this point both upcurrent and downcurrent for the bed G-66.

The bed G-67 shows a small decrease in grain size from the proximal to distal region. However, the extension of the bed further upstream is not known. It may show a decrease in grain size in the upstream direction and give a pattern similar to the bed G-66.

Beds G-68 and G-50 show a non-significant variation in grain size along the strike.

(d) The beds show a convex side up grain size decline curve in the proximal region.

(ii) Sorting improves with decrease in grain size. Well graded beds show an improvement in sorting and change of positive or zero skewness to negative skewness from bottom to top of the bed.

(iii) Matrix content increases with decrease in grain size.

CHAPTER V

DISCUSSION AND INTERPRETATION

The problem of turbidite beds has two facets: one is transportation of coarse sand over long distances without deposition and the other is the mechanism of deposition from the turbidity current and the formation of various features associated with turbidites. Study of ancient turbidites can give clues mainly to solve the second problem.

Study of lateral continuity of greywacke beds from the Cloridorme Formation by Enos (1965) showed that turbidite greywackes are not of as great longitudinal extent as generally thought. Even correlation of beds in sections a few hundred yards apart based on grain size, sole structures and thickness proved to be wrong, when checked by walking out the outcrop. Nearly 68% of all the beds from the lower part of unit G failed to extend the full 2 miles length of the outcrop. The beds under study belong to the lower part of unit G and were chosen for their continuity and easy traceability in the field. Thus though all the beds do not die out in the area of study, the beds may show distinct changes in their sedimentologic characteristics even in this short distance

because of their general short downcurrent persistence.

Changes in Internal Structure

Bouma (1962, p.97) explained the typical composite turbidite sequence in terms of slowing down of the turbidity current. Walker (1965) and Harms and Fahnestock (1965) interpreted the sequence in terms of flow regime (fig. 5.1). It is obvious that a lateral sequence similar to a vertical sequence should occur in a single turbidite bed, since the current slows down as it starts depositing sediment.

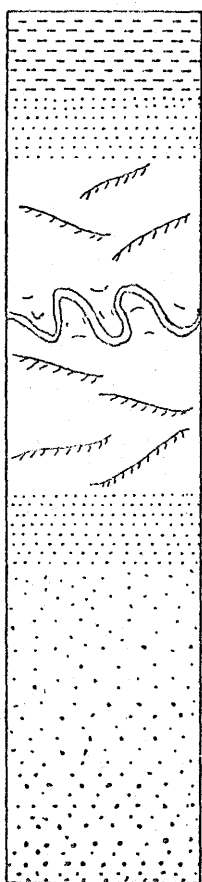
According to Sanders (1965), the drag conditions at the bottom of a turbidity current are very important and determine to a large extent the internal structures formed in the deposited bed. When a turbidity current shears over a cohesionless bottom, the drag is maximum owing to the greater roughness of grains and the 'Bagnold effect' (Sanders, 1965, p.212), and a traction carpet forms at the bottom. When the drag is negative at the base of the current, a "flowing grain layer" forms at the base of the current. Freezing of the 'flowing grain layer' gives rise to the massive graded bed and deposition from the upper part of the current may form a very fine grained graded bed or silt sized laminated or cross-laminated bed. As drag conditions at the bottom along the path of the current may occur in any order, no definite lateral sequence

Fig. 5.1

Complete Turbidite Sequence

Sequence of internal structures in turbidites observed by Bouma (1962)

Corresponding bed forms observed in flume Harms and Fahnestock (1965) and Walker (1965)



- E Pelitic division
- D Upper division of parallel lamination
- C Division of current ripple lamination
- B Lower division of parallel lamination
- A Graded massive division

Lower flow regime

Upper flow regime

Plane bed without movement

Ripples

Plane bed with movement

Standing waves
antidunes

Bed forms not preserved

in a turbidite bed could be expected. The validity of this theoretical speculation cannot be checked in the case of ancient turbidites because of the difficulty of ascertaining the drag conditions at the base at the time of deposition of a bed.

Instead of a regular change in internal structures in the direction of the current similar to the typical vertical turbidite sequence of Bouma (1962), beds G-67, G-66 and G-50 are commonly massive and show plane laminations at places where they are thin in the proximal area. In the distal area, the thinner parts of the beds are also massive.

Enos (1965) explained changes in thickness of the beds due to local irregularities at the bottom. The flow was accelerated over a slight high on the bottom, over which the flow was constricted between the bottom and the static water. As a result, most of the sediment was swept past the local high and was deposited in the depression. The author considers this to be adequate explanation for thinning of the beds in the proximal areas. The proximal regions where the bed is thin, deformation of cross-laminae at the top of the bed, probably caused by higher velocity in this region, provides supporting evidence.

In the plane laminated portion of the beds, where wavy laminae occur, the angle of the dip of laminae is so

slight that it is unlikely that separation of flow could have taken place to form the observed structures by migration of ripples. Also, there is no resemblance to cross bedding formed by migration of antidunes. It is suggested that these laminae resulted due to traction of particles in the plane bed phase of the upper flow regime and that wavy nature of the laminae is simply a result of small undulations on the bottom.

Since on either side of the region with a local high, the velocity of the current was less than that at the local high and a massive bed was deposited on both sides of this point, it is an important corollary that the massive bed formed at velocities less than those at which the plane bed formed. The change in velocity was very small; thus during the deposition of the massive portion of the bed, the velocity might be still in the lower part of the upper flow regime. This interpretation contrasts with the usually accepted idea that the massive bed forms in the upper part of the upper flow regime (Walker, 1965, p.22; Harms and Fahnestock, 1965, p.109).

It seems that the factor determining whether a massive bed or laminated bed will form from deposition in the upper flow regime (and probably also in the lower flow regime) depends on the rate of deposition of the sediment. At any time a layer only a few grain diameters

thick is tracted at the bottom and this traction is responsible for the formation of distinct laminae. With a high rate of deposition, particles coming to rest at the interface will lie there only for a short time before they are buried. Thus these particles will not be tracted and a massive bed will result. A similar conclusion was reached by Walton (1967) from a different line of reasoning with the addition that the rate of deposition is a function of the rate of deceleration of the depositing current.

It is apparent that all gradations from very well developed laminated beds to massive beds should occur in turbidite beds depending upon the rate of deposition. The poorly developed laminae in the upper part of the bed G-58 at section II₆ (fig. 2.29) are examples of an intermediate case. Poorly developed laminations thought by Stauffer (1967) to be formed by some sort of internal shearing may, in fact, have been formed in a similar way.

Argillite and calcisiltite fragments are not present in thin laminated parts of the beds and occur in the upper part of a bed, only where it is massive in nature. These waterlogged fragments were probably quite light and were not likely to be deposited in the thinner laminated part of the bed because of the higher velocity of the current in this region. However, the implication

of general absence of fragments in the laminated beds (Enos, 1965, p.28) and their presence only in the massive beds may be far reaching. It is well known that large fragments at the bottom inhibit the formation of ripples even though all other conditions, such as bottom shear velocity, grain size and supply of the sediment, are favorable (Nevin, 1946). It is suggested that the presence of large fragments at the bottom may also be unfavorable for the traction of particles at the bottom in the plane bed phase of the upper flow regime, even though all other conditions are favourable. Thus if two main ways by which lamination is produced in turbidite beds are eliminated, a massive bed should result. However, it should be noted that there are many massive beds with no large fragments and in the present case, the rock fragments are not considered to play a major role in the formation of beds with massive structure.

Variation in Sole Markings

In the present study, irrespective of internal structure of the beds, the following general change in sole marks from the proximal to the distal area is observed: (1) smooth bed with tool marks such as prod marks, grooves etc., and isolated flutes marks, to

(2) longitudinal ridges, longitudinal ridges with overlapping flute marks and closely spaced flutes, to (3) poorly developed, shallow longitudinal ridges with occasional cusped bars, to (4) smooth bed with occasional groove marks.

For the formation of tool marks, the tool is moved close to the bottom by dragging, rolling or saltation (Dzulynski and Simpson, 1966b). The tool may be taken into suspension temporarily. For this, the current should be dense and turbulent enough to move tools by any of the modes of transportation mentioned above and not so dense that the tools are taken into complete suspension and do not come into contact with the bottom.

Flutes are considered to be the result of current scour brought about by turbulent eddies within the flow over the soft mud bottom (Dzulynski and Walton, 1965, p.47). Dzulynski (1965) proposed that turbulent eddy scouring the flute is vertical and scour of flute is followed by the formation of twin eddies with inverse sense of rotation. The twin vortices change to a horizontal position, as they move down. These horizontal vortices may be responsible for formation of L-ridges. This process may result in sole marks showing all transitions between flutes and L-ridges.

For the formation of L-ridges, the development

of secondary flow such as helical or convection-like flow is necessary. As compared with flutes, scour involved in the formation of L-ridges is negligible and L-ridges result by action of skin friction drag of the flow on the soft mud bottom (Dzulynski and Simpson, 1966b). Studies by Dzulynski (1965) suggest that L-ridges form from flows which are sub-turbulent to very slow in nature. Costello (1968, p.18) has shown experimentally that L-ridges may form even from a turbulent flow.

Obviously the experimental studies of sole mark formation are still of a qualitative nature. So a tentative explanation of the observed sequence of sole marks in the beds under study is attempted. In the initial stages in the proximal region, the depositing current was assumed to have a low concentration of sediment load and was highly turbulent with tools being transported close to the bottom of the current. Scour by turbulent eddies at favorable places, such as small irregularities on the bottom, gave rise to isolated flutes.

As the depositing current slowed down in the downcurrent direction, helicoidal flow developed in the current close to the base to form L-ridges. Due to the slowing down of the current, most of the suspended material moved closer to the bottom of the current and imparted a

high concentration (also effective high density) to the lower part of the flow, such that tools were held high in suspension in the flow and were deposited in the upper part of the bed. Further downcurrent, the current was dilute throughout due to the loss of sediment, tools sank to the lower levels in the current and formed tool marks. Tools are found in all parts of the bed in the distal regions.

Lateral Changes in Sole Mark Directions

In the present study, an increase in variance of sole mark directions can be detected in the downcurrent direction in individual beds. Also, there does not seem to be any preferred trend in the deflection of sole mark directions for a particular type of bed. Sole marks take a direction nearly normal to the previous direction as the bed G-65 is traced along the strike from east to west.

It is proposed that in the proximal region, the turbidity current because of its inertia continued along the direction previously established and as a result, sole marks have a fairly constant mean direction with a very small variance. As the current slowed down in the distal region, the deflection in the direction of the turbidity current might occur due to-

- (i) Coriolis forces (ten Haaf, 1959, p.78)
- (ii) a general slope across the direction of the turbidity current (Scott, 1967)
- (iii) ocean currents flowing at an angle to the direction of the turbidity current (Scott, 1967)
- (iv) the tendency of the current to spread upon debouching from a restricted channel onto an open plane
- (v) the tendency of the slow current to spread out over small slopes (Kuenen, 1967, p.234)
- (vi) increased tendency of the current to meander
- (vii) small irregularities at the bottom

Coriolis forces and a general slope across the direction of flow of the turbidity current would tend to deflect the current in a particular direction. However, the depositing currents were deflected both in clockwise and anticlockwise directions from their mean direction of flow as shown by sole mark directions. Kuenen (1967) has demonstrated that ocean currents require a velocity many times the velocity of turbidity currents to deflect them by large angles and ocean currents with large velocities are unknown.

Also, the explanation of increase in variance of sole mark directions in the downcurrent direction by restriction of the current at first to a channel and later spreading out over an open plane is unacceptable. The

area of deposition of the beds under consideration is considered to be an abyssal plain, as very coarse grained beds are absent and no evidence of large channelling is present in the whole β -7 member (835 meters thick).

Thus the first four factors may be eliminated as causes in the deflection of turbidity currents and deflection of the turbidity currents may be caused by one of or a combination of the three factors, i.e., (i) increased tendency of the current to meander, (ii) deflection of the current by small irregularities, and (iii) the tendency of slow current to spread over small slopes.

Enos (1965) noted that the mean of the sole mark directions is remarkably constant in lateral and vertical sense over large distances and large stratigraphic intervals. However, the study of beds G-66, G-65 and G-49 shows that these beds may have sole directions deviating from the mean direction (274°) up to 90° . These deviations are quite large. It is suggested that a narrow form of the trough imposes the general grand trend in the deposition of greywacke beds and deviations of sole directions around the mean trend are caused by the tendency of the current to meander, to spread over small slopes and to be deflected by microtopography.

Theory of Grain Orientation

In order to understand the factors controlling apposition fabric, or any of the textural properties of a sediment, it is important to understand the processes by which individual particles are brought to rest, i.e., the primary depositional processes. Three types of depositional processes - mass deposition, deposition from suspension and deposition from traction carpet are distinguished here and an attempt is made to deduce the possible fabric patterns that will result from these processes. In the formation of a sedimentary bed, one or all the processes may be involved.

Mass deposition

In this type of deposition, particles are transported 'en masse' to the final site of deposition and the depositional process is a fast 'freezing' of the sediment-fluid mass. All the physical attributes of sediment particles during transportation such as the relative spatial relationship of different particles (grading), fabric, size distribution, sorting, etc., are retained in the deposited sediment. This type of process could further be considered under two headings - deposition from a viscous flow and deposition from a

flowing grain layer.

(i) Deposition from a viscous flow - In sedimentary rocks, consolidation of a highly viscous flow such as a mud flow is an example of mass deposition from a viscous (shear) flow. It will be shown that in the distal areas, clay may be concentrated in the last stages of a turbidity current. Clay may impart high viscosity to the turbidity current, which may behave in a way analogous to a mud flow.

The hydrodynamic behaviour of the ellipsoidal particles in a viscous flow was first analyzed by Jeffreys (1922). Jeffreys (1922) concluded that prolate spheroidal particles would tend to have their largest axis perpendicular to the flow, as this position corresponds to a minimum dissipation of energy. Experiments carried out by Taylor (1923) seem to confirm Jeffreys' conclusions. Later Bhattacharya (1966) has demonstrated that a preferred orientation of particles parallel to the flow should occur in a shear flow as a result of two factors: (i) The particles rotate in a shear flow and have a high residence time in orbits of motion close to the flow direction and (ii) Interaction between particles, even with concentrations as low as 26 parts per million (Mason and Manley, 1956) tends to give a preferred orientation parallel to the flow. Thus a deposit formed by freezing of such a viscous flow will exhibit an excellent current parallel preferred

orientation of particles.

(ii) Deposition from a flowing grain layer -

Bagnold (1954, 1956) has shown that when the tangential component of the attraction of gravity exceeds the internal friction, the bed starts moving downslope. If the intergranular water in a sand bed is charged with silt and clay, the bed may start moving even at slopes of 3° to 4° . This type of granular movement under the influence of gravity has been called a 'flowing grain layer' by Sanders (1965). Massive, coarse grained graded beds are considered by Sanders (1965) to be deposited by freezing of such a grain layer. Theoretical and experimental studies show that beds formed by freezing of high concentration dispersions moving under the influence of gravity as envisaged by Bagnold (1954, 1956) have well developed grain orientation in the direction of the flow of the dispersions (Rees, 1968; Hamilton and others, 1968).

Another mass depositional process has been observed experimentally by Middleton (1967a) and Kuenen (1966). A thick coarse grained 'quick' bed separates out at the bottom of a high concentration flow. Apparently it exhibits no turbulence. The bed moves under the current. The impelling force is provided by the fluid flowing above it. The bed does not show intense saltation similar to

that of 'traction carpet' of Dzulynski and Sanders (1962). Consolidation of such a 'quick' bed gives rise to a massive bed. The interaction of particles on each other and shearing of the 'quick' bed by the current will give rise to excellent current parallel grain orientation. A preliminary study of grain orientation by Middleton (1967a) in a bed formed by freezing of a 'quick' bed confirms this idea.

Thus it seems that all mass depositional processes give rise to a massive bed with current parallel grain orientation.

Direct deposition from suspension

Rukavina (1965) suggested that if the deposition of particles from a current is fast enough, the orientation of particles in suspension may be preserved in the deposited bed. Also, Rusnak (1957) demonstrated that a weightless ellipsoidal cylinder in an inviscid flow will take a current normal direction. Rukavina (1965) has argued that particles with size greater than that of the turbulent eddies will have current normal direction (meaning thereby that they behave as if they were in an inviscid flow); but particles of smaller size will have isotropic orientation, because they will be most affected by turbulence and turbulence is thought to be isotropic over a period.

Thus if deposition from suspension is fast enough, current normal and isotropic orientation of particles will be preserved in the deposited bed.

In Rukavina's (1965) experiments bimodal orientations with modes 90° apart and uniform orientation distributions were present in beds with grain size less than 0.14 mm, but in Schwarzacher's (1951) experiments on particle orientation uniform or 90° apart bimodal orientation distributions developed in coarser sandy beds, when the rate of deposition was high. Similar results were obtained by Vollbrecht (1953). Though there is a large probability that particles greater than 0.14 mm in size will be moved by traction, it is possible that if deposition is fast enough, they may preserve their orientation in suspension. Thus 90° apart bimodal orientation or uniform orientation distributions are characteristics of rapidly deposited beds from suspension and need not be confined to beds with grain size less than 0.14 mm.

Also uniform orientation distribution of particles in rapidly deposited beds may be explained by supposing that particles fall from suspension to the depositional interface in a random manner and get buried rapidly. Thus the uniform orientation distribution of particles in the rapidly deposited beds need not reflect the orientation of particles in suspension.

Deposition from a traction carpet

If the deposition of particles from a low concentration turbidity current is slow, particles may be tracted along the bottom and thus give rise to traction structures - ripples, dunes or plane bed. The formation of a particular bed form is determined by the stream power of the turbidity current (Simons and others, 1965). Formation of ripples and dunes in the lower flow regime involves a number of fundamental processes. Since the present study is confined to plane laminated and massive beds, orientation of particles in beds with ripples and dunes will not be discussed here.

Traction of particles in the plane bed phase of the upper flow regime is a simple process. A thin layer, a few grain diameters thick, moves close to the bottom (Welinkanoff, 1955; in Nachtigall, 1962). Deposition of sediment in the upper flow regime with plane bed results in the formation of the plane-laminated beds.

Many different types of plane laminations have been described from ancient rocks (Einsele, 1963). The present discussion is restricted to two main types of plane laminations. The first type is mostly confined to well sorted sand. Grain size remains almost the same from lamina to lamina. The bed splits along the planes

parallel to the bedding and exhibits 'parting lineation' (Crowell, 1955) along the parting surfaces. Both parting lineation and the mean grain orientation direction from these beds are parallel to the inferred current direction from these beds (Allen, 1964, Martini, 1965). Grain orientation distributions have usually two modes 20° to 40° apart symmetrically distributed about the parting lineation. Experimental study of grain orientation from beds deposited from well sorted source material in the plane bed phase of the upper flow regime gives orientation patterns similar to those observed from the ancient beds (Allen, 1964).

The second type of plane laminations consists of alternating coarse and fine laminae. Kuenen (1965, 1966) produced experimentally similar laminations using poorly sorted material and described the process of formation of these laminations. Particles after coming to rest at the bottom continue to move forward and override each other. In this process, a particle settled among particles of shape and size similar to its own is likely to stay there, since it will receive maximum shielding from the neighbouring particles against current action. A particle resting over particles of much smaller size is likely to be rolled over or lifted to another saltatory leap. A number of patches of different grain size at the bottom grow by

addition of individual particles. This process results in segregation of a heterogeneous mass of sediment into homogeneous laminae of particles of similar shape and size (Kuenen, 1966).

Traction of particles at the bottom involves two processes - rolling and sliding of particles. Depending upon a number of factors, one or the other process may be dominant or both the processes may act together. The orientation pattern of particles during transport may be preserved in the deposited bed. Also, particles may be pivoted during deposition to take a position parallel to the current direction due to the 'combing effect' (cf. Vollbrecht, 1953, Nachtigall, 1962) of the current and due to the fact that in this position particles offer minimum resistance to the flowing fluid (Rusnak, 1957). Thus the deposited bed will show a current parallel, current-normal or bimodal grain orientation distribution with modes 90° apart, and will have a laminated internal structure. A plane bed with alternating coarse and fine laminae probably was deposited in the plane bed phase of the upper flow regime, as cross-laminated beds are deposited over the plane-laminated bed with alternating coarse and fine laminae by slowing down^{of} the experimental current (Kuenen, 1966, fig. 7).

More recently, Kuenen (1967) has observed experi-

mentally that instead of growing of patches of coarse and fine grains by addition of individual particles, a layer of coarse rolling grains appears occasionally and is deposited. The coarse layer is later covered with finer material from the current. In conclusion, rolling of particles does take place with heterogeneous source material, it results in laminated structure of the bed and gives rise to current normal grain orientation.

Sole normal grain orientations from poorly laminated beds reported by Stanley (1963) probably result from rolling of particles.

Explanation of Observed Features of Grain Orientation in Light of Theory.

Degree of preferred orientation

Beds G-68, G-67 and G-66 show non-significant, sole normal or bimodal grain orientation distributions in the eastern, proximal regions. Also, x-ray radiographic examination of specimens II₉-66, II₆-66, II₈-66, II₆-68, and II₈-68 show that these specimens are massive and structureless. Thus their orientation patterns can be explained best by assuming that these beds were deposited directly from suspension. This is in conformity with the conclusion already arrived on the basis of the presence of laminated structure in thin parts of the beds in the

eastern region.

Because of the nature of grain orientation, it may be assumed that the beds G-68, G-67 and G-66 were deposited from suspension particle by particle in the proximal region and that currents were relatively low concentration ones similar to those of Middleton (1967a). In a bed deposited by low concentration flow, good grading also should develop as observed by Middleton (1967a) in experimental turbidites. Beds G-68, G-67 and G-68 show good grading in the eastern regions as expected.

Middleton (1967a) observed a very good orientation parallel to the current in the experimental turbidites deposited from low concentration flows. Also it was observed that particles were tracted along the bottom for about 15 centimeters after coming to rest at the depositional interface. Current-parallel orientation of particles probably resulted from their traction at the bottom. If the rate of deposition is fast enough that the particles are not tracted at the bottom before being buried, it is possible that the deposited bed will have a non-significant preferred grain orientation as observed in beds G-68, G-67 and G-66 in the proximal region.

The massive upper parts of beds G-65A and G-65 at sections II₉ and II₈ with grain size less than 2.5 phi also exhibit non-significant grain orientation. Since

these parts are massive, these are also considered to have been deposited from suspension. During deposition, particles were derived progressively from higher parts of the current, and therefore the ungraded nature of the bed reflects the ungraded nature of the depositing current, i.e., the particles in the depositing current were in auto-suspension. Nordin and others (1963) reported that particles with size less than 0.06 mm are uniformly distributed in a vertical profile of the Rio Grande river. As pointed out by Johnson (1965), this grain size distribution is due to the fact that these grain sizes meet the criteria of auto-suspension. It is suggested that similar auto-suspension took place in the depositing currents for grain sizes less than 2.5 phi and deposition from these currents was responsible for the formation of ungraded massive beds with non-significant grain orientation.

The ungraded nature and non-significant grain orientation of bed G-49 at section II₉ can be explained in a similar way as for beds G-65A and G-65. However, it should be pointed out that grain size in bed G-49 (2.071 phi) is slightly higher than that in beds G-65A and G-65. Also beds with grain size similar to bed G-49 commonly show good grading.

Deviation of graptolites and grain orientations from the sole

Explanations of non-parallel relationship between grain orientation and sole structures in turbidites are mainly of three types. The first assumes that both the sole structures and the preferred grain orientation directions are parallel to the flow direction. The divergence in their directions is attributed to a change in the flow direction subsequent to the production of sole structures (Bouma, 1962; Spotts, 1964; Spotts and Weser, 1964). The second does not require a change in the flow direction. Grain orientation normal to flow direction is assumed to develop because of traction (Stanley, 1963; Ballance, 1964). A third hypothesis is that, in a bed deposited rapidly, grain orientation may be sole normal (Rukavina, 1965; Hand, 1961).

In the present study, significant grain orientations and graptolites are generally parallel to the sole. They show a gradual change from bottom to top of beds from sole parallel to deviations as large as 90° . Deviations of grain orientations from the sole directions are both clockwise and anticlockwise. Also, some of the specimens (II₄-68, II₄-66) showing large deviations of grain orientation from the sole examined by radiographic technique for the presence of internal structures turned out to be

massive and structureless.

The large deviations of grain orientations from the sole could not be caused by rolling as in a rolling process, a layer with a maximum thickness of a few grain diameters moves close to the bottom. If the rolling process is continued for a long time to deposit a bed a few centimeters thick, a laminated structure will result by the processes already described in the last section. However, the beds under consideration are massive. Further evidence comes from the fact that the change in grain orientation direction from bottom to top of the bed is a gradual one. If rolling process had been responsible for sole normal grain orientation, it is expected that the change in grain orientation would have been a sudden one. Also, all the processes giving rise to coarse-grained massive beds produce excellent current-parallel grain orientation. Thus it seems that the depositing current must have changed its direction after the formation of the sole mark.

Dzulynski and Simpson (1966b, p.200) suggested that there is a brief interval between the formation of tool marks and their filling by the sediment from the current. During this small time interval, another set of tool marks may be formed at an angle to the first formed set due to change in the direction of the current. A similar change

in the direction of the current is possible even during the deposition of the bed itself. Thus the depositing current may change its direction after the formation of the first set of sole marks and before the start of deposition as well as during the deposition of the bed.

Deflection of the turbidity currents during the deposition of the beds in distal regions was probably related to the slowing down of the current. The deflection of the slow current was caused by the same factors as caused the deflection in the earlier stages of current flow in the distal region. These factors resulted in a higher variance in the sole mark directions in the distal regions.

Bed G-58 has mostly statistically significant sole normal grain orientations. The bed seems to be massive except for the presence of plane laminations towards the top of the bed at section II₆. The following two explanations are possible: (i) the bed has some sort of internal structure, which is not seen as such, and this internal structure is responsible for sole-normal grain orientation, (ii) soft sediment deformation as evidenced by the presence of load structures at the base of the bed is the cause of the sole normal grain orientation. The latter explanation is favored here, since the fine polished surface of the specimens studied for grain

orientation from the bed G-58 failed to show any sign of the presence of internal structure.

Difference between the directions of tool marks and grain orientation may result from a change in the direction of the depositing current after the formation of the tool marks. However, the divergence between the two may be accounted for in another equally plausible way. In laboratory experiments with straight flumes, it has been observed that tools may be deflected from a direction parallel to the current direction due to wall effects and these tools may give rise to tool marks at an angle to the current direction (Dzulynski and Simpson, 1966b, p.208). In a natural case, an irregularity at the bottom may deflect the tool in a similar way and this may result in a tool mark at an angle to the current direction. Also, large random turbulent eddies in the flow may deflect the tools from a direction parallel to the current. Later deposition will be with grains aligned parallel to the current. A constant angle between the groove mark and grain orientation in specimen II₅-68 may be explained in a similar way.

The sole-normal and sole-parallel grain orientations of specimen II₈-67 and sole-normal grain orientation of specimen II₆-50 are associated with certain internal structures. The specimen II₆-50 has poorly developed

plane laminations. The specimen II₈-67 comes from a region where 'dish structure' is developed in the bed. Traction of particles may be responsible for sole normal grain orientation and laminated structure of the specimen II₆-50. Grain orientation patterns of specimen II₈-67 are probably a result of the so far unknown processes involved in the formation of 'dish structure'.

Grading

Kuenen and Migliorini (1950) visualized a turbidity current as a current with a large amount of suspended sediment, in which the coarse material is concentrated near the head of the current close to bottom. There is lateral and vertical grading towards finer sizes from this high concentration region. At a particular place, the material is deposited by the parts of the turbidity current progressively further behind in the current, and this process results in a vertical grading.

Middleton (1967a) recognized two types of turbidity currents in his experiments - low concentration flows and high concentration flows. In the low concentration flows, the deposition is slow and particle by particle. It gives rise to normal grading or distribution grading. In the high concentration flows, there is a sudden appearance of "quick" bed which is sheared extensively. A similar quick

bed was observed by Kuenen (1966) and he called it a 'traction carpet'. This quick bed is thought to be homogeneous and coarse grains work their way to the bottom;

'freezing' of such a bed gives rise to 'coarse tail' grading. But the bed formed by high concentration flows may be normally graded, if suspended material in the turbidity current is normally graded (Kuenen, 1966).

Kuenen and Menard (1952) attributed poor grading near the source in their experiments to rapid deposition. Middleton (in Walker, 1965; 1966) has suggested that in the earlier, swifter stages of the current, if the slope is steep enough, sediment is transported from the body of the current to the head at a fast rate. Such a current is called an 'immature' current by Walker (1965). Deposition from an 'immature' current gives rise to poorly graded beds (Walker, 1965).

Grain size decrease away from the source has been attributed to decrease in velocity, and thus decrease in the capacity of the current to carry coarse grains, and due to progressive loss of coarse particles (Kuenen and Migliorini, 1950; Rukavina, 1965; Middleton, 1967a).

In all experiments on turbidity currents, deposition of sediment starts just after the formation of the turbidity current due to small size of the apparatus and high settling velocity of the sediment used. However, in nature, a

turbidity current may carry its load of sediment for a long distance probably in auto-suspension (Middleton, 1967a, p.501), before it starts depositing. So the experimental results may not explain all the features observed in natural turbidite beds. This is particularly true in the case of lateral changes in grading characteristics. In the present case, the beds show very good grading in the proximal region, and become ungraded or slightly reverse graded in the distal region, whereas just the reverse is observed in the experimental turbidites (Kuenen and Migliorini, 1950; Middleton, 1967a). Since the natural turbidity currents apparently had travelled long distances, they developed a very good lateral and vertical grading, and deposited beds with good grading in the proximal region.

It has been observed that sandy greywacke beds may pass into argillaceous beds which may pass into argillite (Parkash, Tech. Memo. 66-4, Enos, 1965, p.98). Also, the experimental turbidites formed by strong and swift currents show an increase in clay matter in the distal portions, even though the original source material of the turbidity currents was clean sand (Dzulynski and Walton, 1965, p.200). It suggests that an effective segregation of clay can take place in the late stages of the current in the distal portions.

A number of lines of evidence suggest that clay in

the turbidity currents was probably highly flocculated. Studies of underflows in Lake Mead show that most of the suspended material is highly flocculated clay (Sherman 1953). Sediment deposited by turbidity currents in large reservoirs is found to contain a high percentage of flocculated material (Bell, 1942; Gould, 1951; Sherman, 1953). Flocculation will be a still more important process in salt water. Also, Mizutani (1957) suggested, from grain size and matrix studies, that the fine material in Permian turbidite greywackes of Japan was deposited originally in the form of flocculated aggregates. It is proposed that concentration of clay in the current in the distal regions combined with its highly flocculated nature inhibited the segregation of detrital particles and thus resulted in the ungraded nature of the beds deposited there.

Flocculated clay inhibited the segregation of detrital particles in the distal regions in two ways. Firstly, the clay imparted a high effective density to the fluid, and, secondly, the clay floccules behaved as large particles, and thus there was a high particle-to-particle-interaction under these conditions. Turbulence was a minor factor in the suspension of the sand fraction. Since turbulence is the main factor in the auto-suspension of sand (Bagnold, 1962, p.319), this type of suspension was not auto-suspension.

Clay in the turbidity current may have been present from the beginning of the current or picked up later by the current from the muddy bottom of the ocean and incorporated in it. Incorporation of clay from the muddy bottom by a turbidity current initially carrying clean sand has been observed experimentally by Dzulynski and Walton (1965, p.200).

As the current had travelled a long distance, it developed a very good lateral grading with coarsest grains close to the head and finer grains towards the tail. In the depositional phase, a 'quick' bed separated over a large area simultaneously had similar lateral grading as in the current and freezing of the quick bed gave rise to a bed with a maximum grain size at a point corresponding to the location of the head of the current and with a decreasing grain size in the upstream direction. Also, the deposited bed had a decrease in grain size in the downcurrent direction due to the loss of coarse grains resulting from decrease in velocity of the current. It explains the observed maximum grain size in the middle of the outcrop for bed G-66 and decrease in grain size both in upcurrent and downcurrent directions.

Two Parts of a Bed

In the beds under study, a grain size break at the bedding joint separating the two parts was recognized in

the field. The intrabed lineation at the bedding joint may differ in direction from the sole by as much as 40 degrees. In one case, (bed G-67 close to the 1100 yard point), the upper part of the bed shows the development of small scale dish structure, whereas the lower part of the bed is massive. Also, the lower part may show 'lobate' structure just below the joint. The graptolite orientations from the lower part were found to be parallel to the sole and that from the upper part were more variable, but close to the intrabed lineation direction.

The grain-size break at the bedding joint was later confirmed by laboratory studies. Also, laboratory work has shown that the two parts of the bed may have different grading characteristics. The lower part may be graded or ungraded and the upper part may be ungraded, or slightly reverse graded. Grain orientations show a pattern similar to that of the graptolite orientations. In addition, in the bed G-66 the grain orientations are significant from the lower part, and non-significant or bimodal orientation distributions from the upper part in the proximal region. It is suggested that a significant change in hydrodynamic conditions takes place during the deposition of the bed, which is brought out later by diagenesis and tectonism of the rocks in the form of a bedding joint.

Sanders (1965) interpreted the lower part of a bed as being deposited by a bottom-hugging, 'flowing grain layer' and the upper part as formed by the accompanying current carrying the sediment in suspension. Thus the deposition of the bed took place by two fundamentally different processes. It has been demonstrated elsewhere that the two processes will give rise to very different fabric patterns in the deposited bed, i.e., significantly preferred grain orientation by freezing the flowing grain layer and non-significant preferred grain orientation by deposition from suspension. The fabric pattern studies show, however, mostly significant preferred orientations from both parts of the beds.

Wood and Smith (1958) divided beds with two or more parts into two categories - composite beds and multiple beds. Different parts of composite beds were considered to be deposited in several stages probably from the same current formed by repeated slipping from the same slip-scar. Different parts of multiple beds (amalgamated beds of Walker, 1965) were thought to be deposited by separate distinct currents. Enos (1965, p.126) suggested that successive lobes of an advancing turbidity current, as proposed by ten Haaf (1959, p.36-37), might give rise to two parts of beds under consideration.

A number of observations indicate that the two

parts of a bed do not represent deposition from two separate currents separated from each other in space or time. If the two parts were deposited from two separate currents, the following features should be observed:

(i) Argillite should be present between the two parts of the bed. (ii) If argillite was deposited by the first current and later eroded along with a small portion of the lower bed by the second current, one should observe an erosional surface which is likely to be irregular at places. (iii) The second current may carry material coarser than that carried by the first current. Thus, the grain size of the upper part of the bed may be coarser than that of the lower part.

None of the above mentioned features is observed in the beds under study. Grain size at the base of the upper part is invariably less than that at the base of the lower part. No argillite is observed between the two parts of a bed. The bedding joint marking the discontinuity between the two parts of a bed is a plane surface in all cases. Also, the two parts of a bed can be traced laterally into one part. Thus it seems that the two parts of a bed were deposited by the same current.

The lineation at the joint is suggestive of the fact that the lower part of the bed had consolidated enough that tools (mostly argillite and calcisiltite fragments)

could be dragged over it by the current and lineation could be made and preserved. But 'lobate' structure below the joint indicates that the bed was sheared after only partial consolidation. It seems fair to assume that shearing of the lower part of the bed was caused by the current depositing the upper part of the bed. Thus deposition of the two parts of the bed was separated by only a small time interval and probably the two parts of the bed were deposited by the same current.

The hypothesis of deposition of the two parts of a bed by two frontal lobes of a single current as envisaged by Enos (1965) is unacceptable, as it is difficult to imagine that two lobes of the current areally separated from each other could deposit two parts of a bed with similar sole and intrabed lineation directions as observed in beds G-68, G-67 and G-65 in the proximal region.

Different features of the beds studied can be explained by resorting to the experimental observations made by Middleton (1967a) and Kuenen (1966). A 'quick' bed (Middleton, 1967a) or 'traction carpet' (Kuenen, 1966) separated from a high concentration flow is extensively sheared by the overflowing current. Separation and consolidation of such a 'quick' bed will give rise to the lower part of the bed. Shearing during consolidation will

produce the internal lobate structure in the upper part of the 'quick' bed. Further deposition from the upper part of the current and part of the current close to the tail gives rise to the upper part of the bed. The grain size decreases from bottom to top of the current, thus later deposition from the upper part of the current will give rise to a bed finer grained than the lower part of the bed.

It should be emphasized that separation of the 'quick' bed from the depositing current was a feature associated with the depositional phase of the current. The current transported its load of sediment to the depositional site completely in suspension and in the initial stages, it was similar to the low concentration experimental flow of Middleton (1967a). Formation of flutes, tool marks and even erosion of sediment (erosion of bed G-68 by the current depositing the bed G-67) in the proximal region shows that the current was highly turbulent, underloaded and probably transported its tools close to the bottom.

Separation of a 'quick' bed from a current assumed to have a low concentration needs some explanation, as a 'quick' bed separates from high concentration flows in experiments by Middleton (1967a). In nature, a 'quick' bed could form from even a low concentration flow, if

rate of deposition is high and the deposited material contains a high percentage of fines and flaky minerals (Middleton, 1967a, p.502). High proportion of clay may also induce conditions similar to a high concentration flow (Middleton, 1967a, p.502).

It was not possible to determine in the field with certainty whether the thinner part of a bed in the proximal regions belongs to the upper part of the bed or the whole thickness of the bed elsewhere. However, it seems that the thinner part of the bed is probably equivalent to the upper part of the bed at other places from consideration of variation of thickness. As the thinner part of the bed in the proximal regions is probably deposited over a local high, it seems that the quick bed was sheared past over the local high by the overflowing current except for filling the sole marks with coarse grains. Probably the thinner part of the bed was deposited only from the upper part or the part closer to the tail of the current.

Deposition of the upper part of the bed was rather variable. After the separation of the quick bed from the depositing current, deposition was particle by particle from suspension in the proximal region. Non-significant preferred grain orientations from the upper part of the bed G-66 and presence of traction structures in the thinner parts of the beds G-66, G-67 and G-68 in the

proximal region support this contention. However, in the distal region, the upper parts of the beds have massive structures and significant preferred grain orientations. These might be formed in some cases by separation of another 'quick' bed from the depositing currents.

Synthesis: Depositional Mechanism of Greywackes

The depositing current was initially highly turbulent, low in concentration, underloaded with sediment and carried its tools close to the bottom. The current eroded the bottom to form flute marks, tool marks and smoothed out small irregularities in the proximal region.

The current continued its direction in the proximal region due to inertia. As a result, sole marks have a fairly constant mean direction with a very small variance. As the current slowed down in the distal region, it changed its direction drastically or it followed a more sinuous path with the mean direction as before. Also during the deposition of the bed, the current direction was fairly constant in the proximal region and it changed gradually by as much as 90° in the distal region.

Deposition of beds took place in at least two distinct phases. First, separation of a 'quick' bed took place from the depositing current. It was sheared

extensively by Helmholtz waves in the overflowing current in a manner similar to that observed in experiments of Middleton (1967a) and shearing resulted in the formation of 'lobate' structure. The 'quick' bed was sheared past local highs in the proximal region, except for filling the small depressions and sole marks with coarse grains. Freezing and consolidation of the 'quick' bed gave rise to the lower part of the bed with massive structure and significant preferred grain orientation.

After the separation of the 'quick' bed from the current, deposition from the upper part of the current in the proximal region was particle by particle. After coming to rest at the bottom, particles were tracted to form a laminated bed or if the rate of deposition was fast, particles were buried as soon as they reached the depositional interface and a massive bed with non-significant grain orientation resulted. Deposition from the upper part of the current further downcurrent probably took place in some cases by separation of another 'quick' bed to give rise to the upper part of the bed with massive structure and significant preferred grain orientation.

The depositing current had a very good grain size grading in the proximal region. However, due to the loss of coarse grains and probable concentration of flocculated clay in a way similar to that observed in

experiments of Dzulynski and Walton (1965, p.200), the current was poorly graded in the distal region. These features of the current were reflected in the grading characteristics of the deposited beds.

SUMMARY AND CONCLUSIONS

In an attempt to understand the mechanism of deposition of sediment from turbidity currents, a detailed field study of lateral changes in sole mark types and directions, bed thickness, and internal sedimentary structures was undertaken for eight turbidite greywacke beds from the Cloridorme Formation (Middle Ordovician), Gaspé, Quebec. More than 225 thin sections were studied for vertical and lateral changes in dimensional orientation and size of quartz grains.

The presence of tool marks, flute marks and evidence of erosion in the proximal region suggests that turbidity currents were initially highly turbulent, low concentration ones, under-loaded with sediment and carried their tools close to the bottom.

The downcurrent change of sole mark types (tool marks and isolated flute marks to longitudinal ridges and related structures to smooth bottom with occasional grooves) and distribution of tools in the deposited beds indicate that the lower part of the current developed a higher concentration of suspended sediment (also higher effective density) in early stages before the onset of deposition, such that the tools (calcsiltite and argillite

fragments) were held high in the current and were deposited later in the upper part of the bed. In the distal region, the current was again of uniformly low concentration due to loss of coarse grains and, consequently, tools moved close to the bottom.

The beds under study are traversed by a bedding joint. A distinct break in grain size at the bedding joint, deviation of up to 40° of intrabed lineation at the bedding joint from the sole and the difference in fabric, grading characteristics and internal structure between the two parts of the bed at places suggest that the deposition of the two parts of the bed was separated by a small time interval and that the mode of deposition of the two parts was different.

The grain fabric, grading characteristics and internal sedimentary structures of the two parts and comparison with experiments on turbidites indicate that the lower part of the beds was deposited by consolidation of a 'quick' bed (Middleton, 1967a) separated from the current. The particles in the 'quick' bed were kept in a dispersed state by the internal pore pressure. The quick bed was sheared extensively by the overflowing current and sheared past local highs in the proximal region except for filling the small depressions, such as flute marks, with coarse grains. Partial loss of the

pore pressure during consolidation resulted in some cohesiveness, and shearing of the still 'quick' bed at this stage formed the internal 'lobate' structure.

The deposition of the upper part of the beds was rather variable. The upper part was deposited in the proximal region by settling of individual particles from the dilute upper part of the current and part close to the tail of the current. If the rate of deposition was high, particles were buried as soon as they landed on the depositional interface and when the deposition was slow, particles were tracted at the bottom. The upper part probably was deposited in some parts of the distal region by consolidation of another 'quick' bed separated from the current.

Change from well-graded to poorly graded beds from the proximal to the distal region is just the reverse of that observed in experimental turbidites, suggesting that not all the features of turbidity currents may be adequately modelled in the laboratory. The observed grading characteristics are explained by assuming that the current travelled a long distance before reaching the depositional site and as a result developed a good vertical and lateral grading and deposited a bed with good grading in the proximal region. An ungraded bed was deposited by the current in the distal region due to

the loss of coarse grains and concentration of flocculated clay in a manner similar to that observed in the experiments of Dzulynski and Walton (1965, p.200).

An increase of variance or large changes in the sole mark direction from the proximal to distal region and large deviations of internal flow direction indicators (grain orientation, graptolites, and intrabed lineation) from the sole direction in the distal region, suggest that the depositing currents maintained their previously established courses in the proximal region due to inertia. On slowing down in the distal region, the currents tended to change direction greatly before the onset of deposition as well as during the deposition of the beds. Changes in direction were brought about by microtopography, increased tendency of the currents to meander, and tendency of the slow currents to spread out over small slopes.

As a subsidiary problem, a review of the studies on grain orientation of sediments and related sedimentation processes was undertaken. The grain fabric of sediment seems to be controlled by the way the particles are brought to final rest. Three main depositional processes - mass deposition, direct deposition from suspension and deposition from a traction carpet are recognized. Mass deposition takes place by freezing of a viscous suspension,

a 'flowing grain layer' (Sanders, 1965), or consolidation of a 'quick' bed separated from a high concentration flow (Middleton, 1967a). These processes lead to the formation of a massive bed with flow-parallel grain orientation. Fast deposition of particles from a suspension without traction also produces a massive bed with mostly statistically non-significant grain orientation. Deposition from a traction carpet (plane bed phase of the upper flow regime) produces a plane-laminated bed with current-parallel, current-normal, or bimodal grain orientation distributions.

BIBLIOGRAPHY

- Allen, J. R. L., 1962, Petrology, origin and deposition of the highest Lower Old Red Sandstone of Shropshire, England: *Jour. Sedimentary Petrology*, v. 32, p. 657-697.
- _____, 1964, Primary current lineation in the Lower Old Red Sandstone (Devonian), Anglo-Welsh Basin: *Sedimentology*, v. 3, p. 89-108.
- Bagnold, R. A., 1954, Experiments on a gravity-free dispersion of large solid spheres in a Newtonian fluid under shear: *Proc. Royal Soc. London*, ser. A, v. 225, p. 49-63.
- _____, 1956, The flow of cohesionless grains in fluids: *Trans. Royal Soc. London Philos.*, ser. A, v. 249, p. 235-297.
- _____, 1962, Auto-suspension of transported sediment: turbidity currents: *Proc. Royal Soc.*, ser. A, v. 265, p. 315-319.
- Ballance, P. F., 1964, Streaked-out mid ripples below Miocene turbidites, Puriri Formation: New Zealand: *Jour. Sedimentary Petrology*, v. 34, p. 91-101.
- Bassett, D. A. and Walton, E. K., 1960, The Hell's Mouth Grits, Cambrian greywacke in St. Tudwal's Peninsula, North Wales: *Quart. Jour. Geol. Soc. London*, v. 116, p. 85-110.
- Bell, H. S., 1942, Density currents as agents for transporting sediments: *Jour. Geol.*, v. 50, p. 512-547.
- Berry, Wm. B. N., 1962, Stratigraphy, zonation and age of Schaghticoke, Deepkill and Normanskill Shales, eastern New York: *Bull. Geol. Soc. Am.*, v. 73, p. 695-718.
- Bhattacharyya, D. S., 1966, Orientation of mineral lineation along the flow direction in rocks: *Tectonophysics*, v. 3, no. 1, p. 29-33.

- Bokman, John, 1952, Clastic quartz particles as indices of provenance: *Jour. Sedimentary Petrology*, v. 22, p. 17-24.
- Bouma, A. H., 1962, *Sedimentology of some flysch deposits*: Elsevier Publishing Co., Amsterdam, 168 p.
- Briggs, Garrett, and Cline, L. M., 1967, Paleocurrents and source areas of late Paleozoic sediments of the Ouachita Mountains, Southeastern Oklahoma: *Jour. Sedimentary Petrology*, v. 37, p. 985-1000.
- Carrozi, A. V., 1957, Tracing turbidity current deposits down the slope of an Alpine basin: *Jour. Sedimentary Petrology*, v. 27, p. 271-281.
- Colburn, Ivan P., 1968, Grain fabrics of turbidite sandstone beds and their relationship to sole mark trends on the same beds: *Jour. Sedimentary Petrology*, v. 38, p. 146-158.
- Costello, R. W., 1968, Experimental production of sedimentary structures: B.Sc. Thesis, McMaster Univ., 35 p.
- Crowell, J. C., 1955, Directional-current structures from the Prealpine flysch, Switzerland: *Bull. Geol. Soc. Am.*, v. 66, p. 1351-1384.
- Curry, J. R., 1956, The analysis of two dimensional orientation data: *Jour. Geology*, v. 64, p. 117-131.
- Dapples, E. C. and Rominger, J. F., 1945, Orientation analysis of fine-grained clastic sediments: *Jour. Geol.*, v. 53, 246-261.
- Dzulynski, S., 1965, New data on experimental production of sedimentary structures: *Jour. Sedimentary Petrology*, v. 35, p. 196-212.
- _____, 1966, Sedimentary structures resulting from convection-like pattern of motion: *Ann. Soc. Geol. Pologne*, t. XXXVI, p. 3-21.
- _____, and Sanders, J. E., 1962, Current marks on firm mud bottoms: *Trans. Conn. Acad. Arts Sci.*, v. 42, p. 57-96.

- _____, and Simpson, F., 1966a, Influence of bottom irregularities and transported tools upon experimental scour markings: *Ann. Soc. Geol. Pologne*, v. XXXVI, p. 285-294.
- _____, and Simpson, F., 1966b, Experiments on interfacial current markings: *Geologica Romana*, v. V, p. 197-214.
- _____, and Slaczka, A., 1958, Directional structures and sedimentation of the Krosno beds (Carpathian flysch): *Ann. Soc. Geol. Pologne*, v. 28, p. 205-259.
- _____, and Walton, E. K., 1963, Experimental production of sole marks: *Trans. Edinburgh Geol. Soc.*, v. 19, p. 279-305.
- _____, and Walton, E. K., 1965, Sedimentary features of flysch and greywackes, Elsevier Publishing Co., Amsterdam, p. 274.
- Einsele, Gerhard, 1963, "Convolute bedding" und ähnliche Sedimentstrukturen im rheinischen Oberdevon und anderen Ablagerungen: *N. Jb. Geol. Paläont. Abh.*, v. 116, p. 162-198.
- Enos, P., 1965, Anatomy of a flysch: Cloridorme Formation (Mid. Ordovician), Northern Gaspé Peninsula, Quebec: Ph.D. Thesis, Yale Univ., 145 p.
- Ericson, D. B., Ewing, M., Wollin, G. and Heezen, B. C., 1961, Atlantic deep-sea cores: *Bull. Geol. Soc. Am.*, v. 72, p. 193-286.
- Folk, R. L. and Ward, W. C., 1957, Brazos River bar, a study in the significance of grain-size parameters: *Jour. Sedimentary Petrology*, v. 27, p. 3-27.
- Gould, R. R., 1951, Some quantitative aspects of Lake Mead turbidity currents: *in* Turbidity Currents and the Transportation of Coarse Sediment to Deep Waters: *Soc. Paleontologists and Mineralogists, Spec. Pub.* 2, p. 34-52.
- Griffiths, J. C., 1967, Scientific methods in analysis of sediments: McGraw Hill, 508 p.
- Hamilton, N., Owens, W. H. and Rees, A. I., 1968, Laboratory experiments on the production of grain orientation in shearing sand: *Jour. Geol.*, v. 76, p. 465-472.

- Hand, B. M., 1961, Grain orientation in turbidites: *Compass*, v. 38, p. 133-144.
- Henningsen, D., 1968, Untersuchungen über Korngefüge und Schüttungsrichtungen in Sandsteinen des südöstlichen Rheinischen Schiefergebirges: *N. Jb. Geol. Paläont. Mh.*, v. 3, p. 153-163.
- Hubert, John F., 1966, Sedimentary history of the upper Ordovician geosynclinal rocks, Grivan, Scotland: *Jour. Sedimentary Petrology*, v. 36, p. 677-699.
- _____, 1967, Sedimentology of prealpine flysch sequences, Switzerland: *Jour. Sedimentary Petrology*, v. 37, p. 885-907.
- _____, Scott, Kevin M. and Walton, E. K., 1966, Composite nature of Silurian flysch sandstones shown by groove molds on intra-bed surfaces, Peeblesshire, Scotland: *Jour. Sedimentary Petrology*, v. 36, p. 237-241.
- Jefferys, G. B., 1922, The motion of ellipsoidal particles immersed in a viscous fluid: *Royal Soc. London Proc.*, v. 102A, p. 161-179.
- Johnson, M. A., 1966, Application of theory to an Atlantic turbidity current path: *Sedimentology*, v. 7, p. 117-129.
- Jones, I. W., 1934, Marsoui Map-Area, Gaspé Peninsula: *Quebec Bur. Mines, Ann. Rpt. for 1933, pt. d.*, p. 3-40.
- Kelling, Gilbert, 1962, The petrology and sedimentation of Upper Ordovician rocks in the Rhinns of Galloway, southwest Scotland: *Trans. Roy. Soc. Edinburgh*, v. 65, p. 107-137.
- Kopstein, F. P. H. W., 1954, Graded bedding of Halech Dome: *Ph.D. Thesis, State Univ. of Groningen*, 97 p.
- Kuenen, Ph. H., 1951, Properties of turbidity currents of high density: *in Soc. Econ. Paleontologists Mineralogists, Spec. Publ. 2*, p. 14-33.
- _____, 1965, Experiments in connection with turbidity currents: *Univ. Bristol, Colston Papers*, v. 17, p. 47-74.

- _____, 1966, Experimental turbidite lamination in a circular flume: *Jour. Geol.*, v. 74, p. 523-545.
- _____, 1967, Emplacement of flysch-type sand beds: *Sedimentology*, v. 9, p. 203-243.
- _____, and Migliorini, C. I., 1950, Turbidity currents as cause of graded bedding: *Jour. Geology*, v. 58, p. 91-127.
- _____, and Menard, H. W., 1952, Turbidity currents, graded and non-graded deposits: *Jour. Sedimentary Petrology*, v. 22, p. 83-96.
- Martini, I. P., 1965, The sedimentology of the Medina Formation outcropping along the Niagara escarpment (Ontario and New York State): Ph.D. Thesis, McMaster Univ., 420 p.
- Mason, S. G. and Manley, R. S. J., 1956, Particle motion in sheared suspensions: *Proc. Roy. Soc. London*, v. 238A, p. 117-131.
- McBride, E. F., 1962, Flysch and associated beds of the Martinsburg Formation (Ordovician), Central Appalachians: *Jour. Sedimentary Petrology*, v. 32, p. 39-91.
- McGerrigle, H. W., 1950, The geology of Eastern Gaspé: Quebec Dept. Mines, Geol. Rpt. 35, 174 p.
- _____, 1953, Geology of Gaspé Peninsula: Quebec Dept. Mines, Map No. 1000.
- _____, 1954, An outline of the Geology of Gaspé Peninsula: *Can. Mining Jour.*, v. 45, no. 8, p. 57-63.
- _____, 1959, Madeleine River area: Quebec Dept. Minés, Geol. Rpt. 77, 50 p.
- McIver, N. L., 1961, Upper Devonian marine sedimentation in the central Appalachians: Ph.D. Thesis, The John Hopkins Univ., 375 p.
- Middleton, G. V., 1962, Size and sphericity of quartz grains in two turbidite formations: *Jour. Sedimentary Petrology*, v. 32, p. 725-742.

- _____, 1965, Grain orientation in clastic sediments (with annotated bibliography): California Institute of Technology, Tech. Memo. 65-1, 22 p.
- _____, 1966a, Experiments on density and turbidity currents I. Motion of the head: Can. Jour. Earth Sci., v. 3, p. 523-545.
- _____, 1966b, Experiments on density and turbidity currents II. Uniform flow of density currents: Can. Jour. Earth Sci., v. 3, p. 627-637.
- _____, 1966c, Multivariate statistical methods in Geology: Unpublished Lecture Notes, McMaster Univ.
- _____, 1967a, Experiments on density and turbidity currents III. Deposition of sediment: Can. Jour. Earth Sci., v. 4, p. 475-505.
- _____, 1967b, The orientation of concavo-convex particles deposited from experimental turbidity currents: Jour. Sedimentary Petrology, v. 37, p. 229-232.
- Mizutani, S., 1957, Permian sandstone in the Mugu Area, Gifu Prefecture, Japan: Jour. Earth. Sci., Nagoya Univ., v. 5, p. 133-151.
- Nachtigall, J. O., 1962, Uber die Regelung von Langquarzen in aquatisch sedimentierten Sanden: Meyiniana, v. 12, p. 9-24.
- Nevin, C., 1946, Competency of moving water to transport debris: Geol. Soc. Am. Bull, v. 57, p. 651-674.
- Nordin, C. F. and Dempster, G. R., 1963, Vertical distribution of velocity and suspended sediment, Middle Rio Grande, N.M.: U.S. Geol. Surv. Profess. Paper 462B, 20 p.
- Okada, H., 1966, Non-greywacke "turbidite" sandstones in the Welsh geosyncline: Sedimentology, v. 7, p. 211-232.
- Onions, D., 1965, Dimensional grain orientation of Ordovician turbidite greywackes: M.Sc. Thesis, McMaster Univ., 102 p.
- _____, and Middleton, G. V., 1968, Dimensional grain orientation of Ordovician turbidite greywackes, Jour. Sedimentary Petrology, v. 38, p. 164-174.

- Parkash, B., 1966, Sedimentary structures and lateral variation in a turbidite sequence - Cloridorme Formation (Middle Ordovician), Gaspé, Quebec: McMaster Univ., Department of Geology, Tech. Memo. 66-4, 23 p.
- _____, 1968, A Fortran IV program for grain size data from thin sections: McMaster Univ., Department of Geology, Tech. Mem. 68-2, 11 p.
- Passega, R., 1957, Texture as characteristic of clastic deposition: Bull. Am. Assoc. Petrol. Geologists, v. 41, p. 1952-1984.
- Potter, P. E. and Pettijohn, F. J., 1963, Paleocurrents and Basin Analysis: Springer Verlag, Berlin, 296 p.
- Radomski, Andrzej, 1958, Sedimentological character of the Podhale flysch: Acta Geol. Polonica, v. 8, no. 3, p. 395-408.
- _____, 1960, Remarks on sedimentation of shales in flysch deposits: Acad. Polonaise des Sciences, Bull., v. 8, p. 123-129.
- Raup, O. B. and Miesch, A. T., 1957, A new method for obtaining significant average directional measurements in cross stratification studies: Jour. Sedimentary Petrology, v. 27, p. 313-321.
- Rayleigh, Lord, 1884, The theory of sound: 2nd ed., v. 1, McMillan and Co., New York, 480 p.
- Rees, A. I., 1968, The production of preferred orientation in a concentrated dispersion of elongated and flattened grains: Jour. Geol., v. 76, p. 457-465.
- Rukavina, N. A., 1965, Particle orientation in turbidites; Theory and experiment: Ph.D. Thesis, Rochester Univ., 57 p.
- Rusnak, G. A., 1957, Orientation of sand grains under conditions of unidirectional flow: Jour. Geology, v. 65, p. 384-409.
- Sanders, J. E., 1963, Concepts of fluid mechanics provided by primary sedimentary structures: Jour. Sedimentary Petrology, v. 33, p. 173-179.

- _____, 1965, Primary sedimentary structures formed by turbidity currents and related resedimentation mechanisms: in Primary Sedimentary Structure and Their Hydrodynamic Interpretation: Soc. Econ. Paleontologists Mineralogists, Spec. Publ. 12, 192 p.
- Scheidegger, A. E. and Potter, P. E., 1965, Textural studies of graded bedding: Observation and theory: Sedimentology, v. 5, p. 289-
- Schwarzacher, W., 1951, Grain orientation in sands and sandstones: Jour. Sedimentary Petrology, v. 21, p. 162-172.
- Scott, K. M., 1966, Sedimentology and dispersal pattern of a Cretaceous flysch sequence, Patagonian Andes, Southern Chile. Bull. Am. Assoc. Petroleum Geologists, v. 50, p. 72-107.
- _____, 1967, Intra bed paleocurrent variations in a Silurian flysch sequence, Kirkcudbrightshire, Southern Uplands of Scotland: Scott. Jour. Geol., v. 3, part 2, p. 268-281.
- Sestini, G. and Pranzini, P., 1965, Correlation of sedimentary fabric and sole marks as current indicators in turbidites: Jour. Sedimentary Petrology, v. 35, p. 100-109.
- Sherman, I., 1953, Flocculent structure of sediment suspended in Lake Mead: Trans. Am. Geophys. Union, v. 34, p. 394-406.
- Shiki, T., 1961, Studies on sandstones in the Maizuru zone, Southwest Japan. II. Graded bedding and mineral composition of sandstones of the Maizuru Group: Mem. Coll. Sci. Univ. Kyoto, Ser. B., v. 27, no. 3, p. 293-308.
- Simons, D. B., Richardson, E. V. and Nordin, C. F., 1965, Sedimentary structures generated by flow in alluvial channels: in Primary Structures and their Hydrodynamic Interpretation, Soc. Econ. Paleontologists Mineralogists, Spec. Publ. 12, p. 34-52.
- Smoor, P. B., 1960, Dimensional grain orientation studies of turbidite greywackes: M.Sc. thesis, McMaster Univ., 97 p.

- Snedecor, G. W., 1956, Statistical methods, Iowa State Univ. Press, 534 p.
- Spotts, J. H., 1964, Grains orientation and imbrications in Miocene turbidity current sandstones, California: Jour. Sedimentary Petrology, v. 34, p. 229-253.
- _____, and Weser, O. E., 1964, Directional properties of a Miocene turbidite, California, in Developments in Sedimentology 3, Turbidites. Amsterdam, Elsevier Publishing Co., 264 p.
- Stanley, D. J., 1961, Étude sédimentologique des grès d'Annot et de leurs équivalents latéraux: Rev. Inst. Franc. Pétrol. Ann. Combust. Liquides, v. 16, p. 1231-1254.
- _____, 1963, Vertical petrographic variability in Annot Sandstone turbidites: some preliminary observations and generalizations: Jour. Sedimentary Petrology, v. 33, p. 738-788.
- Stauffer, P. H., 1967, Grain-flow deposits and their implications, Santa Ynez Mountains, California: Jour. Sedimentary Petrology, v. 37, no. 2, p. 487-508.
- Studer, B., 1827, Notice géognostique sur quelques parties de la chaine de Stockhorn et sur la houille du Siemmental, canton Berne: Ann. Sci. Nat. v. XI, Paris, 1.
- Taylor, G. L., 1923, The motion of ellipsoidal particles in a viscous fluid: Proc. Royal Soc. London, v. 103A, p. 58-61.
- Ten Haaf, 1959, Graded beds of the Northern Appenines: Ph.D. Thesis, State Univ. of Groningen, 102 p.
- Unrug, R., 1963, Istebna beds - a fluxoturbidite formation in the Carpathian flysch: Ann. Soc. Geol. Pologne, v. 33, p. 49-92.
- Vollbrecht, K., 1953, Zur Quazachsen-Regelung sandiger Sedimente: Acta Hydrophys., v. 1, p. 1-87.
- Walker, R. G., 1965, The origin and significance of the internal sedimentary structures of turbidites: Proc. Yorkshire Geol. Soc., v. 35, p.1-32.

- Walton, E. K., 1955, Silurian greywackes in Peeblesshire:
Proc. Roy. Soc. Edinburgh, Ser. B, v. 65, p. 327-357.
- _____, 1967, The sequence of internal structures in
turbidites: Scott. Jour. Geol., v. 3, part 2,
p. 306-317.
- Webby, B. D., 1959, Sedimentation of alternating greywacke
and argillite strata in the Porirua district:
N.Z. Jour. Geol. and GEoph., v. 2, p. 461-478.
- Welikanoff, M., 1955, Dynamik der Stromungen, Bd. 2,
Geschiebe und Flussbett, - Moskau, zitiert in
Yalin, S., 1957, Die theoretische Analyse der
Geschiebebewegung. Mitt.-Bl. Bundesanstalt
Wasserbau, Heft 8.
- Wood, A. and Smith, A. J., 1959, The sedimentation and
sedimentary history of the Aberystwyth Grits
(Upper Llandoveryan): Quart. Jour. Geol. Soc.
London, v. 114, p. 163-195.
- Yule, G. U. and Kendall, M. G., 1950, An introduction to
the theory of statistics: 14th ed. Haffner,
New York, 701 p.

APPENDIX I

Grain Orientation Statistics

Thin Section	Ht. above the base (cms)	Sole Direction	No. of measurements	Vector mean θ_m	Deviation	Unimodal Test			Bimodal Test	
						Rayleigh Prob.	Vector Mag. % L%	95% Conf. interval		
II ₉ -68-4	7.5		very		fine		grained			
II ₉ -68-3	5.0	277°	100	289.1°	12.1°c	0.000	**	42.18	± 7.14°	
II ₉ -68-2	2.5	277°	100	202.1°	74.9°a	0.518	N.S.	8.11	± 9.61°	0.019 **
II ₉ -68-1	0.0	277°	100	248.3°	28.7°a	0.953	N.S.	2.31	± 9.95°	0.610 N.S.
II ₆ -68-4	7.5	278°	100	252.0°	26.0°a	0.001	**	25.80	± 8.38°	
II ₆ -68-3	5.0	278°	100	282.5°	4.5°c	0.372	N.S.	9.94	± 9.51°	0.176 N.S.
II ₆ -68-2	2.5	278°	100	236.1°	42.9°a	0.123	N.S.	14.49	± 9.22°	0.492 N.S.
II ₆ -68-1	0.0	278°	100	316.5°	38.5°c	0.464	N.S.	8.76	± 9.55°	0.078 **
II ₈ -68-5	10.0	300°	100	305.6°	5.6°c	0.002	**	25.29	± 8.76°	
II ₈ -68-4	7.2	300°	100	310.0°	10.0°c	0.000	**	32.35	± 7.93°	
II ₈ -68-3	4.5	300°	100	280.8°	19.2°a	0.120	N.S.	14.57	± 9.14°	0.057 *
	6.6			Bedding Joint						
II ₈ -68-2	2.3	282°	100	290.6°	8.6°c	0.000	**	35.29	± 7.73°	
II ₈ -68-1	0.0	282°	100	242.6°	39.4°a	0.164	N.S.	13.45	± 9.24°	0.002 **
II ₅ -68-6	11.5	267°	100	315.4°	48.4°c	0.073	*	16.18	± 9.12°	
II ₅ -68-5	9.5	267°	100	279.8°	12.8°c	0.725	N.S.	5.67	± 9.87°	0.768 N.S.
II ₅ -68-4	7.5	267°	82	313.8°	46.8°c	0.000	**	30.71	± 9.01°	
II ₅ -68-3	5.0	267°	100	313.5°	46.5°c	0.000	**	37.95	± 7.49°	
	3.5			Bedding Joint						
II ₅ -68-2	2.5	267°	100	312.0°	45.0°c	0.000	**	29.19	± 8.21°	
II ₅ -68-1	0.0	267°	100	311.0°	44.0°c	0.339	N.S.	10.41	± 9.51°	0.336 N.S.

Thin Section	Ht. above the base (cms)	Sole Direction	No. of measurements	Vector mean θ_m	Deviation	Unimodal Test.			Bimodal Test Rayleigh Prob.
						Rayleigh Prob.	Vector Mag. % L%	95% Conf. interval	
II ₄ -68-6	12.0	262°	100	289.3°	27.3° _c	0.035 **	18.30	± 8.96°	
II ₄ -68-5	9.0	262°	100	341.9°	79.9° _c	0.040 **	17.75	± 9.00°	
II ₄ -68-4	6.0	262°	100	330.0°	68.0° _c	0.000 **	29.65	± 8.13°	
II ₄ -68-3	3.1	262°	100	302.0°	40.0° _c	0.000 **	32.42	± 7.97°	
	3.0			Bedding Joint					
II ₄ -68-2	2.5	262°	100	293.0°	31.0° _c	0.026 **	19.13	± 8.92°	
II ₄ -68-1	0.0	262°	100	274.0°	12.0° _c	0.116 N.S.	14.68	± 9.28°	0.434 N.S.
II ₉ -67-5	10.6		70	316.3°		0.155 N.S.	16.31	± 9.15°	0.096 **
II ₉ -67-4	8.4		100	200.3°		0.003 **	24.48	± 8.58°	
II ₉ -67-3	6.2		100	291.5°		0.161 N.S.	13.51	± 9.37°	0.160 N.S.
II ₉ -67-2	3.0		100	346.7°		0.078 *	15.96	± 9.18°	
II ₉ -67-1	0.6		100	217.7°		0.268 N.S.	11.48	± 9.53°	0.891 N.S.
II ₆ -67-6	15.0		76	289.9°		0.007 **	25.64	± 9.81°	
II ₆ -67-5	12.0		100	321.0°		0.002 **	24.80	± 8.54°	
II ₆ -67-4	9.0		100	290.0°		0.000 **	50.13	± 6.53°	
II ₆ -67-3	6.0		100	314.8°		0.033 **	18.44	± 9.01°	
II ₆ -67-2	3.0		100	281.2°		0.000 **	29.14	± 8.25°	
II ₆ -67-1	0.0		100	205.2°		0.022 **	19.50	± 8.93°	

Thin Section	Ht. above the base (cms)	Sole Direction	No. of measurements	Vector mean θ_m	Deviation	R ^y leigh Prob.	Unimodal Test Vector Mag. % L%	95% Conf. interval	Bimodal Test R ^y leigh Prob.
II ₈ -67-9	16.4	288°	91	307.3°	19.3° _c	0.072 *	16.99	± 9.57°	
II ₈ -67-8	14.5	288°	100	344.4°	56.4° _c	0.029 **	18.85	± 8.97°	
II ₈ -67-7	12.5	288°	83	245.9°	42.1° _a	0.000 **	39.05	± 7.42°	
II ₈ -67-6	10.5	288°	100	351.5°	63.5° _c	0.001 **	27.38	± 8.36°	
II ₈ -67-5	8.5	288°	100	293.1°	5.1° _c	0.000 **	30.52	± 8.11°	
	6.5	288°	Bedding Joint						
II ₈ -67-4	6.5	288°	87	347.0°	59.0° _c	0.005 **	24.50	± 8.58°	
II ₈ -67-3	4.5	288°	100	289.8°	1.8° _c	0.000 **	40.37	± 7.33°	
II ₈ -67-2	2.5	288°	100	278.0°	10.0° _a	0.000 **	30.33	± 8.13°	
II ₈ -67-1	0.0	288°	100	353.2°	65.2° _c	0.001 **	25.60	± 8.48°	
II ₄ -67-8	14.4	298°	100	277.4°	20.6° _a	0.001 **	26.64	± 8.41°	
II ₄ -67-7	11.7	298°	100	317.2°	19.2° _c	0.509 N.S.	8.22	± 9.73°	0.715 N.S.
II ₄ -67-6	9.0	298°	100	306.3°	8.3° _c	0.000 **	42.11	± 7.18°	
II ₄ -67-5	6.3	298°	100	311.6°	13.8° _c	0.000 **	40.23	± 7.34°	
II ₄ -67-4	3.7	298°	100	311.1°	13.1° _c	0.000 **	30.56	± 8.11°	
	3.6		Bedding Joint						
II ₄ -67-3	3.5	283°	100	298.0°	15.0° _c	0.000 **	35.67	± 7.70°	
II ₄ -67-2	1.8	283°	100	320.5°	37.5° _c	0.142 N.S.	13.98	± 9.32°	0.676 N.S.
II ₄ -67-1	0.0	283°	100	328.8°	45.8° _c	0.000 **	28.20	± 8.31°	

Thin Section	Ht. above the base (cms)	Sole Direction	No. of measurements	Vector mean θ_m	Deviation	Raleigh Prob.	Unimodal Test Vector Mag. % L%	95% Conf. interval	Bimodal Test Raleigh Prob.
II ₉ -66-1	0.0	271°	100	195.9°	75.1° _a	0.001 **	27.51	± 8.27°	
II ₆ -66-6	13.3	282°	100	280.0°	2.0° _a	0.637 N.S.	6.71	± 9.85°	0.126 N.S.
II ₆ -66-5	9.8	282°	100	282.0°	0.0°	0.316 N.S.	10.74	± 9.56°	0.225 N.S.
II ₆ -66-4	5.1	282°	100	357.0°	75.0° _c	0.884 N.S.	3.51	±10.11°	0.786 N.S.
	5.0		Bedding Joint						
II ₆ -66-3	4.9	282°	100	301.0°	19.0° _c	0.001 **	26.50	± 8.42°	
II ₆ -66-2	2.5	282°	100	305.6°	23.6° _c	0.000 **	29.07	± 8.26°	
II ₆ -66-1	0.0	282°	100	181.1°	79.0° _a	0.003 **	24.07	± 8.59°	
II ₈ -66-6	12.0	333°	97	268.0°	65.0° _a	0.007 **	22.68	± 8.82°	
II ₈ -66-5	8.5	333°	100	356.0°	23.0° _c	0.772 N.S.	5.08	± 9.92°	0.140 N.S.
II ₈ -66-4	5.1	333°	100	245.4°	87.6° _a	0.238 N.S.	11.99	± 9.48°	0.971 N.S.
	5.0		Bedding Joint						
II ₈ -66-3	4.5	288°	100	298.7°	10.7° _c	0.000 **	42.57	± 7.14°	
II ₈ -66-2	2.0	288°	100	300.0°	12.0° _c	0.000 **	27.63	± 8.35°	
II ₈ -66-1	0.0	288°	100	284.6°	3.4° _a	0.000 **	33.30	± 7.88°	

Thin Section	Ht. above the base (cms)	Sole Direction	No. of measurements	Vector mean θ_m	Deviation	Unimodal Test			Bimodal Test Raleigh Prob.
						Raleigh Prob.	Vector Mag. % L%	95% Conf. interval	
II ₅ -66-6	11.0	292°	100	268.0°	24.0° _a	0.169 N.S.	13.34	± 9.30°	0.120 N.S.
II ₅ -66-5	7.5	292°	100	300.5°	8.5° _c	0.000 **	31.48	± 8.05°	
II ₅ -66-4	4.5	292°	100	308.0°	16.0° _c	0.000 **	43.88	± 7.03°	
	4.0		Bedding Joint						
II ₅ -66-3	3.3	292°	100	315.0°	23.0° _c	0.000 **	34.63	± 7.86°	
II ₅ -66-2	1.7	292°	100	306.9°	14.9° _c	0.307 N.S.	10.86	± 9.56°	0.354 N.S.
II ₅ -66-1	0.0	292°	100	284.8°	7.2° _a	0.001 *	27.30	± 8.37°	
II ₄ -66-7	9.0	253°	100	334.8°	81.8° _c	0.054 *	17.06	± 9.03°	
II ₄ -66-6	7.5	253°	100	325.7°	72.7° _c	0.002 **	25.00	± 8.43°	
II ₄ -66-5	6.0	253°	100	306.2°	53.2° _c	0.003 **	24.18	± 8.56°	
II ₄ -66-4	4.0	253°	100	252.8°	0.2° _a	0.051 *	17.25	± 9.09°	
II ₄ -66-3	1.5	253°	100	240.1°	12.9° _a	0.002 **	25.31	± 8.49°	
	1.5		Bedding Joint						
II ₄ -66-2	1.3	253°	100	312.5°	59.5° _c	0.000 **	42.26	± 7.17°	
II ₄ -66-1	0.0	253°	100	253.8°	0.8° _c	0.105 N.S.	15.00	± 9.25°	0.540 N.S.

Thin Section	Ht. above the base (cms)	Sole Direction	No. of measurements	Vector mean θ_m	Deviation	Unimodal Test			Bimodal Test Raleigh Prob.
						Raleigh Prob.	Vector Mag. % L%	95% Conf. interval	
II ₉ -65A-8	13.9	289°	84	298.8°	9.8° _c	0.000 **	30.63	± 8.85°	
II ₉ -65A-7	11.6	289°	73	289.4°	0.4° _c	0.701 N.S.	6.98	±11.52°	0.426 N.S.
II ₉ -65A-6	9.3	289°	70	283.1°	5.9° _a	0.004 **	28.20	± 9.97°	
II ₉ -65A-5	7.0	289°	92	306.5°	17.5° _c	0.538 N.S.	8.20	±10.15°	0.404 N.S.
	6.9		Bedding Joint						
II ₉ -65A-4	6.8	289°	100	265.0°	24.0° _a	0.013 **	20.89	± 8.82°	
II ₉ -65A-3	4.6	289°	100	271.0°	18.0° _a	0.063 *	16.65	± 9.14°	
II ₉ -65A-2	2.4	289°	100	304.9°	15.9° _c	0.001 **	26.72	± 8.40°	
II ₉ -65A-1	0.2	289°	100	312.4°	23.4° _c	0.959 N.S.	2.04	±11.11°	0.569 N.S.
II ₆ -65A-4	7.7	287°	very	fine grained					
II ₆ -65A-3	5.2	287°	very	fine grained					
II ₆ -65A-2	2.7	287°	75	291.5°	4.5° _c	0.000 **	41.22	± 8.38°	
II ₆ -65A-1	0.2	287°	87	291.5°	4.5° _c	0.890 N.S.	3.65	±11.67°	0.795 N.S.

Thin Section	Ht. above the base (cms)	Sole Direction	No. of measurements	Vector mean \ominus_m	Deviation	Unimodal Test			Bimodal Test
						Raleigh Prob.	Vector Mag. % L%	95% Conf. interval	
II ₈ -65A-8	12.2	317°	84	232.5°	84.5° _a	0.717 N.S.	6.29	±10.76°	0.087 *
II ₈ -65A-7	10.2	317°	100	349.1°	32.1° _c	0.000 **	33.55	± 7.86°	
II ₈ -65A-6	8.2	317°	100	209.4°	72.4° _c	0.561 N.S.	7.61	± 9.80°	0.092 *
	8.0		Bedding Joint						
II ₈ -65A-5	7.6	317°	100	319.4°	2.4° _c	0.001 **	27.70	± 8.34°	
II ₈ -65A-4	5.4	317°	100	288.3°	28.7° _a	0.000 **	32.09	± 7.98°	
II ₈ -65A-3	3.2	317°	100	214.6°	77.6° _c	0.134 N.S.	14.18	± 9.32°	0.806 N.S.
	3.0		Bedding Joint						
II ₈ -65A-2	2.6	317°	100	215.0°	78.0° _c	0.743 N.S.	5.46	± 9.96°	0.135 N.S.
II ₈ -65A-1	0.2	317°	100	310.0°	7.0° _a	0.153 N.S.	13.69	± 9.36°	0.280 N.S.
II ₉ -65-5	10.3	290°	100	279.9°	10.1° _a	0.198 N.S.	12.72	± 9.93°	0.767 N.S.
II ₉ -65-4	7.8	290°	100	314.9°	24.9° _c	0.125 N.S.	14.42	± 0.31°	0.507 N.S.
	6.3		Bedding Joint						
II ₉ -65-3	5.3	290°	100	263.2°	26.8° _a	0.000 **	28.72	± 8.28°	
II ₉ -65-2	2.8	290°	100	267.5°	22.5° _a	0.000 **	30.21	± 8.13°	
II ₉ -65-1	0.3	290°	100	292.7°	2.7° _c	0.000 **	32.58	± 7.93°	

Thin Section	Ht. above the base (cms)	Sole Direction	No. of measurements	Vector mean θ_m	Deviation	Raleigh Prob.	Unimodal Test Vector Mag. % L%	95% Conf. interval	Bimodal Test Raleigh Prob.
Bedding Joint at a height of 9.9 cm									
II ₆ -65-6	9.5	296°	100	316.1°	20.1° _c	0.001 **	25.78	± 8.47°	
II ₆ -65-5	7.0	296°	100	270.9°	25.1° _a	0.527 N.S.	8.01	± 9.76°	0.615 N.S.
II ₆ -65-4	4.5	296°	100	347.0°	51.0° _c	0.000 **	37.85	± 7.54°	
Bedding Joint									
II ₆ -65-3	4.0	309°	100	324.6°	15.6° _c	0.000 **	31.82	± 8.01°	
II ₆ -65-2	2.0	309°	100	314.8°	15.8° _c	0.034 **	18.37	± 9.01°	
II ₆ -65-1	0.5	309°	100	301.0°	8.0° _a	0.016 **	20.39	± 8.85°	
Bedding Joint									
II ₈ -65-8	13.7	292°	very	fine	grained				
II ₈ -65-7	11.7	292°	80	248.9°	43.1° _a	0.636 N.S.	7.52	± 9.58°	0.008 **
II ₈ -65-6	9.7	292°	59	318.7°	26.7° _c	0.295 N.S.	14.40	±12.22°	0.848 N.S.
II ₈ -65-5	7.2	292°	77	195.6°	83.6° _c	0.326 N.S.	12.06	±10.81°	0.216 N.S.
Bedding Joint									
II ₈ -65-4	5.9	292°	100	321.0°	29.0° _c	0.000 **	28.64	± 8.29°	
II ₈ -65-3	3.7	292°	100	304.7°	12.7° _c	0.000 **	34.93	± 7.74°	
Bedding Joint									
II ₈ -65-2	2.5	257°	100	311.5°	54.5° _c	0.000 **	37.27	± 7.57°	
II ₈ -65-1	0.3	257°	100	257.3°	0.3° _c	0.187 N.S.	12.96	± 9.42°	0.165 N.S.

Thin Section	Ht. above the base (cms)	Sole Direction	No. of measurements	Vector mean Θ_m	Deviation	Raleigh Prob.	Unimodal Test Vector Mag. % L%	95% Conf. interval	Bimodal Test Raleigh Prob.
II ₄ -65-7	14.2	250°			very fine grained				
II ₄ -65-6	12.2	250°	74	295.2°	45.2°c	0.023 **	22.60	±10.83°	
II ₄ -65-5	10.0	250°	92	264.0°	14.0°c	0.001 **	28.68	± 6.60°	
II ₄ -65-4	7.5	250°	100	199.9°	50.1°a	0.001 **	26.17	± 8.45°	
II ₄ -65-3	5.0	250°	72	246.0°	4.0°a	0.001 **	30.19	± 9.59°	
II ₄ -65-2	2.5	250°	100	273.5°	23.5°c	0.026 **	19.16	± 8.95°	
II ₄ -65-1	0.0	250°	100	234.3°	15.7°a	0.023 **	19.48	± 8.93°	
II ₉ -58-3	4.5	251°	100	315.0°	64.0°c	0.026 **	19.11	± 8.95°	
II ₉ -58-2	2.5	251°	100	245.8°	5.2°a	0.018 **	20.09	± 8.89°	
II ₉ -58-1	0.5	251°	100	303.6°	52.6°c	0.000 **	38.10	± 7.51°	
II ₆ -58-6	14.0	244°			very fine grained				
II ₆ -58-5	11.5	244°			very fine grained				
II ₆ -58-4	9.0	244°	74	207.6°	36.4°a	0.002 **	29.09	± 6.82°	
II ₆ -58-3	6.0	244°	95	199.7°	44.3°a	0.027 **	19.47	± 9.16°	
II ₆ -58-2	3.0	244°	100	316.7°	72.7°c	0.000 **	28.68	± 8.29°	
II ₆ -58-1	0.0	244°			very fine grained				
II ₈ -58-5	12.0	260°			very fine grained				
II ₈ -58-4	9.0	260°	86	214.3°	45.7°a	0.004 **	25.42	± 9.23°	
II ₈ -58-3	6.0	260°	100	289.0°	29.0°c	0.087 *	15.61	± 9.21°	
II ₈ -58-2	3.0	260°	100	322.4°	62.4°c	0.000 **	33.99	± 7.83°	
II ₈ -58-1	0.0	260°	100	195.3°	64.7°a	0.126 N.S.	14.40	± 9.31°	0.971 N.S.

Thin Section	Ht. above the base (cms)	Sole Direction	No. of measurements	Vector mean θ_m	Deviation	Raleigh Prob.	Unimodal Test Vector Mag. % L%	95% Conf. interval	Bimodal Test Raleigh Prob.
II ₅ -58-5	10.0	255°			very fine grained				
II ₅ -58-4	7.5	255°	82	191.0°	64.0° _a	0.183 N.S.	14.40	±10.37°	0.531 N.S.
II ₅ -58-3	5.0	255°	100	210.5°	44.5° _a	0.001 **	26.74	± 8.40°	
II ₅ -58-2	2.5	255°	100	300.7°	45.7° _c	0.005 **	22.96	± 8.71°	
II ₅ -58-1	0.0	255°	100	336.4°	81.4° _c	0.000 **	41.45	± 7.22°	
II ₄ -58-5	12.0	247°	100	350.3°	76.7° _a	0.038 **	18.56	± 8.99°	
II ₄ -58-4	9.0	247°	100	247.2°	0.2° _c	0.046 **	17.52	± 9.09°	
II ₄ -58-3	6.0	247°	100	321.6°	74.6° _c	0.000 **	35.91	± 7.68°	
II ₄ -58-2	3.0	247°	100	194.6°	52.4° _a	0.000 **	28.94	± 8.25°	
II ₄ -58-1	0.0	247°	100	332.0°	85.0° _c	0.000 **	39.46	± 7.38°	
II ₉ -50-4	6.1	223°	100	296.0°	73.0° _c	0.021 **	19.63	± 8.91°	
II ₉ -50-3	4.3	223°	100	289.6°	66.6° _c	0.001 **	27.04	± 8.39°	
II ₉ -50-2	2.3	223°	100	292.0°	69.0° _c	0.021 **	19.67	± 8.92°	
II ₉ -50-1	0.3	233°	100	189.0°	34.0° _a	0.321 N.S.	10.66	± 9.58°	0.118 N.S.
II ₆ -50-5	8.4	294°			very fine grained				
II ₆ -50-4	6.4	294°			very fine grained				
II ₆ -50-3	4.4	294°	83	223.6°	71.0° _a	0.225 N.S.	13.41	±10.31°	0.400 N.S.
II ₆ -50-2	2.4	294°	100	203.6°	89.6° _a	0.001 **	26.49	± 8.42°	
II ₆ -50-1	0.4	294°	100	182.6°	68.6° _c	0.765 N.S.	5.17	± 9.98°	0.920 N.S.

Thin Section	Ht. above the base (cms)	Sole Direction	No. of measurements	Vector mean θ_m	Deviation	Unimodal Test			Bimodal Test Raleigh Prob.
						Raleigh Prob.	Vector Mag. % L%	95% Conf. interval	
II ₈ -50-4	8.3	307°	71	310.8°	3.8°c	0.099 *	18.07	±10.74°	
II ₈ -50-3	5.8	307°	84	284.3°	22.7°c	0.553 N.S.	8.40	±10.61°	0.726 N.S.
	5.2		Bedding Joint						
II ₈ -50-2	3.2	272°	100	306.9°	34.9°c	0.001 **	27.31	± 8.36°	
II ₈ -50-1	0.7	272°	100	299.7°	27.7°c	0.001 **	26.75	± 8.40°	
II ₅ -50-3	4.7	269°	100	277.0°	8.0°c	0.001 **	22.12	± 8.73°	
II ₅ -50-2	2.8	269°	100	297.0°	28.0°c	0.000 **	40.80	± 7.29°	
II ₅ -50-1	0.3	269°	100	239.3°	29.7°a	0.797 N.S.	4.76	±10.02°	0.305 N.S.
II ₄ -50-5	9.6		fine grained						
II ₄ -50-4	6.9		84	336.0°		0.000 **	32.45	± 8.71°	
II ₄ -50-3	3.7		100	307.1°		0.003 **	23.92	± 8.50°	
II ₄ -50-2	2.6		10	296.8°		0.043 **	17.75	± 9.07°	
II ₄ -50-1	0.8		100	276.6°		0.003 **	23.89	± 8.61°	

Thin Section	Ht. above the base (cms)	Sole Direction	No. of measurements	Vector mean θ_m	Deviation	Unimodal Test			Bimodal Test Raleigh Prob.	
						Raleigh Prob.	Vector Mag. % L%	95% Conf. interval		
II ₉ -49-9	18.5	330°	100	293.9°	36.1° _a	0.123 N.S.	14.48	± 9.30°	0.840 N.S.	
II ₉ -49-8	15.5	330°	100	290.2°	39.8° _a	0.037 **	18.18	± 9.03°		
II ₉ -49-7	12.5	330°	100	297.9°	32.1° _a	0.691 N.S.	6.08	± 9.92°	0.767 N.S.	
II ₉ -49-6	9.5	330°	100	249.8°	80.2° _a	0.602 N.S.	7.12	± 9.82°	0.897 N.S.	
II ₉ -49-5	6.5	330°	100	253.9°	76.1° _a	0.178 N.S.	13.14	± 9.41°	0.954 N.S.	
	6.4		Bedding Joint							
II ₉ -49-4	6.3	330°	100	286.6°	43.4° _a	0.100 *	15.17	± 9.26°		
II ₉ -49-3	4.5	330°	100	199.3°	30.7° _a	0.806 N.S.	4.64	±10.04°	0.197 N.S.	
II ₉ -49-2	2.3	330°	100	316.6°	13.4° _a	0.013 **	20.94	± 8.81°		
II ₉ -49-1	0.0	330°	100	320.9°	9.1° _a	0.091 *	15.49	± 9.23°		
			Bedding Joint at a height of 9.8 cm							
II ₆ -49-5	9.3	309°	89	292.6°	16.4° _a	0.000 **	41.20	± 7.75°		
II ₆ -49-4	7.0	309°	100	297.7°	11.3° _a	0.000 **	38.56	± 7.48°		
II ₆ -49-3	4.6	309°	100	312.0°	3.0° _c	0.281 N.S.	11.26	± 9.52°	0.407 N.S.	
II ₆ -49-2	2.4	309°	100	298.0°	11.0° _a	0.246 N.S.	11.84	± 9.51°	0.275 N.S.	
II ₆ -49-1	0.2	309°	100	300.5°	8.5° _a	0.002 **	25.41	± 8.49°		

Thin Section	Ht. above the base (cms)	Sole Direction	No. of measurements	Vector mean θ_m	Deviation	Unimodal Test			Bimodal Test Raleigh Prob.
						Raleigh Prob.	Vector Mag. % L%	95% Conf. interval	
II ₄ -49-6	7.8	292°	100	265.1°	26.9° _a	0.001 **	27.20	± 8.37°	
II ₄ -49-5	5.7	292°	100	283.1°	8.9° _a	0.096 *	15.31	± 9.25°	
II ₄ -49-4	3.7	292°	100	267.8°	24.2° _a	0.292 N.S.	11.09	± 9.55°	0.456 N.S.
	3.6		Bedding Joint						
II ₄ -49-3	3.5	292°	100	272.4°	19.6° _a	0.952 N.S.	2.23	±10.21°	0.921 N.S.
II ₄ -49-2	1.8	292°	100	235.6°	56.4° _a	0.007 **	22.38	± 8.71°	
II ₄ -49-1	0.0	292°	100	272.3°	19.7° _a	0.488 N.S.	8.47	± 9.72°	0.495 N.S.

- ** indicates significance at $\alpha = 0.05$
 * indicates significance at $\alpha = 0.10$
 N.S. indicates non-significance at $\alpha = 0.10$
 c deviation of vector mean from sole mark in clockwise direction
 a deviation of vector mean from sole mark in anticlockwise direction

APPENDIX II

Grain Imbrication Statistics

Thin Section Number	Direction of thin section	Height in cm above the base	No. of measurements	Imbrication	L%	Standard Deviation	95% Confidence limits	Raleigh Prob.	Level of significance	t-test of significance diff. from zero
II ₉ -68-5	202°	2.5	100	19.0° NE	29.31	41.50	± 8.23°	0.000	**	*
II ₆ -68-5	282°	5.0	92	25.1° SE	58.72	29.30	± 6.06°	0.000	**	*
II ₈ -68-6	290°	2.3	100	10.0° SE	60.73	28.50	± 5.65°	0.000	**	*
II ₈ -68-7	307°	8.5	100	4.7° SE	55.02	30.87	± 6.12°	0.000	**	N.S.
II ₅ -68-7	312°	1.6	100	12.1° SE	60.38	28.60	± 5.67°	0.000	**	*
II ₅ -68-8	315°	10.5	90	8.7° SE	40.84	36.75	± 7.69°	0.000	**	*
II ₄ -68-7	284°	1.2	100	15.8° SE	60.47	28.55	± 5.66°	0.000	**	*
II ₄ -68-8	335°	8.0	100	14.7° SE	48.51	33.60	± 6.67°	0.000	**	*
II ₆ -67-9	281°	3.0	84	11.0° SE	31.21	40.60	± 8.85°	0.000	**	*
II ₆ -67-10	321°	12.0	100	10.3° SE	50.88	32.60	± 6.47°	0.000	**	*
II ₈ -67-10	290°	4.5	100	15.5° SE	50.25	32.80	± 6.51°	0.000	**	*
II ₈ -67-11	344°	14.0	100	11.0° SE	31.21	40.60	± 8.06°	0.000	**	*
II ₄ -67-9	320°	1.8	100	7.5° SE	51.72	32.20	± 6.39°	0.000	**	*
II ₄ -67-10	306°	8.7	100	15.5° SE	50.25	32.80	± 6.51°	0.000	**	*
II ₆ -66-7	305°	2.5	100	12.4° SE	62.43	27.75	± 5.51°	0.000	**	*
II ₆ -66-8	202°	10.0	100	13.1° SE	45.91	34.65	± 6.87°	0.000	**	*
II ₈ -66-7	300°	2.5	100	15.3° SE	41.45	36.40	± 7.22°	0.000	**	*
II ₈ -66-8	356°	8.5	100	26.2° SE	40.42	36.95	± 7.33°	0.000	**	*

Thin Section Number	Direction of thin section	Height in cm above the base	No. of measurements	Imbrication	L%	Standard Deviation	95% Confidence limits	Rayleigh Prob.	Level of significance	t-test of significance diff. from zero
II ₅ -66-7	310°	2.0	100	0.0°	50.40	32.75	± 6.50°	0.000	**	N.S.
II ₅ -66-8	304°	5.5	100	5.0° SE	69.19	25.00	± 4.96°	0.000	**	*
II ₄ -66-8	312°	0.6	100	13.9° SE	44.17	35.20	± 6.98°	0.000	**	*
II ₄ -66-9	325°	8.5	100	10.6° SE	52.47	31.92	± 6.33°	0.000	**	*
II ₉ -65A-9	304°	2.4	100	28.7° SE	66.31	26.00	± 5.16°	0.000	**	*
II ₉ -65A-10	289°	11.6	100	16.7° SE	43.86	35.40	± 7.02°	0.000	**	*
II ₆ -65A-5	291°	2.7	100	8.4° SE	54.93	30.95	± 6.14°	0.000	**	*
II ₈ -65A-9	214°	1.6	100	3.6° SW	35.62	38.80	± 7.70°	0.000	**	N.S.
II ₂ -65A-10	319°	6.5	100	13.7° SE	40.43	36.95	± 7.33°	0.000	**	*
II ₈ -65A-11	319°	10.0	100	3.8° SE	48.13	33.70	± 6.69°	0.000	**	N.S.
II ₉ -65-6	267°	2.8	100	15.5° NE	41.68	36.35	± 7.21°	0.000	**	*
II ₉ -65-7	315°	2.0	100	4.5° SE	52.83	31.82	± 6.31°	0.000	**	N.S.
II ₆ -65-7	314°	2.0	100	19.1° SE	39.06	37.40	± 7.42°	0.000	**	*
II ₆ -65-8	316°	8.2	100	18.4° SE	48.81	33.40	± 6.63°	0.000	**	*
II ₈ -65-9	257°	1.2	100	3.3° NE	55.57	30.50	± 6.05°	0.000	**	N.S.
II ₈ -65-10	320°	5.5	100	16.4° SE	62.17	27.80	± 5.52°	0.000	**	*
II ₈ -65-11	249°	11.7	100	22.9° NE	17.66	45.75	± 9.08°	0.044	**	*
II ₄ -65-8	273°	2.5	100	12.4° SE	45.99	34.64	± 6.88°	0.000	**	*
II ₄ -65-9	250°	5.0	88	1.4° SW	41.87	36.30	± 7.70°	0.000	**	N.S.
II ₉ -58-4	245°	2.4	100	14.2° NE	56.22	30.25	± 6.00°	0.000	**	*

Thin Section Number	Direction of thin section	Height in cm above the base	No. of measurements	Imbrication	L%	Standard Deviation	95% Confidence limits	Rayleigh Prob.	Level of significance	t-test of significance diff. from zero
II ₆ -58-7	316°	6.0	100	2.4° SE	57.65	29.70	± 5.89°	0.000	**	*
II ₈ -58-6	322°	3.0	100	0.2° NW	12.62	47.60	± 9.44°	0.204	N.S.	N.S.
II ₅ -58-6	300°	2.5	100	17.2° NW	40.99	36.65	± 7.27°	0.000	**	*
II ₅ -58-7	207°	5.8	74	19.1° NE	64.63	26.90	± 6.25°	0.000	**	*
II ₄ -58-6	194°	2.5	100	47.2° SW	20.65	44.50	± 8.83°	0.014	**	*
II ₄ -58-7	247°	9.0	100	30.7° NE	49.79	33.01	± 6.55°	0.000	**	*
II ₉ -50-5	292°	2.5	100	9.8° SE	52.07	30.87	± 6.12°	0.000	**	*
II ₆ -50-6	203°	2.4	100	17.9° SW	49.53	33.10	± 6.57°	0.000	**	*
II ₈ -50-5	300°	3.0	100	14.9° SE	55.26	30.70	± 6.09°	0.000	**	*
II ₈ -50-6	284°	6.4	100	26.4° SE	46.53	34.40	± 6.82°	0.000	**	*
II ₅ -50-4	297°	2.8	100	3.5° SE	47.75	33.90	± 6.72°	0.000	**	N.S.
II ₉ -49-10	317°	2.3	100	26.0° SE	19.70	44.95	± 8.92°	0.021	**	*
II ₉ -49-11	250°	8.0	100	19.7° NE	38.64	37.70	± 7.48°	0.000	**	*
II ₉ -49-12	297°	13.5	100	15.2° SE	27.57	42.08	± 8.35°	0.001	**	*
II ₆ -49-6	298°	2.4	100	12.4° SE	66.05	26.20	± 5.20°	0.000	**	*
II ₄ -49-7	236°	1.8	100	2.0° SW	29.28	41.50	± 8.23°	0.000	**	N.S.
II ₄ -49-8	283°	5.7	100	2.7° SE	42.94	35.94	± 7.13°	0.000	**	N.S.

** indicates significance at $\alpha = 0.05$
* indicates significance at $\alpha = 0.10$
N.S. indicates non-significance at $\alpha = 0.10$

APPENDIX III

Moment Measure Statistics

Thin Section	No. of measure- ments	k_1	k_2	k_3	k_4	m_2	m_3	m_4	g_1	g_2
II ₉ -68-4				very	fine	grained				
II ₉ -68-3	100	2.400	0.440	0.032	-0.087	0.435	0.031	0.477	0.109	-0.447
II ₉ -68-2	100	2.130	0.541	0.015	-0.081	0.536	0.014	0.769	0.037	-0.278
II ₉ -68-1	100	1.961	0.655	-0.039	-0.413	0.648	-0.038	0.851	-0.073	-0.963*
II ₆ -68-4	100	1.720	1.125	0.162	-1.554	1.114	0.157	2.202	0.136	-1.227*
II ₆ -68-3	100	2.596	0.350	0.046	-0.052	0.346	0.044	0.304	0.222	-0.428
II ₆ -68-2	100	2.244	0.332	0.061	-0.072	0.329	0.059	0.252	0.319	-0.647
II ₆ -68-1	100	1.786	0.698	0.017	-0.418	0.691	0.017	1.014	0.030	-0.859
II ₈ -68-5	100	2.445	0.411	-0.057	-0.026	0.407	-0.056	0.463	-0.217	-0.154
II ₈ -68-4	100	2.290	0.485	-0.010	-0.038	0.480	-0.010	0.643	-0.029	-0.160
II ₈ -68-3	100	2.427	0.598	0.059	-0.300	0.592	0.058	0.750	0.128	-0.841
II ₈ -68-2	100	1.893	0.546	0.166	-0.063	0.541	0.161	0.801	0.411	-0.211
II ₈ -68-1	100	1.792	0.775	0.367	-0.230	0.768	0.356	1.518	0.538*	-0.383
II ₅ -68-6	100	2.050	0.503	-0.059	-0.081	0.498	-0.057	0.654	-0.164	-0.320
II ₅ -68-5	100	2.226	0.592	0.023	-0.129	0.586	0.023	0.891	0.051	-0.367
II ₅ -68-4	91	2.377	0.458	-0.104	-0.121	0.453	-0.101	0.490	-0.335	-0.577
II ₅ -68-3	100	2.174	0.544	-0.034	-0.062	0.538	-0.033	0.794	-0.085	-0.209
II ₅ -68-2	100	1.930	0.520	0.060	-0.164	0.515	0.058	0.627	0.160	-0.605
II ₅ -68-1	100	1.850	0.750	0.028	-0.402	0.742	0.027	1.246	0.043	-0.715

Thin Section	No. of measure- ments	k_1	k_2	k_3	k_4	m_2	m_3	m_4	g_1	g_2
II ₄ -68-6	100	2.036	0.657	-0.340	0.264	0.651	-0.329	1.491	-0.637*	0.610
II ₄ -68-5	100	2.162	0.484	-0.020	-0.011	0.479	-0.019	0.664	-0.059	-0.047
II ₄ -68-4	100	2.293	0.537	-0.062	-0.085	0.531	-0.061	0.751	-0.159	-0.296
II ₄ -68-3	100	2.301	0.367	0.005	-0.052	0.367	0.005	0.347	0.022	-0.381
II ₄ -68-2	100	2.094	0.593	-0.078	-0.166	0.587	-0.075	0.859	-0.170	-0.472
II ₄ -68-1	100	2.054	0.458	0.135	-0.075	0.454	0.131	0.535	0.435	-0.359
II ₉ -67-5	100	2.512	0.310	-0.048	-0.018	0.307	-0.047	0.260	-0.277	-0.191
II ₉ -67-4	100	2.162	0.354	0.000	0.015	0.350	0.000	0.375	0.000	0.122
II ₉ -67-3	100	1.772	0.436	0.301	0.222	0.431	0.292	0.754	1.049*	1.171*
II ₉ -67-2	100	1.380	0.613	0.204	-0.086	0.607	0.198	1.002	0.426	-0.229
II ₉ -67-1	100	1.498	0.527	0.197	0.243	0.522	0.191	1.027	0.515	0.874
II ₆ -67-6	100	2.543	0.380	-0.046	-0.047	0.377	-0.045	0.374	-0.197	-0.323
II ₆ -67-5	100	2.365	0.346	-0.001	-0.040	0.342	-0.001	0.307	-0.004	-0.338
II ₆ -67-4	100	2.135	0.477	-0.080	-0.178	0.472	-0.078	0.490	-0.243	-0.780
II ₆ -67-3	100	2.036	0.490	0.145	-0.040	0.485	0.140	0.655	0.422	-0.166
II ₆ -67-2	100	2.058	0.675	0.229	-0.138	0.668	0.222	1.184	0.413	-0.303
II ₆ -67-1	100	1.705	0.927	0.514	-0.006	0.918	0.499	2.470	0.576*	-0.007

Thin Section	No. of measure- ments	k_1	k_2	k_3	k_4	m_2	m_3	m_4	g_1	g_2
II ₈ -67-9	100	2.270	0.555	0.045	-0.247	0.550	0.044	0.658	0.110	-0.802
II ₈ -67-8	100	2.449	0.485	0.034	-0.050	0.480	0.033	0.631	0.101	-0.214
II ₈ -67-7	100	2.086	0.802	-0.386	0.297	0.794	-0.375	2.132	-0.537*	0.461
II ₈ -67-6	100	2.165	0.592	-1.230	6.075	0.586	-1.193	6.669	-2.703*	17.360*
II ₈ -67-5	100	2.073	0.633	0.020	-0.316	0.626	0.019	0.859	0.040	-0.789
II ₈ -67-4	100	2.245	0.606	0.129	-0.417	0.600	0.126	0.669	0.274	-1.137
II ₈ -67-3	100	1.937	0.641	0.154	-0.264	0.635	0.149	0.939	0.300	-0.641
II ₈ -67-2	100	1.959	0.601	0.068	-0.109	0.595	0.066	0.940	0.146	-0.301
II ₈ -67-1	100	1.632	0.593	0.121	0.004	0.587	0.117	1.018	0.264	0.011
II ₄ -67-8	100	2.226	0.621	0.049	-0.208	0.615	0.047	0.919	0.100	-0.538
II ₄ -67-7	100	2.131	0.598	0.142	-0.218	0.592	0.138	0.827	0.308	-0.610
II ₄ -67-6	100	2.021	0.810	-0.059	-0.621	0.802	-0.058	1.311	-0.082	-0.947*
II ₄ -67-5	100	2.038	0.461	-0.056	-0.032	0.456	-0.055	0.583	-0.180	-0.152
II ₄ -67-4	100	1.998	0.666	-0.036	-0.122	0.660	-0.035	1.166	-0.066	-0.275
II ₄ -67-3	100	2.106	0.707	0.033	-0.300	0.700	0.032	1.610	0.056	-0.601
II ₄ -67-2	100	1.855	0.669	0.340	0.005	0.662	0.330	1.294	0.621*	0.012
II ₄ -67-1	100	1.808	0.723	0.018	0.146	0.716	0.017	1.645	0.029	0.279

Thin Section	No. of measure- ments	k ₁	k ₂	k ₃	k ₄	m ₂	m ₃	m ₄	g ₁	g ₂
II ₉ -66-3				very	fine	grained				
II ₉ -66-2				very	fine	grained				
II ₉ -66-1	71	2.174	0.825	-0.027	-0.542	0.813	-0.026	1.437	-0.036	-0.798
II ₆ -66-6	100	2.491	0.517	-0.016	-0.131	0.511	-0.015	0.646	-0.042	-0.493
II ₆ -66-5	100	2.498	0.747	0.097	-0.472	0.740	0.094	1.170	0.149	-0.844
II ₆ -66-4	100	1.975	0.603	0.139	-0.013	0.597	0.135	1.036	0.298	-0.035
II ₆ -66-3	100	2.104	0.723	-0.013	0.132	0.716	-0.013	1.630	-0.022	0.252
II ₆ -66-2	100	1.384	0.587	0.362	0.135	0.581	0.351	1.118	0.804*	0.390
II ₆ -66-1	100	2.036	1.519	-0.161	-3.007	1.504	-0.156	3.848	-0.086	-1.303*
II ₈ -66-6	88	2.325	0.686	0.086	-0.278	0.678	0.083	1.093	0.151	-0.590
II ₈ -66-5	100	1.952	0.617	-0.027	-0.124	0.611	-0.026	0.981	-0.056	-0.325
II ₈ -66-4	100	2.223	0.543	0.155	-0.098	0.537	0.150	0.758	0.387	-0.333
II ₈ -66-3	100	1.423	0.562	0.260	0.228	0.557	0.252	1.124	0.616*	0.722
II ₈ -66-2	100	1.519	0.480	0.324	0.275	0.475	0.314	0.921	0.973*	1.193*
II ₈ -66-1	100	0.993	0.749	0.513	0.302	0.741	0.498	1.896	0.792*	0.538
II ₅ -66-6	100	2.402	0.824	-0.010	-0.644	0.816	-0.010	1.357	-0.013	-0.948*
II ₅ -66-5	100	1.980	0.499	0.094	-0.083	0.494	0.092	0.641	0.268	-0.332
II ₅ -66-4	100	2.129	0.658	0.187	-0.246	0.651	0.181	1.017	0.350	-0.569
II ₅ -66-3	100	1.443	0.395	0.133	-0.041	0.391	0.129	0.410	0.538*	-0.265
II ₅ -66-2	100	1.781	0.694	0.184	-0.158	0.687	0.179	1.240	0.318	-0.329
II ₅ -66-1	100	1.675	0.488	0.182	-0.059	0.483	0.177	0.632	0.534*	-0.247

Thin Section	No. of measurements	k_1	k_2	k_3	k_4	m_2	m_3	m_4	g_1	g_2
II ₄ -66-7	85	2.002	0.835	0.385	-0.288	0.826	0.371	1.732	0.504*	-0.413
II ₄ -66-6	100	2.040	0.721	0.062	-0.158	0.714	0.060	1.353	0.101	-0.303
II ₄ -66-5	100	2.283	0.823	0.007	-0.347	0.815	0.007	1.630	0.010	-0.512
II ₄ -66-4	100	2.228	0.652	0.086	-0.254	0.646	0.083	0.990	0.163	-0.596
II ₄ -66-3	100	2.337	0.760	0.161	-0.605	0.752	0.157	1.100	0.244	-1.048*
II ₄ -66-2	100	2.161	1.119	0.284	-1.334	1.108	0.275	2.365	0.240	-1.066*
II ₄ -66-1	100	1.611	0.928	0.307	-0.463	0.918	0.298	2.049	0.343	-0.538
II ₉ -65A-8	100	2.728	0.437	-0.068	-0.088	0.433	-0.066	0.468	-0.235	-0.462
II ₉ -65A-7	100	2.778	0.374	-0.086	-0.081	0.370	-0.083	0.327	-0.376	-0.579
II ₉ -65A-6	100	2.841	0.326	-0.036	0.035	0.323	-0.035	0.340	-0.191	0.332
II ₉ -65A-5	100	2.689	0.367	-0.110	-0.061	0.363	-0.106	0.331	-0.493*	-0.456
II ₉ -65A-4	100	2.372	0.504	0.081	-0.082	0.499	0.079	0.654	0.227	-0.324
II ₉ -65A-3	100	1.839	0.383	-0.031	0.101	0.380	-0.030	0.518	-0.131	0.689
II ₉ -65A-2	100	1.828	0.403	0.213	0.144	0.399	0.207	0.601	0.834*	0.888
II ₉ -65A-1	100	1.576	0.542	0.218	0.009	0.537	0.212	0.855	0.546*	0.029
II ₆ -65A-4					very fine	grained				
II ₆ -65A-3					very fine	grained				
II ₆ -65A-2	100	2.696	0.493	-0.296	0.281	0.488	-0.287	0.964	-0.854*	1.155*
II ₆ -65A-1	100	2.593	0.436	-0.082	-0.045	0.432	-0.079	0.506	0.284	-0.237

Thin Section	No. of measure- ments	k_1	k_2	k_3	k_4	m_2	m_3	m_4	g_1	g_2
II ₈ -65A-8	100	2.495	0.638	-0.154	-0.174	0.632	-0.149	1.011	-0.302	-0.427
II ₈ -65A-7	100	2.594	0.488	0.044	-0.181	0.483	0.042	0.516	0.128	-0.764
II ₈ -65A-6	100	2.486	0.428	0.064	-0.138	0.424	0.062	0.399	0.228	-0.755
II ₈ -65A-5	100	1.962	0.558	0.207	-0.046	0.552	0.201	0.853	0.498*	-0.147
II ₈ -65A-4	100	1.812	0.358	-0.017	0.009	0.355	-0.016	0.378	-0.078	0.070
II ₈ -65A-3	100	2.172	0.514	-0.052	-0.020	0.509	-0.051	0.742	-0.142	-0.077
II ₈ -65A-2	100	1.763	0.423	0.134	0.001	0.419	0.130	0.517	0.488*	0.005
II ₈ -65A-1	100	1.918	0.342	0.071	-0.042	0.338	0.069	0.298	0.356	-0.356
II ₉ -65-5	100	2.225	0.446	0.104	-0.044	0.442	0.101	0.533	0.350	-0.221
II ₉ -65-4	100	2.227	0.434	0.077	-0.114	0.430	0.075	0.438	0.269	-0.604
II ₉ -65-3	100	2.164	0.653	0.009	0.043	0.646	0.009	1.268	0.018	0.101
II ₉ -65-2	100	1.814	0.419	0.092	-0.102	0.414	0.089	0.409	0.339	-0.586
II ₉ -65-1	100	1.675	0.618	0.012	-0.103	0.612	0.012	1.005	0.025	-0.270
II ₆ -65-6	100	2.326	0.621	0.030	-0.239	0.615	0.029	0.889	0.061	-0.619
II ₆ -65-5	100	2.358	0.559	0.074	-0.138	0.554	0.072	0.773	0.178	-0.441
II ₆ -65-4	100	2.164	0.503	0.069	-0.148	0.498	0.067	0.591	0.192	-0.587
II ₆ -65-3	100	1.935	0.418	0.047	0.009	0.414	0.046	0.512	0.175	0.051
II ₆ -65-2	100	2.053	0.642	0.083	-0.265	0.636	0.081	0.941	0.162	-0.643
II ₆ -65-1	100	1.742	0.581	0.208	0.084	0.575	0.202	1.051	0.471*	0.250

Thin Section	No. of measurements	k_1	k_2	k_3	k_4	m_2	m_3	m_4	g_1	g_2
II ₈ -65-7	100	2.594	0.488	0.044	-0.181	0.483	0.042	0.516	0.128	-0.764
II ₈ -65-6	100	2.558	0.358	-0.007	-0.072	0.355	-0.007	0.303	-0.032	-0.561
II ₈ -65-5	100	2.460	0.452	0.025	-0.156	0.447	0.025	0.442	0.084	-0.767
II ₈ -65-4	100	2.207	0.619	0.181	-0.159	0.613	0.176	0.956	0.373	-0.415
II ₈ -65-3	100	2.043	0.447	0.025	-0.179	0.442	0.025	0.408	0.085	-0.899
II ₈ -65-2	100	1.939	0.567	-0.247	0.130	0.561	-0.240	1.046	-0.579*	0.404
II ₈ -65-1	100	1.970	0.583	0.130	0.076	0.577	0.126	1.048	0.292	0.223
II ₄ -65-6	100	2.394	0.522	-0.060	-0.048	0.517	-0.058	0.742	-0.158	-0.174
II ₄ -65-5	100	2.470	0.465	0.058	-0.177	0.460	0.057	0.458	0.184	-0.820
II ₄ -65-4	100	2.529	0.375	-0.001	-0.037	0.371	-0.001	0.371	-0.004	-0.260
II ₄ -65-3	100	2.589	0.671	0.035	-0.374	0.664	0.034	0.949	0.063	-0.831
II ₄ -65-2	100	2.292	0.430	0.071	-0.026	0.425	0.069	0.508	0.251	-0.140
II ₄ -65-1	100	2.033	0.462	0.078	0.010	0.458	0.076	0.626	0.249	0.049
II ₉ -58-3	100	2.305	0.593	-0.288	0.083	0.587	-0.280	1.091	-0.631*	0.235
II ₉ -58-2	100	1.662	0.422	0.010	-0.061	0.418	0.010	0.457	0.038	-0.342
II ₉ -58-1	100	1.603	0.571	0.212	-0.082	0.566	0.206	0.865	0.492*	-0.250
II ₆ -58-4	83	2.993	0.222	-0.033	0.001	0.219	-0.031	0.142	-0.312	0.026
II ₆ -58-3	100	2.420	0.484	-0.021	-0.069	0.479	-0.020	0.612	-0.063	-0.293
II ₆ -58-2	100	1.764	0.533	0.031	-0.107	0.527	0.030	0.719	0.080	-0.376
II ₆ -58-1					very fine	grained				

Thin Section	No. of measurements	k_1	k_2	k_3	k_4	m_2	m_3	m_4	g_1	g_2
II ₄ -58-5	100	2.597	0.487	-0.154	-0.079	0.482	-0.149	0.611	-0.452	-0.331
II ₄ -58-4	100	2.377	0.517	-0.180	0.222	0.512	-0.175	0.978	-0.484	0.831
II ₄ -58-3	100	1.984	0.468	0.070	-0.161	0.463	0.068	0.481	0.218	-0.737
II ₄ -58-2	100	1.872	0.567	-0.045	0.035	0.561	-0.043	0.959	-0.104	0.108
II ₄ -58-1	100	1.434	0.810	0.312	-0.205	0.802	0.303	1.701	0.428	-0.313
II ₅ -58-5					very fine	grained				
II ₅ -58-6	96	2.961	0.271	-0.029	0.015	0.268	-0.028	0.226	-0.205	0.217
II ₅ -58-3	100	2.499	0.329	-0.125	0.023	0.326	-0.121	0.334	-0.661*	0.216
II ₅ -58-2	100	2.135	0.566	-0.015	0.034	0.560	-0.015	0.954	-0.036	0.108
II ₅ -58-1	100	1.526	1.019	0.518	-0.801	1.009	0.503	2.247	0.504*	-0.771
II ₈ -58-5					very fine	grained				
II ₈ -58-4	100	2.751	0.220	0.003	0.014	0.218	0.003	0.153	0.033	0.297
II ₈ -58-3	100	2.242	0.373	0.031	-0.121	0.369	0.030	0.288	0.136	-0.873
II ₈ -58-2	100	1.911	0.603	0.154	-0.269	0.597	0.149	0.797	0.329	-0.741
II ₈ -58-1	100	1.491	0.761	0.241	-0.487	0.753	0.234	1.215	0.363	-0.841
II ₉ -50-4	100	2.314	0.574	-0.057	-0.085	0.568	-0.055	0.869	-0.131	-0.258
II ₉ -50-3	100	2.378	0.475	-0.058	-0.050	0.470	-0.056	0.605	-0.176	-0.220
II ₉ -50-2	100	2.365	0.413	-0.011	-0.051	0.409	-0.011	0.444	-0.041	-0.299
II ₉ -50-1	100	2.124	0.649	-0.021	-0.361	0.642	-0.020	0.877	-0.040	-0.857

Thin Section	No. of measure- ments	k_1	k_2	k_3	k_4	m_2	m_3	m_4	g_1	g_2
II ₆ -50-5				very	fine	grained				
II ₆ -50-4										
II ₆ -50-3	100	2.597	0.330	-0.057	0.000	0.326	-0.055	0.313	-0.299	0.000
II ₆ -50-2	100	2.319	0.553	-0.059	0.005	0.547	-0.057	0.885	-0.143	0.016
II ₆ -50-1	100	1.875	0.512	0.243	-0.040	0.507	0.236	0.719	0.663*	-0.152
II ₈ -50-4	100	2.583	0.536	-0.105	-0.260	0.530	-0.101	0.585	-0.267	-0.906
II ₈ -50-3	100	2.378	0.371	0.021	-0.074	0.367	0.020	0.328	0.093	-0.540
II ₈ -50-2	100	2.374	0.405	0.032	-0.068	0.401	0.030	0.410	0.123	-0.412
II ₈ -50-1	100	1.989	0.648	0.170	-0.133	0.641	0.165	1.085	0.327	-0.318
II ₅ -50-3	100	2.130	0.544	-0.018	-0.067	0.539	-0.017	0.792	-0.044	-0.227
II ₅ -50-2	100	2.152	0.491	0.104	-0.113	0.486	0.101	0.590	0.302	-0.467
II ₅ -50-1	100	2.126	0.549	-0.122	-0.155	0.543	-0.119	0.724	-0.301	-0.516
II ₄ -50-5	100	2.163	0.505	-0.020	-0.103	0.500	-0.020	0.638	-0.057	-0.404
II ₄ -50-4	100	2.326	0.438	0.065	-0.004	0.434	0.063	0.550	0.225	-0.022
II ₄ -50-3	100	2.167	0.413	-0.001	-0.096	0.409	-0.001	0.402	-0.005	-0.565
II ₄ -50-2	100	1.894	0.435	0.046	-0.086	0.431	0.045	0.465	0.160	-0.456
II ₄ -50-1	100	1.863	0.553	0.022	-0.273	0.547	0.021	0.626	0.053	0.894

Thin Section	No. of measurements	k_1	k_2	k_3	k_4	m_2	m_3	m_4	g_1	g_2
II ₉ -49-9	100	1.941	0.545	0.083	0.106	0.539	0.081	0.954	0.207	0.357
II ₉ -49-8	100	2.022	0.622	-0.034	-0.014	0.616	-0.033	1.102	-0.068	-0.036
II ₉ -49-7	100	2.029	0.538	0.064	-0.040	0.533	0.062	0.797	0.162	-0.140
II ₉ 049-6	100	2.165	0.399	0.050	-0.088	0.395	0.049	0.377	0.200	-0.551
II ₉ -49-5	100	2.133	0.424	0.114	0.107	0.420	0.111	0.617	0.413	0.593
II ₉ -49-4	100	2.032	0.488	0.205	0.054	0.483	0.199	0.736	0.603*	0.229
II ₉ -49-3	100	2.114	0.381	0.015	0.045	0.378	0.014	0.461	0.062	0.309
II ₉ -49-2	100	2.134	0.479	0.130	-0.042	0.474	0.127	0.621	0.394	-0.182
II ₉ -49-1	100	1.925	0.555	0.122	-0.085	0.549	0.119	0.808	0.296	-0.275
II ₆ -49-5	100	2.604	0.350	-0.021	-0.053	0.346	-0.020	0.303	-0.100	-0.437
II ₆ -49-4	100	2.393	0.286	-0.054	-0.030	0.283	-0.052	0.207	-0.353	-0.371
II ₆ -49-3	100	2.216	0.530	-0.309	0.193	0.525	-0.300	0.989	-0.801*	0.688
II ₆ -49-2	100	2.263	0.359	0.050	0.094	0.355	0.049	0.459	0.233	0.731
II ₆ -49-1	100	2.342	0.370	0.025	-0.057	0.367	0.025	0.342	0.113	-0.415
II ₄ -49-6	100	2.325	0.554	-0.047	-0.168	0.548	-0.046	0.727	-0.114	-0.548
II ₄ -49-5	84	1.486	2.338	-3.441	0.900	2.315	-3.338	16.594	-0.962*	0.165
II ₄ -49-4	100	2.072	0.543	0.039	-0.172	0.538	0.086	0.690	0.221	-0.583
II ₄ -49-3	100	2.275	0.579	0.032	-0.328	0.573	0.031	0.660	0.072	-0.980*
II ₄ -49-2	100	2.052	0.562	0.184	0.143	0.556	0.178	1.043	0.437	0.452
II ₄ -49-1	100	1.855	0.618	0.191	-0.097	0.611	0.185	1.009	0.394	-0.254

* indicates significant deviation from normality at $\alpha = 0.05$.